ANALYTICAL HEAT TRANSFER

Mihir Sen

Department of Aerospace and Mechanical Engineering
University of Notre Dame
Notre Dame, IN 46556

May 6, 2008

Preface

These are lecture notes for *AME60634: Intermediate Heat Transfer,* a second course on heat transfer for undergraduate seniors and beginning graduate students. At this stage the student can begin to apply knowledge of mathematics and computational methods to the problems of heat transfer. Thus, in addition to some undergraduate knowledge of heat transfer, students taking this course are expected to be familiar with vector algebra, linear algebra, ordinary differential equations, particle and rigid-body dynamics, thermodynamics, and integral and differential analysis in fluid mechanics. The use of computers is essential both for the purpose of computation as well as for display and visualization of results.

At present these notes are in the process of being written; the student is encouraged to make extensive use of the literature listed in the bibliography. The students are also expected to attempt the problems at the end of each chapter to reinforce their learning.

I will be glad to receive comments on these notes, and have mistakes brought to my attention.

Mihir Sen
Department of Aerospace and Mechanical Engineering
University of Notre Dame

Contents

Part I

Review

Chapter 1

Introductory heat transfer

It is assumed that the reader has had an introductory course in heat transfer of the level of [12, 14, 19, 20, 22, 24, 26, 34, 65, 76, 80, 88, 90, 106, 111, 112, 117, 122, 138, 155, 177, 183, 188, 207, 210, 211]. More advanced books are, for example, [206, 212]. A classic work is that of Jakob [94].

1.1 Fundamentals

1.1.1 Definitions

Temperature is associated with the motion of molecules within a material, being directly related to the kinetic energy of the molecules, including vibrational and rotational motion. *Heat* is the energy transferred between two points at different temperatures. The laws of thermodynamics govern the transfer of heat. Two bodies are in *thermal equilibrium* with each other if there is no transfer of heat between them. The *zeroth* law states that if each of two bodies are in thermal equilibrium with a third, then they also are in equilibrium with each other. Both heat transfer and work transfer increase the *internal energy* of the body. The change in internal energy can be written in terms of a coefficient of specific heat[1] as $Mc\ dT$. According to the *first* law, the increase in internal energy is equal to the net heat and work transferred in. The *third* law says that the *entropy* of an isolated system cannot decrease over time.

Example 1.1

Show that the above statement of the third law implies that heat is always transferred from a high temperature to a low.

1.1.2 Energy balance

The first law gives a quantitative relation between the heat and work input to a system. If there is no work transfer, then

$$Mc\frac{\partial T}{\partial t} = Q \tag{1.1}$$

where Q is the heat rate over the surface of the body. A surface cannot store energy, so that the heat flux coming in must be equal to that going out.

[1] We will not distinguish between the specific heat at constant pressure and that a constant volume.

1.1.3 States of matter

We will be dealing with solids, liquids and gases as well as the transformation of on to the other. Again, thermodynamics dictates the rules under which these changes are possible. For the moment, we will define the enthalpy of transformation[2] as the change in enthalpy that occurs when matter is transformed from one state to another.

1.2 Conduction

[31, 66, 68, 77, 100, 136, 137, 149]

The Fourier law of conduction is

$$\mathbf{q} = -k\nabla T \tag{1.2}$$

where $\mathbf{q}$ is the heat flux vector, $T(\mathbf{x})$ is the temperature field, and $k(T)$ is the coefficient of thermal conductivity.

1.2.1 Governing equation

$$\frac{\partial T}{\partial t} = \alpha\nabla\left(k \cdot \nabla T\right) + g \tag{1.3}$$

1.2.2 Fins

Fin effectiveness ϵ_f: This is the ratio of the fin heat transfer rate to the rate that would be if the fin were not there.
Fin efficiency η_f: This is the ratio of the fin heat transfer rate to the rate that would be if the entire fin were at the base temperature.

Longitudinal heat flux

$$q''_x = O(k_s\frac{T_b - T_\infty}{L}) \tag{1.4}$$

Transverse heat flux

$$q''_t = O(h(T_b - T_\infty)) \tag{1.5}$$

The transverse heat flux can be neglected compared to the longitudinal if

$$q''_x \gg q''_t \tag{1.6}$$

which gives a condition on the Biot number

$$Bi = \frac{hL}{k} \ll 1 \tag{1.7}$$

Consider the fin shown shown in Fig. 1.1. The energy flows are indicated in Fig. 1.2. The conductive heat flow along the fin, the convective heat loss from the side, and the radiative loss from the side are

$$q_k = -k_s A\frac{dT}{dx} \tag{1.8}$$

$$q_h = hdA_s(T - T_\infty) \tag{1.9}$$

$$q_r = \sigma dA_s(T^4 - T_\infty^4) \tag{1.10}$$

[2] Also called the latent heat.

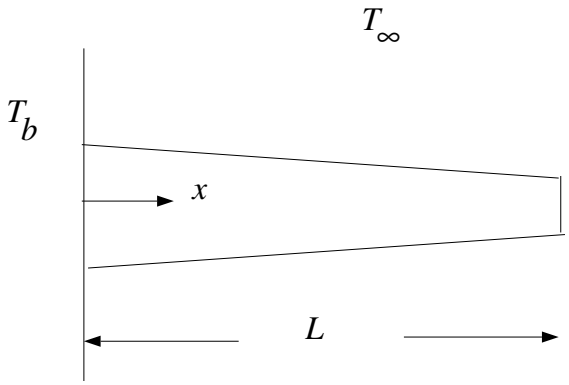

Figure 1.1: Schematic of a fin.

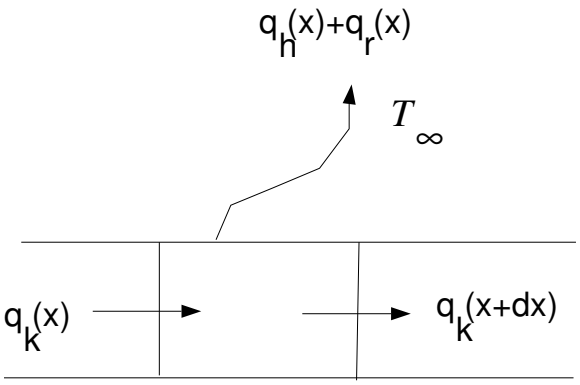

Figure 1.2: Energy balance.

where, for a small enough slope, $P(x) \approx dA_s/dx$ is the perimeter. Heat balance gives

$$\rho Ac\frac{\partial T}{\partial t} + \frac{\partial q_k}{\partial x}dx + q_h + q_r = 0 \tag{1.11}$$

from which

$$\rho Ac\frac{\partial T}{\partial t} - k_s\frac{\partial}{\partial x}(A\frac{\partial T}{\partial x}) + Ph(T - T_\infty) + \sigma P(T^4 - T_\infty^4) = 0 \tag{1.12}$$

where k_s is taken to be a constant.

The initial temperature is $T(x, 0) = T_i(x)$. Usually the base temperature T_b is known. The different types of boundary conditions for the tip are:

- Convective: $\partial T/\partial x = a$ at $x = L$
- Adiabatic: $\partial T/\partial x = 0$ at $x = L$
- Known tip temperature: $T = T_L$ at $x = L$

- Long fin: $T = T_\infty$ as $x \to \infty$

  Taking

$$\theta = \frac{T - T_\infty}{T_b - T_\infty} \tag{1.13}$$

$$\tau = \frac{k_s t}{L^2 \rho c} \quad \text{Fourier modulus} \tag{1.14}$$

$$\xi = \frac{x}{L} \tag{1.15}$$

$$a(\xi) = \frac{A}{A_b} \tag{1.16}$$

$$p(\xi) = \frac{P}{P_b} \tag{1.17}$$

where the subscript indicates quantities at the base, the fin equation becomes

$$a\frac{\partial \theta}{\partial \tau} - \frac{\partial}{\partial \xi}\left(a\frac{\partial \theta}{\partial \xi}\right) + m^2 p\theta + \epsilon p\left[(\theta + \beta)^4 - \beta^4\right] = 0 \tag{1.18}$$

where

$$m^2 = \frac{P_b h L^2}{k_s A_b} \tag{1.19}$$

$$\epsilon = \frac{\sigma P_b L^2 (T_b - T_\infty)^3}{k_s A_b} \tag{1.20}$$

$$\beta = \frac{T_\infty}{T_b - T_\infty} \tag{1.21}$$

1.2.3 Separation of variables

Steady-state coduction in a rectangular plate.

$$\nabla^2 T = 0 \tag{1.22}$$

Let $T(x, y) = X(x)Y(y)$.

1.2.4 Similarity variable

$$\frac{\partial T}{\partial t} = \alpha \frac{\partial^2 T}{\partial x^2} \tag{1.23}$$

1.2.5 Lumped-parameter approximation

Consider a wall with fluid on both sides as shown in Fig. 1.3. The fluid temperatures are $T_{\infty,1}$ and $T_{\infty,2}$ and the wall temperatures are $T_{w,1}$ and $T_{w,2}$. The initial temperature in the wall is $T(x, 0) = f(x)$.

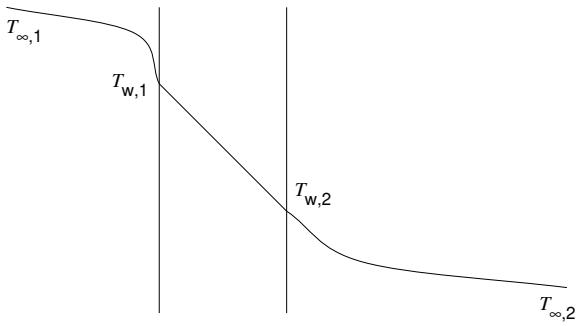

Figure 1.3: Wall with fluids on either side.

Steady state

In the steady state, we have

$$h_1(T_{\infty,1} - T_{w,1}) = k_s \frac{T_{w,1} - T_{w,2}}{L} = h_2(T_{w,2} - T_{\infty,2}) \tag{1.24}$$

from which

$$\frac{h_1 L}{k_s} \frac{T_{\infty,1} - T_{w,1}}{T_{\infty,1} - T_{\infty,2}} = \frac{T_{w,1} - T_{w,2}}{T_{\infty,1} - T_{\infty,2}} = \frac{h_2 L}{k_s} \frac{T_{w,2} - T_{\infty,2}}{T_{\infty,1} - T_{\infty,2}} \tag{1.25}$$

Thus we have

$$\frac{T_{w,1} - T_{w,2}}{T_{\infty,1} - T_{\infty,2}} \ll \frac{T_{\infty,1} - T_{w,1}}{T_{\infty,1} - T_{\infty,2}} \quad \text{if } \frac{h_1 L}{k_s} \ll 1 \tag{1.26}$$

$$\frac{T_{w,1} - T_{w,2}}{T_{\infty,1} - T_{\infty,2}} \ll \frac{T_{w,2} - T_{\infty,2}}{T_{\infty,1} - T_{\infty,2}} \quad \text{if } \frac{h_2 L}{k_s} \ll 1 \tag{1.27}$$

The Biot number is defined as

$$Bi = \frac{hL}{k_s} \tag{1.28}$$

Transient

$$\frac{\partial T}{\partial t} = \frac{k_s}{\rho c} \frac{\partial^2 T}{\partial x^2} \tag{1.29}$$

There are two time scales: the short (conductive) $t_0^k = L^2 \rho c / k_s$ and the long (convective) $t_0^h = L\rho c / h$. In the short time scale conduction within the slab is important, and convection from the sides is not. In the long scale, the temperature within the slab is uniform, and changes due to convection. The ratio of the two $t_0^k / t_0^h = Bi$. In the long time scale it is possible to show that

$$L\rho_s c \frac{dT}{dt} + h_1(T - T_{\infty,1}) + h_2(T - T_{\infty,2}) = 0 \tag{1.30}$$

where $T = T_{w,1} = T_{w,2}$.

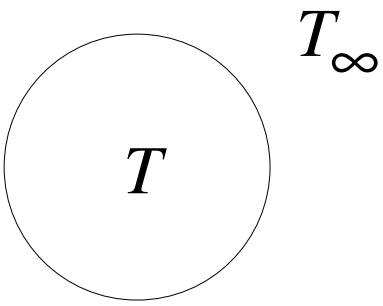

Figure 1.4: Convective cooling.

Convective cooling

A body at temperature T, such as that shown in Fig. 1.4, is placed in an environment of different temperature, T_∞, and is being convectively cooled. The governing equation is

$$Mc\frac{dT}{dt} + hA(T - T_\infty) = 0 \tag{1.31}$$

with $T(0) = T_i$. We nondimensionalize using

$$\theta = \frac{T - T_\infty}{T_i - T_\infty} \tag{1.32}$$

$$\tau = \frac{hAt}{Mc} \tag{1.33}$$

The nondimensional form of the governing equation (1.31) is

$$\frac{d\theta}{d\tau} + \theta = 0 \tag{1.34}$$

the solution to which is

$$\theta = e^{-\tau} \tag{1.35}$$

This is shown in Fig. 1.5 where the nondimensional temperature goes from $\theta = 1$ to $\theta = 0$. The dimensional time constant is Mc/hA.

1.3 Convection

[11, 21, 27, 67, 95, 98, 99, 102, 104, 133].

Newton's law of cooling: The rate of convective heat transfer from a body is proportional the difference in temperature between the body and the surrounding fluid. Thus, we can write

$$\mathbf{q} = hA(T_b - T_f), \tag{1.36}$$

where A is the surface area of the body, T_b is its temperature, T_f is that of the fluid, and h is the coefficient of thermal convection.

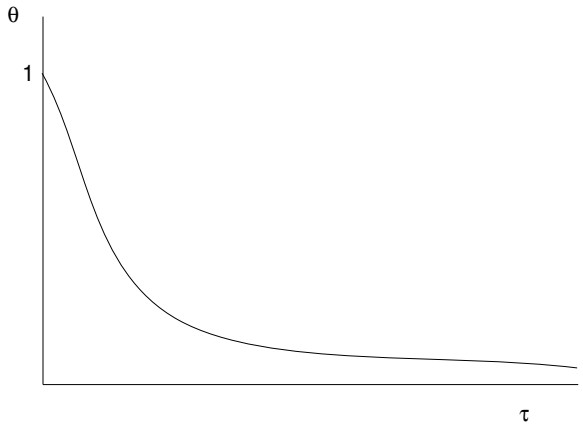

Figure 1.5: Convective cooling.

1.3.1 Governing equations

For incompressible flow

$$\nabla \cdot \mathbf{V} = 0 \tag{1.37}$$

$$\rho\left(\frac{\partial \mathbf{V}}{\partial t} + \mathbf{V} \cdot \nabla \mathbf{V}\right) = -\nabla p + \mu \nabla^2 \mathbf{V} + \mathbf{f} \tag{1.38}$$

$$\rho c\left(\frac{\partial T}{\partial t} + \mathbf{V} \cdot \nabla T\right) = \nabla\left(k \cdot \nabla T\right) + \Phi \tag{1.39}$$

1.3.2 Flat-plate boundary-layer theory

Forced convection

Natural convection

1.3.3 Heat transfer coefficients

Overall heat transfer coefficient
- Fouling
- Bulk temperature
- Nondimensional groups

$$\text{Reynolds number } Re = \frac{UL}{\nu} \tag{1.40}$$

$$\text{Prandtl number} = \frac{\nu}{\kappa} \tag{1.41}$$

$$\text{Nusselt number } Nu = \frac{hL}{k} \tag{1.42}$$

$$\text{Stanton number } St = Nu/Pr\ Re \tag{1.43}$$

$$\text{Colburn } j\text{-factor } j = St\ Pr^{2/3} \tag{1.44}$$

$$\text{Friction factor } f = \frac{2\tau_w}{\rho U^2} \tag{1.45}$$

1.4 Radiation

[25, 58, 127, 209]

Emission can be from a surface or volumetric. Monochromatic radiation is at a single wavelength. The direction distribution of radiation from a surface may be either specular (i.e. mirror-like with angles of incidence and reflection equal) or diffuse (i.e. equal in all directions).

The spectral intensity of emission is the radiant energy leaving per unit time, unit area, unit wavelength, and unit solid angle. The emissive power is the emission of an entire hemisphere. Irradiations is the radiant energy coming in, while the radiosity is the energy leaving including the emission plus the reflection.

The absorptivity α_λ, the reflectivity ρ_λ, and transmissivity τ_λ are all functions of the wavelkength λ. Also

$$\alpha_\lambda + \rho_\lambda + \tau_\lambda = 1 \tag{1.46}$$

Integrating over all wavelengths

$$\alpha + \rho + \tau = 1 \tag{1.47}$$

The emissivity is defined as

$$\epsilon_\lambda = \frac{E_\lambda(\lambda, T)}{E_{b\lambda}(\lambda, T)} \tag{1.48}$$

where the numerator is the actual energy emitted and the denominator is that that would have been emitted by a blackbody at the same temperature. For the overall energy, we have a similar definition

$$\epsilon = \frac{E(T)}{E_b(T)} \tag{1.49}$$

so that the emission is

$$E = \epsilon\sigma T^4 \tag{1.50}$$

For a gray body ϵ_λ is independent of λ.

Kirchhoff's law: $\alpha_\lambda = \epsilon_\lambda$ and $\alpha = \epsilon$.

1.4.1 Electromagnetic radiation

[173]

Electromagnetic radiation travels at the speed of light $c = 2.998 \times 10^8$ m/s. Thermal radiation is the part of the spectrum in the 0.1–100 μm range. The frequency f and wavelength λ of a wave are related by

$$c = f\lambda \tag{1.51}$$

The radiation can also be considered a particles called phonons with energy

$$E = \hbar f \tag{1.52}$$

where $\hbar$ is Planck's constant.

Maxwell's equations of electromagnetic theory are

$$\begin{aligned} \nabla \times \mathbf{H} &= \mathbf{J} + \frac{\partial \mathbf{D}}{\partial t} && (1.53)\\ \nabla \times \mathbf{E} &= -\frac{\partial \mathbf{B}}{\partial t} && (1.54)\\ \nabla \cdot \mathbf{D} &= \rho && (1.55)\\ \nabla \cdot \mathbf{B} &= 0 && (1.56) \end{aligned}$$

where $\mathbf{H}$, $\mathbf{B}$, $\mathbf{E}$, $\mathbf{D}$, $\mathbf{J}$, and ρ are the magnetic intensity, magnetic induction, electric field, electric displacement, current density, and charge density, respectively. For linear materials $\mathbf{D} = \epsilon\mathbf{E}$, $\mathbf{J} = g\mathbf{E}$ (Ohm's law), and $\mathbf{B} = \mu\mathbf{H}$, where ϵ is the permittivity, g is the electrical conductivity, and μ is the permeability. For free space $\epsilon = 8.8542 \times 10^{-12}$ $\mathrm{C^2N^{-1}m^{-2}}$, and $\mu = 1.2566 \times 10^{-6}$ $\mathrm{NC^{-2}s^2}$,

For $\rho = 0$ and constant ϵ, g and μ, it can be shown that

$$\begin{aligned} \nabla^2\mathbf{H} - \epsilon\mu\frac{\partial^2\mathbf{H}}{\partial t^2} - g\mu\frac{\partial \mathbf{H}}{\partial t} &= 0 && (1.57)\\ \nabla^2\mathbf{E} - \epsilon\mu\frac{\partial^2\mathbf{E}}{\partial t^2} - g\mu\frac{\partial \mathbf{E}}{\partial t} &= 0 && (1.58) \end{aligned}$$

The speed of an electromagnetic wave in free space is $c = 1/\sqrt{\mu\epsilon}$.

Blackbody radiation

Planck distribution [147]

$$E_\lambda = \frac{C_1}{\lambda^5 \left[\exp\left(C_2/\lambda T\right) - 1\right]} \tag{1.59}$$

Wien's law: Putting $dE_\lambda/d\lambda = 0$, the maximum of is seen to be at $\lambda = \lambda_m$, where

$$\lambda_m T = C_3 \tag{1.60}$$

and $C_3 = 2897.8$ μmK.

Stefan-Boltzmann's law: The total radiation emitted is

$$\begin{aligned} E_b &= \int_0^\infty E_\lambda \, d\lambda \\ &= \sigma T^4 && (1.61) \end{aligned}$$

where $\sigma = 5.670 \times 10^{-8}$ $\mathrm{W/m^2K^4}$.

$$\frac{d^2T}{dx^2} = \lambda^2 T^4 \tag{1.62}$$

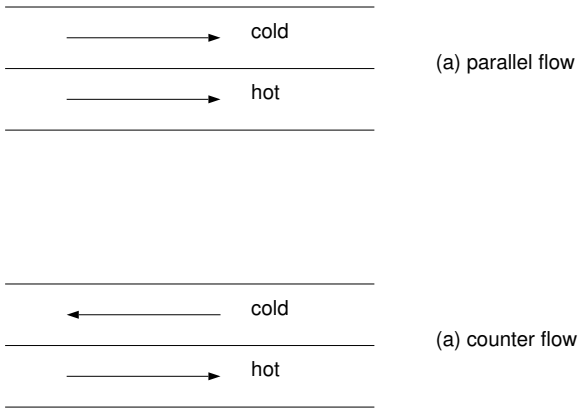

Figure 1.6: Parallel and counter flow.

1.4.2 View factors

1.5 Boiling and condensation

[29, 42, 198]

1.5.1 Boiling curve

1.5.2 Critical heat flux

1.5.3 Film boiling

1.5.4 Condensation

Nusselt's solution

1.6 Heat exchangers

[105, 154]

Shell and tube heat exchangers are commonly used for large industrial applications. Compact heat exchangers are also common in industrial and engineering applications that exchanger heat between two separated fluids. The term *compact* is understood to mean a surface to volume ratio of more than about 700 m^2/m^3. The advantages are savings in cost, weight and volume of the heat exchanger.

The fin efficiency concept was introduced by Harper and Brown (1922). The effectiveness-NTU method was introduced by London and Seban in 1941.

A possible classification of HXs is shown in Table 1.1.

Table 1.1: Classification of HX (due to Shah [170], 1981

According to	*Types of HXs*	*Examples*
Transfer processes	Direct contact	
	Indirect contact	(a) direct transfer, (b) storage, (c) fluidized bed
Surface compactness	Compact	
	Non-compact	
Construction	Tubular	(a) double pipe (b) shell and tube (c) spiral tube
	Plate	(a) gasketed, (b) spiral, (c) lamella
	Extended surface	(a) plate fin, (b) tube fin
	Regenerative	(a) rotary disk (b) rotary drum (c) fixed matrix
Flow arrangement	Single pass	(a) parallel flow (b) counterflow (c) crossflow
	Multipass	(a) extended surface cross counter flow, (b) extended surface cross parallel flow, (c) shell and tube parallel counterflow shell and tube mixed, (d) shell and tube split flow, (e) shell and tube divided flow Plate
Number of fluids	Two fluid	
	Three fluid	
	Multifluid	
Heat transfer	Single-phase convection mechanisms on both sides	
	Single-phase convection on one side, two-phase convection on other side	
	Two-phase convection on both sides	
	Combined convection and radiative heat transfer	

1.6.1 Parallel- and counter-flow

We define the subscripts h and c to mean hot and cold fluids, i and o for inlet and outlet, 1 the end where the hot fluids enters, and 2 the other end. Energy balances give

$$dq = U(T_h - T_c)\, dA \tag{1.63}$$
$$dq = \pm \dot{m}_c C_c\, dT_c \tag{1.64}$$
$$dq = -\dot{m}_h C_h\, dT_h \tag{1.65}$$

where the upper and lower signs are for parallel and counterflow, respectively. From equations (1.64) and (1.65), we get

$$-dq \left(\frac{1}{\dot{m}_h C_h} \pm \frac{1}{\dot{m}_c C_c} \right) = d(T_h - T_c) \tag{1.66}$$

Using (1.63), we find that

$$-U\, dA \left(\frac{1}{\dot{m}_h C_h} \pm \frac{1}{\dot{m}_c C_c} \right) = \frac{d(T_h - T_c)}{T_h - T_c} \tag{1.67}$$

which can be integrated from 1 to 2 to give

$$-UA \left(\frac{1}{\dot{m}_h C_h} \pm \frac{1}{\dot{m}_c C_c} \right) = \ln \frac{(T_h - T_c)_1}{(T_h - T_c)_2} \tag{1.68}$$

From equation (1.66), we get

$$-q_T \left(\frac{1}{\dot{m}_h C_h} + \frac{1}{\dot{m}_c C_c} \right) = (T_h - T_c)_2 - (T_h - T_c)_1 \tag{1.69}$$

where q_T is the total heat transfer rate. The last two equations can be combined to give

$$q_T = UA\Delta T_{lmtd} \tag{1.70}$$

where

$$\Delta T_{lmtd} = \frac{(T_h - T_c)_1 - (T_h - T_c)_2}{\ln[(T_h - T_c)_1/(T_h - T_c)_2]} \tag{1.71}$$

is the logarithmic mean temperature difference.

For parallel flow, we have

$$\Delta T_{lmtd} = \frac{(T_{h,i} - T_{c,i}) - (T_{h,o} - T_{c,o})}{\ln[(T_{h,i} - T_{c,i})/(T_{h,o} - T_{c,o})]} \tag{1.72}$$

while for counterflow it is

$$\Delta T_{lmtd} = \frac{(T_{h,i} - T_{c,o}) - (T_{h,o} - T_{c,i})}{\ln[(T_{h,i} - T_{c,o})/(T_{h,o} - T_{c,i})]} \tag{1.73}$$

We an write the element of area dA in terms of the perimeter P as $dA = P\, dx$, so that

$$T_c(x) = T_{c,1} \pm \frac{q(x)}{\dot{m}_c C_c} \tag{1.74}$$
$$T_h(x) = T_{h,1} - \frac{q(x)}{\dot{m}_h C_h} \tag{1.75}$$

Thus

$$\frac{dq}{dx} + qUP\left(\frac{1}{\dot{m}_h C_h} \pm \frac{1}{\dot{m}_c C_c}\right) \tag{1.76}$$

With the boundary condition $q(0) = 0$, the solution is

$$q9x) = \frac{T_{h,1} - T_{c,1}}{\frac{1}{\dot{m}_h C_h} \pm \frac{1}{\dot{m}_c C_c}} \left\{1 - \exp\left[-UP\left(\frac{1}{\dot{m}_h C_h} \pm \frac{1}{\dot{m}_c C_c}\right)\right]\right\} \tag{1.77}$$

1.6.2 HX relations

The HX effectiveness is

$$\begin{aligned} \epsilon &= \frac{Q}{Q_{max}} && (1.78)\\ &= \frac{C_h(T_{h,i} - T_{h,o})}{C_{min}(T_{h,i} - T_{c,i})} && (1.79)\\ &= \frac{C_c(T_{c,o} - T_{c,i})}{C_{min}(T_{h,i} - T_{c,i})} && (1.80) \end{aligned}$$

where

$$C_{min} = \min(C_h, C_c) \tag{1.81}$$

Assuming U to be a constant, the number of transfer units is

$$NTU = \frac{AU}{C_{min}} \tag{1.82}$$

The heat capacity rate ratio is $C_R = C_{min}/C_{max}$.

Effectiveness-NTU relations

In general, the effectiveness is a function of the HX configuration, its NTU and the C_R of the fluids.
(a) Counterflow

$$\epsilon = \frac{1 - \exp[-NTU(1 - C_R)]}{1 - C_R \exp[-NTU(1 - C_R)]} \tag{1.83}$$

so that $\epsilon \to 1$ as $NTU \to \infty$.
(b) Parallel flow

$$\epsilon = \frac{1 - \exp[-NTU(1 - C_R)]}{1 + C_R} \tag{1.84}$$

(c) Crossflow, both fluids unmixed
Series solution (Mason, 1954)
(d) Crossflow, one fluid mixed, the other unmixed
If the unmixed fluid has $C = C_{min}$, then

$$\epsilon = 1 - \exp[-C_R(1 - \exp\{-NTUC_r\})] \tag{1.85}$$

But if the mixed fluid has $C = C_{min}$

$$\epsilon = C_R(1 - \exp\{-C_R(1 - e^{-NTU})\}) \tag{1.86}$$

(e) Crossflow, both fluids mixed
(f) Tube with wall temperature constant

$$\epsilon = 1 - \exp(-NTU) \tag{1.87}$$

Pressure drop

It is important to determine the pressure drop through a heat exchanger. This is given by

$$\frac{\Delta p}{p_1} = \frac{G^2}{2\rho_1 p_1}\left[(K_c + 1 - \sigma^2) + 2(\frac{\rho_1}{\rho_2} - 1) + f\frac{A\rho_1}{A_c\rho_m} - (1 - \sigma^2 - K_e)\frac{\rho_1}{\rho_2}\right] \tag{1.88}$$

where K_c and K_e are the entrance and exit loss coefficients, and σ is the ratio of free-flow area to frontal area.

1.6.3 Design methodology

Mean temperature-difference method

Given the inlet temperatures and flow rates, this method enables one to find the outlet temperatures, the mean temperature difference, and then the heat rate.

Effectiveness-NTU method

The order of calculation is NTU, ϵ, q_{max} and q.

1.6.4 Correlations

1.6.5 Extended surfaces

$$\eta_0 = 1 - \frac{A_f}{A}(1 - \eta_f) \tag{1.89}$$

where η_0 is the total surface temperature effectiveness, η_f is the fin temperature effectiveness, A_f is the HX total fin area, and A is the HX total heat transfer area.

Problems

1. For a perimeter corresponding to a fin slope that is not small, derive Eq. 1.11.
2. The two sides of a plane wall are at temperatures T_1 and T_2. The thermal conductivity varies with temperature in the form $k(T) = k_0 + \alpha(T - T_1)$. Find the temperature distribution within the wall.
3. Consider a cylindrical pin fin of diameter D and length L. The base is at temperature T_b and the tip at T_∞; the ambient temperature is also T_∞. Find the steady-state temperature distribution in the fin, its effectiveness, and its efficiency. Assume that there is only convection but no radiation.
4. Show that the efficiency of the triangular fin shown in Fig. 1.7 is

   $$\eta_f = \frac{1}{mL}\frac{I_1(2mL)}{I_0(2mL)},$$

   where $m = (2h/kt)^{1/2}$, and I_0 and I_1 are the zeroth- and first-order Bessel functions of the first kind.
5. A constant-area fin between surfaces at temperatures T_1 and T_2 is shown in Fig. 1.8. If the external temperature, $T_\infty(x)$, is a function of the coordinate x, find the general steady-state solution of the fin temperature $T(x)$ in terms of a Green's function.

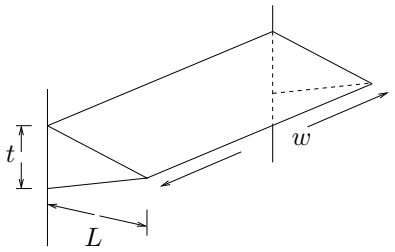

Figure 1.7: Triangular fin.

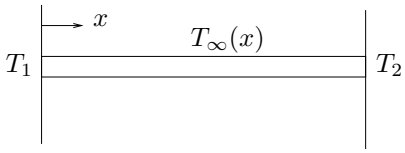

Figure 1.8: Constant-area fin.

6. Using a lumped parameter approximation for a vertical flat plate undergoing laminar, natural convection, show that the temperature of the plate, $T(t)$, is governed by

$$\frac{dT}{dt} + \alpha(T - T_\infty)^{5/4} = 0$$

Find $T(t)$ if $T(0) = T_0$.

7. Show that the governing equation in Problem 3 *with* radiation can be written as

$$\frac{d^2T}{dx^2} - m^2(T - T_\infty) - \epsilon(T^4 - T_\infty^4) = 0.$$

Find a two-term perturbation solution for $T(x)$ if $\epsilon \ll 1$ and $L \to \infty$.

8. The fin in Problem 3 has a *non-uniform* diameter of the form

$$D = D_0 + \epsilon x.$$

Determine the equations to be solved for a two-term perturbation solution for $T(x)$ if $\epsilon \ll 1$.

Part II

No spatial dimension

Chapter 2

Dynamics

2.1 Variable heat transfer coefficient

If, however, the h is slightly temperature-dependent, then we have

$$\frac{d\theta}{d\tau} + (1 + \epsilon\theta)\theta = 0 \tag{2.1}$$

which can be solved by the method of perturbations. We assume that

$$\theta(\tau) = \theta_0(\tau) + \epsilon\theta_1(\tau) + \epsilon^2\theta_2(\tau) + \dots \tag{2.2}$$

To order ϵ^0, we have

$$\begin{aligned} \frac{d\theta_0}{d\tau} + \theta_0 &= 0 && (2.3)\\ \theta_0(0) &= 1 && (2.4) \end{aligned}$$

which has the solution

$$\theta_0 = e^{-\tau} \tag{2.5}$$

To the next order ϵ^1, we get

$$\begin{aligned} \frac{d\theta_1}{d\tau} + \theta_1 &= -\theta_0^2 && (2.6)\\ &= -e^{-2\tau} && (2.7)\\ \theta_1(0) &= 0 && (2.8) \end{aligned}$$

the solution to which is

$$\theta_1 = -e^{-t} + e^{-2\tau} \tag{2.9}$$

Taking the expansion to order ϵ^2

$$\begin{aligned} \frac{d\theta_2}{d\tau} + \theta_2 &= -2\theta_0\theta_1 && (2.10)\\ &= -2e^{-2t} - 2e^{-3\tau} && (2.11)\\ \theta_2(0) &= 1 && (2.12) \end{aligned}$$

with the solution

$$\theta_2 = e^{-\tau} - 2e^{-2\tau} + e^{-3\tau} \tag{2.13}$$

And so on. Combining, we get

$$\theta = e^{-\tau} - \epsilon(e^{-\tau} - e^{-2\tau}) + \epsilon^2(e^{-\tau} - 2e^{-2\tau} + e^{-3\tau}) + \dots \tag{2.14}$$

Alternatively, we can find an exact solution to equation (2.1). Separating variables, we get

$$\frac{d\theta}{(1+\epsilon\theta)\theta} = d\tau \tag{2.15}$$

Integrating

$$\ln\frac{\theta}{\epsilon\theta+1} = -\tau + C \tag{2.16}$$

The condition $\theta(0) = 1$ gives $C = -\ln(1+\epsilon)$, so that

$$\ln\frac{\theta(1+\epsilon)}{1+\epsilon\theta} = -\tau \tag{2.17}$$

This can be rearranged to give

$$\theta = \frac{e^{-\tau}}{1+\epsilon(1-e^{-\tau})} \tag{2.18}$$

A Taylor-series expansion of the exact solution gives

$$\begin{aligned} \theta &= e^{-\tau}\left[1+\epsilon(1-e^{-\tau}\right]^{-1} && (2.19)\\ &= e^{-\tau}\left[1-\epsilon(1-e^{-\tau}) + \epsilon^2(1-e^{-\tau})^2 + \dots\right] && (2.20)\\ &= e^{-\tau} - \epsilon(e^{-\tau} - e^{-2\tau}) + \epsilon^2(e^{-\tau} - 2e^{-2\tau} + e^{-3\tau}) + \dots && (2.21) \end{aligned}$$

2.1.1 Radiative cooling

If the heat loss is due to radiation, we can write

$$Mc\frac{dT}{dt} + \sigma A(T^4 - T_\infty^4) = 0 \tag{2.22}$$

Taking the dimensionless temperature to be defined in equation (1.32), and time to be

$$\tau = \frac{\sigma A(T_i - T_\infty)^3 t}{Mc} \tag{2.23}$$

and introducing the parameter

$$\beta = \frac{T_\infty}{T_i - T_\infty} \tag{2.24}$$

we get

$$\frac{d\phi}{d\tau} + \phi^4 = \beta^4 \tag{2.25}$$

where

$$\phi = \theta + \beta \tag{2.26}$$

Writing the equation as

$$\frac{d\phi}{\phi^4 - \beta^4} = -d\tau \tag{2.27}$$

the integral is

$$\frac{1}{4\beta^3} \ln\left(\frac{\phi - \beta}{\phi + \beta}\right) - \frac{1}{2\beta^3} \tan^{-1}\left(\frac{\phi}{\beta}\right) = -\tau + C \tag{2.28}$$

Using the initial condition $\theta(0) = 1$, we get (?)

$$\tau = \frac{1}{2\beta^3}\left[\frac{1}{2} \ln \frac{(\beta + T)(\beta - 1)}{(\beta - T)(\beta + 1)} + \tan^{-1} \frac{T - 1}{\beta + (T/\beta)}\right] \tag{2.29}$$

2.1.2 Convective with weak radiation

The governing equationis

$$Mc\frac{dT}{dt} + hA(T - T_\infty) + \sigma A(T^4 - T_\infty^4) = 0 \tag{2.30}$$

with $T(0) = T_i$. Using the variables defined by equations (1.32) and (1.33), we get

$$\frac{d\theta}{d\tau} + \theta + \epsilon\left[(\theta + \beta^4)^4 - \beta^4\right] = 0 \tag{2.31}$$

where β is defined in equation (2.24), and

$$\epsilon = \frac{\sigma(T_i - T_\infty)^3}{h} \tag{2.32}$$

If radiative effects are small compared to the convective (for $T_i - T_\infty = 100$ K and $h = 10$ W/m^{2}K we get $\epsilon = 5.67 \times 10^{-3}$), we can take $\epsilon \ll 1$. Substituting the perturbation series, equation (2.2), in equation (2.31), we get

$$\begin{aligned} &\frac{d}{d\tau}\left(\theta_0 + \epsilon\theta_1 + \epsilon^2\theta_2 + \ldots\right) + \left(\theta_0 + \epsilon\theta_1 + \epsilon^2\theta_2 + \ldots\right) \\ &+\epsilon\big[\left(\theta_0 + \epsilon\theta_1 + \epsilon^2\theta_2 + \ldots\right)^4 + 4\beta\left(\theta_0 + \epsilon\theta_1 + \epsilon^2\theta_2 + \ldots\right)^3 \\ &+6\beta^2\left(\theta_0 + \epsilon\theta_1 + \epsilon^2\theta_2 + \ldots\right)^2 4\beta^3\left(\theta_0 + \epsilon\theta_1 + \epsilon^2\theta_2 + \ldots\right)\big] = 0 \end{aligned} \tag{2.33}$$

In this case

$$\frac{d\theta}{d\tau} + (\theta - \theta_0) + \epsilon(\theta^4 - \theta_s^4) = 0 \tag{2.34}$$

$$\theta(0) = 1 \tag{2.35}$$

As a special case, of we take $\beta = 0$, i.e. $T_\infty = 0$, we get

$$\frac{d\theta}{d\tau} + \theta + \epsilon\theta^4 = 0 \tag{2.36}$$

which has an exact solution

$$\tau = \frac{1}{3} \ln \frac{1 + \epsilon\theta^3}{(1 + \epsilon)\theta^3} \tag{2.37}$$

2.2 Radiation in an enclosure

Consider a closed enclosure with N walls radiating to each other and with a central heater H. The walls have no other heat loss and have different masses and specific heats. The governing equations are

$$M_i c_i \frac{dT_i}{dt} + \sigma \sum_{j=1}^{N} A_i F_{ij}(T_i^4 - T_j^4) + \sigma A_i F_{iH}(T_i^4 - T_H^4) = 0 \tag{2.38}$$

where the view factor F_{ij} is the fraction of radiation leaving surface i that falls on j. The steady state is

$$\overline{T}_i = T_H \quad (i = 1, \ldots, N) \tag{2.39}$$

Linear stability is determined by a small perturbation of the type

$$T_i = T_H + T_i' \tag{2.40}$$

from which

$$M_i c_i \frac{dT_i'}{dt} + 4\sigma T_H^3 \sum_{j=1}^{N} A_i F_{ij}(T_i' - T_j') + 4\sigma T_H^3 A_i F_{iH} T_i' = 0 \tag{2.41}$$

This can be written as

$$\mathbf{M}\frac{d\mathbf{T}'}{dt} = -4\sigma T_H^3 \mathbf{A}\mathbf{T}' \tag{2.42}$$

2.3 Long time behavior

The general form of the equation for heat loss from a body with internal heat generation is

$$\frac{d\theta}{d\tau} + f(\theta) = a \tag{2.43}$$

with $\theta(0) = 1$. Let

$$f(\overline{\theta}) = a \tag{2.44}$$

Then we would like to show that $\theta \to \overline{\theta}$ as $t \to \infty$. Writing

$$\theta = \overline{\theta} + \theta' \tag{2.45}$$

we have

$$\frac{d\theta'}{d\tau} + f(\overline{\theta} + \theta') = a \tag{2.46}$$

2.3.1 Linear analysis

If we assume that θ' is small, then a Taylor series gives

$$f(\overline{\theta} + \theta') = f(\overline{\theta}) + \theta' f'(\overline{\theta}) + \ldots \tag{2.47}$$

from which

$$\frac{d\theta'}{d\tau} + b\theta' = 0 \tag{2.48}$$

where $b = f'(\overline{\theta})$. The solution is

$$\theta' = Ce^{-b\tau} \tag{2.49}$$

so that $\theta' \to 0$ as $t \to \infty$ if $b > 0$.

2.3.2 Nonlinear analysis

Multiplying equation (2.46) by θ', we get

$$\frac{1}{2}\frac{d}{d\tau}(\theta')^2 = -\theta'\left[f(\bar{\theta}+\theta') - f(\bar{\theta})\right] \tag{2.50}$$

Thus

$$\frac{d}{d\tau}(\theta')^2 \leq 0 \tag{2.51}$$

if θ' and $[f(\bar{\theta}+\theta') - f(\bar{\theta})]$, as shown in Fig. 2.1, are both of the same sign or zero. Thus $\theta' \to 0$ as $\tau \to \infty$.

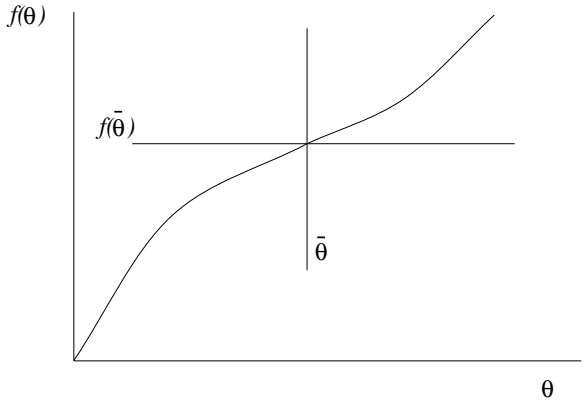

Figure 2.1: Convective cooling.

2.4 Time-dependent T_∞

Let

$$Mc\frac{dT}{dt} + hA(T - T_\infty(t)) = 0 \tag{2.52}$$

with

$$T(0) = T_i \tag{2.53}$$

2.4.1 Linear

Let

$$T_\infty = T_{\infty,0} + at \tag{2.54}$$

Defining the nondimensional temperature as

$$\theta = \frac{T - T_{\infty,0}}{T_i - T_{\infty,0}} \tag{2.55}$$

and time as in equation (1.33), we get

$$\frac{d\theta}{d\tau} + \theta = A\tau \tag{2.56}$$

where

$$A = \frac{aMc}{hA(T_i - T_{\infty,0})} \tag{2.57}$$

The nondimensional ambient temperature is

$$\theta_\infty = \frac{aMc}{hA(T_i - T_{\infty,0})}\tau \tag{2.58}$$

The solution to equation (2.56) is

$$\theta = Ce^{-\tau} + A\tau - A \tag{2.59}$$

The condition $\theta(0) = 1$ gives $C = 1 + A$, so that

$$\theta = (1 + A)e^{-\tau} + A(\tau - 1) \tag{2.60}$$

The time shown in Fig. 2.2 at crossover is

$$\tau_c = \ln \frac{1 + A}{A} \tag{2.61}$$

and the offset is

$$\delta\theta = A \tag{2.62}$$

as $\tau \to \infty$.

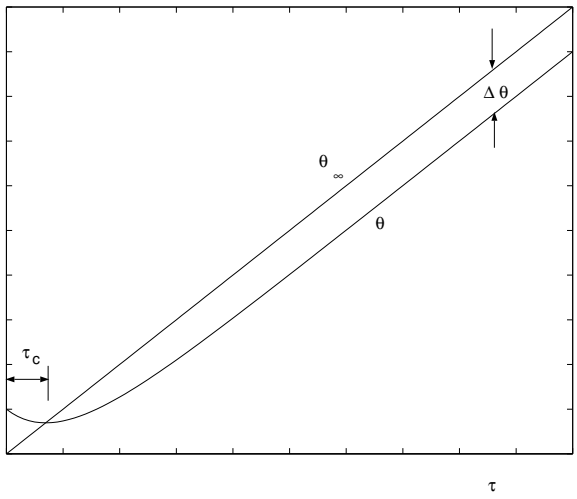

Figure 2.2: Response to linear ambient temperature.

2.4.2 Oscillatory

Let

$$T_\infty = \overline{T}_\infty + \delta T \sin \omega t \tag{2.63}$$

where $T(0) = T_i$. Defining

$$\theta = \frac{T - \overline{T}_\infty}{T_i - \overline{T}_\infty} \tag{2.64}$$

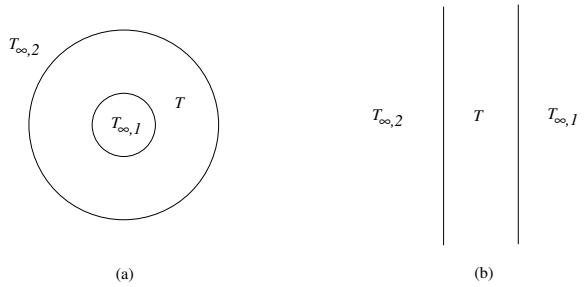

Figure 2.3: Two-fluid problems.

and using equation (1.33), the nondimensional equation is

$$\frac{d\theta}{d\tau} + \theta = \delta\theta \sin \Omega\tau \tag{2.65}$$

where

$$\delta\theta = \frac{\delta T}{T_i - \overline{T}_\infty} \tag{2.66}$$

$$\Omega = \frac{\omega Mc}{hA} \tag{2.67}$$

The solution is

$$\theta = Ce^{-\tau} + \frac{\delta\theta}{(1+\Omega^2)\cos\phi} \sin(\Omega\tau - \phi) \tag{2.68}$$

where

$$\phi = \tan^{-1} \Omega \tag{2.69}$$

From the condition $\theta(0) = 1$, we get $C = 1 + \delta\Omega/(1+\Omega^2)$, so that

$$\theta = \left(1 + \delta\theta \frac{\Omega}{1+\Omega^2}\right) e^{-\tau} + \frac{\delta\theta}{(1+\Omega^2)\cos\phi} \sin(\Omega\tau - \phi) \tag{2.70}$$

2.5 Two-fluid problem

Suppose there is a body in contact with two fluids at different temperatures $T_{\infty,1}$ and $T_{\infty,2}$, like in the two examples shown in Fig. 2.3. The governing equation is

$$Mc\frac{dT}{dt} + h_1A_1(T - T_{\infty,1}) + h_2A_2(T - T_{\infty,2}) = 0 \tag{2.71}$$

where $T(0) = T_i$. If $T_{\infty,1}$ and $T_{\infty,2}$ are constants, we can nondimensionalize the equation using the parameters for one of them, fluid 1 for instance. Thus we have

$$\theta = \frac{T - T_{\infty,1}}{T_i - T_{\infty,1}} \tag{2.72}$$

$$\tau = \frac{h_1A_1t}{Mc} \tag{2.73}$$

from which

$$\frac{d\theta}{d\tau} + \theta + \alpha(\theta + \beta) = 0 \tag{2.74}$$

with $\theta(0) = 1$, where

$$\alpha = \frac{h_2 A_2}{h_1 A_1} \tag{2.75}$$

$$\beta = \frac{T_{\infty,1} - T_{\infty,2}}{T_i - T_{\infty,1}} \tag{2.76}$$

The equation can be written as

$$\frac{d\theta}{d\tau} + (1 + \alpha)\theta = -\alpha\beta \tag{2.77}$$

with the solution

$$\theta = Ce^{-(1+\alpha)\tau} - \frac{\alpha\beta}{1 + \alpha} \tag{2.78}$$

The condition $\theta(0) = 1$ gives $C = 1 + \alpha\beta/(1 + \alpha)$, from which

$$\theta = \left(1 + \frac{\alpha\beta}{1 + \alpha}\right) e^{-(1+\alpha)\tau} - \frac{\alpha\beta}{1 + \alpha} \tag{2.79}$$

For $\alpha = 0$, the solution reduces to the single-fluid case, equation (1.35). Otherwise the time constant of the general system is

$$t_0 = \frac{Mc}{h_1 A_1 + h_2 A_2} \tag{2.80}$$

2.6 Two-body problem

2.6.1 Convective

Suppose now that there are two bodies at temperatures T_1 and T_2 in thermal contact with each other and exchanging heat with a single fluid at temperature T_∞ as shown in Fig. 2.4.

Figure 2.4: Two bodies in thermal contact.

The mathematical model of the thermal process is

$$M_1 c_1 \frac{dT_1}{dt} + \frac{k_s A_c}{L}(T_1 - T_2) + hA(T_1 - T_\infty) = Q_1 \tag{2.81}$$

$$M_2 c_2 \frac{dT_2}{dt} + \frac{k_s A_c}{L}(T_2 - T_1) + hA(T_2 - T_\infty) = Q_2 \tag{2.82}$$

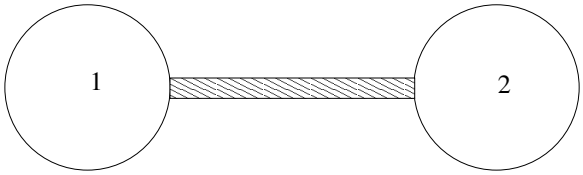

Figure 2.5: Bodies with radiation.

2.6.2 Radiative

$$M_1 c_1 \frac{dT_1}{dt} + \frac{k_s A_c}{L}(T_1 - T_2) + A_1 \sigma F_{1s}(T_1^4 - T_s^4) + A_1 \sigma F_{12}(T_1^4 - T_2^4) = Q_1 \quad (2.83)$$

$$M_2 c_2 \frac{dT_2}{dt} + \frac{k_s A_c}{L}(T_2 - T_1) + +A_1 F_{2s}(T_2^4 - T_s^4) + A_2 \sigma F_{21}(T_2^4 - T_1^4) = Q_2 \quad (2.84)$$

Without radiation

$$Q_1 = Q_2 = -\frac{2kA}{L}\left(\overline{T}_1 - \overline{T}_2\right) \quad (2.85)$$

Problems

1. Show that the temperature distribution in a sphere subject to convective cooling tends to become uniform as $Bi \to 0$.
2. Check one of the perturbation solutions against a numerical solution.
3. Plot all real $\overline{\theta}(\beta, \epsilon)$ surfaces for the convection with radiation problem, and comment on the existence of solutions.
4. Complete the problem of radiation in an enclosure (linear stability, numerical solutions).
5. Lumped system with convective-radiative cooling with nonzero θ_0 and θ_s.
6. Find the steady-state temperatures for the two-body problem and explore the stability of the system for constant ambient temperature.
7. Consider the change in temperature of a lumped system with convective heat transfer where the ambient temperature, $T_\infty(t)$, varies with time in the form shown. Find (a) the long-time solution of the system temperature, $T(t)$, and (b) the amplitude of oscillation of the system temperature, $T(t)$, for a small period δt.

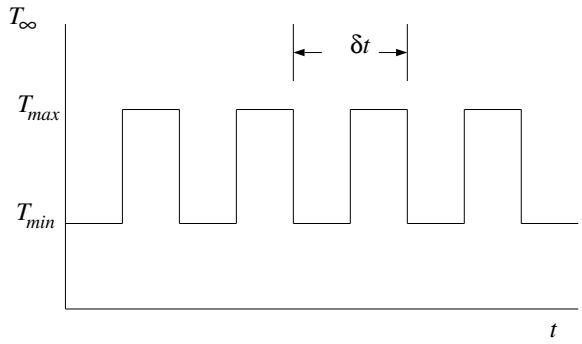

Figure 2.6: Ambient temperature variation.

Chapter 3

Control

3.1 Introduction

There are many kinds of thermal systems in common industrial, transportation and domestic use that need to be controlled in some manner, and there are many ways in which that can be done. One can give the example of heat exchangers [85, 114], environmental control in buildings [70, 72, 82, 115, 152, 218], satellites [101, 172, 184, 221], thermal packaging of electronic components [150, 185], manufacturing [54], rapid thermal processing of computer chips [84, 158, 200], and many others. If precise control is not required, or if the process is very slow, control may simply be *manual*; otherwise some sort of mechanical or electrical feedback system has to be put in place for it to be *automatic*.

Most thermal systems are generally *complex* involving diverse physical processes. These include natural and forced convection, radiation, complex geometries, property variation with temperature, nonlinearities and bifurcations, hydrodynamic instability, turbulence, multi-phase flows, or chemical reaction. It is common to have large uncertainties in the values of heat transfer coefficients, approximations due to using lumped parameters instead of distributed temperature fields, or material properties that may not be accurately known. In this context, a complex system can be defined as one that is made up of sub-systems, each one of which can be analyzed and computed, but when put together presents such a massive computational problem so as to be practically intractable. For this reason large, commonly used engineering systems are hard to model exactly from first principles, and even when this is possible the dynamic responses of the models are impossible to determine computationally in real time. Most often some degree of approximation has to be made to the mathematical model. Approximate correlations from empirical data are also heavily used in practice. The two major reasons for which control systems are needed to enable a thermal system to function as desired are the approximations used during design and the existence of unpredictable external and internal disturbances which were not taken into account.

There are many aspects of thermal control that will not be treated in this brief review. The most important of these are hardware considerations; all kinds of sensors and actuators [59, 187] developed for measurement and actuation are used in the control of thermal systems. Many controllers are also computer based, and the use of microprocessors [87, 180] and PCs in machines, devices and plants is commonplace. Flow control, which is closely related to and is often an integral part of thermal control, has its own extensive literature [64]. Discrete-time (as opposed to continuous-time) systems will not be described. The present paper will, however, concentrate only on the basic principles relating to the theory of control as applied to thermal problems, but even then it will be impossible to go into any depth within the space available. This is only an introduction,

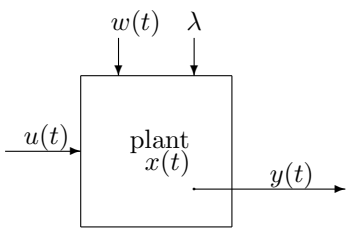

Figure 3.1: Schematic of a system without controller.

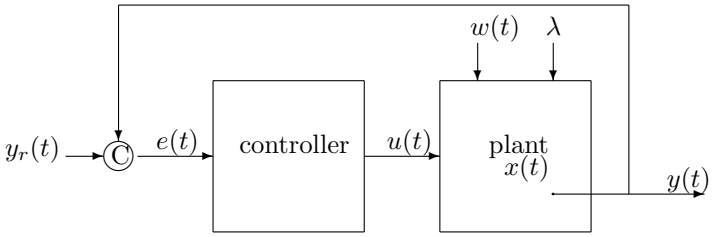

Figure 3.2: Schematic of a system with comparator C and controller.

and the interested reader should look at the literature that is cited for further details. There are good texts and monographs available on the basics of control theory [116, 132, 144, 157], process control [28,75,93,151], nonlinear control [91], infinite-dimensional systems [39,89], and mathematics of control [9, 179] that can be consulted. These are all topics that include and are included within thermal control.

3.2 Systems

Some basic ideas of systems will be defined here even though, because of the generality involved, it is hard to be specific at this stage.

3.2.1 Systems without control

The dynamic behavior of any thermal system (often called the open-loop system or *plant* to distinguish it from the system with controller described below), schematically shown in Fig. 3.1, may be mathematically represented as

$$\mathcal{L}_s(x, u, w, \lambda) = 0, \tag{3.1}$$

where $\mathcal{L}_s$ is a system operator, t is time, $x(t)$ is the state of the system, $u(t)$ is its input, $w(t)$ is some external or internal disturbance, and λ is a parameter that defines the system. Each one of these quantities belongs to a suitable set or vector space and there are a large number of possibilities. For example $\mathcal{L}_s$ may be an algebraic, integral, ordinary or partial differential operator, while x may be a finite-dimensional vector or a function. $u(t)$ is usually a low-dimensional vector.

In general, the output of the system $y(t)$ is different from its state $x(t)$. For example, x may be a spatial temperature distribution, while y are the readings of one or more temperature measurement devices at a finite number of locations. The relation between the two may be written as

$$\mathcal{L}_o(y, x, u, w, \lambda) = 0, \tag{3.2}$$

where $\mathcal{L}_o$ is the output operator.

The system is *single-input single-output* (SISO) if both u and y are scalars. A system is said to be *controllable* if it can be taken from one specific state to another within a prescribed time with the help of a suitable input. It is *output* controllable if the same can be done to the output. It is important to point out that output controllability does not imply system controllability. In fact, in practice for many thermal systems the former is all that is required; it has been reported that most industrial plants are controlled quite satisfactorily though they are not system controllable [156]. All possible values of the output constitute the *reachable* set. A system is said to be *observable* if its state x can be uniquely determined from the input u and output y alone. The *stability* of a system is a property that leads to a bounded output if the input is also bounded.

3.2.2 Systems with control

The objective of control is to have a given output $y = y_r(t)$, where the *reference* or *set* value y_r is prescribed. The problem is called *regulation* if y_r is a constant, and *tracking* if it is function of time.

In *open-loop* control the input is selected to give the desired output without using any information from the output side; that is one would have to determine $u(t)$ such that $y = y_r(t)$ using the mathematical model of the system alone. This is a *passive* method of control that is used in many thermal systems. It will work if the behavior of the system is exactly predictable, if precise output control is not required, or if the output of the system is not very sensitive to the input. If the changes desired in the output are very slow then manual control can be carried out, and that is also frequently done. A self-controlling approach that is sometimes useful is to design the system in such a way that any disturbance will bring the output back to the desired value; the output in effect is then insensitive to changes in input or disturbances.

Open-loop control is not usually effective for many systems. For thermal systems contributing factors are the uncertainties in the mathematical model of the plant and the presence of unpredictable disturbances. Internal disturbances may be noise in the measuring or actuating devices or a change in surface heat transfer characteristics due to fouling, while external ones may be a change in the environmental temperature. For these cases *closed-loop* control is an appropriate alternative. This is done using *feedback* from the output, as measured by a *sensor*, to the input side of the system, as shown in Fig. 3.2; the figure actually shows unit feedback. There is a comparator which determines the error signal $e(t) = e(y_r, y)$, which is usually taken to be

$$e = y_r - y. \tag{3.3}$$

The key role is played by the *controller* which puts out a signal that is used to move an *actuator* in the plant.

Sensors that are commonly used are temperature-measuring devices such as thermocouples, resistance thermometers or thermistors. The actuator can be a fan or a pump if the flow rate is to be changed, or a heater if the heating rate is the appropriate variable. The controller itself is either entirely mechanical if the system is not very complex, or is a digital processor with appropriate software. In any case, it receives the error in the output $e(t)$ and puts out an appropriate control input $u(t)$ that leads to the desired operation of the plant.

The control process can be written as

$$\mathcal{L}_c(u, e, \lambda) = 0, \tag{3.4}$$

where $\mathcal{L}_c$ is a control operator. The controller designer has to propose a suitable $\mathcal{L}_c$, and then Eqs. (C.9)–(3.4) form a set of equations in the unknowns $x(t)$, $y(t)$ and $u(t)$. Choice of a control strategy defines $\mathcal{L}_o$ and many different methodologies are used in thermal systems. It is common to use *on-off* (or bang-bang, relay, etc.) control. This is usually used in heating or cooling systems in which the heat coming in or going out is reduced to zero when a predetermined temperature is reached and set at a constant value at another temperature. Another method is Proportional-Integral-Derivative (PID) control [214] in which

$$u = K_p e(t) + K_i \int_0^t e(s)\, ds + K_d \frac{de}{dt}. \tag{3.5}$$

3.3 Linear systems theory

The term *classical* control is often used to refer to theory derived on the basis of Laplace transforms. Since this is exclusively for linear systems, we will be using the so-called *modern* control or *state-*

space analysis which is based on dynamical systems, mainly because it can be extended to nonlinear systems. Where they overlap, the issue is only one of preference since the results are identical. Control theory can be developed for different linear operators, and some of these are outlined below.

3.3.1 Ordinary differential equations

Much is known about a linear differential system in which Eqs. (C.9) and (3.2) take the form

$$\frac{dx}{dt} = Ax + Bu, \tag{3.6}$$

$$y = Cx + Du, \tag{3.7}$$

where $x \in \mathbb{R}^n$, $u \in \mathbb{R}^m$, $y \in \mathbb{R}^p$, $A \in \mathbb{R}^{n\times n}$, $B \in \mathbb{R}^{n\times m}$, $C \in \mathbb{R}^{p\times n}$, $D \in \mathbb{R}^{p\times m}$. x, u and y are vectors of different lengths and A, B, C, and D are matrices of suitable sizes. Though A, B, C, and D can be functions of time in general, here they will be treated as constants.

The solution of Eq. (3.6) is

$$x(t) = e^{A(t-t_0)}x(t_0) + \int_{t_0}^{t} e^{A(t-s)}Bu(s)\ ds. \tag{3.8}$$

where the exponential matrix is defined as

$$e^{At} = I + At + \frac{1}{2!}A^2t^2 + \frac{1}{3!}A^3t^3 + \ldots,$$

with I being the identity matrix. From Eq. (3.7), we get

$$y(t) = C\left[e^{At}x(t_0) + \int_{t_0}^{t} e^{A(t-s)}\ Bu(s)\ ds\right] + Du. \tag{3.9}$$

Eqs. (3.8) and (3.9) define the state $x(t)$ and output $y(t)$ if the input $u(t)$ is given.

It can be shown that for the system governed by Eq. (3.6), a $u(t)$ can be found to take $x(t)$ from $x(t_0)$ at $t = t_0$ to $x(t_f) = 0$ at $t = t_f$ if and only if the matrix

$$M = \left[B \vdots AB \vdots A^2B \vdots \ \ldots \ \vdots A^{n-1}B\right] \in \mathbb{R}^{n\times nm} \tag{3.10}$$

is of rank n. The system is then controllable. For a linear system, controllability from one state to another implies that the system can be taken from *any* state to any other. It must be emphasized that the $u(t)$ that does this is not unique.

Similarly, it can be shown that the output $y(t)$ is controllable if and only if

$$N = \left[D \vdots CB \vdots CAB \vdots CA^2B \vdots \ \ldots \ \vdots CA^{n-1}B\right] \in \mathbb{R}^{p\times(n+1)m} \tag{3.11}$$

is of rank p. Also, the state $x(t)$ is observable if and only if the matrix

$$P = \left[C \vdots CA \vdots CA^2 \ \ldots \ \vdots CA^{n-1}\right]^T \in \mathbb{R}^{pn\times n} \tag{3.12}$$

is of rank n.

3.3.2 Algebraic-differential equations

This is a system of equations of the form

$$E\frac{dx}{dt} = A\ x + B\ u, \tag{3.13}$$

where the matrix $E \in \mathbb{R}^{n\times n}$ is singular [113]. This is equivalent to a set of equations, some of which are ordinary differential and the rest are algebraic. As a result of this, Eq. (3.13) cannot be converted into (3.6) by substitution. The index of the system is the least number of differentiations of the algebraic equations that is needed to get the form of Eq. (3.6). The system may not be completely controllable since some of the components of x are algebraically related, but it may have restricted or R-controllability [45].

3.4 Nonlinear aspects

The following are a few of the issues that arise in the treatment of nonlinear thermal control problems.

3.4.1 Models

There are no general mathematical models for thermal systems, but one that can be used is a generalization of Eq. (3.6) such as

$$\frac{dx}{dt} = f(x,u). \tag{3.14}$$

where $f : \mathbb{R}^n \times \mathbb{R}^m \mapsto \mathbb{R}^n$. If one is interested in local behavior about an equilibrium state $x = x_0$, $u = 0$, this can be linearized in that neighborhood to give

$$\begin{aligned}\frac{dx}{dt} &= \left.\frac{\partial f}{\partial x}\right|_0 x' + \left.\frac{\partial f}{\partial u}\right|_0 u' \\ &= Ax' + Bu',\end{aligned} \tag{3.15}$$

where $x = x_0 + x'$ and $u = u'$. The Jacobian matrices $(\partial f/\partial x)_0$ and $(\partial f/\partial u)_0$, are evaluated at the equilibrium point. Eq. (3.15) has the same form as Eq. (3.6).

3.4.2 Controllability and reachability

General theorems for the controllability of nonlinear systems are not available at this point in time. Results obtained from the linearized equations generally do not hold for the nonlinear equations. The reason is that in the nonlinear case one can take a path in state space that travels far from the equilibrium point and then returns close to it. Thus regions of state space that are unreachable with the linearized equations may actually be reachable. In a thermal convection loop it is possible to go from one branch of a bifurcation solution to another in this fashion [1].

3.4.3 Bounded variables

In practice, due to hardware constraints it is common to have the physical variables confined to certain ranges, so that variables such as x and u in Eqs. (C.9) and (3.2), being temperatures, heat rates, flow rates and the like, are bounded. If this happens, even systems locally governed by Eqs. (3.6) and (3.7) are now nonlinear since the sum of solutions may fall outside the range in which x

exists and thus may not be a valid solution. On the other hand, for a controllable system in which only u is bounded in a neighborhood of zero, x can reach any point in $\mathbb{R}^n$ if the eigenvalues of A have zero or positive real parts, and the origin is reachable if the eigenvalues of A have zero or negative real parts [179].

3.4.4 Relay and hysteresis

A relay is an element of a system that has an input-output relationship that is not smooth; it may be discontinuous or not possess first or higher-order derivatives. This may be accompanied by hysteresis where the relationship also depends on whether the input is increasing or decreasing. Valves are typical elements in flow systems that have this kind of behavior.

3.5 System identification

To be able to design appropriate control systems, one needs to have some idea of the dynamic behavior of the thermal system that is being controlled. Mathematical models of these systems can be obtained in two entirely different ways: from first principles using known physical laws, and empirically from the analysis of experimental information (though combinations of the two paths are not only possible but common). The latter is the process of *system identification*, by which a complex system is reduced to mathematical form using experimental data [75, 121, 129]. There are many different ways in which this can be done, the most common being the fitting of parameters to proposed models [141]. In this method, a form of $\mathcal{L}_s$ is assumed with unknown parameter values. Through optimization routines the values of the unknowns are chosen to obtain the best fit of the results of the model with experimental information. Apart from the linear Eq. (3.6), other models that are used include the following.

- There are many forms based on Eq. (3.14), one of which is the closed-affine model

$$\frac{dx}{dt} = F_1(x) + F_2(x)u \tag{3.16}$$

  The bilinear equation for which $F_1(x) = Ax$ and $F_2(x) = Nx + b$ is a special case of this.

- Volterra models, like

$$y(t) = y_0(t) + \sum_{i=1}^{\infty} \int_{-\infty}^{\infty} \dots \int_{-\infty}^{\infty} k_i(t; t_1, t_2, t_3, \dots, t_i) u(t_1) \dots u(t_i)\ dt_1 \dots dt_i \tag{3.17}$$

  for a SISO system, are also used.

- Functional [71], difference [23] or delay [57] equations such as

$$\frac{dx}{dt} = A\ x(t-s) + B\ u \tag{3.18}$$

  also appear in the modeling of thermal systems.

- Fractional-order derivatives, of which there are several different possible definitions [10, 17, 134, 135, 148] can be used in differential models. As an example, the Riemann-Liouville definition of the nth derivative of $f(t)$ is

$${}_a\mathcal{D}_t^n f(t) = \frac{1}{\Gamma(m-n+1)}\ \frac{d^{m+1}}{dt^{m+1}}\ \int_a^t (t-s)^{m-n} f(s)\ ds, \tag{3.19}$$

  where a and n are real numbers and m is the largest integer smaller than n.

3.6 Control strategies

3.6.1 Mathematical model

Consider a body that is cooled from its surface by convection to the environment with a constant ambient temperature T_∞. It also has an internal heat source $Q(t)$ to compensate for this heat loss, and the control objective is to maintain the temperature of the body at a given level by manipulating the heat source. The Biot number for the body is $Bi = hL/k$, where h is the convective heat transfer coefficient, L is a characteristics length dimension of the body, and k is its thermal conductivity. If $Bi < 0.1$, the body can be considered to have a uniform temperature $T(t)$. Under this lumped approximation the energy balance is given by

$$Mc\frac{dT}{dt} + hA_s(T - T_\infty) = Q(t), \tag{3.20}$$

where M is the mass of the body, c is its specific heat, and A_s is the surface area for convection.

Using Mc/hA_s and $hA_s(T_i - T_\infty)$ as the characteristic time and heat rate, this equation becomes

$$\frac{d\theta}{dt} + \theta = Q(t) \tag{3.21}$$

Here $\theta = (T - T_\infty)/(T_i - T_\infty)$ where $T(0) = T_i$ so that $\theta(0) = 1$. The other variables are now non-dimensional. With $x = \theta$, $u = Q$, $n = m = 1$ in Eq. (3.6), we find from Eq. (3.10) that rank(M)=1, so the system is controllable.

Open-loop operation to maintain a given non-dimensional temperature θ_r is easily calculated. Choosing $Q = \theta_r$, it can be shown from the solution of Eq. (3.21), that is

$$\theta(t) = (1 - \theta_r)e^{-t} + \theta_r, \tag{3.22}$$

that $\theta \to \theta_r$ as $t \to \infty$. In practice, to do this the dimensional parameters hA_s and T_∞ must be exactly known. Since this is usually not the case some form of feedback control is required.

3.6.2 On-off control

In this simple form of control the heat rate in Eq. (3.20) has only two values; it is is either $Q = Q_0$ or $Q = 0$, depending on whether the heater is on or off, respectively. With the system in its *on* mode, $T \to T_{max} = T_\infty + Q_0/hA_s$ as $t \to \infty$, and in its *off* mode, $T \to T_{min} = T_\infty$. Taking the non-dimensional temperature to be

$$\theta = \frac{T - T_{min}}{T_{max} - T_{min}} \tag{3.23}$$

the governing equation is

$$\frac{d\theta}{dt} + \theta = \begin{cases} 1 & \text{on} \\ 0 & \text{off} \end{cases}, \tag{3.24}$$

the solution for which is

$$\theta = \begin{cases} 1 + C_1 e^{-t} & \text{on} \\ C_2 e^{-t} & \text{off} \end{cases}. \tag{3.25}$$

We will assume that the heat source comes on when temperature falls below a value T_L, and goes off when it is rises above T_U. These lower and upper bounds are non-dimensionally

$$\theta_L = \frac{T_L - T_{min}}{T_{max} - T_{min}}, \tag{3.26}$$

$$\theta_U = \frac{T_U - T_{min}}{T_{max} - T_{min}}. \tag{3.27}$$

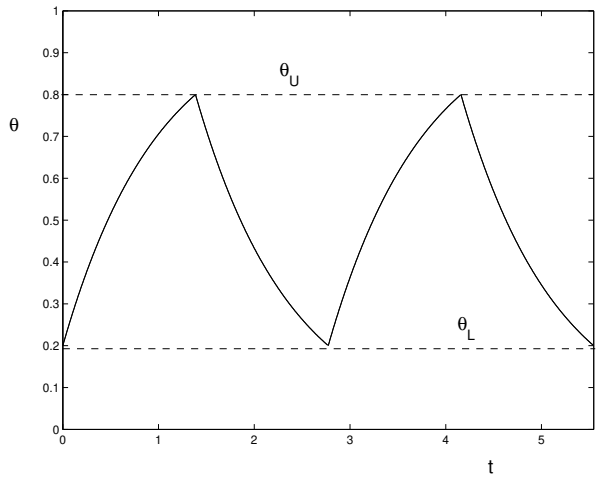

Figure 3.3: Lumped approximation with on-off control.

The result of applying this form of control is an oscillatory temperature that looks like that in Fig. 3.3, the period and amplitude of which can be chosen using suitable parameters. It can be shown that the on and off time periods are

$$t_{on} = \ln \frac{1-\theta_L}{1-\theta_U}, \tag{3.28}$$

$$t_{off} = \ln \frac{\theta_U}{\theta_L}, \tag{3.29}$$

respectively. The total period of the oscillation is then

$$t_p = \ln \frac{\theta_U(1-\theta_L)}{\theta_L(1-\theta_U)}. \tag{3.30}$$

If we make a small dead-band assumption, we can write

$$\theta_L = \theta_r - \delta, \tag{3.31}$$

$$\theta_U = \theta_r + \delta, \tag{3.32}$$

where $\delta \ll 1$. A Taylor-series expansion gives

$$t_p = 2\ \delta \left(\frac{1}{\theta_r} + \frac{1}{1-\theta_r} \right) + \ldots \tag{3.33}$$

The period is thus proportional to the width of the dead band. The frequency of the oscillation increases as its amplitude decreases.

3.6.3 PID control

The error $e = \theta_r - \theta$ and control input $u = Q$ can be used in Eq. (3.5), so that the derivative of Eq. (3.21) gives

$$(K_d + 1)\frac{d^2\theta}{dt^2} + (K_p + 1)\frac{d\theta}{dt} + K_i\theta = K_i\theta_r, \tag{3.34}$$

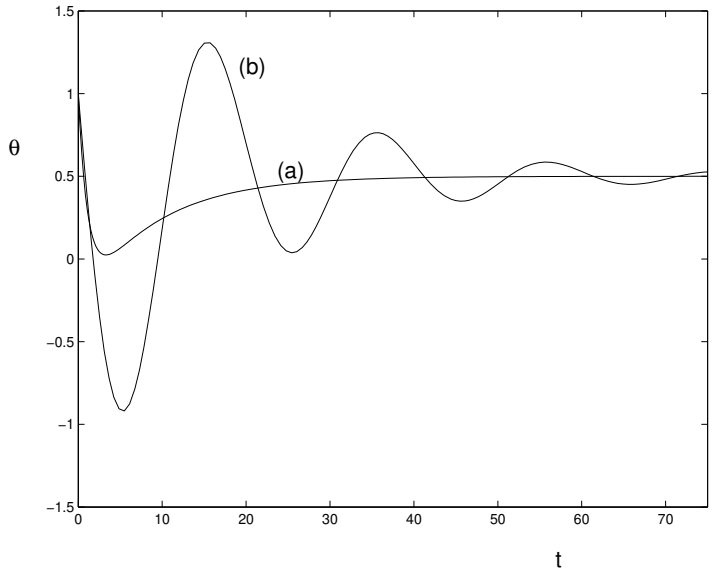

Figure 3.4: Lumped approximation with PID control; $K_i = K_d = -0.1$, $\theta_r = 0.5$, (a) $K_p = -0.1$, (b) $K_p = -0.9$.

with the initial conditions

$$\theta = \theta_0 \quad \text{at} \quad t = 0, \tag{3.35}$$

$$\frac{d\theta}{dt} = -\frac{K_p + 1}{K_d + 1}\theta_0 + \frac{K_p \theta_r}{K_d + 1} \quad \text{at} \quad t = 0. \tag{3.36}$$

The response of the closed-loop system can be obtained as a solution. The steady-state for $K_i \neq 0$ is given by $\theta = \theta_r$. It can be appreciated that different choices of the controller constants K_p, K_i and K_d will give overdamped or underdamped oscillatory or unstable behavior of the system. Fig. 3.4 shows two examples of closed-loop behavior with different parameter values.

Problems

1. Two lumped bodies A and B in thermal contact (contact thermal resistance R_c) exchange heat between themselves by conduction and with the surroundings by convection. It is desired to control their temperatures at T_A and T_B using separate internal heat inputs Q_A and Q_B.

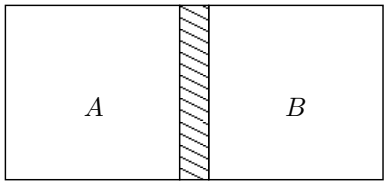

   (a) Check that the system is controllable.

(b) Set up a PID controller where its constants are matrices. Determine the condition for linear stability of the control system. Show that the case of two independent bodies is recovered as $R_c \to \infty$.

(c) Calculate and plot $T_A(t)$ and $T_B(t)$ for chosen values of the controller constants.

2. Apply an on-off controller to the previous problem. Plot $T_A(t)$ and $T_B(t)$ for selected values of the parameters. Check for phase synchronization.

3. A number of identical rooms are arranged in a circle as shown, with each at a uniform temperature $T_i(t)$. Each room exchanges heat by convection with the outside which is at T_∞, and with its neighbors with a conductive thermal resistance R. To maintain temperatures, each room has a heater that is controlled by independent but identical proportional controllers. (a) Derive the governing equations for the system, and nondimensionalize. (b) Find the steady state temperatures. (c) Write the dynamical system in the form $\dot{\mathbf{x}} = \mathbf{A}\mathbf{x}$ and determine the condition for stability[1].

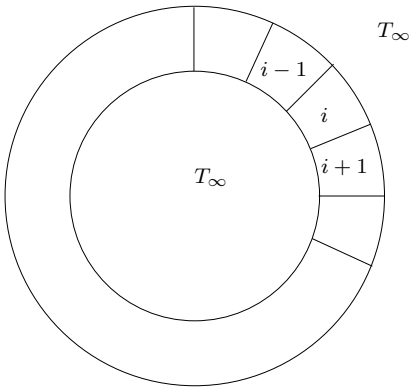

[1] Eigenvalues of an $N \times N$, circulant, banded matrix of the form

$$\begin{bmatrix} b & c & 0 & \dots & 0 & a \\ a & b & c & \dots & 0 & 0 \\ 0 & a & b & \dots & 0 & 0 \\ \vdots & \vdots & \vdots & \vdots & \vdots & \\ 0 & \dots & 0 & a & b & c \\ c & 0 & \dots & 0 & a & b \end{bmatrix}$$

are $\lambda_j = b + (a+c)\cos\{2\pi(j-1)/N\} - i(a-c)\sin\{2\pi(j-1)/N\}$, where $j = 1, 2, \dots, N$.

Part III

One spatial dimension

Chapter 4

Conduction

4.1 Structures

Fig. 4.1 shows a complex shape consisting of conductive bars. At each node

$$\sum_i q_i = 0 \tag{4.1}$$

For each branch

$$\sum_i \frac{k_i A_i}{L_i} (T_i - T_0) = 0 \tag{4.2}$$

from which

$$T_0 = \frac{\sum_i \frac{k_i A_i}{L_i} T_i}{\sum_i \frac{k_i A_i}{L_i}} \tag{4.3}$$

4.2 Fin theory

4.2.1 Long time solution

The general fin equation is

$$a\frac{\partial \theta}{\partial \tau} - \frac{\partial}{\partial \xi}\left(a\frac{\partial \theta}{\partial \xi}\right) + f(\theta) = 0 \tag{4.4}$$

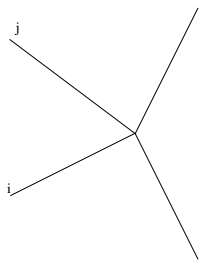

Figure 4.1: Complex conductive structures.

where $f(\theta)$ includes heat transfer from the sides due to convection and radiation. The boundary conditions are either Dirichlet or Neumannn type at $\xi = 0$ and $\xi = 1$. The steady state is determined from

$$-\frac{d}{d\xi}\left(a\frac{d\theta}{d\xi}\right) + f(\overline{\theta}) = 0 \tag{4.5}$$

with the same boundary conditions. Substituting $\theta = \overline{\theta} + \theta'$ in equation (4.4) and subtracting (4.5), we have

$$a\frac{\partial\theta'}{\partial\tau} - \frac{\partial}{\partial\xi}\left(a\frac{\partial\theta'}{\partial\xi}\right) + \left[f(\overline{\theta}+\theta') - f(\overline{\theta})\right] = 0 \tag{4.6}$$

where θ' is the perturbation from the steady state. The boundary conditions for θ' are homogeneous. Multiplying by θ' and integrating from $\xi = 0$ to $\xi = 1$, we have

$$\frac{dE}{d\tau} = I_1 + I_2 \tag{4.7}$$

where

$$E = \frac{1}{2}\int_0^1 a(\theta')^2 \, d\xi \tag{4.8}$$

$$I_1 = \int_0^1 \theta' \frac{\partial}{\partial\xi}\left(a\frac{\partial\theta'}{\partial\xi}\right) \, d\xi \tag{4.9}$$

$$I_2 = -\int_0^1 \theta' \left[f(\overline{\theta}+\theta') - f(\overline{\theta})\right] \, d\xi \tag{4.10}$$

Integrating by parts we can show that

$$I_1 = \theta' a\frac{\partial\theta'}{\partial\xi}\bigg|_0^1 - \int_0^1 a\left(\frac{d\theta'}{d\xi}\right)^2 \, d\xi \tag{4.11}$$

$$= -\int_0^1 a\left(\frac{d\theta'}{d\xi}\right)^2 \, d\xi \tag{4.12}$$

since the first term on the right side of equation (4.11) is zero due to boundary conditions. Thus we know from the above that I_1 is nonpositive and from equation (4.8) that E is nonnegative. If we also assume that

$$I_2 \leq 0 \tag{4.13}$$

then equation (4.7) tells us that E must decrease with time until reaching zero. Thus the steady state is globally stable. Condition (4.13) holds if [θ' and $f(\overline{\theta}+\theta') - f(\overline{\theta})$] are of the same sign or both zero; this is a consequence of the Second Law of Thermodynamics.

4.2.2 Shape optimization of convective fin

Consider a rectangular fin of length L and thickness δ as shown in Fig. 4.2. The dimensional equation is

$$\frac{d^2T}{dx^2} - m^2(T - T_\infty) = 0 \tag{4.14}$$

where

$$m = \left(\frac{2h}{k_s\delta}\right)^{1/2} \tag{4.15}$$

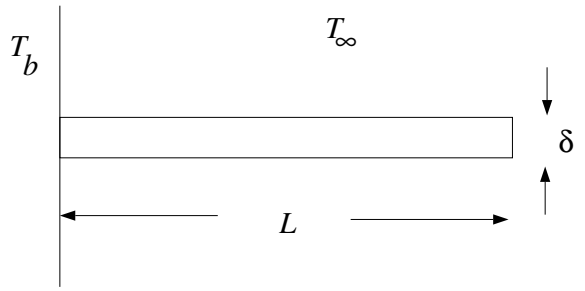

Figure 4.2: Rectangular fin.

We will take the boundary conditions

$$T(0) = T_b \tag{4.16}$$

$$\frac{dT}{dx}(L) = 0 \tag{4.17}$$

The solution is

$$T = T_\infty - (T - T_\infty)\left[\tanh mL \sinh mx - \cosh mx\right] \tag{4.18}$$

The heat rate through the base per unit width is

$$q = -k_s \delta \left.\frac{dT}{dx}\right|_{x=0} \tag{4.19}$$

$$= k_s \delta (T_b - T_\infty) m \tanh mL \tag{4.20}$$

Writing $L = A_p/\delta$, we get

$$q = k_s \delta \left(\frac{2h}{k_s \delta}\right)^{1/2} (T_b - T_\infty) \tanh \left[\frac{A_p}{\delta}\left(\frac{2h}{k_s \delta}\right)^{1/2}\right] \tag{4.21}$$

Keeping A_p constant, i.e. constant fin volume, the heat rate can be maximized if

$$\delta_{opt}^{1/2} \mathrm{sech}^2 \left[\frac{A_p}{\delta}\left(\frac{2h}{k_s \delta_{opt}}\right)\right] A_p \frac{2h}{k_s}^{1/2} (-\frac{3}{2}) \delta_{opt}^{-5/2} + \frac{1}{2}\delta_{opt}^{-1/2} \tanh \left[\frac{A_p}{\delta}\left(\frac{2h}{k_s \delta_{opt}}\right)^{1/2}\right] = 0 \tag{4.22}$$

This is equivalent to

$$3\beta_{opt} \mathrm{sech}^2 \beta_{opt} = \tanh \beta_{opt} \tag{4.23}$$

where

$$\beta_{opt} = \frac{A_p}{\delta_{opt}}\left(\frac{2h}{k_s \delta_{opt}}\right) \tag{4.24}$$

Numerically, we find that $\beta_{opt} = 1.4192$. Thus

$$\delta_{opt} = \left[\frac{A_p}{\beta_{opt}}\left(\frac{k_s A_p}{2h}\right)^{1/2}\right]^{2/3} \tag{4.25}$$

$$L_{opt} = \left[\beta_{opt}\left(\frac{k_s A_p}{2h}\right)^{1/2}\right]^{2/3} \tag{4.26}$$

4.3 Fin structure

Consider now Fig. 4.1 with convection.

4.4 Fin with convection and radiation

Steady state solutions

Equation (4.4) reduces to

$$-\frac{d}{d\xi}\left(a\frac{d\theta}{d\xi}\right)+m^2p\theta+\epsilon p\left[(\theta+\beta)^4-\beta^4\right]=0 \tag{4.27}$$

Uniform cross section

For this case $a=p=1$, so that

$$-\frac{d^2\theta}{d\xi^2}+m^2\theta+\epsilon\left[(\theta+\beta)^4-\beta^4\right]=0 \tag{4.28}$$

Convective

With only convective heat transfer, we have

$$-\frac{d^2\theta}{d\xi^2}+m^2\theta=0 \tag{4.29}$$

the solution to whiich is

$$\theta=C_1\sinh m\xi+C_2\cosh m\xi \tag{4.30}$$

the constants are determined from the boundary conditions. For example, if

$$\theta(0) = 1 \tag{4.31}$$

$$\frac{d\theta}{d\xi}(1) = 0 \tag{4.32}$$

we get

$$\theta=-\tanh m\sinh m\xi+\cosh m\xi \tag{4.33}$$

Example 4.1

If

$$T(0) = T_0 \tag{4.34}$$

$$T(L) = T_1 \tag{4.35}$$

then show that

$$T(x)=\left[T_1-T_0\cosh\left(L\sqrt{\frac{hP}{kA}}\right)\right]\frac{\sinh\left(x\sqrt{\frac{hP}{kA}}\right)}{\sinh\left(L\sqrt{\frac{hP}{kA}}\right)}+T_0\cosh\left(x\sqrt{\frac{hP}{kA}}\right) \tag{4.36}$$

Radiative

The fin equation is

$$-\frac{d^2\theta}{d\xi^2} + \epsilon\left[(\theta+\beta)^4 - \beta^4\right] = 0 \tag{4.37}$$

Let

$$\phi = \theta + \beta \tag{4.38}$$

so that

$$-\frac{d^2\phi}{d\xi^2} + \epsilon\phi^4 = -\epsilon\beta^4 \tag{4.39}$$

As an example, we will find a perturbation solution with the boundary conditions

$$\phi(0) = 1+\beta \tag{4.40}$$

$$\frac{d\phi}{d\xi}(1) = 0 \tag{4.41}$$

We write

$$\phi = \phi_0 + \epsilon\phi_1 + \epsilon^2\phi_2 + \ldots \tag{4.42}$$

The lowest order equation is

$$\frac{d_0^\phi}{d\xi^2} = 0, \quad \phi_0(0) = 1+\beta, \quad \frac{d\phi_0}{d\xi}(1) = 0 \tag{4.43}$$

which gives

$$\phi_0 = 1+\beta \tag{4.44}$$

To the next order

$$\frac{d_1^\phi}{d\xi^2} = \phi_0^4 - \beta^4, \quad \phi_1(0) = 0, \quad \frac{d\phi_1}{d\xi}(1) = 0 \tag{4.45}$$

with the solution

$$\phi_1 = [(1+\beta)^4 - \beta^4]\frac{\xi^2}{2} - [(1+\beta)^4 - \beta^4]\xi \tag{4.46}$$

The complete solution is

$$\phi = (1+\beta) + \epsilon\left\{[(1+\beta)^4 - \beta^4]\frac{\xi^2}{2} - [(1+\beta)^4 - \beta^4]\xi\right\} + \ldots \tag{4.47}$$

so that

$$\theta = 1 + \epsilon\left\{[(1+\beta)^4 - \beta^4]\frac{\xi^2}{2} - [(1+\beta)^4 - \beta^4]\xi\right\} + \ldots \tag{4.48}$$

Convective and radiative

(4.49)

4.4.1 Annular fin

Example 4.2

Show that under suitable conditions, the temperature distribution in a two-dimensional rectangle tends to that given by a one-dimensional approximation.

4.5 Perturbations of one-dimensional conduction

4.5.1 Temperature-dependent conductivity

[13]

The governing equation is

$$\frac{d}{dx}\left(k(T)\frac{dT}{dx}\right) - \frac{Ph}{A}\left(T - T_\infty\right) = 0 \tag{4.50}$$

with the boundary conditions

$$T(0) = T_b \tag{4.51}$$

$$\frac{dT}{dx}(L) = 0 \tag{4.52}$$

we use the dimensionless variables

$$\theta = \frac{T - T_\infty}{T_b - T_\infty} \tag{4.53}$$

$$\xi = \frac{x}{L} \tag{4.54}$$

Consider the special case of a linear variation of conductivity

$$k(T) = k_0\left(1 + \epsilon\frac{T - T_\infty}{T_b - T_\infty}\right) \tag{4.55}$$

so that

$$\left(1 + \epsilon\theta\right)\frac{d^2\theta}{d\xi^2} + \epsilon\left(\frac{d\theta}{d\xi}\right)^2 - m^2\theta = 0 \tag{4.56}$$

$$\theta(0) = 1 \tag{4.57}$$

$$\frac{d\theta}{d\xi}(L) = 0 \tag{4.58}$$

where

$$m^2 = \frac{PhL^2}{Ak_0(T_b - T_\infty)} \tag{4.59}$$

Introduce

$$\theta(\xi) = \theta_0(\xi) + \epsilon\theta_1(\xi) + \epsilon\theta_2(\xi) + \ldots \tag{4.60}$$

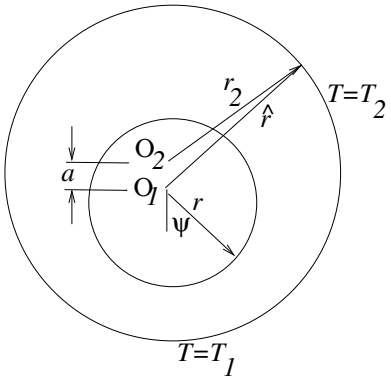

Figure 4.3: Eccentric annulus.

Collect terms of $O(\epsilon^0)$

$$\frac{d^2\theta_0}{d\xi^2} - m^2\theta = 0 \tag{4.61}$$

$$\theta_0(0) = 1 \tag{4.62}$$

$$\frac{d\theta_0}{d\xi}(1) = 0 \tag{4.63}$$

The solution is

$$\theta(\xi) = \cosh m\xi - \tanh m \sinh m\xi \tag{4.64}$$

To $O(\epsilon^1)$

$$\frac{d^2\theta_1}{d\xi^2} - m^2\theta_1 = -\theta_0\frac{d^2\theta_0}{d\xi^2} - \left(\frac{d\theta_0}{d\xi}\right)^2 \tag{4.65}$$

$$= -m^2(1 - \tanh^2 m)\cosh 2m\xi - m^2 \tanh m \ \sinh 2m\xi \tag{4.66}$$

$$\theta_1(0) = 0 \tag{4.67}$$

$$\frac{d\theta_1}{d\xi}(1) = 0 \tag{4.68}$$

The solution is

4.5.2 Eccentric annulus

Steady-state conduction in a slightly eccentric annular space, as shown in Fig. 4.3 can be solved by regular perturbation [13]. The radii of the two circles are r_1 and r_2.

We will use polar coordinates (r, ψ) with the center of the small circle as origin. The two circles are at $r = r_1$ and $r = \widehat{r}$, where

$$r_2^2 = a^2 + \widehat{r}^2 + 2a\widehat{r}\cos\psi. \tag{4.69}$$

Solving for $\widehat{r}$, we have

$$\widehat{r} = \sqrt{r_2^2 - a^2(1 - \cos^2\psi)} - a\cos\psi. \tag{4.70}$$

In the quadratic solution, the positive sign corresponding to the geometry shown in the figure has been kept.

The governing equation for the temperature is

$$\left(\frac{\partial^2}{\partial r^2}+\frac{1}{r}\frac{\partial}{\partial r}+\frac{1}{r^2}\frac{\partial^2}{\partial \psi^2}\right)T(r,\psi)=0. \tag{4.71}$$

The boundary conditions are

$$\begin{aligned} T(r_1,\psi) &= T_1, & (4.72)\\ T(\widehat{r},\psi) &= T_2. & (4.73)\end{aligned}$$

With the variables

$$\begin{aligned} \theta &= \frac{T-T_2}{T_1-T_2}. & (4.74)\\ R &= \frac{r-r_1}{r_2-r_1}. & (4.75)\\ d &= \frac{r_1}{r_2-r_1}. & (4.76)\\ \epsilon &= \frac{a}{r_2-r_1}, & (4.77)\end{aligned}$$

we get

$$\left(\frac{\partial^2}{\partial R^2}+\frac{1}{R+d}\frac{\partial}{\partial R}+\frac{1}{(R+d)^2}\frac{\partial^2}{\partial \psi^2}\right)\theta(R,\psi)=0, \tag{4.78}$$

and

$$\begin{aligned} \theta(0,\psi) &= 1, & (4.79)\\ \theta(\widehat{R},\psi) &= 0, & (4.80)\end{aligned}$$

where

$$\begin{aligned} \widehat{R}(\psi) &= \frac{\widehat{r}-r_1}{r_2-r_1}\\ &= \sqrt{(1+d)^2-\epsilon^2(1-\cos^2\psi)}-\epsilon\cos\psi-d, & (4.81)\end{aligned}$$

The perturbation expansion is

$$\theta(R,\psi)=\theta_0(R,\psi)+\epsilon\theta_1(R,\psi)+\epsilon^2\theta_2(R,\psi)+\ldots. \tag{4.82}$$

Substituting in the equations, we get

$$\left(\frac{\partial^2}{\partial R^2}+\frac{1}{R+d}\frac{\partial}{\partial R}+\frac{1}{(R+d)^2}\frac{\partial^2}{\partial \psi^2}\right)\left(\theta_0+\epsilon\theta_1+\epsilon^2\theta_2+\ldots\right)=0, \tag{4.83}$$

$$\widehat{R}(\psi)=1-\epsilon\cos\psi-\frac{\epsilon^2}{2}(1-\cos^2\psi)+\ldots, \tag{4.84}$$

$$\theta_0(0,\psi)+\epsilon\theta_1(0,\psi)+\epsilon^2\theta_2(0,\psi)+\ldots=1, \tag{4.85}$$

$$\theta_0(\widehat{R},\psi)+\epsilon\theta_1(\widehat{R},\psi)+\epsilon^2\theta_2(\widehat{R},\psi)+\ldots=0. \tag{4.86}$$

Using Eq. (4.84), (4.86) can be further expanded in a Taylor series around $\widehat{R} = 1$ to give

$$\theta_0(1,\psi) + \epsilon\left(\theta_1(1,\psi) - \cos\psi \frac{d\theta_0}{dR}(1,\psi)\right) + \ldots = 0. \tag{4.87}$$

Collecting terms to order $O(\epsilon^0)$, we get

$$\left(\frac{\partial^2}{\partial R^2} + \frac{1}{R+d}\frac{\partial}{\partial R} + \frac{1}{(R+d)^2}\frac{\partial^2}{\partial \psi^2}\right)\theta_0 = 0, \tag{4.88}$$

$$\theta_0(0,\psi) = 1, \tag{4.89}$$

$$\theta_0(1,\psi) = 0, \tag{4.90}$$

which has the solution

$$\theta_0(R,\psi) = 1 - \frac{\ln(1+R/h)}{\ln(1+1/h)}. \tag{4.91}$$

To order $O(\epsilon^1)$

$$\left(\frac{\partial^2}{\partial R^2} + \frac{1}{R+d}\frac{\partial}{\partial R} + \frac{1}{(R+d)^2}\frac{\partial^2}{\partial \psi^2}\right)\theta_1 = 0, \tag{4.92}$$

$$\theta_1(0,\psi) = 0, \tag{4.93}$$

$$\theta_1(1,\psi) = \cos\psi \frac{d\theta_0}{dR}(1,\psi), \tag{4.94}$$

$$= \frac{\cos\psi}{(1+h)\ \ln(1+1/h)}. \tag{4.95}$$

The solution is

$$\theta_1(R,\psi) = \pm\frac{R\cos\psi}{(1+2h)\ \ln(1+1/h)}\ \frac{R-2h}{R+h}. \tag{4.96}$$

4.6 Transient conduction

Let us propose a similarity solution of the transient conduction equation

$$\frac{\partial^2 T}{\partial x^2} - \frac{1}{\kappa}\frac{\partial T}{\partial t} = 0 \tag{4.97}$$

as

$$T = A\ \mathrm{erf}\left(\frac{x}{2\sqrt{\kappa t}}\right) \tag{4.98}$$

Taking derivatives we find

$$\frac{\partial T}{\partial x} = A\frac{1}{\sqrt{\pi\kappa t}}\exp\left(-\frac{x^2}{4\kappa t}\right) \tag{4.99}$$

$$\frac{\partial^2 T}{\partial x^2} = -A\frac{x}{2\sqrt{\pi\kappa^3 t^3}}\exp\left(-\frac{x^2}{4\kappa t}\right) \tag{4.100}$$

$$\frac{\partial T}{\partial t} = -A\frac{x}{2\sqrt{\pi\kappa t^3}}\exp\left(-\frac{x^2}{4\kappa t}\right) \tag{4.101}$$

so that substitution verifies that equation (4.98) is a solution to equation (4.97).

4.7 Linear diffusion

Let $T = T(x,t)$ and

$$\frac{\partial T}{\partial t} = \alpha \frac{\partial^2 T}{\partial x^2} \tag{4.102}$$

in $0 \leq x \leq L$, with the boundary and initial conditions $T(0,t) = T_1$, $T(L,t) = T_2$, and $T(x,0) = f(x)$. The steady state solution is

$$\overline{T}(x) = T_1 + \frac{T_2 - T_1}{L} x. \tag{4.103}$$

With

$$T'(x,t) = T - \overline{T} \tag{4.104}$$

we have the same equation

$$\frac{\partial T'}{\partial t} = \alpha \frac{\partial^2 T'}{\partial x^2} \tag{4.105}$$

but with the conditions: $T'(0,t) = 0$, $T'(L,t) = 0$, and $T'(x,0) = f(x) - \overline{T}$.

Following the methodology outlined in Section A.6.1, we consider the eigenvalue problem

$$\frac{d^2\phi}{dx^2} = \lambda\phi \tag{4.106}$$

with $\phi(0) = \phi(L) = 0$. The operator is self-adjoint. Its eigenvalues are

$$\lambda_i = -\frac{i^2\pi^2}{L^2}, \tag{4.107}$$

and its orthonormal eigenfunctions are

$$\phi_i(x) = \sqrt{\frac{2}{L}}\ \sin\frac{i\pi x}{L}. \tag{4.108}$$

Thus we let

$$\theta(x,t) = \sum_{i=1}^{\infty} a_i(t)\phi_i(x), \tag{4.109}$$

so that

$$\frac{da_j}{dt} = -\alpha\left(\frac{j\pi}{L}\right)^2 a_j, \tag{4.110}$$

with the solution

$$a_j = C_j \exp\left\{-\alpha\left(\frac{j\pi}{L}\right)^2 t\right\}. \tag{4.111}$$

Thus

$$T'(x,t) = \sum_{i=1}^{\infty} C_j \exp\left\{-\alpha\left(\frac{j\pi}{L}\right)^2 t\right\}\sqrt{\frac{2}{L}}\ \sin\frac{i\pi x}{L}. \tag{4.112}$$

The solution shows that $T' \to 0$, as $t \to \infty$. Thus $\theta = 0$ is a stable solution of the problem. It must be noted that there has been no need to linearize, since Eq. (4.105) was already linear.

4.8 Nonlinear diffusion

The following diffusion problem with heat generation is considered in [81]

$$\frac{\partial T}{\partial t} = \epsilon \frac{\partial^2 T}{\partial x^2} + f(T), \tag{4.113}$$

with $-\infty < x < \infty$, $t \geq 0$, and $\epsilon \ll 1$. The initial condition is taken to be

$$\begin{aligned} T(x,0) &= g(x) && (4.114)\\ &= \frac{1}{1+e^{\lambda x}}. && (4.115) \end{aligned}$$

Consider two time scales, a fast, short one $t_1 = t$, and a slow, long scale $t_2 = \epsilon t$. Thus

$$\frac{\partial}{\partial t} = \frac{\partial}{\partial t_1} + \epsilon \frac{\partial}{\partial t_2}. \tag{4.116}$$

Assuming an asymptotic expansion of the type

$$T = T_0(x, t_1, t_2) + \epsilon T_1(x, t_1, t_2) + \ldots \tag{4.117}$$

we have a Taylor series expansion

$$f(T) = f(T_0) + \epsilon f'(T_0) + \ldots \tag{4.118}$$

Substituting and collecting terms of $O(\epsilon^0)$, we get

$$\frac{\partial T_0}{\partial t_1} = f(T_0), \tag{4.119}$$

with the solution

$$\int_{1/2}^{T_0} \frac{dr}{f(r)} = t_1 + \theta(x, t_2). \tag{4.120}$$

The lower limit of the integral is simply a convenient value at which $g(x) = 0.5$. Applying the initial condition gives

$$\theta = \int_{1/2}^{g(x)} \frac{dr}{f(r)}. \tag{4.121}$$

The terms of $O(\epsilon)$ are

$$\frac{\partial T_1}{\partial t_1} = f'(T_0)T_1 + \frac{\partial^2 T_0}{\partial x^2} - \frac{\partial T_0}{\partial t_2} \tag{4.122}$$

Differentiating Eq. 4.120 with respect to x gives

$$\frac{\partial T_0}{\partial x} = f(T_0)\frac{\partial \theta}{\partial x}, \tag{4.123}$$

so that

$$\begin{aligned} \frac{\partial^2 T_0}{\partial x^2} &= f'(T_0)\frac{\partial T_0}{\partial x}\frac{\partial \theta}{\partial x} + f(T_0)\frac{\partial^2 \theta}{\partial x^2}\\ &= f'(T_0)f(T_0)\left(\frac{\partial \theta}{\partial x}\right)^2 + f(T_0)\frac{\partial @2\theta}{\partial x^2} && (4.124) \end{aligned}$$

Also, differentiating with respect to t_2 gives

$$\frac{\partial T_0}{\partial t_2} = f(T_0)\frac{\partial \theta}{\partial t_2} \tag{4.125}$$

Substituting in Eq. 4.122,

$$\frac{\partial T_1}{\partial t_1} = f'(T_0)T_1 + f(T_0)\left[\frac{\partial^2 \theta}{\partial x^2} - \frac{\partial \theta}{\partial t_2} + f'(T_0)\left(\frac{\partial \theta}{\partial x}\right)^2\right]. \tag{4.126}$$

Since

$$\begin{aligned} \frac{\partial}{\partial t_1}\ln f(T_0) &= \frac{f'(T_0)}{f(T_0)}\frac{\partial T_0}{\partial t_1} && (4.127)\\ &= f'(T_0) && (4.128) \end{aligned}$$

we have

$$\frac{\partial T_1}{\partial t_1} = f'(T_0)T_1 + f(T_0)\left[\frac{\partial^2 \theta}{\partial x^2} - \frac{\partial \theta}{\partial t_2} + \frac{\partial}{\partial t_1}\ln f(T_0)\right]. \tag{4.129}$$

The solution is

$$T_1 = \left[A(x,t_2) + t_1\left(\frac{\partial^2 \theta}{\partial x^2} - \frac{\partial \theta}{\partial t_2} + \left(\frac{\partial \theta}{\partial x}\right)^2 \ln f(T_0)\right)\right] f(T_0) \tag{4.130}$$

which can be checked by differentiation since

$$\begin{aligned} \frac{\partial T_1}{\partial t_1} &= \left[\frac{\partial^2 \theta}{\partial x^2} - \frac{\partial \theta}{\partial t_2} + f'(T_0)\left(\frac{\partial \theta}{\partial x}\right)^2\right] f(T_0) && (4.131)\\ &\quad + \left[A + t_1\left(\frac{\partial^2 \theta}{\partial x^2} - \frac{\partial \theta}{\partial t_2}\right) + \left(\frac{\partial \theta}{\partial x}\right)^2 \ln f(T_0)\right] f'(T_0)\frac{\partial T_0}{\partial t_1} && (4.132)\\ &= \left[\frac{\partial^2 \theta}{\partial x^2} - \frac{\partial \theta}{\partial t_2} + f'(T_0)\left(\frac{\partial \theta}{\partial x}\right)^2\right] f(T_0) + T_1 f'(T_0). && (4.133) \end{aligned}$$

where Eq. 4.119 has been used.

To suppress the secular term in Eq. 4.130, we take

$$\frac{\partial^2 \theta}{\partial x^2} - \frac{\partial \theta}{\partial t_2} + \kappa(x,t_1)\left(\frac{\partial \theta}{\partial x}\right)^2 = 0. \tag{4.134}$$

where $\kappa = f'(T_0)$. Let

$$w(x,t_2) = e^{\kappa\theta}, \tag{4.135}$$

so that its derivatives are

$$\begin{aligned} \frac{\partial w}{\partial x} &= \kappa e^{\kappa\theta}\frac{\partial \theta}{\partial x} && (4.136)\\ \frac{\partial^2 w}{\partial x^2} &= \kappa^2 e^{\kappa\theta}\left(\frac{\partial \theta}{\partial x}\right)^2 + \kappa e^{\kappa\theta}\frac{\partial^2 \theta}{\partial x^2} && (4.137)\\ \frac{\partial w}{\partial t_2} &= \kappa e^{\kappa\theta}\frac{\partial \theta}{\partial t_2} && (4.138) \end{aligned}$$

We find that

$$\frac{\partial^2 w}{\partial x^2} - \frac{\partial w}{\partial t_2} = \kappa e^{\kappa\theta}\left[\frac{\partial^2\theta}{\partial x^2} - \frac{\partial\theta}{\partial t_2} + \kappa\left(\frac{\partial\theta}{\partial x}\right)^2\right] \tag{4.139}$$

$$= 0. \tag{4.140}$$

The solution is

$$w = \frac{1}{\sqrt{\pi}}\int_\infty^\infty R(x + 2r\sqrt{t_2})e^{-r^2}\ dr, \tag{4.141}$$

where $R(x) = w(x, 0)$. This can be confirmed by finding the derivatives

$$\frac{\partial^2 w}{\partial x^2} = \frac{1}{\sqrt{\pi}}\int_\infty^\infty R''(x + 2r\sqrt{t_2})e^{-r^2}\ dr \tag{4.142}$$

$$\frac{\partial w}{\partial t_2} = \frac{1}{\sqrt{\pi}}\int_\infty^\infty R'(x + 2r\sqrt{t_2})\frac{r}{\sqrt{t_2}}e^{-r^2}\ dr$$

$$= -\frac{1}{2\sqrt{\pi}}\left[R'(x + 2r\sqrt{t_2})\Big|_\infty^\infty - \int_\infty^\infty R''(x + 2r\sqrt{t_2})2\sqrt{t_2}e^{-r^2}\ dr\right] \tag{4.143}$$

$$= \frac{1}{\sqrt{\pi}}\int_\infty^\infty R''(x + 2r\sqrt{t_2})e^{-r^2}\ dr \tag{4.144}$$

and substituting. Also,

$$R(x) = \exp\left[\kappa\theta(x, 0)\right] \tag{4.145}$$

$$= \exp\left[\kappa\int_{1/2}^{g(x)}\frac{dr}{f(r)}\right] \tag{4.146}$$

so that the final (implicit) solution is

$$\int_{1/2}^{T_0}\frac{dr}{f(r)} = t_1 + \frac{1}{\kappa}\ln\left[\frac{1}{\sqrt{\pi}}\int_\infty^\infty R(x + 2r\sqrt{t_2})e^{-r^2}\ dr\right] \tag{4.147}$$

Fisher's equation: As an example, we take $f(T) = T(1 - T)$, so that the integral in Eq. 4.120 is

$$\int_{1/2}^{T_0}\frac{dr}{r(1-r)} = \ln\frac{T_0}{T_0 - 1} \tag{4.148}$$

Substituting in the equation, we get

$$T_0 = \frac{1}{1 + e^{-(t_1+\theta)}} \tag{4.149}$$

$$= \frac{w}{w + e^{-t_1}} \tag{4.150}$$

Thus

$$w = \frac{T_0 e^{-t_1}}{1 - T_0} \tag{4.151}$$

and from Eq. 4.115,

$$R(x) = w(x, 0) \tag{4.152}$$

$$= e^{-\lambda x} \tag{4.153}$$

Substituting in Eq. 4.141 and integrating,

$$w = \exp\left(-\lambda x + \lambda^2 t_2\right) \tag{4.154}$$

so that

$$T_0 = \frac{1}{1 + \exp\left[x - t(1 + \lambda^2\epsilon)/\lambda\right]} \tag{4.155}$$

This is a wave that travels with a phase speed of $(1 + \lambda^2\epsilon)/\lambda$.

4.9 Stability by energy method

4.9.1 Linear

As an example consider the same problem as in Section 4.7. The deviation from the steady state is governed by

$$\frac{\partial T'}{\partial t} = \alpha \frac{\partial^2 T'}{\partial x^2} \tag{4.156}$$

with $T'(0,t) = 0$, $T'(L,t) = 0$.

Define

$$E(t) = \frac{1}{2}\int_0^L T'^2 \, dx \tag{4.157}$$

so that $E \geq 0$. Also

$$\begin{aligned}
\frac{dE}{dt} &= \int_0^L T' \frac{\partial T'}{\partial t} \, dx \\
&= \alpha \int_0^L T' \frac{\partial^2 T'}{\partial x^2} \, dx \\
&= \alpha \left[\int_0^L T' \frac{\partial T'}{\partial x} \bigg|_0^L - \int_0^L \left(\frac{\partial T'}{\partial x}\right)^2 \, dx \right] \\
&= -\alpha \int_0^L \left(\frac{\partial T'}{\partial x}\right)^2 \, dx
\end{aligned} \tag{4.158}$$

so that

$$\frac{dE}{dt} \leq 0. \tag{4.159}$$

Thus $E \to 0$ as $t \to \infty$ whatever the initial conditions.

4.9.2 Nonlinear

Let us now re-do the problem for a bar with temperature-dependent conductivity. Thus

$$\frac{\partial T}{\partial t} = \frac{\partial}{\partial x}\left\{k(T)\frac{\partial T}{\partial x}\right\}, \tag{4.160}$$

with $T(0,t) = T_1$ and $T(L,t) = T_2$. The steady state, $\overline{T}(x)$, is governed by

$$\frac{d}{dx}\left\{k(\overline{T})\frac{d\overline{T}}{dx}\right\} = 0. \tag{4.161}$$

Let the deviation from the steady state be

$$\theta(x,t) = T(x,t) - \overline{T}(x). \tag{4.162}$$

Thus

$$\frac{\partial\theta}{\partial t} = \frac{\partial}{\partial x}\left\{k(\theta)\frac{\partial\theta}{\partial x}\right\}, \tag{4.163}$$

where $\theta = \theta(x,t)$, with $\theta(0,t) = \theta(L,t) = 0$. The steady state is $\theta = 0$. Let

$$E(t) = \frac{1}{2}\int_0^L \theta^2\, dx. \tag{4.164}$$

so that $E \geq 0$. Then

$$\begin{aligned}
\frac{dE}{dt} &= \int_0^L \theta\frac{\partial\theta}{\partial t}\, dx && (4.165)\\
&= \int_0^L \theta\frac{\partial}{\partial x}\left\{k(\theta)\frac{\partial\theta}{\partial x}\right\}\, dx && (4.166)\\
&= \theta k(\theta)\frac{\partial\theta}{\partial x}\bigg|_0^L - \int_0^L k(\theta)\left(\frac{\partial\theta}{\partial x}\right)^2\, dx. && (4.167)
\end{aligned}$$

Due to boundary conditions the first term on the right is zero, so that $dE/dt \leq 0$. Thus $E \to 0$ as $t \to \infty$.

4.10 Self-similar structures

Consider the large-scale structure shown in Fig. 4.4 in which each line i (indicated by $i = 0, 1, \ldots$) is a conductive bar. The length of each bar is $L_i = L/\beta^i$ and its diameter is $D_i = D/\beta^i$. The beginning is at temperature T_0 and the ambient is T_∞.

The total length of the structure is

$$\begin{aligned}
L_T &= L_0 + 2L_1 + 4L_2 + 8L_3 + \ldots\\
&= \ldots
\end{aligned} \tag{4.168}$$

The total volume of the material is

$$\begin{aligned}
V_T &= \frac{\pi}{4}\left(D_0^2 L_0 + 2D_1^2 L_1 + 4D_2^2 L_2 + 8D_3^2 L_3 + \ldots\right)\\
&= \ldots
\end{aligned} \tag{4.169}$$

Both of these are finite if $\beta < \beta_c = \ldots$.

4.11 Non-Cartesian coordinates

Toroidal, bipolar.

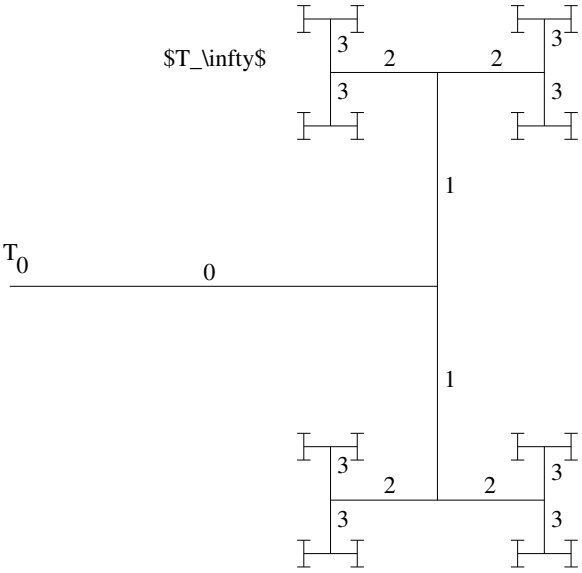

Figure 4.4: Large-scale self-similar structure.

4.12 Thermal control

Partial differential equations (PDEs) are an example of infinite-dimensional systems that are very common in thermal applications [2,110]. *Exact* controllability exists if the function representing the state can be taken from an initial to a final target state, and is *approximate* if it can be taken to a neighborhood of the target [118]. Determination of approximate controllability is usually sufficient for practical purposes.

Consider a system governed by

$$\frac{\partial X}{\partial t} = \mathcal{A}X + \mathcal{B}u, \tag{4.170}$$

with homogeneous boundary and suitable initial conditions, where $\mathcal{A}$ is a bounded semi-group operator [2], and $\mathcal{B}$ is a another linear operator. The state $X(\xi, t)$ is a function of spatial coordinates ξ and time t. If $\mathcal{A}$ is self-adjoint, then it has real eigenvalues and a complete orthonormal set of eigenfunctions $\phi_m(\xi)$, with $m = 0, 1, 2 \ldots$, which forms a complete spatial basis for X. It is known [110] that the system is approximately state controllable if and only if all the inner products

$$\langle \mathcal{B}, \phi_m \rangle \neq 0. \tag{4.171}$$

The lumped approximation in this chapter, valid for $Bi \ll 1$, is frequently not good enough for thermal systems, and the spatial variation of the temperature must be taken into account. The system is then described by PDEs that represent a formidable challenge for control analysis. The simplest examples occur when only one spatial dimension is present.

Fig. 4.5 shows a fin of length L with convection to the surroundings [4]. It is thin and long enough such that the transverse temperature distribution may be neglected. The temperature field is governed by

$$\frac{\partial T}{\partial t} = \alpha \frac{\partial^2 T}{\partial \xi^2} - \zeta (T - T_\infty), \tag{4.172}$$

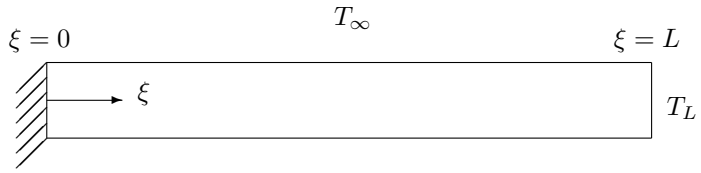

Figure 4.5: One-dimensional fin with convection.

where $T(\xi, t)$ is the temperature distribution that represents the state of the system, T_∞ is the temperature of the surroundings, t is time, and ξ is the longitudinal coordinate measured from one end. The thermal diffusivity is α, and $\zeta = hP/\rho c A_c$ where h is the convective heat transfer coefficient, A_c is the constant cross-sectional area of the bar, P is the perimeter of the cross section, ρ is the density, and c is the specific heat. For simplicity it will be assumed that ζ is independent of ξ. The end $\xi = 0$ will be assumed to be adiabatic so that $(\partial T/\partial \xi)(0, t) = 0$.

Since a linear system that is controllable can be taken from any state to any other, we can arbitrarily assume the fin to be initially at a uniform temperature. There are two ways in which the temperature distribution on the bar can be controlled: in *distributed* control[1] the surrounding temperature T_∞ is the control input and in *boundary* control it is the temperature of the other end $T(L, t)$ of the fin.

(a) *Distributed control:* The boundary temperature $T(L, t) = T_L$ is fixed. Using it as a reference temperature and defining $\theta = T - T_L$, Eq. (4.172) becomes,

$$\frac{\partial \theta}{\partial t} = \alpha \frac{\partial^2 \theta}{\partial \xi^2} - \zeta\theta + \zeta\theta_\infty(t) \tag{4.173}$$

with the homogeneous boundary and initial conditions $(\partial\theta/\partial\xi)(0, t) = 0$, $\theta(L, t) = 0$, and $\theta(\xi, 0) = 0$.

The operators in Eq. (4.170) are $\mathcal{A} = \alpha\partial^2/\partial\xi^2 - \zeta$, $\mathcal{B} = \zeta$, and $u = \theta_\infty$. $\mathcal{A}$ is a self-adjoint operator with the eigenvalues and eigenfunctions

$$\begin{aligned} \beta_m &= -\frac{(2m+1)^2\pi^2}{4L^2} - \zeta, \\ \phi_m &= \sqrt{\frac{2}{L}} \cos\frac{(2m+1)\pi\xi}{2L}, \end{aligned}$$

respectively. Inequality (4.171) is satisfied for all m, so the system is indeed state controllable. It can be shown that the same problem can also be analyzed using a finite-difference approximation [5].

(b) *Boundary control:* Using the constant outside temperature T_∞ as reference and defining $\theta = T - T_\infty$, Eq. (4.172) becomes

$$\frac{\partial \theta}{\partial t} = \alpha \frac{\partial^2 \theta}{\partial \xi^2} - \zeta\theta, \tag{4.174}$$

with the initial and boundary conditions $(\partial\theta/\partial\xi)(0, t) = 0$, $\theta(L, t) = T_L(t) - T_\infty$, and $\theta(\xi, 0) = 0$.

To enable a finite-difference approximation [5], the domain $[0, L]$ is divided into n equal parts of size $\Delta\xi$, so that Eq. (4.174) becomes

$$\frac{d\theta_i}{dt} = \sigma\theta_{i-1} - (2\sigma + \zeta)\theta_i + \sigma\theta_{i-1}, \tag{4.175}$$

[1] This term is also used in other senses in control theory.

where $\sigma = \alpha/\Delta\xi^2$. The nodes are $i = 1, 2, \ldots, n+1$, where $i = 1$ is at the left and $i = n+1$ at the right end of the fin in Fig. 4.5. With this Eq. (4.174) can be discretized to take the form of Eq. (3.6), where x is the vector of unknown θ_i. Thus we find

$$A = \begin{bmatrix} -(2\sigma+\zeta) & 2\sigma & 0 & \cdots & 0 \\ \sigma & -(2\sigma+\zeta) & \sigma & & \vdots \\ 0 & \ddots & \ddots & \ddots & \\ \vdots & & & & \sigma \\ 0 & \cdots & 0 & \sigma & -(2\sigma+\zeta) \end{bmatrix} \in \mathbb{R}^{n\times n}, \tag{4.176}$$

$$B = [0, \cdots, \sigma]^T \in \mathbb{R}^n. \tag{4.177}$$

The boundary conditions have been applied to make A non-singular: at the left end the fin is adiabatic, and at the right end θ_{n+1} is the control input u.

The controllability matrix M is

$$M = \begin{bmatrix} 0 & \cdots & \cdots & 0 & \sigma^n \\ 0 & \cdots & 0 & \sigma^{n-1} & \cdots \\ \vdots & \vdots & \vdots & \vdots & \vdots \\ 0 & 0 & \sigma^3 & \cdots & \cdots \\ 0 & \sigma^2 & -2\sigma^2(2\sigma+\zeta) & \cdots & \cdots \\ \sigma & -\sigma(2\sigma+\zeta) & \sigma^3+\sigma(2\sigma+\zeta)^2 & \cdots & \cdots \end{bmatrix} \tag{4.178}$$

The rank of M is n, indicating that the state of the system is also boundary controllable.

4.13 Multiple scales

Solve

$$\frac{\partial T_1}{\partial t} = \alpha \frac{\partial^2 (T_1 - T_2)}{\partial x^2} \tag{4.179}$$

$$\frac{\partial T_2}{\partial t} = R\alpha \frac{\partial^2 (T_2 - T_1)}{\partial x^2} \tag{4.180}$$

where $\epsilon \ll 1$, and with a step change in temperature at one end. Let

$$t = t_0 + \epsilon t_1 \tag{4.181}$$

Problems

1. From the governing equation for one-dimensional conduction

$$\frac{d}{dx}\left[k(x,T)\ \frac{dT}{dx}\right] = 0,$$

with boundary conditions

$$T(0) = \overline{T} + \frac{\Delta T}{2},$$

$$T(L) = \overline{T} - \frac{\Delta T}{2}.$$

show that the magnitude of the heat rate is independent of the sign of ΔT if we can write $k(x,T) = A(x)\ \lambda(T)$.

2. Consider a rectangular fin with convection, radiation and Dirichlet boundary conditions. Calculate numerically the evolution of an initial temperature distribution at different instants of time. Graph the results for several values of the parameters.
3. Consider a longitudinal fin of concave parabolic profile as shown in the figure, where $\delta = [1 - (x/L)]^2 \delta_b$. δ_b is the thickness of the fin at the base. Assume that the base temperature is known. Neglect convection from the thin sides. Find (a) the temperature distribution in the fin, and (b) the heat flow at the base of the fin. Optimize the fin assuming the fin volume to be constant and maximizing the heat rate at the base. Find (c) the optimum base thickness δ_b, and (d) the optimum fin height L.

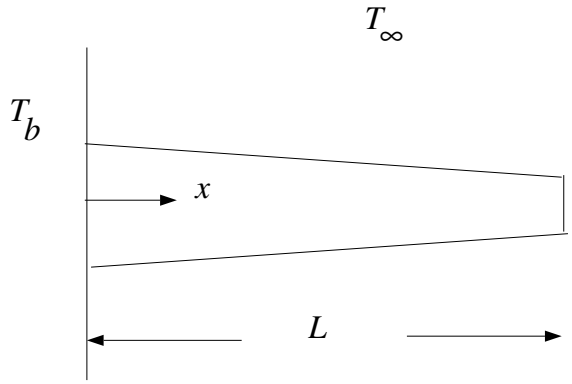

Figure 4.6: Longitudinal fin of concave parabolic profile.

Chapter 5

Forced convection

In this chapter we will considering the heat transfer in pipe flows. We will take a one-dimensional approach and neglect transverse variations in the velocity and temperature. In addition, for simplicity, we will assume that fluid properties are constant and that the area of the pipe is also constant.

5.1 Hydrodynamics

5.1.1 Mass conservation

For a duct of constant cross-sectional area and a fluid of constant density, the mean velocity of the fluid, V, is also constant.

5.1.2 Momentum equation

The forces on an element of length ds, shown in Fig. 5.1, in the positive s direction are: f_v, the viscous force and f_p, the pressure force. We can write

$$f_v = -\tau_w \; P \; ds \tag{5.1}$$

$$f_p = -A\frac{\partial p}{\partial s}ds \tag{5.2}$$

where τ_w is the magnitude of the wall shear stress, and p is the pressure in the fluid. Since the mass of the element is $\rho A \; ds$, we can write the momentum equation as

$$\rho A \; ds\frac{dV}{dt} = f_v + f_p \tag{5.3}$$

from which we get

$$\frac{dV}{dt} + \frac{\tau_w P}{\rho A} = -\frac{1}{\rho}\frac{\partial p}{\partial s} \tag{5.4}$$

Integrating over the length L of a pipe, we have

$$\frac{dV}{dt} + \frac{4\tau_w}{\rho D} = \frac{p_1 - p_2}{\rho L} \tag{5.5}$$

where p_1 and p_2 are the pressures at the inlet and outlet respectively, and the hydraulic diameter is defined by $D = 4A/P$.

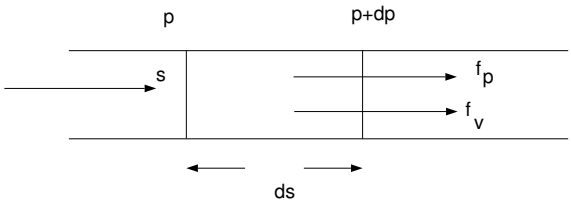

Figure 5.1: Forces on an element of fluid.

For fully developed flow we can assume that τ_w is a function of V that depends on the mean velocity profile, and acts in a direction opposite to V, so that we can write

$$\frac{dV}{dt} + T(|V|)V = \beta\ \Delta p \tag{5.6}$$

where $T(V) = |4\tau_w/\rho DV|$ is always positive, $\beta = 1/\rho L$, and $\Delta p = p_1 - p_2$ is the pressure difference that is driving the flow. The wall shear stress is estimated below for laminar and turbulent flows.

Laminar

The fully developed laminar velocity profile in a circular duct is given by the Poiseuille flow result

$$u_x(r) = u_m \left(1 - \frac{4r^2}{D^2}\right) \tag{5.7}$$

where u is the local velocity, r is the radial coordinate, u_m is the maximum velocity at the centerline, and D is the diameter of the duct. The mean velocity is given by

$$V = \frac{4}{\pi D^2} \int_0^{D/2} u_x(r)\ 2\pi r\ dr \tag{5.8}$$

Substituting the velocity profile, we get

$$V = \frac{u_m}{2} \tag{5.9}$$

The shear stress at the wall τ_w is given by

$$\tau_w = -\mu \left.\frac{\partial u_x}{\partial r}\right|_{r=D/2} \tag{5.10}$$

$$= \mu u_m \frac{4}{D} \tag{5.11}$$

$$= \frac{8\mu V}{D} \tag{5.12}$$

The wall shear stress is linear relationship

$$\tau_w = \alpha V \tag{5.13}$$

where

$$\alpha = \frac{8\mu}{D} \tag{5.14}$$

so that

$$T(|V|)V = \frac{32\mu}{\rho D^2} V \tag{5.15}$$

Turbulent

For turbulent flow the expression for shear stress at the wall of a duct that is usually used is

$$\tau_w = \frac{f}{4}\left(\frac{1}{2}\rho V^2\right) \tag{5.16}$$

so that

$$T(V) = \frac{f}{2D}|V|V. \tag{5.17}$$

Here f is the Darcy-Weisbach friction factor[1]. The friction factor is also a fucntion of $|V|$, and may be calculated from the Blasius equation for smooth pipes

$$f = \frac{0.3164}{Re^{1/4}} \tag{5.18}$$

where the Reynolds number is $Re = |V|D/\nu$, or the Colebrook equation for rough pipes

$$\frac{1}{f^{1/2}} = -2.0\ \log\left(\frac{e/D_h}{3.7} + \frac{2.51}{Re\ f^{1/2}}\right) \tag{5.19}$$

where e is the roughness at the wall, or similar expressions.

In the flow in a length of duct, L, without acceleration, the pressure drop is given by

$$\Delta p\ A = \tau_w P L \tag{5.20}$$

where A is the cross-sectional area, and P is the inner perimeter. Thus

$$\Delta p = f\left(\frac{L}{4A/P}\right)\left(\frac{1}{2}\rho V^2\right) \tag{5.21}$$

$$= f\left(\frac{L}{D}\right)\left(\frac{1}{2}\rho|V|V\right) \tag{5.22}$$

Example 5.1

Consider a long, thin pipe with pressures p_1 and p_2 ate either end. For $t \leq 0$, $p_1 - p_2 = 0$ and there is no flow. For $t > 0$, $p_1 - p_2$ is a nonzero constant. Find the resulting time-dependent flow. Make the assumption that the axial velocity is only a function of radial position and time.

5.1.3 Long time behavior

Consider the flow in a single duct of finite length with a constant driving pressure drop. The governing equation for the flow velocity is equation (5.6). The flow velocity in the steady state is a solution of

$$T(\overline{V})\overline{V} = \beta\ \Delta p \tag{5.23}$$

[1] Sometimes, confusingly, the Fanning friction factor, which is one-fourth the Darcy-Weisbach value, is used in the literature.

where Δp and $\overline{V}$ are both of the same sign, say nonnegative. We can show that under certain conditions the steady state is globally stable. Writing $V = \overline{V} + V'$, equation (5.6) becomes

$$\frac{dV'}{dt} + T(\overline{V} + V')(\overline{V} + V') = \beta\ \Delta p \tag{5.24}$$

Subtracting equation (5.23), we get

$$\frac{dV'}{dt} = -T(\overline{V} + V')(\overline{V} + V') + T(\overline{V})(\overline{V}) \tag{5.25}$$

Defining

$$E = \frac{1}{2}V'^2 \tag{5.26}$$

so that $E \geq 0$, we find that

$$\begin{aligned} \frac{dE}{dt} &= V'\frac{dV'}{dt} && (5.27)\\ &= -V'\left[T(\overline{V} + V')(\overline{V} + V') - T(\overline{V})\overline{V}\right] && (5.28)\\ &= -V'\overline{V}\left[T(\overline{V} + V') - T(\overline{V})\right] - V'^2 T(\overline{V} + V') && (5.29) \end{aligned}$$

If we assume that $T(V)$ is a non-decreasing function of V, we see that

$$V'\overline{V}\left[T(\overline{V} + V') - T(\overline{V})\right] \geq 0 \tag{5.30}$$

regardless of the sign of either V' or $\overline{V}$, so that

$$\frac{dE}{dt} \leq 0 \tag{5.31}$$

Thus, $E(V)$ is a Lyapunov function, and $V = \overline{V}$ is globally stable to all perturbations.

5.2 Energy equation

Consider a section of a duct shown in Fig. 5.2, where an elemental control volume is shown. The heat rate going in is given by

$$Q^- = \rho A V c T - kA\frac{\partial T}{\partial s} \tag{5.32}$$

where the first term on the right is due to the advective and second the conductive transports. c is the specific heat at constant pressure and k is the coefficient of thermal conductivity. The heat rate going out is

$$Q^+ = Q^- + \frac{\partial Q^-}{\partial s}\ ds \tag{5.33}$$

The difference between the two is

$$\begin{aligned} Q^+ - Q^- &= \frac{\partial Q^-}{\partial s}\ ds \\ &= \left[\rho A V c\frac{\partial T}{\partial s} - kA\frac{\partial^2 T}{\partial s^2}\right]\ ds && (5.34) \end{aligned}$$

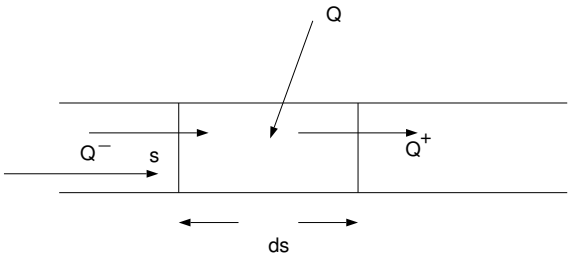

Figure 5.2: Forces on an element of fluid.

Furthermore, heat is gained from the side at a rate dQ, which can be written as

$$dQ = q\ ds \tag{5.35}$$

where q is the rate of gain of heat per unit length of the duct.

An energy balance for the elemental control volume gives

$$Q^- + dQ = Q^+ + \rho A\ ds\ c\frac{\partial T}{\partial t} \tag{5.36}$$

where the last term is the rate of accumulation of energy within the control volume.

Substituting equations (5.34) and (5.35) in (5.36) we get the energy equation

$$\frac{\partial T}{\partial t} + V\frac{\partial T}{\partial s} = \frac{q}{\rho A c} + \frac{k}{\rho c}\frac{\partial^2 T}{\partial s^2} \tag{5.37}$$

The two different types of heating conditions to consider are:

5.2.1 Known heat rate

The heat rate per unit length, $q(s)$, is known all along the duct. Defining

$$\xi = \frac{x}{L} \tag{5.38}$$

$$\theta = \frac{(T - T_i)\rho V A C}{Lq} \tag{5.39}$$

$$\tau = \frac{tV}{L} \tag{5.40}$$

gives

$$\frac{\partial \theta}{\partial \tau} + \frac{\partial \theta}{\partial \xi} - \lambda\frac{d^2\theta}{d\xi^2} = 1 \tag{5.41}$$

where

$$\lambda = \frac{k}{LV\rho c} \tag{5.42}$$

Boundary conditions may be $\theta = 0$ at $\xi = 0$, $\theta = \theta_1$ at $\xi = 1$.

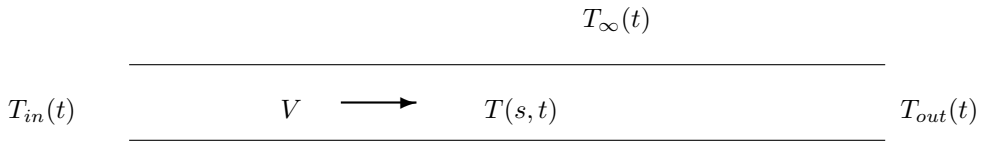

Figure 5.3: Fluid duct with heat loss.

5.2.2 Convection with known outside temperature

The heating is now convective with a heat transfer coefficient U, and an external temperature of $T_\infty(s)$. Thus,

$$q = PU(T_\infty - T) \tag{5.43}$$

Defining

$$\xi = \frac{x}{L} \tag{5.44}$$

$$\theta = \frac{T - T_i}{T_\infty - T_i} \tag{5.45}$$

$$\tau = \frac{tV}{L} \tag{5.46}$$

gives

$$\frac{\partial\theta}{\partial\tau} + \frac{\partial\theta}{\partial\xi} - \lambda\frac{d^2\theta}{d\xi^2} + H\theta = H \tag{5.47}$$

where

$$\lambda = \frac{k}{LV\rho c} \tag{5.48}$$

$$H = \frac{U\rho L}{\rho V Ac} \tag{5.49}$$

5.3 Single duct

Consider the duct that is schematically shown in Fig. 5.3. The inlet temperature is $T_{in}(t)$, and the outlet temperature is $T_{out}(t)$, and the fluid velocity is V. The duct is subject to heat loss through its surface of the form $UP\,(T - T_\infty)$ per unit length, where the local fluid temperature is $T(s,t)$ and the ambient temperature is $T_\infty(t)$. U is the overall heat transfer coefficient and P the cross-sectional perimeter of the duct.

We assume that the flow is one-dimensional, and neglect axial conduction through the fluid and the duct. Using the same variables to represent non-dimensional quantities, the governing non-dimensional equation is

$$\frac{\partial\theta}{\partial\tau} + \frac{\partial\theta}{\partial\xi} + H\theta = 0 \tag{5.50}$$

where the nondimensional variables are

$$\xi = \frac{s}{L} \tag{5.51}$$

$$\tau = \frac{tV}{L} \tag{5.52}$$

$$\theta = \frac{T - \overline{T}_\infty}{\Delta T} \tag{5.53}$$

The characteristic time is the time taken to traverse the length of the duct, i.e. the residence time. The ambient temperature is

$$T_\infty(t) = \overline{T}_\infty + \widetilde{T}_\infty(t) \tag{5.54}$$

where the time-averaged and fluctuating parts have been separated. Notice that the nondimensional mean ambient temperature is, by definition, zero. The characteristic temperature difference ΔT will be chosen later. The parameter $\gamma = UPL/\rho AVc$ represents the heat loss to the ambient.

5.3.1 Steady state

No axial conduction

The solution of the equation

$$\frac{d\theta}{d\xi} + H(\theta - 1) = 0 \tag{5.55}$$

with boundary condition $\theta(0) = 0$ is

$$\theta(\xi) = 1 - e^{-H\xi} \tag{5.56}$$

With small axial conduction

We have

$$\lambda \frac{d^2\theta}{d\xi^2} - \frac{d\theta}{d\xi} - H(\theta - 1) = 0 \tag{5.57}$$

where $\lambda \ll 1$, and with the boundary conditions $\theta(0) = 0$ and $\theta(1) = \theta_1$.

We can use a boundary layer analysis for this singular perturbation problem. The outer solution is

$$\theta_{out} = 1 - e^{-H\xi} \tag{5.58}$$

The boundary layer is near $\xi = 1$, where we make the transformation

$$X = \frac{\xi - 1}{\lambda} \tag{5.59}$$

This gives the equation

$$\frac{d^2\theta_{in}}{dX^2} - \frac{d\theta_{in}}{dX} - \lambda H(\theta_{in} - 1) = 0 \tag{5.60}$$

To lowest order, we have

$$\lambda \frac{d^2\theta_{in}}{dX^2} - \frac{d\theta_{in}}{dX} = 0 \tag{5.61}$$

with the solution

$$\theta_{in} = A + Be^X \tag{5.62}$$

The boundary condition $\theta_{in}(X = 0) = \theta_1$ gives $\theta_1 = A + B$, so that

$$\theta_{in} = A + (\theta_1 - A)e^X \tag{5.63}$$

The matching conditions is

$$\theta_{outer}(\xi = 1) = \theta_{in}(X \to -\infty) \tag{5.64}$$

so that

$$A = 1 - e^{-H} \tag{5.65}$$

The composite solution is then

$$\theta = 1 - e^{-H} + (\theta_1 - 1 + e^{-H})e^{(\xi-1)/\lambda} + \ldots \tag{5.66}$$

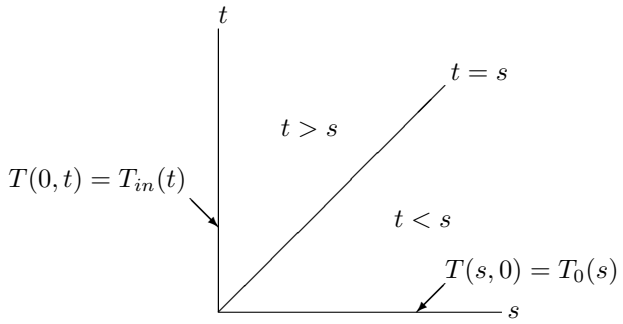

Figure 5.4: Solution in s-t space.

5.3.2 Unsteady dynamics

The general solution of this equation is

$$T(s,t) = \left[f(s-t) + \gamma \int_0^t e^{Ht'} \widetilde{T}_\infty(t')\, dt' \right] e^{-Ht} \tag{5.67}$$

The boundary conditions $T(0,t) = T_{in}(t)$ and $T(s,0) = T_0(s)$ are shown in Fig. 5.4. The solution becomes

$$T(s,t) = \begin{cases} T_{in}(t-s)e^{-Hs} + He^{-Ht} \int_{t-s}^t e^{Ht'} \widetilde{T}_\infty(t')\, dt' & \text{for } t \geq s \\ T_0(s-t)e^{-Ht} + He^{-Ht} \int_0^t e^{Ht'} \widetilde{T}_\infty(t')\, dt' & \text{for } t < s \end{cases} \tag{5.68}$$

The $t < s$ part of the solution is applicable to the brief, transient period of time in which the fluid at time $t = 0$ has still not left the duct. The later $t > s$ part depends on the temperature of the fluid entering at $s = 0$. The temperature, $T_{out}(t)$, at the outlet section, $s = 1$, is given by

$$T_{out}(t) = \begin{cases} T_{in}(t-1)e^{-H} + He^{-Ht} \int_{t-1}^t e^{Ht'} \widetilde{T}_\infty(t')\, dt' & \text{for } t \geq 1 \\ T_0(1-t)e^{-Ht} + He^{-Ht} \int_0^t e^{Ht'} \widetilde{T}_\infty(t')\, dt' & \text{for } t < 1 \end{cases} \tag{5.69}$$

It can be observed that, after an initial transient, the inlet and outlet temperatures are related by a unit delay. The outlet temperature is also affected by the heat loss parameter, γ, and the ambient temperature fluctuation, $\widetilde{T}_\infty$. The following are some special cases of equation (5.69).

5.3.3 Perfectly insulated duct

If $H = 0$ the outlet temperature simplifies to

$$T_{out}(t) = \begin{cases} T_{in}(t-1) & \text{for } t \geq 1 \\ T_0(1-t) & \text{for } t < 1 \end{cases} \tag{5.70}$$

The outlet temperature is the same as the inlet temperature, but at a previous instant in time.

5.3.4 Constant ambient temperature

For this $\widetilde{T}_\infty = 0$, and equation (5.69) becomes

$$T_{out}(t) = \begin{cases} T_{in}(t-1)e^{-H} & \text{for } t \geq 1 \\ T_0(1-t)e^{-Ht} & \text{for } t < 1 \end{cases} \tag{5.71}$$

This is similar to the above, but with an exponential drop due to heat transfer.

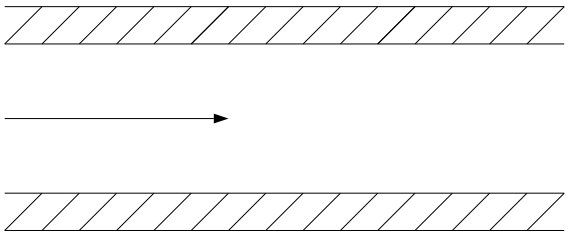

Figure 5.5: Effect of wall.

5.3.5 Periodic inlet and ambient temperature

We take

$$T_{in}(t) = \overline{T}_{in} + \widehat{T}_{in} \sin \omega t \tag{5.72}$$

$$\widetilde{T}_{\infty}(t) = \widehat{T}_{\infty} \sin \Omega t \tag{5.73}$$

so that equation (5.69) becomes

$$T_{out}(t) = \begin{cases} \left[\overline{T}_{in} + \widehat{T}_{in} \sin \omega(t-1)\right] e^{-H} \\ \qquad + \widehat{T}_{\infty} H \sqrt{\frac{-2e^{-H}\cos 1 + e^{-2H}}{H^2+\Omega^2}} \sin(\Omega t + \phi) & \text{for } t \geq 1 \\ T_0(1-t)e^{-Ht} + \frac{H}{H^2+\Omega^2} \widehat{T}_{\infty} \sqrt{H^2+\Omega^2} \sin(\Omega t + \phi') & \text{for } t < 1 \end{cases}$$

where

$$\tan \phi = -\frac{H(1 - e^{-H}\cos 1) + e^{-H}\Omega \sin 1}{\Omega(1 - e^{-H}\cos 1) - He^{-H}\sin 1} \tag{5.74}$$

$$\tan \phi' = -\frac{\Omega}{H} \tag{5.75}$$

The outlet temperature has frequencies which come from oscillations in the inlet as well as the ambient temperatures. A properly-designed control system that senses the outlet temperature must take the frequency dependence of its amplitude and phase into account. There are several complexities that must be considered in practical applications to heating or cooling networks, some of which are analyzed below.

5.3.6 Effect of wall

The governing equations are

$$\rho A c \frac{\partial T}{\partial t} + \rho V A c \frac{\partial T}{\partial x} - kA \frac{\partial^2 T}{\partial x^2} + h_i P_i (T - T_{\infty}) = 0 \tag{5.76}$$

$$\rho_w A_w c_w \frac{\partial T_w}{\partial t} - k_w A_w \frac{\partial^2 T_w}{\partial x^2} + h_i P_i (T_w - T) + h_o P_o (T_w - T_{\infty}) = 0 \tag{5.77}$$

$$\tag{5.78}$$

Nondimensionalize, using

$$\xi = \frac{x}{L} \tag{5.79}$$

$$\tau = \frac{tV}{L} \tag{5.80}$$

$$\theta = \frac{T - T_\infty}{T_i - T_\infty} \tag{5.81}$$

$$\theta_w = \frac{T_w - T_\infty}{T_i - T_\infty} \tag{5.82}$$

we get

$$\frac{\partial \theta}{\partial \tau} + \frac{\partial \theta}{\partial \xi} - \lambda \frac{\partial^2 \theta}{\partial \xi^2} + H_{in}(\theta - \theta_w) = 0 \tag{5.83}$$

$$\frac{\partial \theta_w}{\partial \tau} - \lambda_w \frac{\partial^2 \theta_w}{\partial \xi^2} + H_{in}(\theta_w - \theta) + H_{out}\theta_w = 0 \tag{5.84}$$

where

$$\lambda_w = \frac{k_w}{\rho_w V A_w c_w L} \tag{5.85}$$

$$H_{in} = \frac{h_{in} P_{in} L}{\rho_w A_w c_w V} \tag{5.86}$$

$$H_{out} = \frac{h_{out} P_{out} L}{\rho_w A_w c_w V} \tag{5.87}$$

In the steady state and with no axial conduction in the fluid

$$\frac{d\theta}{d\xi} + H_{in}(\theta - \theta_w) = 0 \tag{5.88}$$

$$-\lambda_w \frac{d^2 \theta_w}{d\xi^2} + H_{in}(\theta_w - \theta) + H_{out}\theta_w = 0 \tag{5.89}$$

If we assume $\lambda_w = 0$ also, we get

$$\theta_w = \frac{H_{in}}{H_{in} + H_{out}} \theta \tag{5.90}$$

The governing equation is

$$\frac{dT}{d\xi} + H_w \theta = 0 \tag{5.91}$$

where

$$H_w = \frac{H_{in}^w H_{out}^w}{H_{in}^w + H_{out}^w} \tag{5.92}$$

5.4 Two-fluid configuration

Consider the heat balance in Fig. 5.6. Neglecting axial conduction, we have

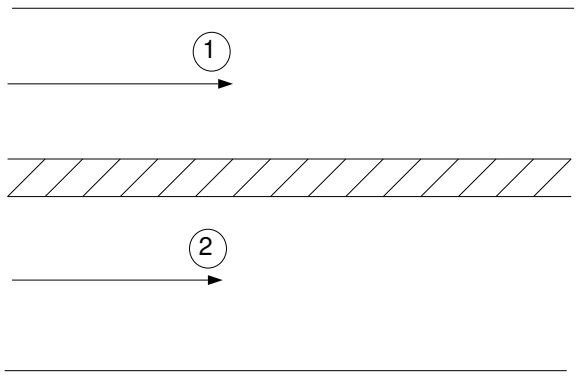

Figure 5.6: Two-fluids with wall.

$$\rho_w A_w c_w \frac{\partial T_w}{\partial t} + h_1(T_w - T_1) + h_2(T_w - T_2) = 0 \tag{5.93}$$

$$\rho_1 A_1 c_1 \frac{\partial T_1}{\partial t} + \rho_1 V_1 c_1 \frac{\partial T_1}{\partial x} + h_1(T_1 - T_w) = 0 \tag{5.94}$$

$$\rho_2 A_2 c_2 \frac{\partial T_2}{\partial t} + \rho_2 V_2 c_2 \frac{\partial T_2}{\partial x} + h_2(T_2 - T_w) = 0 \tag{5.95}$$

5.5 Flow between plates with viscous dissipation

Consider the steady, laminar flow of an incompressible, Newtonian fluid between fixed, flat plates at $y = -h$ and $y = h$. The flow velocity $u(y)$ is in the x-direction due to a constant pressure gradient $P < 0$. The plane walls are kept isothermal at temperature $T = T_0$, and the viscosity is assumed to decrease exponentially with temperature according to

$$\mu = \exp(1/T).) \tag{5.96}$$

The momentum equation is then

$$\frac{d}{dy}\left(\mu(T)\frac{du}{dy}\right) = P \tag{5.97}$$

with boundary conditions $u = 0$ at $y = \pm h$. Integrating, we get

$$\mu(T)\frac{du}{dy} = Py + C \tag{5.98}$$

Due to symmetry $du/dy = 0$ at $y = 0$ so that $C = 0$. There is also other evidence for this.

The energy equation can be written as

$$k\frac{d^2T}{dy^2} + \mu(T)\left(\frac{du}{dy}\right)^2 = 0 \tag{5.99}$$

with $T = T_0$ at $y = \pm h$, where k has been taken to be a constant. The second term corresponds to viscous heating or dissipation, and the viscosity is assumed to be given by Eq. (5.96). We non-

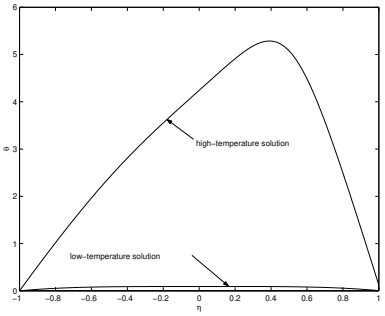

Figure 5.7: Two solutions of Eq. (5.102) with boundary conditions (5.104) for $a = 1$.

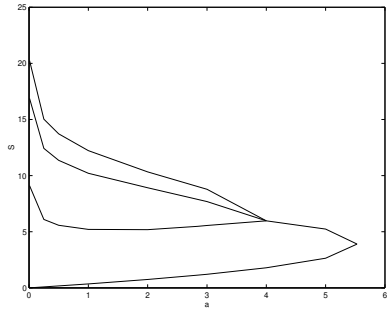

Figure 5.8: Bifurcation diagram.

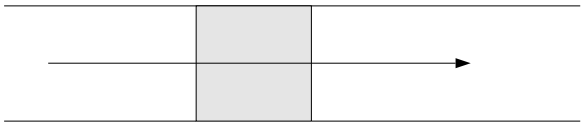

Figure 5.9: Schematic of regenerator.

dimensionalize using

$$\theta = \beta(T - T_0) \tag{5.100}$$

$$\eta = \frac{y}{h} \tag{5.101}$$

The energy equation becomes

$$\frac{d^2\theta}{d\eta^2} + a\ \eta^2 e^{\theta} = 0 \tag{5.102}$$

where

$$a = \frac{\beta P^2 h^4}{k\mu_0} \tag{5.103}$$

The boundary conditions are

$$\theta = 0 \text{ for } \eta = \pm 1 \tag{5.104}$$

There are two solutions that can be obtained numerically (by the shooting method, for instance) for the boundary-value problem represented by Eqs. (5.102) and (5.104) for $a < a_c$ and above which there are none. There are other solutions also but they do not satisfy the boundary conditions on the velocity. As examples, two numerically obtained solutions for $a = 1$ are shown in Fig. 5.7.

The bifurcation diagram corresponding to this problem is shown in Fig. 5.8 where S is the slope of the temperature gradient on one wall.

5.6 Regenerator

A regenerator is schematically shown in Fig. 5.9.

$$Mc\frac{dT}{dt} + \dot{m}c(T_{in} - T_{out}) = 0 \tag{5.105}$$

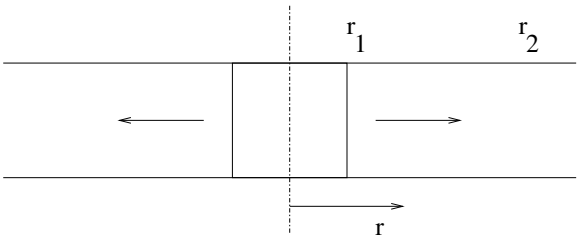

Figure 5.10: Flow between disks.

5.7 Radial flow between disks

This is shown in Fig. 5.10.

$$u_r = \frac{C}{r} \tag{5.106}$$

$$q_r = u_r 2\pi r H T - k 2\pi r H \frac{dT}{dr} \tag{5.107}$$

where H is the distance between the disks. With $dq_r/dr = 0$, we get

$$\frac{d}{dr}(r u_r T) = k \frac{d}{dr}(r \frac{dT}{dr}) \tag{5.108}$$

For the boundary conditions $T(r_1) = T_1$ and $T(r_2) = T_2$, the temperature field is

$$T(r) = \frac{T_1 \ln(r_2/r) - T_2 \ln(r_1/r)}{\ln(r_2/r_1)} \tag{5.109}$$

Example 5.2

Redo the previous problem with a slightly eccentric flow.

5.8 Networks

A network consists of a number of ducts that are united at certain points. At each junction, we must have

$$\sum_i A_i V_i = 0 \tag{5.110}$$

where A_i are the areas and V_i the fluid velocities in the ducts coming in, the sum being over all the ducts entering the junction. Furthermore, for each duct, the momentum equation is

$$\frac{dV_i}{dt} + T(V_i) V_i = \beta \ \left[p_i^{in} - p_i^{out} + \Delta p \right] \tag{5.111}$$

where Δp is the pressure developed by a pump, if there happens to be one on that line. We must distinguish between two possible geometries.

(a) Two-dimensional networks: A planar or two-dimensional network is one that is topologically equivalent to one on a plane in which every intersection of pipes indicates fluid mixing. For such a graph, we know that

$$E = V + F - 1 \tag{5.112}$$

where E, V and F are the number of edges, vertices and faces, respectively. In the present context, these are better referred to as branches, junctions and circuits, respectively.

The unknowns are the E velocities in the ducts and the V pressures at the junctions, except for one pressure that must be known. The number of unknowns thus are $E+V-1$. The momentum equation in the branches produce E independent differential equations, while mass conservation at the juntions give $V-1$ independent algebraic relations. Thus the number of

(b) Three-dimensional networks: For a three-dimensioanl network, we have

$$E = V + F - 2 \tag{5.113}$$

If there are n junctions, they can have a maximum of $n(n-1)/2$ lines connecting them. The number of circuits is then $(n^2 - 3n + 4)/2$. The number of equations to be solved is thus quite large if n is large.

5.8.1 Hydrodynamics

The global stability of flow in a network can be demonstrated in a manner similar to that in a finite-length duct. In a general network, assume that there are n junctions, and each is connected to all the rest. Also, p_i is the pressure at junction i, and V_{ij} is the flow velocity from junction i to j defined to be positive in that direction. The flow velocity matrix V_{ij} is anti-symmetric, so that V_{ii} which has no physical meaning is considered zero.

The momentum equation for V_{ij} is

$$\frac{dV_{ij}}{dt} + T_{ij}(V_{ij})V_{ij} = \beta_{ij}(p_i - p_j) \tag{5.114}$$

The network properties are represented by the symmetric matrix β_{ij}. The resistance T_{ij} may or may not be symmetric. To simplify the analysis the network is considered fully connected, but T_{ij} is infinite for those junctions that are not physically connected so that the flow velocity in the corresponding branch is zero. We take the diagonal terms in T_{ij} to be also infinite, so as to have $V_{ii} = 0$.

The mass conservation equation at junction j for all flows arriving there is

$$\sum_{i=1}^{n} A_{ij}V_{ij} = 0 \quad \text{for } j = 1, \ldots, n \tag{5.115}$$

where A_{ij} is a symmetric matrix. The symmetry of A_{ij} and antisymmetry of V_{ij} gives the equivalent form

$$\sum_{i=1}^{n} A_{ji}V_{ji} = 0 \quad \text{for } j = 1, \ldots, n \tag{5.116}$$

which is simply the mass conservation considering all the flows leaving junction j.

The steady states are solutions of

$$T_{ij}(\overline{V}_{ij})\overline{V}_{ij} = \beta_{ij}(\overline{p}_i - \overline{p}_j) \tag{5.117}$$

$$\sum_{i=1}^{n} A_{ij}\overline{V}_{ij} = 0 \quad \text{or} \quad \sum_{i=1}^{n} A_{ji}\overline{V}_{ji} = 0 \tag{5.118}$$

We write

$$V_{ij} = \overline{V}_{ij} + V'_{ij} \tag{5.119}$$

$$p_i = \overline{p} + p'_i \tag{5.120}$$

Substituting in equations (5.114)–(5.116), and subtracting equations (5.117) and (5.118) we get

$$\frac{dV'_{ij}}{dt} = -\left[T_{ij}(\overline{V}_{ij} + V'_{ij})(\overline{V}_{ij} + V'_{ij}) - T_{ij}(\overline{V}_{ij})\overline{V}_{ij}\right] + \beta_{ij}(p'_i - p'_j) \tag{5.121}$$

$$\sum_{i=1}^{n} A_{ij}V'_{ij} = 0 \quad \text{or} \quad \sum_{i=1}^{n} A_{ji}V'_{ji} = 0 \tag{5.122}$$

Defining

$$E = \frac{1}{2}\sum_{j=1}^{n}\sum_{i=1}^{n}\frac{A_{ij}}{\beta_{ij}}V'^{2}_{ij}, \quad \beta_{ij} > 0 \tag{5.123}$$

we get

$$\frac{dE}{dt} = \sum_{j=1}^{n}\sum_{i=1}^{n}\frac{A_{ij}}{\beta_{ij}}V'_{ij}\frac{dV'_{ij}}{dt} \tag{5.124}$$

$$= -\sum_{j=1}^{n}\sum_{i=1}^{n}\frac{A_{ij}}{\beta_{ij}}V'_{ij}\left[T_{ij}(\overline{V}_{ij} + V'_{ij})(\overline{V}_{ij} + V'_{ij}) - T_{ij}(\overline{V}_{ij})\overline{V}_{ij}\right] + \sum_{j=1}^{n}\sum_{i=1}^{n}A_{ij}V'_{ij}(p'_i - p'_j) \tag{5.125}$$

The pressure terms vanish since

$$\sum_{j=1}^{n}\sum_{i=1}^{n}A_{ij}V'_{ij}p'_i = \sum_{i=1}^{n}\sum_{j=1}^{n}A_{ij}V'_{ij}p'_i \tag{5.126}$$

$$= \sum_{i=1}^{n}\left(p'_i\sum_{j=1}^{n}A_{ij}V'_{ij}\right) \tag{5.127}$$

$$= 0 \tag{5.128}$$

and

$$\sum_{j=1}^{n}\sum_{i=1}^{n}A_{ij}V'_{ij}p'_j = \sum_{j=1}^{n}\left(p'_j\sum_{i=1}^{n}A_{ij}V'_{ij}\right) \tag{5.129}$$

$$= 0 \tag{5.130}$$

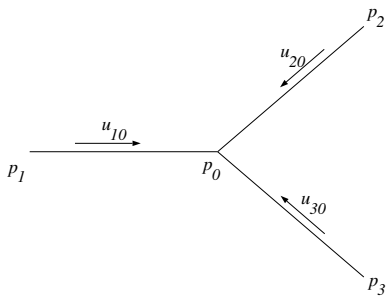

Figure 5.11: Star network.

The terms that are left in equation (5.125) are similar to those in equation (5.30) and satisfy the same inequality. Since $E \geq 0$ and $dE/dt \leq 0$, the steady state is globally stable. For this reason the steady state is also unique.

Example 5.3

Show that the flow in the the star network shown in Fig. 5.11 is globally stable. The pressures p_1, p_2 and p_3 are known while the pressure p_0 and velocities V_{10}, V_{20} and V_{30} are the unknowns.

For branches $i = 1, 2, 3$, equation (5.6) is

$$\frac{dV_{i0}}{dt} + T_{i0}(V_{i0})V_{i0} = \beta_{i0}(p_i - p_0) \tag{5.131}$$

Equation (5.110) at the junction gives

$$\sum_{i=1}^{3} A_{i0}V_{i0} = 0 \tag{5.132}$$

In the steady state

$$T_{i0}(\overline{V}_{i0})\overline{V}_{i0} = \beta_{i0}(p_i - \overline{p}_0) \tag{5.133}$$

$$\sum_{i=1}^{3} A_{i0}\overline{V}_{i0} = 0 \tag{5.134}$$

Substituting $V_{i0} = \overline{V}_{i0} + V'_{i0}$ and $p_0 = \overline{p}_0 + p'_0$ in equations (5.131) and (5.132) and subtracting equations (5.133) and (5.134), we find that

$$\frac{dV'_{i0}}{dt} = -\left[T_{i0}(\overline{V}_{i0} + V'_{i0})(\overline{V}_{i0} + V'_{i0}) - T_{i0}(\overline{V}_{i0})\overline{V}_{i0}\right] - \beta_{i0}p'_0 \tag{5.135}$$

$$\sum_{i=1}^{3} A_{i0}V'_{i0} = 0 \tag{5.136}$$

If we define

$$E = \frac{1}{2}\sum_{i=1}^{3} \frac{A_{i0}}{\beta_{i0}} V'^2_i \tag{5.137}$$

we find that

$$\frac{dE}{dt} = \sum_{i=1}^{3} \frac{A_{i0}}{\beta_{i0}} V'_{i0}\frac{dV'_{i0}}{dt} \tag{5.138}$$

$$= -\sum_{i=1}^{3} \frac{A_{i0}}{\beta_{i0}} V'_{i0}\left[T_{i0}(\overline{V}_{i0} + V'_{i0})(\overline{V}_{i0} + V'_{i0}) - T_{i0}(\overline{V}_{i0})\overline{V}_{i0}\right] - p'_0\sum_{i=1}^{3} A_{i0}V'_{i0} \tag{5.139}$$

The last term vanishes because of equation (5.136). Thus

$$\frac{dE}{dt} = -\sum_{i=1}^{3} \frac{A_{i0}}{\beta_{i0}} V'_{i0} \overline{V}_{i0} \left[T_{i0}(\overline{V}_{i0} + V'_{i0}) - T_{i0}(\overline{V}_{i0}) \right] - \sum_{i=1}^{3} \frac{A_{i0}}{\beta_{i0}} V'^{2}_{i0} T_{i0}(\overline{V}_{i0} + V'_{i0}) \tag{5.140}$$

Since $E \geq 0$ and $dE/dt \leq 0$, E is a Lyapunov function and the steady state is globally stable.

5.8.2 Thermal networks

[61]

5.9 Thermal control

5.9.1 Control with heat transfer coefficient

5.9.2 Multiple room temperatures

Let there be n interconnected rooms. The wall temperature of room i is T_i^w and the air temperature is T_i^a. The heat balance equation for this room is

$$M_i^a c^w \frac{dT_i^w}{dt} = h_i A_i (T_i^a - T_i^w) + U_i A_i^e (T^e - T_i^w) \tag{5.141}$$

$$M_i^a c^a \frac{dT_i^a}{dt} = h_i A_i (T_i^w - T_i^a) + \frac{1}{2} c^a \sum_j (m_{ji}^a + |m_{ji}^a|) T_j^a - \frac{1}{2} c^a \sum_j (m_{ij}^a + |m_{ij}^a|) T_i^a + q_i \tag{5.142}$$

where T^e is the exterior temperature, m_{ij} is the mass flow rate of air from room i to room j. By definition $m_{ij} = -m_{ji}$. Since m_{ii} has no meaning and can be arbitrarily taken to be zero, m_{ij} is an anti-symmetric matrix. Also, from mass conservation for a single room, we know that

$$\sum_j m_{ji}^a = 0 \tag{5.143}$$

Analysis

The unknowns in equations (5.141) and (5.142) are the $2n$ temperatures T_i^w and T_i^a.
(i) Steady state with $U = 0$
(a) The equality

$$\sum_i \sum_j (m_{ji}^a + |m_{ji}^a|) T_j^a - \sum_i \sum_j (m_{ij}^a + |m_{ij}^a|) T_i^a = 0 \tag{5.144}$$

can be shown by interchanging i and j in the second term. Using this result, the sum of equations (5.141) and (5.142) for all rooms gives

$$\sum_i q_i = 0 \tag{5.145}$$

which is a necessary condition for a steady state.
(b) Because the sum of equations (5.141) and (5.142) for all rooms gives an identity, the set of equations is not linearly independent. Thus the steady solution is not unique unless one of the room temperatures is known.

Control

The various proportional control schemes possible are:

- Control of individual room heating

$$q_i = -K_i(T_i^a - T_i^{set}) \tag{5.146}$$

- Control of mass flow rates

$$m_{ji}^a = f_{ij}(T_j^a, T_i^a, T_i^{set}) \tag{5.147}$$

Similar on-off control schemes can also be proposed.

5.9.3 Two rooms

Consider two interconnected rooms 1 and 2 with mass flow m from 1 to 2. Also there is leakage of air into room 1 from the exterior at rate m, and leakage out of room 2 to the exterior at the same rate. The energy balances for the two rooms give

$$\begin{aligned} M_1 c^a \frac{dT_1}{dt} &= U_1 A_1 (T^e - T_1) + \frac{1}{2}(m + |m|)(T^e - T_1) \\ &\quad -\frac{1}{2}(m - |m|)(T_2 - T_1) + q_1 \end{aligned} \tag{5.148}$$

$$\begin{aligned} M_2 c^a \frac{dT_2}{dt} &= U_2 A_2 (T^e - T_2) - \frac{1}{2}(m - |m|)(T^e - T_2) \\ &\quad +\frac{1}{2}(m + |m|)(T_1 - T_2) + q_2 \end{aligned} \tag{5.149}$$

The overall mass balance can be given by the sum of the two equations to give

$$\begin{aligned} M_1 c^a \frac{dT_1}{dt} + M_2 c^a \frac{dT_2}{dt} &= U_1 A_1 (T^e - T_1) + U_2 A_2 (T^e - T_2) + |m| T^e \\ &\quad +\frac{1}{2}(m - |m|)T_1 - \frac{1}{2}(m + |m|)T_2 \\ &\quad +q_1 + q_2 \end{aligned} \tag{5.150}$$

One example of a control problem would be to change m to keep the temperatures of the two rooms equal. Delay can be introduced by writing $T_2 = T_2(t - \tau)$ and $T_1 = T_1(t - \tau)$ in the second to last terms of equations (5.148) and (5.149), respectively, where τ is the time taken for the fluid to get from one room to the other.

5.9.4 Temperature in long duct

The diffusion problem of the previous section does not have advection. Transport of fluids in ducts introduces a delay between the instant the particles of fluid go into the duct and when they come out, which creates a difficulty for outlet temperature control. The literature includes applications to hot-water systems [43, 128] and buildings [8, 159]; transport [197] and heater [40, 41] delay and the effect of the length of a duct on delay [46] have also been looked at.

A long duct of constant cross section, schematically shown in Fig. 5.12 where the flow is driven by a variable-speed pump, illustrates the basic issues [4, 7]. The fluid inlet temperature T_{in} is kept

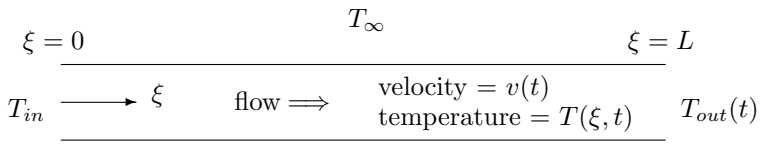

Figure 5.12: Schematic of duct.

constant, and there is heat loss to the constant ambient temperature T_∞ through the surface of the duct.

With a one-dimensional approximation, energy conservation gives

$$\frac{\partial T}{\partial t} + v\frac{\partial T}{\partial \xi} + \frac{4h}{\rho c D}\,(T - T_\infty) = 0, \tag{5.151}$$

with the boundary condition $T(0,t) = T_{in}$, where $T(\xi,t)$ is the fluid temperature, t is time, ξ is the distance along the duct measured from the entrance, $v(t)$ is the flow velocity, h is the coefficient of heat transfer to the exterior, ρ is the fluid density, c is its specific heat, and D is the hydraulic diameter of the duct. The flow velocity is taken to be always positive, so that the $\xi = 0$ end is always the inlet and $\xi = L$ the outlet, where L is the length of the duct. The temperature of the fluid coming out of the duct is $T_{out}(t)$.

Using the characteristic quantities of L for length, $\rho c D/4h$ for time, and $hL/\rho c D$ for velocity, the non-dimensional version of Eq. (5.151) is

$$\frac{\partial \theta}{\partial t} + v\frac{\partial \theta}{\partial \xi} + \theta = 0, \tag{5.152}$$

where $\theta = (T - T_\infty)/(T_{in} - T_\infty)$, with $\theta(0,t) = 1$. The other variables are now non-dimensional. Knowing $v(t)$, this can be solved to give

$$\theta(\xi, t) = e^{-t}\; f\left(\xi - \int_0^t v(s)\; ds\right), \tag{5.153}$$

where the initial startup interval in which the fluid within the duct is flushed out has been ignored; f is an arbitrary function. Applying the boundary condition at $\xi = 0$ gives

$$1 = e^{-t}\; f\left(-\int_0^t v(s)\; ds\right). \tag{5.154}$$

The temperature at the outlet of the duct, *i.e.* at $\xi = 1$, is

$$\theta_{out}(t) = e^{-t}\; f\left(1 - \int_0^t v(s).\; ds\right) \tag{5.155}$$

Eqs. (5.154) and (5.155) must be simultaneously solved to get the outlet temperature $\theta_{out}(t)$ in terms of the flow velocity v.

The problem is non-linear if the outlet temperature $T_{out}(t)$ is used to control the flow velocity $v(t)$. The delay between the velocity change and its effect on the outlet temperature can often lead instability, as it does in other applications [16, 69, 74, 174]. Fig. 5.13 shows a typical result using PID control in which the system is unstable. Shown are the outlet temperature, flow velocity and residence time of the fluid in the duct, all of which ultimately achieve constant amplitude oscillations.

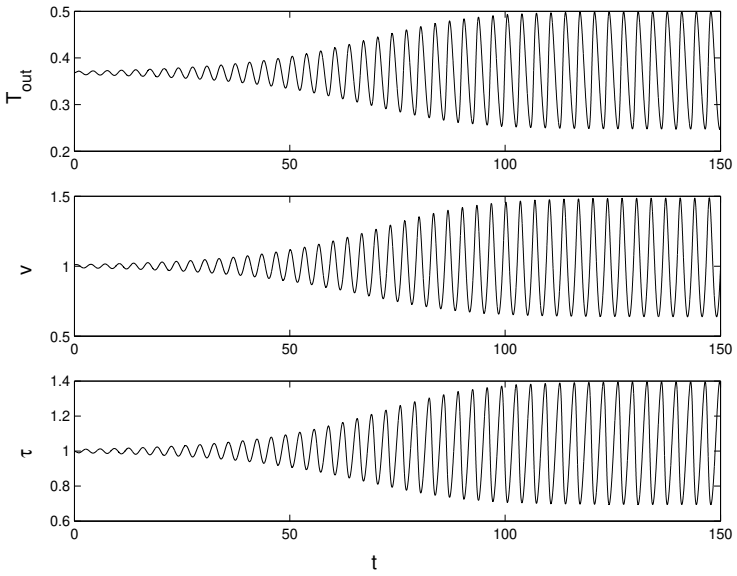

Figure 5.13: Outlet temperature, velocity and residence time for $K_i = -5$ and $K_p = 2.5$ [4].

Problems

1. Determine the single duct solutions for heat loss by radiation $q = P\epsilon\sigma(T_{sur}^4 - T^4)$.
2. A sphere, initially at temperature T_i is being cooled by natural convection to fluid at T_∞. Churchill's correlation for natural convection from a sphere is

$$\overline{Nu} = 2 + \frac{0.589\ Ra_D^{1/4}}{\left[1 + (0.469/Pr)^{9/16}\right]^{4/9}},$$

where

$$Ra_D = \frac{g\beta(T_s - T_\infty)D^3}{\nu\alpha}.$$

Assume that the temperature within the sphere $T(t)$ is uniform, and that the material properties are all constant. Derive the governing equation, and find a two-term perturbation solution.

3. The velocity field, $u(r)$, for forced convection in a cylindrical porous medium is given by

$$u'' + r^{-1}u' - s^2u + s^2\ Da = 0,$$

where s and the Darcy number Da are parameters. A WKB solution for small Da has been reported as[2]

$$u = Da\left[1 - \frac{e^{-s(1-r)}}{\sqrt{r}}\right].$$

Re-do to check the analysis.

4. Consider one-dimensional steady-state flow along a pipe with advection and conduction in the fluid and lateral convection from the side. The fluid inlet and outlet temperatures given. Use the nondimensional version of the governing equation to find the inner and outer matched temperature distributions if the fluid thermal conductivity is small.

[2]K. Hooman and A.A. Ranjbar-Kani, Forced convection in a fluid-saturated porous-medium tube with isoflux wall, International Communcications in Heat and Mass Transfer, Vol. 30, No. 7, pp. 1015–1026, 2003.

5. Plot the exact analytical and the approximate boundary layer solutions for Problem 4 for a small value of the conduction parameter.
6. Show that no solution is possible in Problem 4 if the boundary layer is assumed to be on the wrong side.
7. Consider one-dimensional unsteady flow in a tube with a non-negligible wall thickness, as shown in Fig. 17.1. There is conduction along the fluid as well as along the wall of the tube. There is also convection from the outer surface of the tube to the environment as well as from its inner surface to the fluid. Find the governing equations and their boundary conditions. Nondimensionalize.

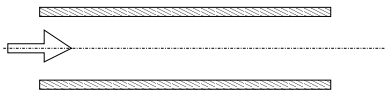

Figure 5.14: Flow in tube with non-negligible wall thickness.

Chapter 6

Natural convection

6.1 Modeling

Let us consider a closed loop, shown in Fig. 6.1, of length L and constant cross-sectional area A filled with a fluid. The loop is heated in some parts and cooled in others. The temperature differences within the fluid leads to a change in density and hence a buoyancy force that creates a natural circulation. The spatial coordinate is s, measured from some arbitrary origin and going around the loop in the counterclockwise direction.

We will make the Boussinesq approximation by which the fluid density is constant except in the buoyancy term. We will also approximate the behavior of the fluid using one spatial dimensions. Thus, we will assume that the velocity u and temperature T are constant across a section of the loop. In general both u and T are functions of space s and time t, though we will find that $u = u(t)$.

6.1.1 Mass conservation

Consider an elemental control volume as shown in Fig. 6.2. The mass fluxes in and out are

$$m^- = \rho_0 u A \tag{6.1}$$

$$m^+ = m^- + \frac{\partial m^-}{\partial s}\, ds \tag{6.2}$$

For a fluid of constant density, there is no accumulation of mass within an elemental control volume, so that the mass flow rate into and out of the control volume must be the same, i.e. $m^- = m^+$. For

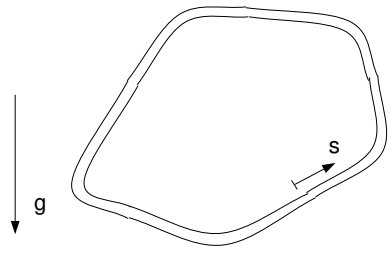

Figure 6.1: A general natural convective loop.

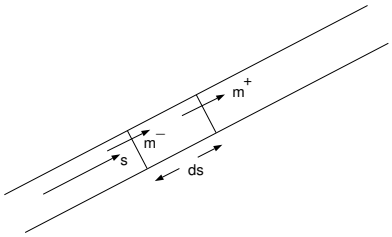

Figure 6.2: Mass flows in an elemental control volume.

a loop of constant cross-sectional area, this implies that u is the same into and out of the control volume. Thus u is independent of s, and must be a function of t alone.

6.1.2 Momentum equation

The forces on an element of length ds, shown in Fig. 6.3, in the positive s direction are: f_v, the viscous force, f_p, the pressure force, and f_g, the component of the gravity force. We can write

$$f_v = -\tau_w \, P \, ds \tag{6.3}$$

$$f_p = -A\frac{\partial p}{\partial s}ds \tag{6.4}$$

$$f_g = -\rho A \, ds \, \tilde{g} \tag{6.5}$$

where τ_w is the wall shear stress, and p is the pressure in the fluid. It is impossible to determine the viscous force f_v through a one-dimensional model, since it is a velocity profile in the tube that is responsible for the shear streass at the wall. For simplicity, however, we will assume a linear relationship between the wall shear stress and the mean fluid velocity, i.e. $\tau_w = \alpha u$. For Poiseuille flow in a duct, which is strictly not the case here but gives an order of magnitude value for the coefficient, this would be

$$\alpha = \frac{8\mu}{D} \tag{6.6}$$

The local component of the acceleration due to gravity has been written in terms of

$$\tilde{g}(s) = g\cos\theta \tag{6.7}$$

$$= g\frac{dz}{ds} \tag{6.8}$$

where g is the usual acceleration in the vertical direction, $\tilde{g}$ is its component in the negative s direction, and dz is the difference in height at the two ends of the element, with z being measured upwards. The integral around a closed loop should vanish, so that

$$\int_0^L \tilde{g}(s) \, ds = 0 \tag{6.9}$$

The density in the gravity force term will be taken to decrease linearly with temperature, so that

$$\rho = \rho_0 \left[1 - \beta(T - T_0)\right] \tag{6.10}$$

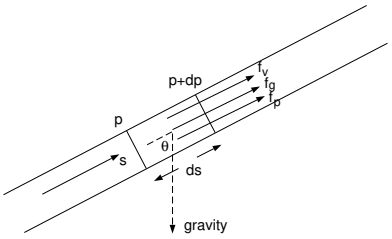

Figure 6.3: Forces on an element of fluid.

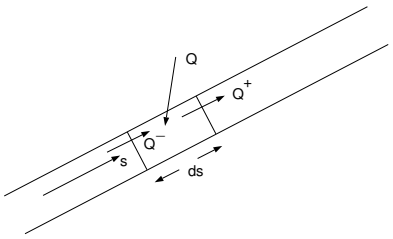

Figure 6.4: Heat rates on an elemental control volume.

Since the mass of the element is $\rho_0 A\ ds$, we can write the momentum equation as

$$\rho_0 A\ ds \frac{du}{dt} = f_v + f_p + f_g \tag{6.11}$$

from which we get

$$\frac{du}{dt} + \frac{P\alpha}{\rho_0 A} u = -\frac{1}{\rho_0}\frac{\partial p}{\partial s} - \left[1 - \beta(T - T_0)\right] \tilde{g} \tag{6.12}$$

Integrating around the loop, we find that the pressure term disappears, and

$$\frac{du}{dt} + \frac{P\alpha}{\rho_0 A} u = \frac{\beta}{L} \int_0^L T\tilde{g}(s)\ ds \tag{6.13}$$

where $u = u(t)$ and $T = T(s,t)$.

6.1.3 Energy equation

Fig. 6.4 shows the heat rates going into and out of an elemental control volume. The heat rate going in is given by

$$Q^- = \rho_0 A u c_p T - kA\frac{\partial T}{\partial s} \tag{6.14}$$

where the first term on the right is due to the advective and second the conductive transports. c_p is the specific heat at constant pressure and k is the coefficient of thermal conductivity. The heat rate going out is

$$Q^+ = Q^- + \frac{\partial Q^-}{\partial s}\ ds \tag{6.15}$$

The difference between the two is

$$\begin{aligned} Q^+ - Q^- &= \frac{\partial Q^-}{\partial s}\ ds \\ &= \left[\rho_0 A u c_p \frac{\partial T}{\partial s} - kA\frac{\partial^2 T}{\partial s^2}\right]\ ds \end{aligned} \tag{6.16}$$

Furthermore, heat is gained from the side at a rate Q, which can be written as

$$Q = q\ ds \tag{6.17}$$

where q is the rate of gain of heat per unit length of the duct.

An energy balance for the elemental control volume gives

$$Q^- + Q = Q^+ + \rho_0 A \; ds \; c_p \frac{\partial T}{\partial t} \tag{6.18}$$

where the last term is the rate of accumulation of energy within the control volume.

Substituting equations (6.16) and (6.17) in (6.18) we get the energy equation

$$\frac{\partial T}{\partial t} + u\frac{\partial T}{\partial s} = \frac{q}{\rho_0 A c_p} + \frac{k}{\rho_0 c_p}\frac{\partial^2 T}{\partial s^2} \tag{6.19}$$

6.2 Known heat rate

[164, 165]

The simplest heating condition is when the heat rate per unit length, $q(s)$, is known all along the loop. For zero mean heating, we have

$$\int_0^L q(s) \; ds = 0 \tag{6.20}$$

$q(s) > 0$ indicates heating, and $q(s) < 0$ cooling.

6.2.1 Steady state, no axial conduction

Neglecting axial conduction, the steady-state governing equations are

$$\frac{P\alpha}{\rho_0 A}\overline{u} = \frac{\beta}{L}\int_0^L \overline{T}(s)\tilde{g}(s) \; ds \tag{6.21}$$

$$\overline{u}\frac{d\overline{T}}{ds} = \frac{q(s)}{\rho_0 A c_p} \tag{6.22}$$

The solution of equation (6.22) gives us the temperature field

$$\overline{T}(s) = \frac{1}{\rho_0 A c_p \overline{u}}\int_0^s q(s') \; ds' + T_0 \tag{6.23}$$

where $\overline{T}(0) = T_0$. Using equation (6.9) it can be checked that $T(L) = T_0$ also. Substituting in equation (6.21), we get

$$\frac{P\alpha}{\rho_0 A}\overline{u} = \frac{\beta}{\rho_0 A c_p L \overline{u}}\int_0^L \left[\int_0^s q(s') \; ds'\right] \tilde{g}(s) \; ds \tag{6.24}$$

from which

$$\overline{u} = \pm\sqrt{\frac{\beta}{P\alpha L c_p}\int_0^L \left[\int_0^s q(s') \; ds'\right] \tilde{g}(s) \; ds} \tag{6.25}$$

Two real solutions exist for

$$\int_0^L \left[\int_0^s q(s') \; ds'\right] \tilde{g}(s) \; ds \geq 0 \tag{6.26}$$

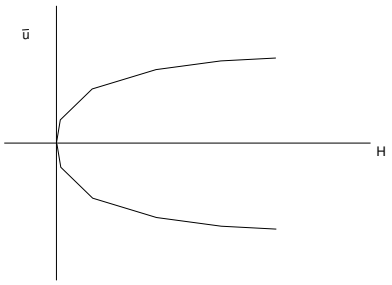

Figure 6.5: Bifurcation with respect to parameter H.

and none otherwise. Thus there is a bifurcation from no solution to two as the parameter H passes through zero, where

$$H = \int_0^L \left[\int_0^s q(s')\ ds' \right] \tilde{g}(s)\ ds \tag{6.27}$$

The pressure distribution can be found from equation (6.12)

$$\frac{d\overline{p}}{ds} = -\frac{P\alpha\overline{u}}{A} - \rho_0 \left[1 - \beta(\overline{T} - T_0)\right] \tilde{g} \tag{6.28}$$

$$= -\frac{P\alpha\overline{u}}{A} - \rho_0\tilde{g} + \frac{\beta}{Ac_p\overline{u}} \left[\int_0^s q(s')\ ds' \right] \tilde{g} \tag{6.29}$$

from which

$$\overline{p}(s) = p_0 - \frac{P\alpha\overline{u}}{A}\ s - \rho_0 \int_0^s \tilde{g}(s')\ ds' + \frac{\beta}{Ac_p\overline{u}} \int_0^s \left[\int_0^{s''} q(s')\ ds' \right] \tilde{g}(s'')\ ds'' \tag{6.30}$$

where $\overline{p}(0) = p_0$. Using equations (6.9) and (6.24), it can be shown that $\overline{p}(L) = p_0$ also.

Example 6.1

Find the temperature distributions and velocities in the three heating and cooling distributions corresponding to Fig. 6.6. (a) Constant heating between points c and d, and constant cooling between h and a. (b) Constant heating between points c and d, and constant cooling between g and h. (c) Constant heating between points d and e, and constant cooling between h and a. (d) Constant heating between points a and c, and constant cooling between e and g. The constant value is $\hat{q}$, and the total length of the loop is L.

Let us write

$$F(s) = \int_0^s q(s')\ ds' \tag{6.31}$$

$$G(s) = F(s)g(s) \tag{6.32}$$

$$H = \int_0^L G(s)\ ds \tag{6.33}$$

The functions $F(s)$ and $G(s)$ are shown in Fig. 6.7. The origin is at point a, and the coordinate s runs counterclockwise. The integral H in the four cases is: (a) $H = 0$, (b) $H = \hat{q}L/8$, (c) $H = -\hat{q}L/8$, (d) $H = \hat{q}L/4$.

The fluid velocity is

$$\overline{u} = \pm\sqrt{\frac{\beta H}{P\alpha L c_p}} \tag{6.34}$$

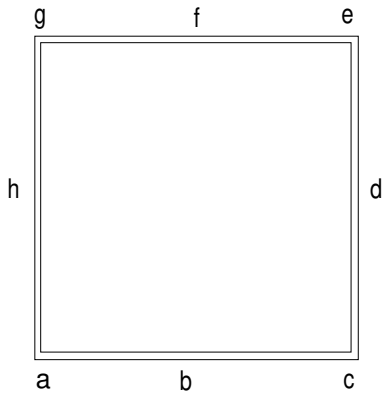

Figure 6.6: Geometry of a square loop.

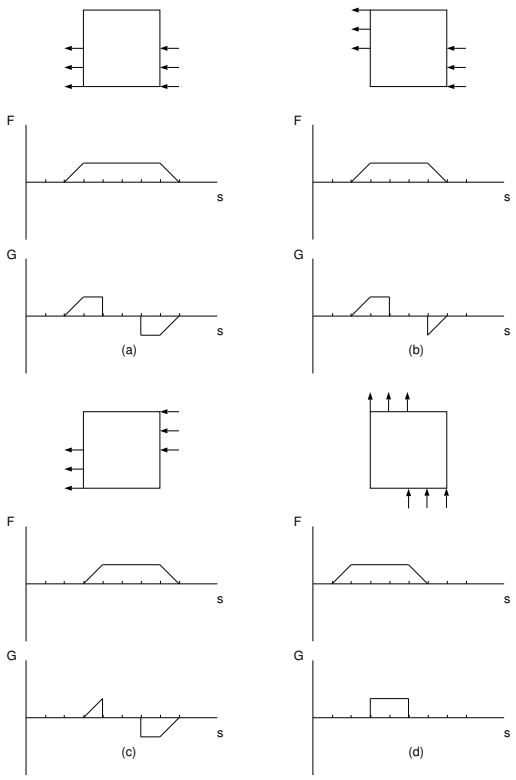

Figure 6.7: Functions $F(s)$ and $G(s)$ for the four cases.

No real solution exists for case (c); the velocity is zero for (a); the other two cases have two solutions each, one positive and the other negative. The temperature distribution is given by

$$\overline{T} - T_0 = \frac{F(s)}{\rho_0 A c_p \overline{u}} \tag{6.35}$$

The function $F(s)$ is shown in Fig. 6.7. There is no real; solution for case (c); for (a), the temperature is unbounded since the fluid is not moving; for the other two cases there are two temperature fields, one the negative of the other.

The pressure distribution can be found from equation (6.29).

Example 6.2

What is the physical interpretation of condition (6.26)?

Let us write

$$H = \int_0^L \left[\int_0^s q(s')\ ds'\right]\ \tilde{g}(s)\ ds \tag{6.36}$$

$$= \int_0^L \left[\int_0^s q(s')\ ds'\right]\ d\left[\int_0^s \tilde{g}(s')\ ds'\right] \tag{6.37}$$

$$= \left[\int_0^s q(s')\ ds'\right]_0^L \left[\int_0^s \tilde{g}(s')\ ds'\right]_0^L - \int_0^L \left[q(s)\int_0^s \tilde{g}(s')\ ds'\right]\ ds \tag{6.38}$$

The first term on the right vanishes due to equations (6.20) and (6.9). Using equation (6.8), we find that

$$H = -g\int_0^L q(s)z(s)\ ds \tag{6.39}$$

The function $z(s)$ is another way of describing the geometry of the loop. We introduce the notation

$$q(s) = q^+(s) - q^-(s) \tag{6.40}$$

where

$$q^+ = \begin{cases} q(s) & \text{for} \quad q(s) > 0 \\ 0 & \text{for} \quad q(s) \le 0 \end{cases} \tag{6.41}$$

and

$$q^- = \begin{cases} 0 & \text{for} \quad q(s) \ge 0 \\ -q(s) & \text{for} \quad q(s) < 0 \end{cases} \tag{6.42}$$

Equations (6.20) and (6.39) thus becomes

$$\int_0^L q^+(s)\ ds = \int_0^L q^-(s)\ ds \tag{6.43}$$

$$H = -g\left[\int_0^L q^+(s)z(s)\ ds - \int_0^L q^-(s)z(s)\ ds\right] \tag{6.44}$$

From these, condition (6.26) which is $H \ge 0$ can be found to be equivalent to

$$\frac{\int_0^L q^+(s)z(s)\ ds}{\int_0^L q^+(s)\ ds} < \frac{\int_0^L q^-(s)z(s)\ ds}{\int_0^L q^-(s)\ ds} \tag{6.45}$$

This implies that the height of the centroid of the heating rate distribution should be above that of the cooling.

6.2.2 Axial conduction effects

To nondimensionalize and normalize equations (6.13) and (6.19), we take

$$t^* = \frac{t}{\tau} \tag{6.46}$$

$$s^* = \frac{s}{L} \tag{6.47}$$

$$u^* = \frac{u}{VG^{1/2}} \tag{6.48}$$

$$T^* = \frac{T - T_0}{\Delta T\ G^{1/2}} \tag{6.49}$$

$$\tilde{g}^* = \frac{\tilde{g}}{g} \tag{6.50}$$

$$q^* = \frac{q}{q_m} \tag{6.51}$$

where

$$V = \frac{P\alpha L}{\rho_0 A} \tag{6.52}$$

$$\Delta T = \frac{P^2\alpha^2 L}{\beta g \rho_0^2 A^2} \tag{6.53}$$

$$\tau = \frac{\rho_0 A}{P\alpha} \tag{6.54}$$

$$G = \frac{q_m \beta g \rho_0^2 A^2}{P^3 \alpha^3 L c_p} \tag{6.55}$$

Substituting, we get

$$\frac{du^*}{dt^*} + u^* = \int_0^1 T^* \tilde{g}^*\ ds^* \tag{6.56}$$

$$\frac{\partial T^*}{\partial t^*} + G^{1/2} u^* \frac{\partial T^*}{\partial s^*} = G^{1/2} q^* + K \frac{\partial^2 T^*}{\partial s^{*2}} \tag{6.57}$$

where

$$K = \frac{kA}{P\alpha L^2 c_p} \tag{6.58}$$

The two nondimensional parameters which govern the problem are G and K.

Under steady-state conditions, and neglecting axial conduction, the temperature and velocity are

$$\overline{T}^*(s) = \frac{1}{\overline{u}^*} \int_0^{s^*} q^*(s_1^*)\ ds_1^* \tag{6.59}$$

$$\overline{u}^* = \pm \sqrt{\int_0^1 \left[\int_0^{s^*} q^*(s_1^*)\ ds_1^* \right] \tilde{g}^*(s^*)\ ds^*} \tag{6.60}$$

All variables are of unit order indicating that the variables have been appropriately normalized.

For $\alpha = 8\mu/D$, $A = \pi D^2/4$, and $P = \pi D$, we get

$$G = \frac{1}{8192\pi}\,\frac{Gr}{Pr}\,\left(\frac{D}{L}\right)^4 \tag{6.61}$$

$$K = \frac{1}{32\ Pr}\,\left(\frac{D}{L}\right)^2 \tag{6.62}$$

where the Prandtl and Grashof numbers are

$$Pr = \frac{\mu c_p}{k} \tag{6.63}$$

$$Gr = \frac{q_m g \beta L^3}{\nu^2 k} \tag{6.64}$$

respectively. Often the Rayleigh number defined by

$$Ra = Gr\ Pr \tag{6.65}$$

is used instead of the Grashof number.

Since $\overline{u}^*$ is of $O(1)$, the dimensional velocity is of order $(8\nu L/D^2)Gr^{1/2}$. The ratio of axial conduction to the advective transport term is

$$\epsilon = \frac{K}{G^{1/2}} \tag{6.66}$$

$$= \left(\frac{8\pi}{Ra}\right)^{1/2} \tag{6.67}$$

Taking typical numerical values for a loop with water to be: $\rho = 998$ kg/m^3, $\mu = 1.003 \times 10^{-3}$ kg/m s, $k = 0.6$ W/m K, $q_m = 100$ W/m, $g = 9.91$ m/s^2, $\beta = 0.207 \times 10^{-3}$ K^{-1}, $D = 0.01$ m, $L = 1$ m, $c_p = 4.18 \times 10^3$ J/kgK, we get the velocity and temperature scales to be

$$VG^{1/2} = \tag{6.68}$$

$$\Delta T G^{1/2} = \tag{6.69}$$

and the nondimensional numbers as

$$G = 1.86 \times 10^{-2} \tag{6.70}$$

$$K = 4.47 \times 10^{-7} \tag{6.71}$$

$$Gr = 3.35 \times 10^{11} \tag{6.72}$$

$$Ra = 2.34 \times 10^{12} \tag{6.73}$$

$$\epsilon = 3.28 \times 10^{-6} \tag{6.74}$$

Axial conduction is clearly negligible in this context.

For a steady state, equations (6.56) and (6.57) are

$$\overline{u}^* = \int_0^1 \overline{T}^* \tilde{g}^*\ ds^* \tag{6.75}$$

$$\epsilon \frac{d^2\overline{T}^*}{ds^{*2}} - \overline{u}^* \frac{d\overline{T}^*}{ds^*} = -q^*(s^*) \tag{6.76}$$

Integrating over the loop from $s^* = 0$ to $s^* = 1$, we find that continuity of $\overline{T}^*$ and equation (6.20) imply continuity of $d\overline{T}^*/ds^*$ also.

Conduction-dominated flow

If $\lambda = G^{1/2}/\epsilon \ll 1$, axial conduction dominates. We can write

$$\overline{u} = \overline{u}_0 + \lambda\overline{u}_1 + \lambda^2\overline{u}_2 + \ldots \tag{6.77}$$

$$\overline{T}(s) = \overline{T}_0(s) + \lambda\overline{T}_1(s) + \lambda^2\overline{T}_2(s) + \ldots \tag{6.78}$$

where, for convenience, the asterisks have been dropped. Substituting into the governing equations, and collecting terms of $O(\lambda^0)$, we have

$$\overline{u}_0 = \int_0^1 \overline{T}_0\tilde{g}\ ds \tag{6.79}$$

$$\frac{d^2\overline{T}_0}{ds^2} = 0 \tag{6.80}$$

The second equation, along with conditions that $\overline{T}_0$ and $d\overline{T}_0/ds$ have the same value at $s = 0$ and $s = 1$, gives $\overline{T}_0 =$ an arbitrary constant. The first equation gives $\overline{u}_0 = 0$.

The terms of $O(\lambda)$ give

$$\overline{u}_1 = \int_0^1 \overline{T}_1\tilde{g}\ ds \tag{6.81}$$

$$\frac{d^2\overline{T}_1}{ds^2} = -q(s) + \overline{u}_0\frac{d\overline{T}_0}{ds} \tag{6.82}$$

The second equation can be integrated once to give

$$\frac{d\overline{T}_1}{ds} = -\int_0^s q(s')\ ds' + A \tag{6.83}$$

and again

$$\overline{T}_1 = -\int_0^s \left[\int_0^{s''} q(s')\ ds'\right]\ ds'' + As + B \tag{6.84}$$

Continuity of $\overline{T}_1(s)$ and $d\overline{T}_1/ds$ at $s = 0$ and $s = 1$ give

$$B = -\int_0^1 \left[\int_o^{s''} q(s')\ ds'\right]\ ds'' + A + B \tag{6.85}$$

$$A = A \tag{6.86}$$

respectively, from which

$$A = \int_0^1 \left[\int_0^{s''} q(s')\ ds'\right]\ ds'' \tag{6.87}$$

and that B can be arbitrary. Thus

$$\overline{T}_1 = \int_0^s \left[\int_0^{s''} q(s')\ ds'\right]\ ds'' + s\int_0^1 \left[\int_0^{s''} q(s')\ ds'\right]\ ds'' + T_1(0) \tag{6.88}$$

where $\overline{T}(0)$ is an arbitrary constant. Substituting in equation (6.81), gives

$$\overline{u}_1 = -\int_0^1 \left\{ \int_0^s \left[\int_0^{s''} q(s')\ ds' \right]\ ds'' \right\} \tilde{g}\ ds + \int_0^1 \left[\int_0^{s''} q(s')\ ds' \right]\ ds'' \int_0^1 s\tilde{g}\ ds \tag{6.89}$$

The temperature distribution is determined by axial conduction, rather than by the advective velocity, so that the resulting solution is unique.

Advection-dominated flow

The governing equations are

$$\overline{u} = \int_0^1 \overline{T}\tilde{g}\ ds \tag{6.90}$$

$$\overline{u}\frac{d\overline{T}}{ds} = q + \epsilon\frac{d^2\overline{T}}{ds^2} \tag{6.91}$$

where $\epsilon \ll 1$. Expanding in terms of ϵ, we have

$$\overline{u} = \overline{u}_0 + \epsilon\overline{u}_1 + \epsilon^2\overline{u}_2 + \ldots \tag{6.92}$$

$$\overline{T} = \overline{T}_0 + \epsilon\overline{T}_1 + \epsilon^2\overline{T}_2 + \ldots \tag{6.93}$$

$$\tag{6.94}$$

To $O(\epsilon^0)$, we get

$$\overline{u}_0 = \int_0^1 \overline{T}_0\tilde{g}\ ds \tag{6.95}$$

$$\overline{u}_0\frac{d\overline{T}_0}{ds} = q \tag{6.96}$$

from which

$$\overline{T}_0 = \frac{1}{\overline{u}_0}\int_0^s q(s')\ ds' \tag{6.97}$$

$$\overline{u}_0 = \pm\int_0^1 \left[\int_0^s q(s')\ ds' \right] \tilde{g}\ ds \tag{6.98}$$

Axial conduction. therefore, slightly modifies the two solutions obtained without it.

6.2.3 Toroidal geometry

The dimensional gravity function can be expanded in a Fourier series in s, to give

$$\tilde{g}(s) = \sum_{n=1}^{\infty} \left[g_n^c \cos\frac{2\pi ns}{L} + g_1^s \sin\frac{2\pi ns}{L} \right] \tag{6.99}$$

The simplest loop geometry is one for which we have just the terms

$$\tilde{g}(s) = g_1^c \cos\frac{2\pi s}{L} + g_1^s \sin\frac{2\pi s}{L} \tag{6.100}$$

corresponds to a toroidal geometry. Using

$$g^2 = (g_1^c)^2 + (g_1^s)^2 \tag{6.101}$$

$$\phi_0 = \tan^{-1}\frac{g_1^c}{g_1^s} \tag{6.102}$$

equation (6.100) becomes

$$\tilde{g}(s) = g\cos\left(\frac{2\pi s}{L} - \phi_0\right) \tag{6.103}$$

Without loss of generality, we can measure the angle from the horizontal, i.e. from three o'clock point, and take $\phi_0 = 0$ so that

$$\tilde{g}(s) = g\cos\left(2\pi s/L\right) \tag{6.104}$$

The nondimensional gravity component is

$$\tilde{g} = \cos(2\pi s) \tag{6.105}$$

where the * has been dropped.

Assuming also a sinusoidal distribution of heating

$$q(s) = -\sin(2\pi s - \phi) \tag{6.106}$$

the momentum and energy equations are

$$\overline{u} = \int_0^1 T(s)\cos(2\pi s)\, ds \tag{6.107}$$

$$\overline{u}\frac{d\overline{T}}{ds} = -\sin(2\pi s - \phi) + \epsilon\frac{d^2\overline{T}}{ds^2} \tag{6.108}$$

The homogeneous solution is

$$\overline{T}_h = Be^{\overline{u}s/\epsilon} + A \tag{6.109}$$

The particular integral satisfies

$$\frac{d^2T_p}{ds^2} - \frac{\overline{u}}{\epsilon}\frac{d\overline{T}_p}{ds} = \frac{1}{\epsilon}\sin(2\pi s - \phi) \tag{6.110}$$

Integrating, we have

$$\frac{dT_p}{ds} - \frac{\overline{u}}{\epsilon}\overline{T}_p = -\frac{1}{2\pi\epsilon}\cos(2\pi s - \phi) \tag{6.111}$$

$$= -\frac{1}{2\pi\epsilon}\left[\cos(2\pi s)\cos\phi + \sin(2\pi s)\sin\phi\right] \tag{6.112}$$

Take

$$\overline{T}_p = a\cos(2\pi s) + b\sin(2\pi s) \tag{6.113}$$

from which

$$\frac{d\overline{T}_p}{ds} = -2\pi a\sin(2\pi s) + 2\pi b\cos(2\pi s) \tag{6.114}$$

Substituting and collecting the coefficients of $\cos(2\pi s)$ and $\sin(2\pi s)$, we get

$$-\frac{\overline{u}}{\epsilon}a + 2\pi b = -\frac{\cos\phi}{2\pi\epsilon} \tag{6.115}$$

$$-2\pi a - \frac{\overline{u}}{\epsilon}b = -\frac{\sin\phi}{2\pi\epsilon} \tag{6.116}$$

The constants are

$$a = \frac{(\overline{u}/2\pi\epsilon^2)\cos\phi + (1/\epsilon)\sin\phi}{4\pi^2 + \overline{u}^2/\epsilon^2} \tag{6.117}$$

$$b = \frac{-(1/\epsilon)\cos\phi + (\overline{u}/2\pi\epsilon^2)\sin\phi}{4\pi^2 + \overline{u}^2/\epsilon^2} \tag{6.118}$$

The temperature field is given by

$$\overline{T} = \overline{T}_h + \overline{T}_p \tag{6.119}$$

Since $\overline{T}(0) = \overline{T}(1)$, we must have $B = 0$. Taking the other arbitrary constant A to be zero, we have

$$\overline{T} = \frac{1}{4\pi^2 + \overline{u}^2/\epsilon^2}\left[\left(\frac{\overline{u}}{2\pi\epsilon^2}\cos\phi + \frac{1}{\epsilon}\sin\phi\right)\cos(2\pi s) + \left(-\frac{1}{\epsilon}\cos\phi + \frac{\overline{u}}{2\pi\epsilon^2}\sin\phi\right)\sin(2\pi s)\right] \tag{6.120}$$

The momentum equation gives

$$\overline{u} = \frac{(\overline{u}/2\pi\epsilon^2)\cos\phi + (1/\epsilon)\sin\phi}{2(4\pi^2 + \overline{u}^2/\epsilon^2)} \tag{6.121}$$

which can be written as

$$\overline{u}^3 + \overline{u}\left(4\pi^2\epsilon^2 - \frac{1}{4\pi}\cos\phi\right) - \frac{\epsilon}{2}\sin\phi = 0 \tag{6.122}$$

Special cases are:

- $\epsilon = 0$

  Equations (6.107) and (6.108) can be solved to give

  $$\overline{T} = \frac{1}{2\pi\overline{u}}\left[\cos(2\pi s)\cos\phi + \sin(2\pi s)\sin\phi\right] \tag{6.123}$$

  $$\overline{u} = \pm\sqrt{\frac{\cos\phi}{4\pi}} \tag{6.124}$$

  On the other hand substituting $\epsilon = 0$ in equation (6.122) gives an additional spurious solution $\overline{u} = 0$.

- $\epsilon \to \infty$

  We get that $\overline{u} \to 0$.

- $\phi = 0$

  We get

  $$\overline{u} = \begin{cases} 0 \\ \sqrt{\frac{1}{4\pi} - 4\pi^2\epsilon^2} \\ -\sqrt{\frac{1}{4\pi} - 4\pi^2\epsilon^2} \end{cases} \tag{6.125}$$

  The last two solutions exist only when $\epsilon < (16\pi^3)^{-1/2}$.

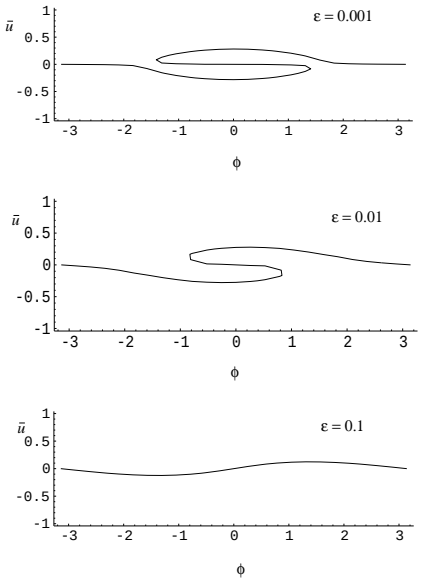

Figure 6.8: $\overline{u}$-ϕ curves.

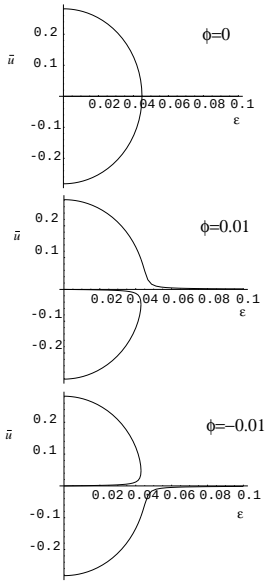

Figure 6.9: $\overline{u}$-ϵ curves.

- $\phi = \pi/2$

  The velocity is a solution of

$$\overline{u}^3 + \overline{u} 4\pi^2 \epsilon^2 - \frac{\epsilon}{2} = 0 \tag{6.126}$$

Figure 6.8 shows $\overline{u}$-ϕ curves for three different values of ϵ. Figure 6.9 and 6.10 show $\overline{u}$-ϵ curves for different values of ϕ. It is also instructive to see the curve u-Ra, shown in Figure 6.11, since the Rayleigh number is directly proportional to the strength of the heating.

The bifurcation set is the line dividing the regions with only one real solution and that with three real solutions. A cubic equation

$$x^3 + px + q = 0 \tag{6.127}$$

has a discriminant

$$D = \frac{p^3}{27} + \frac{q^2}{4} \tag{6.128}$$

For $D < 0$, there are three real solutions, and for $D > 0$, there is only one. The discriminant for the cubic equation (6.122) is

$$D = \frac{1}{27}\left(4\pi^2\epsilon^2 - \frac{1}{4\pi}\cos\phi\right)^3 + \frac{1}{4}\left(\epsilon \sin\phi\right)^2 \tag{6.129}$$

The result is shown in Fig. 6.12.

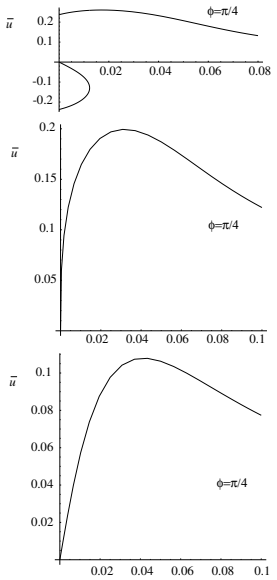

Figure 6.10: More $\overline{u}$-ϵ curves.

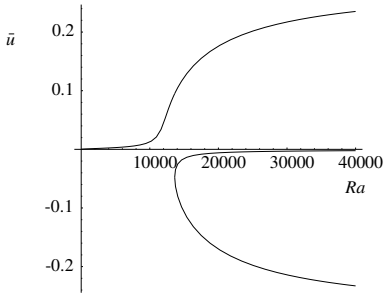

Figure 6.11: $\overline{u}$-Ra for $\phi = 0.01$ radians.

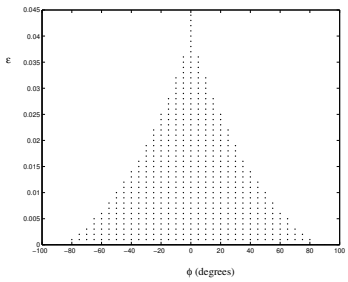

Figure 6.12: Region with three solutions.

6.2.4 Dynamic analysis

We rescale the nondimensional governing equations (6.56) and (6.57) by

$$u^* = \frac{1}{2\pi G^{1/2}}\,\widehat{u} \tag{6.130}$$

$$T^* = \frac{1}{2\pi G^{1/2}}\,\widehat{T} \tag{6.131}$$

to get

$$\frac{du}{dt} + u = \int_0^1 T\tilde{g}\; ds \tag{6.132}$$

$$\frac{\partial T}{\partial t} + \frac{1}{2\pi}\; u\frac{\partial T}{\partial s} = Gq + \frac{G^{1/2}K}{2\pi}\frac{\partial^2 T}{\partial s^2} \tag{6.133}$$

where the hats and stars have been dropped.

We take $\tilde{g} = \cos(2\pi s)$ and $q = -\sin(2\pi s - \phi)$. Expanding the temperature in a Fourier series, we get

$$T(s,t) = T_0(t) + \sum_{n=1}^{\infty}\left[T_n^c(t)\cos(2\pi ns) + T_n^s(t)\sin(2\pi ns)\right] \tag{6.134}$$

Substituting, we have

$$\frac{du}{dt} + u = \frac{1}{2}T_1^c \tag{6.135}$$

and

$$\begin{aligned}
&\frac{dT_0}{dt} + \sum_{n=1}^{\infty}\left[\frac{dT_n^c}{dt}\cos(2\pi ns) + \frac{dT_n^c}{dt}\sin(2\pi ns)\right] \\
&+u\sum_{n=1}^{\infty}\left[-nT_n^c\sin(2\pi ns) + nT_n^s\cos(2\pi ns)\right] \\
&= -G\left[\sin(2\pi s)\cos\phi - \cos(2\pi s)\sin\phi\right] \\
&-2\pi n^2 G^{1/2}K\sum_{n=1}^{\infty}\left[T_n^c\cos(2\pi ns) + T_n^s\sin(2\pi ns)\right]
\end{aligned} \tag{6.136}$$

Integrating, we get

$$\frac{dT_0}{dt} = 0 \tag{6.137}$$

Multiplying by $\cos(2\pi ms)$ and integrating

$$\frac{1}{2}\frac{dT_m^c}{dt} + \frac{m}{2}uT_m^s = \frac{1}{2}G\sin\phi - \pi m^2 G^{1/2}KT_m^c \tag{6.138}$$

Now multiplying by $\sin(2\pi ms)$ and integrating

$$\frac{1}{2}\frac{dT_m^s}{dt} - \frac{m}{2}uT_m^c = -\frac{1}{2}G\cos\phi - \pi m^2 G^{1/2}KT_m^s \tag{6.139}$$

Choosing the variables

$$x = u \tag{6.140}$$
$$y = \frac{1}{2}T_1^c \tag{6.141}$$
$$z = \frac{1}{2}T_1^s \tag{6.142}$$

and the parameters

$$a = \frac{G}{2}\sin\phi \tag{6.143}$$
$$b = \frac{G}{2}\cos\phi \tag{6.144}$$
$$c = 2\pi G^{1/2}K \tag{6.145}$$

we get the dynamical system

$$\frac{dx}{dt} = y - x \tag{6.146}$$
$$\frac{dy}{dt} = a - xz - cy \tag{6.147}$$
$$\frac{dz}{dt} = -b + xy - cz \tag{6.148}$$

The physical significance of the variables are: x is the fluid velocity, y is the horizontal temperature difference, and z is the vertical temperature difference. The parameter c is positive, while a and b can have any sign.

The critical points are found by equating the vector field to zero, so that

$$\overline{y} - \overline{x} = 0 \tag{6.149}$$
$$a - \overline{x}\overline{z} - c\overline{y} = 0 \tag{6.150}$$
$$-b + \overline{x}\overline{y} - c\overline{z} = 0 \tag{6.151}$$

From equation (6.149), we have $\overline{y} = \overline{x}$, and from equation (6.151), we get $\overline{z} = (-b + \overline{x}^2)/c$. Substituting these in equation (6.150), we get

$$\overline{x}^3 + \overline{x}(c^2 - b) - ac = 0 \tag{6.152}$$

This corresponds to equation (6.122), except in different variables.

To analyze the stability of a critical point $(\overline{x}, \overline{y}, \overline{z})$ we add perturbations of the form

$$x = \overline{x} + x' \tag{6.153}$$
$$y = \overline{y} + y' \tag{6.154}$$
$$z = \overline{z} + z' \tag{6.155}$$

Substituting in equation (6.146)-(6.148), we get the local form

$$\frac{d}{dt}\begin{bmatrix} x' \\ y' \\ z' \end{bmatrix} = \begin{bmatrix} -1 & 1 & 0 \\ -\overline{z} & -c & -\overline{x} \\ \overline{y} & \overline{x} & -c \end{bmatrix}\begin{bmatrix} x' \\ y' \\ z' \end{bmatrix} + \begin{bmatrix} 0 \\ -x'z' \\ x'y' \end{bmatrix} \tag{6.156}$$

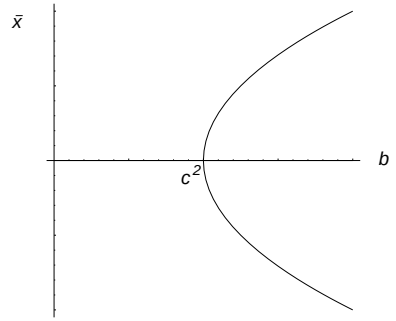

Figure 6.13: Bifurcation diagram for $\overline{x}$.

The linearized version is

$$\frac{d}{dt}\begin{bmatrix} x' \\ y' \\ z' \end{bmatrix} = \begin{bmatrix} -1 & 1 & 0 \\ -\overline{z} & -c & -\overline{x} \\ \overline{y} & \overline{x} & -c \end{bmatrix} \begin{bmatrix} x' \\ y' \\ z' \end{bmatrix} \tag{6.157}$$

No tilt, with axial conduction $(a = 0, c \neq 0)$

From equation (6.152), for $a = 0$ we get

$$\overline{x}^3 + \overline{x}(c^2 - b) = 0 \tag{6.158}$$

from which

$$\overline{x} = \overline{y} = \begin{cases} 0 \\ \sqrt{b - c^2} \\ -\sqrt{b - c^2} \end{cases} \tag{6.159}$$

The z coordinate is

$$\overline{z} = \begin{cases} -b/c \\ -c \\ -c \end{cases} \tag{6.160}$$

The bifurcation diagram is shown in Figure 6.13.

Stability of conductive solution

The critical point is $(0, 0, -b/c)$. To examine its linear stability, we look at the linearized equation (6.157) to get

$$\frac{d}{dt}\begin{bmatrix} x' \\ y' \\ z' \end{bmatrix} = \begin{bmatrix} -1 & 1 & 0 \\ b/c & -c & 0 \\ 0 & 0 & -c \end{bmatrix} \begin{bmatrix} x' \\ y' \\ z' \end{bmatrix} \tag{6.161}$$

The eigenvalues of the matrix are obtained from the equation

$$\begin{vmatrix} -(1+\lambda) & 1 & 0 \\ b/c & -(c+\lambda) & 0 \\ 0 & 0 & -(c+\lambda) \end{vmatrix} = 0 \tag{6.162}$$

which simplifies to

$$(c + \lambda)\left[(1 + \lambda)(c + \lambda) - \frac{b}{c}\right] = 0 \tag{6.163}$$

One eigenvalue is

$$\lambda_1 = -c \tag{6.164}$$

Since $c \geq 0$ this eigenvalue indicates stability. The other two are solutions of

$$\lambda^2 + (c+1)\lambda + (c - \frac{b}{c}) = 0 \tag{6.165}$$

which are

$$\lambda_2 = \frac{1}{2}\left[-(c+1) - \sqrt{(c+1)^2 - 4(c-\frac{b}{c})}\right] \tag{6.166}$$

$$\lambda_3 = \frac{1}{2}\left[-(c+1) + \sqrt{(c+1)^2 - 4(c-\frac{b}{c})}\right] \tag{6.167}$$

λ_2 is also negative and hence stable. λ_3 is negative as long as

$$-(c+1) + \sqrt{(c+1)^2 - 4(c-\frac{b}{c})} < 0 \tag{6.168}$$

which gives

$$b < c^2 \tag{6.169}$$

This is the condition for stability.

In fact, one can also prove global stability of the conductive solution. Restoring the nonlinear terms in equation (6.156) to equation (6.161), we have

$$\frac{dx'}{dt} = y' - x' \tag{6.170}$$

$$\frac{dy'}{dt} = \frac{b}{c}x' - cy' - x'z' \tag{6.171}$$

$$\frac{dz'}{dt} = -cz' + x'y' \tag{6.172}$$

Let

$$E(x,y,z) = \frac{b}{c}x'^2 + y'^2 + z'^2 \tag{6.173}$$

Thus

$$\frac{1}{2}\frac{dE}{dt} = \frac{b}{c}x'\frac{dx'}{dt} + y'\frac{dy'}{dt} + z'\frac{dz'}{dt} \tag{6.174}$$

$$= -\frac{b}{c}x'^2 + \frac{2b}{c}x'y' - cy'^2 - cz'^2 \tag{6.175}$$

$$= -\frac{b}{c}(x'-y')^2 - (c-\frac{b}{c})y'^2 - cz'^2 \tag{6.176}$$

Since

$$E \geq 0 \tag{6.177}$$

$$\frac{dE}{dt} \leq 0 \tag{6.178}$$

for $0 \leq b \leq c^2$, E is a Liapunov function, and the critical point is stable to all perturbations in this region. The bifurcation at $b = c^2$ is thus supercritical.

Stability of convective solution

For $b > c^2$, only one critical point $(\sqrt{b-c^2}, \sqrt{b-c^2}, -c)$ will be considered, the other being similar. We use the linearized equations (6.157). Its eigenvalues are solutions of

$$\begin{vmatrix} -(1+\lambda) & 1 & 0 \\ c & -(c+\lambda) & -\sqrt{b-c^2} \\ \sqrt{b-c^2} & \sqrt{b-c^2} & -(c+\lambda) \end{vmatrix} = 0 \tag{6.179}$$

This can be expanded to give

$$\lambda^3 + \lambda^2(1+2c) + \lambda(b+c) + 2(b-c^2) = 0 \tag{6.180}$$

The Hurwitz criteria for stability require that all coefficients be positive, which they are. Also the determinants

$$D_1 = 1 + 2c \tag{6.181}$$

$$D_2 = \begin{vmatrix} 1+2c & 2(b-c^2) \\ 1 & b+c \end{vmatrix} \tag{6.182}$$

$$D_3 = \begin{vmatrix} 1+2c & 2(b-c^2) & 0 \\ 1 & b+c & 0 \\ 0 & 1+2c & 2(b-c^2) \end{vmatrix} \tag{6.183}$$

should be positive. This requires that

$$b < \frac{c(1+4c)}{1-2c} \quad \text{if} \quad c < 1/2 \tag{6.184}$$

$$b > \frac{c(1+4c)}{1-2c} \quad \text{if} \quad c > 1/2 \tag{6.185}$$

$$\tag{6.186}$$

With tilt, no axial conduction ($a \neq 0$, $c = 0$)

The dynamical system (6.146)-(6.148) simplifies to

$$\frac{dx}{dt} = y - x \tag{6.187}$$

$$\frac{dy}{dt} = a - xz \tag{6.188}$$

$$\frac{dz}{dt} = -b + xy \tag{6.189}$$

The critical points are $\pm(\sqrt{b}, \sqrt{b}, a/\sqrt{b})$. The linear stability of the point P^+ given by $(\sqrt{b}, \sqrt{b}, a/\sqrt{b})$ will be analyzed. From equation (6.157), the solutions of

$$\begin{vmatrix} -(1+\lambda) & 1 & 0 \\ -a/\sqrt{b} & -\lambda & -\sqrt{b} \\ \sqrt{b} & \sqrt{b} & -\lambda \end{vmatrix} = 0 \tag{6.190}$$

are the eigenvalues. This simplifies to

$$\lambda^3 + \lambda^2 + \lambda(b + \frac{a}{\sqrt{b}}) + 2b = 0 \tag{6.191}$$

For stability the Hurwitz criteria require all coefficients to be positive, which they are. The determinants

$$D_1 = 1 \tag{6.192}$$

$$D_2 = \begin{vmatrix} 1 & 2b \\ 1 & b + a/\sqrt{b} \end{vmatrix} \tag{6.193}$$

$$D_3 = \begin{vmatrix} 1 & 2b & 0 \\ 1 & b + a/\sqrt{b} & 0 \\ 0 & 1 & 2b \end{vmatrix} \tag{6.194}$$

should also be positive. This gives the condition $(b + a/\sqrt{b}) - 2b > 0$, from which, we have

$$a > b^{3/2} \tag{6.195}$$

for stability. The stable and unstable region for P^+ is shown in Figure 6.14. Also shown is the stability of the critical point P^- with coordinates $-(\sqrt{b}, \sqrt{b}, a/\sqrt{b})$. The dashed circles are of radius $G/2$, and the angleof tile ϕ is also indicated. Using equations (6.143) and (6.144), the stability condition (6.195) can be written as

$$\frac{\sin\phi}{\cos^{3/2}\phi} > \left(\frac{G}{2}\right)^{1/2} \tag{6.196}$$

As a numerical example, for the value of G in equation (6.70), P^+ is stable for the tilt angle range $\phi > 7.7°$, and P^- is stable for $\phi < -7.7°$. In fact, for $G \ll 1$, the stability condition for P^+ can be approximated as

$$\phi > \left(\frac{G}{2}\right)^{1/2} \tag{6.197}$$

The same information can be shown in slightly different coordinates. Using $\overline{x} = \sqrt{b}$ for P^+ and equation (6.144), we get

$$\frac{G}{2} = \frac{\overline{x}^2}{\cos\phi} \tag{6.198}$$

The stability condition (6.195) thus becomes

$$\tan\phi < \overline{x} \tag{6.199}$$

The stability regions for both $P+$ and P^- are shown in Figure 6.15.

The loss of stability is through imaginary eigenvalues. In fact, for P^+, substituting $a = b^{3/2}$ in equation (6.191), the equation can be factorized to give the three eigenvalues $-1, \pm i\sqrt{2b}$. Thus the nondimensional radian frequency of the oscillations in the unstable range is approximately $\sqrt{2b}$.

The effect of a small nonzero axial conduction parameter c is to alter the Figure 6.195 in the zone $0 < b < c$.

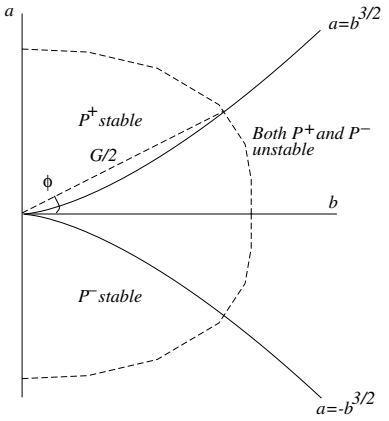

Figure 6.14: Stability of critical points P^+ and P^- in (b, a) space.

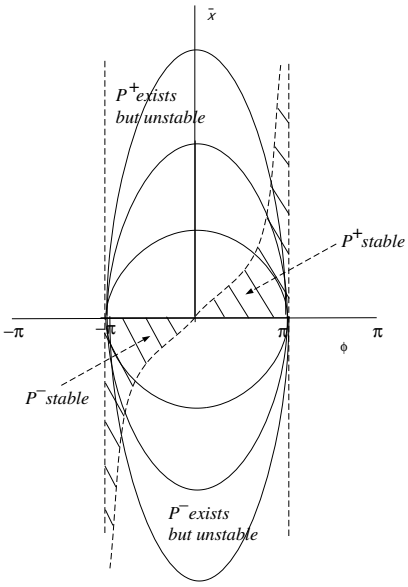

Figure 6.15: Stability of critical points P^+ and P^- in $(\phi, \overline{x})$ space.

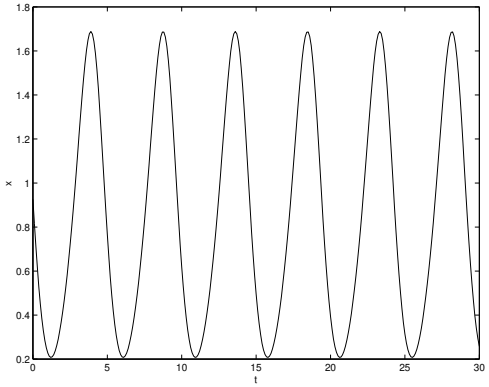

Figure 6.16: x-t for $a = 0.9$, $b = 1$.

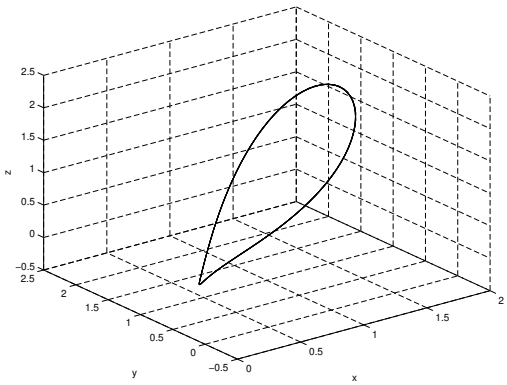

Figure 6.17: Phase-space trajectory for $a = 0.9$, $b = 1$.

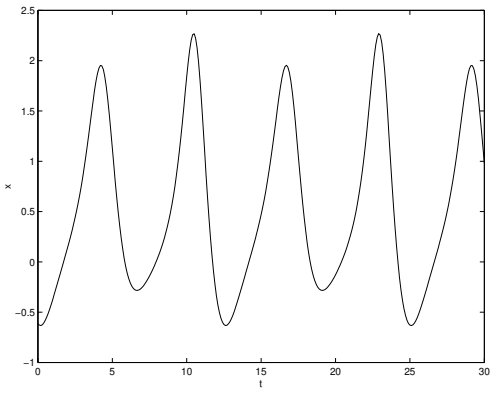

Figure 6.18: x-t for $a = 0.55$, $b = 1$.

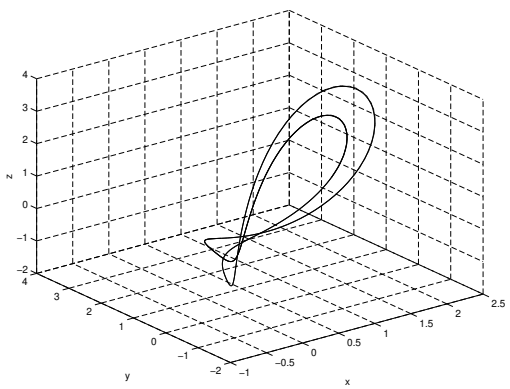

Figure 6.19: Phase-space trajectory for $a = 0.55$, $b = 1$.

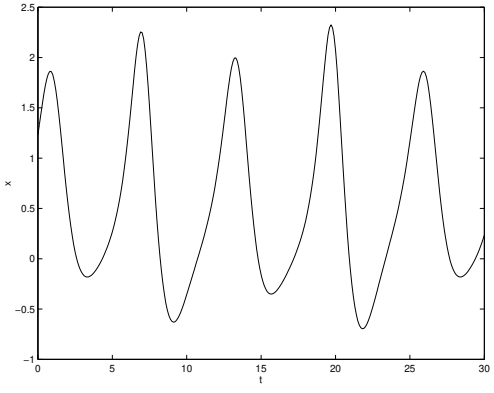

Figure 6.20: x-t for $a = 0.53$, $b = 1$.

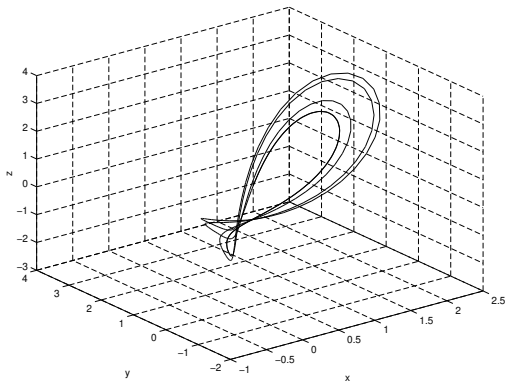

Figure 6.21: Phase-space trajectory for $a = 0.53$, $b = 1$.

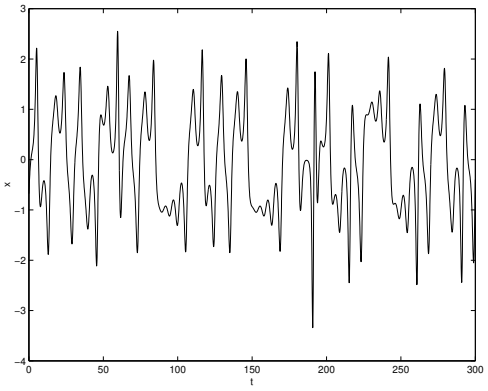

Figure 6.22: x-t for $a = 0$, $b = 1$.

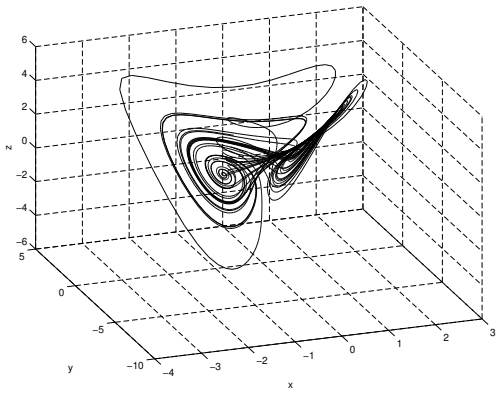

Figure 6.23: Phase-space trajectory for $a = 0$, $b = 1$.

6.2.5 Nonlinear analysis

Numerical

Let us choose $b = 1$, and reduce a. Figures 6.16 and 6.17 show the x-t and phase space representation for $a = 0.9$, Figures 6.18 and 6.19 for $a = 0.55$, and Figures 6.20 and 6.21 for $a = 0.53$.

The strange attractor is shown in Figures 6.22 and 6.23.

Comparison of the three figures in Figures 6.24 shows that vestiges of the shape of the closed curves for $a = -0.9$ and $a = 0.9$ can be seen in the trajectories in $a = 0$.

Analytical

The following analysis is by W. Franco.

We start with the dynamical system which models a toroidal thermosyphon loop with known heat flux

$$\begin{aligned} \frac{dx}{dt} &= y - x \\ \frac{dy}{dt} &= a - zx \\ \frac{dz}{dt} &= xy - b \end{aligned} \tag{6.200}$$

For $b > 0$ two critical points P^+ and P^- appear

$$(\bar{x}, \bar{y}, \bar{z}) = \pm \left(\sqrt{b}, \sqrt{b}, \frac{a}{\sqrt{b}} \right) \tag{6.201}$$

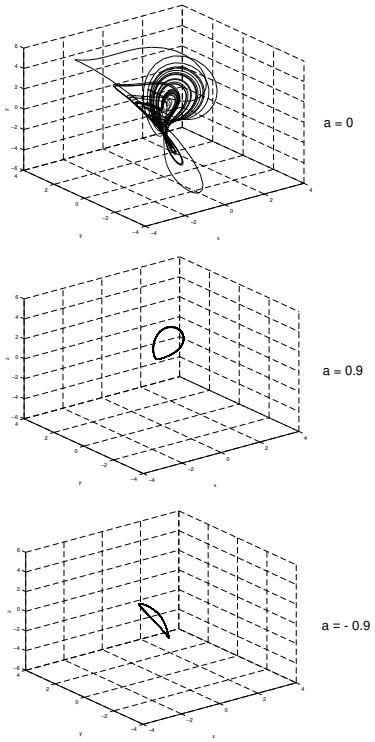

Figure 6.24: Phase-space trajectories for $b = 1$.

The local form respect to P^+ is

$$\begin{aligned} \frac{dx'}{dt} &= y' - x' \\ \frac{dy'}{dt} &= -\frac{a}{\sqrt{b}}x' - \sqrt{b}z' \\ \frac{dz'}{dt} &= \sqrt{b}x' + \sqrt{b}y' \end{aligned} \tag{6.202}$$

For stability $a > b^{\frac{3}{2}}$. At $a = b^{\frac{3}{2}}$ the eigenvalues are $-1, \pm\sqrt{2b}i$, thus a nonlinear analysis through the center manifold projection is possible. Let's introduce a perturbation of the form $a = b^{\frac{3}{2}} + \epsilon$ and the following change of variables

$$\begin{aligned} \alpha &= \frac{a}{\sqrt{b}} \\ \beta &= \sqrt{b} \end{aligned}$$

rewriting the local form, dropping the primes and regarding the perturbation the system becomes

$$\begin{aligned} \frac{dx}{dt} &= y - x \\ \frac{dy}{dt} &= \left(\beta^2 + \frac{\epsilon}{\beta}\right)x - \beta z \\ \frac{dz}{dt} &= \beta x - \beta y \end{aligned} \tag{6.203}$$

for stability $\alpha > \beta^2$.

Let's apply the following transformation:

$$\begin{aligned} x &= w_1 + \frac{2}{2\beta^2+1}w_2 + \frac{2\beta\sqrt{2}}{2\beta^2+1} \\ y &= 2w_2 \\ z &= -\beta w_1 - \frac{2\beta}{2\beta^2+1}w_2 + \frac{2\sqrt{2}\left(\beta^2+1\right)}{2\beta^2+1}w_3 \end{aligned} \tag{6.204}$$

in the new variables

$$\dot{\mathbf{w}} = \begin{pmatrix} -1 & 0 & 0 \\ 0 & 0 & -\sqrt{2}\beta \\ 0 & \sqrt{2}\beta & 0 \end{pmatrix}\mathbf{w} + \hat{\mathbf{P}}\mathbf{w} + \mathbf{l}(\mathbf{w}) \tag{6.205}$$

The center manifold projection is convenient to use if the large-time dynamic behavior is of interest. In many dimensional systems, the system often settles into the same large-time dynamics irrespective of the initial condition; this is usually less complex than the initial dynamics and can be described by far simple evolution equations.

We first state the definition of an invariant manifold for the equation

$$\dot{x} = N(x) \tag{6.206}$$

where $x \in R^n$. A set $S \subset R^n$ is a local invariant manifold for (6.206) if for $x_0 \subset S$, the solution $x(t)$ of (6.206) is in S for $\mid t \mid < T$ where $T > 0$. If we can always choose $T = \infty$, then S is an invariant

manifold. Consider the system

$$\begin{aligned} \dot{x} &= Ax + f(x,y) \\ \dot{y} &= By + g(x,y) \end{aligned} \tag{6.207}$$

where $x \in R^n$, $y \in R^m$ and A and B are constant matrices such that all the eigenvalues of A have zero real parts while all the eigenvalues of B have negative real parts. If $y = h(x)$ is an invariant manifold for (6.207) and h is smooth, then it is called a center manifold if $h(0) = 0$,$h'(0) = 0$. The flow on the center manifold is governed by the n-dimensional system

$$\dot{x} = Ax + f(x, h(x)) \tag{6.208}$$

The last equation contains all the necessary information needed to determine the asymptotic behavior of small solutions of (6.207).

Now we calculate, or at least approximate the center manifold $h(\mathbf{w})$. Substituting $w_1 = h(w_2, w_3)$ in the first component of (6.205) and using the chain rule, we obtain

$$\dot{w}_1 = \left(\frac{\partial h}{\partial w_2}, \frac{\partial h}{\partial w_3} \right) \begin{pmatrix} \dot{w}_2 \\ \\ \dot{w}_3 \end{pmatrix} = -h + l_1 \left(w_2, w_3, h \right) \tag{6.209}$$

We seek a center manifold

$$h = a w_2^2 + b w_2 w_3 + c w_3^2 + O(3) \tag{6.210}$$

substituting in (6.209)

$$\begin{aligned} (2aw_2 + bw_3, 2cw_3 + bw_2) \begin{pmatrix} -\sqrt{2}\beta w_3 \\ \\ \sqrt{2}\beta w_2 \end{pmatrix} &= \\ -\left(a w_2^2 + b w_2 w_3 + c w_3^2 \right) &+ \left(k_1 w_2^2 + k_2 w_2 w_3 + k_3 w_3^2 \right) + O(3) \end{aligned}$$

Equating powers of x^2,xy and y^2, we find that

$$\begin{aligned} a &= k_1 - b\sqrt{2}\beta \\ c &= k_3 + b\sqrt{2}\beta \\ b &= \frac{k_2 + 2\sqrt{2}\beta \left(k_1 - k_3 \right)}{8\beta^2 + 1} \end{aligned}$$

The reduced system is therefore given by

$$\begin{aligned} \dot{w}_2 &= -\sqrt{2}\beta w_3 + s^2 \left(w_2, w_3 \right) \\ \dot{w}_3 &= \sqrt{2}\beta w_2 + s^3 \left(w_2, w_3 \right) \end{aligned} \tag{6.211}$$

Normal form: Now we carry out a smooth nonlinear coordinate transform of the type

$$\mathbf{w} = \mathbf{v} + \psi(\mathbf{v}) \tag{6.212}$$

to simplify (6.211) by transforming away many nonlinear terms. The system in the new coordinates is

$$\dot{\mathbf{v}} = \begin{pmatrix} 0 & -\sqrt{2}\beta \\ \sqrt{2}\beta & 0 \end{pmatrix} + \begin{pmatrix} \left(\nu v_1 - \gamma v_2 \right) \left(v_1^2 + v_2^2 \right) \\ \\ \left(\nu v_2 + \gamma v_1 \right) \left(v_1^2 + v_2^2 \right) \end{pmatrix} \tag{6.213}$$

where ν and γ depend on the nonlinear part of (6.211). This is the unfolding of the Hopf bifurcation.

Although the normal form theory presented in class pertains to a Jacobian whose eigenvalues all lie on the imaginary axis, one can also present a perturbed version. The eigenvalues are then close to the imaginary axis but not quite on it. Consider the system

$$\dot{\mathbf{v}} = \mathbf{A}\mathbf{v} + \hat{\mathbf{A}}\mathbf{v} + \mathbf{f}(\mathbf{v}) \tag{6.214}$$

where the Jacobian $\mathbf{A}$ has been evaluated at a point in the parameter space where all its eigenvalues are on the imaginary axis, $\hat{\mathbf{A}}$ represents a linear expansion of order μ in the parameters above that point; a perturbed Jacobian. The perturbation parameter represents the size of the neighborhood in the parameter space. We stipulate the order of μ such that the real part of the eigenvalues of $\mathbf{A} + \hat{\mathbf{A}}$ is such that, to leading order, $\hat{\mathbf{A}}$ does not change the coefficients of the leading order nonlinear terms of the transformed equation. The linear part $\mathbf{A} + \hat{\mathbf{A}}$ of perturbed Hopf can always be transformed to

$$\begin{pmatrix} \mu & -\omega \\ \omega & \mu \end{pmatrix}$$

The required transformation is a near identity linear transformation

$$\mathbf{v} = \mathbf{u} + \mathbf{B}\mathbf{u}$$

such that the linear part of (6.214) is transformed to

$$\dot{\mathbf{u}} = \left(\mathbf{A} + \mathbf{A}\mathbf{B} - \mathbf{B}\mathbf{A} + \hat{\mathbf{A}}\right)\mathbf{z}$$

For the Hopf bifurcation if

$$\hat{\mathbf{A}} = \begin{pmatrix} a_1 & a_2 \\ a_3 & a_4 \end{pmatrix}$$

then

$$\mu = \frac{a1 + a4}{\omega}$$

Therefore for ϵ small we can write (6.213) as

$$\dot{\mathbf{v}} = \begin{pmatrix} 0 & -\sqrt{2}\beta \\ \sqrt{2}\beta & 0 \end{pmatrix}\mathbf{v} + \begin{pmatrix} p_{22} & p_{23} \\ p_{32} & p_{33} \end{pmatrix}\mathbf{v} + \begin{pmatrix} f_1(\mathbf{v}) \\ \\ f_2(\mathbf{v}) \end{pmatrix} \tag{6.215}$$

where the perturbation matrix comes from (6.205). Applying a near identity transformation of the form $\mathbf{v} = \mathbf{u} + \mathbf{B}\mathbf{u}$ the system becomes

$$\dot{\mathbf{u}} = \begin{pmatrix} \mu & -\sqrt{2}\beta \\ \sqrt{2}\beta & \mu \end{pmatrix}\mathbf{u} + \begin{pmatrix} (\nu u_1 - \gamma u_2)\left(u_1^2 + u_2^2\right) \\ \\ (\nu u_2 + \gamma u_1)\left(u_1^2 + u_2^2\right) \end{pmatrix} \tag{6.216}$$

which is the unfolding for the perturbed Hopf bifurcation. In polar coordinates we have

$$\begin{aligned} \dot{r} &= \mu r + \nu r^3 \\ \dot{\theta} &= \sqrt{2}\beta \end{aligned} \tag{6.217}$$

where

$$\mu = -\frac{\epsilon\sqrt{2}}{2\beta^2\left(2\beta^2 + 1\right)} \tag{6.218}$$

$$\nu = -\frac{40\beta^6 + 40\beta^4 + 12\beta^3 + 10\beta^2 + 12\beta + 3}{4\left(8\beta^2+1\right)\left(2\beta^2+1\right)^4} \tag{6.219}$$

Appendix

$$\begin{aligned} k_1 &= -\frac{8\beta\left(\beta^2+1\right)}{\left(2\beta^2+1\right)^3} \\ k_2 &= \frac{\left(\beta^2+1\right)\left(4\sqrt{2}-8\sqrt{2}\beta^2\right)}{\left(2\beta^2+1\right)^3} \\ k_3 &= \frac{8\beta\left(\beta^2+1\right)}{\left(2\beta^2+1\right)^3} \end{aligned} \tag{6.220}$$

$$\begin{aligned} p_{22} &= -\frac{\epsilon}{\beta\left(2\beta^2+1\right)} \\ p_{23} &= -\frac{\epsilon\sqrt{2}}{2\beta^2+1} \end{aligned} \tag{6.221}$$

From the literature

$$\begin{aligned} \nu &= \frac{1}{16}\left(f_{xxx} + f_{xyy} + g_{xxy} + g_{yyy}\right) \\ &+ \frac{1}{16\omega}\left(f_{xy}(f_{xx}+f_{yy}) - g_{xy}(g_{xx}-g_{yy}) - f_{xx}g_{xx} - f_{yy}g_{yy}\right) \end{aligned} \tag{6.222}$$

in our problem $f = f_1$, $g = f_2$, $x = v_1$, $y = v_2$ and $\omega = \sqrt{2}\beta$.

6.3 Known wall temperature

The heating is now convective with a heat transfer coefficient U, and an external temperature of $T_w(s)$. Thus,

$$q = PU(T - T_w) \tag{6.223}$$

Neglecting axial conduction

$$\frac{P\alpha}{\rho_0 A}\overline{u} = \frac{\beta}{L}\int_0^L \overline{T}(s)\tilde{g}(s)\, ds \tag{6.224}$$

$$\overline{u}\frac{d\overline{T}}{ds} = \gamma\left[\overline{T} - T_w(s)\right] \tag{6.225}$$

where $\gamma = UP/\rho_0 A c_p$[1]. Multiplying the second equation by $e^{-\gamma s/\overline{u}}/\overline{u}$, we get

$$\frac{d}{ds}\left(e^{-\gamma s/\overline{u}}\overline{T}\right) = -\frac{\gamma}{\overline{u}}e^{-\gamma s/\overline{u}}T_w \tag{6.226}$$

Integrating, we get

$$\overline{T} = e^{\gamma s/\overline{u}}\left[-\frac{\gamma}{\overline{u}}\int_0^s e^{-\gamma s'/\overline{u}}T_w(s')\, ds' + T_0\right] \tag{6.227}$$

[1] The sign of γ appears to be wrong.

Since $\overline{T}(L) = \overline{T}(0)$, we get

$$T_0 = \frac{\gamma}{\overline{u}} \frac{e^{\gamma L/\overline{u}} \int_0^L e^{-\gamma s'/\overline{u}} T_w(s')\, ds'}{e^{\gamma L/\overline{u}} - 1} \tag{6.228}$$

The velocity is obtained from

$$\frac{P\alpha}{\rho_0 A}\overline{u} = \frac{\beta}{L}\int_0^L \left[e^{\gamma s/\overline{u}} \left\{ -\frac{\gamma}{\overline{u}} \int_0^s e^{-\gamma s'/\overline{u}} T_w(s')\, ds' + T_0 \right\} \right] \tilde{g}(s)\, ds \tag{6.229}$$

This is a transcendental equation that may have more than one real solution.

Example 6.3

Show that there is no motion if the wall temperature is uniform.

Take T_w to be a constant. Then equation (6.225) can be written as

$$\frac{d(\overline{T} - T_w)}{\overline{T} - T_w} = \frac{\gamma}{\overline{u}}\, ds \tag{6.230}$$

The solution to this is

$$\overline{T} = T_w + K\, e^{\gamma s/\overline{u}} \tag{6.231}$$

where K is a constant. Continuity of T at $s = 0$ and $s = L$ gives $K = 0$. Hence $T = T_w$, and, from equation (6.224), $\overline{u} = 0$.

Assume the wall temperature to be

$$T_w(s) = -\sin(2\pi s - \phi) \tag{6.232}$$

The temperature field is

$$T = \frac{b}{r_2 - r_1}\left(\frac{\cos(2\pi s - \phi)}{2\pi(1 + r_2^2/4\pi^2)}\right) - \left(\frac{\cos(2\pi s - \phi)}{2\pi(1 + r_1 62/4\pi^2)}\right) \tag{6.233}$$

6.4 Mixed condition

The following has been written by A. Pacheco-Vega.

It is common, especially in experiments, to have one part of the loop heated with a known heat rate and the rest with known wall temperature. Thus for part of the loop the wall temperature is known so that $q = PU(T - T_w(s))$, while $q(s)$ is known for the rest. As an example, consider

$$q = \begin{cases} PU(T - T_0) & \text{for} \quad \frac{\phi}{2\pi} \le s \le \pi + \frac{\phi}{2\pi} \\ q_0 & \text{for} \quad \pi + \frac{\phi}{2\pi} < s < 2\pi + \frac{\phi}{2\pi} \end{cases} \tag{6.234}$$

where T_0 and q_0 are constants.

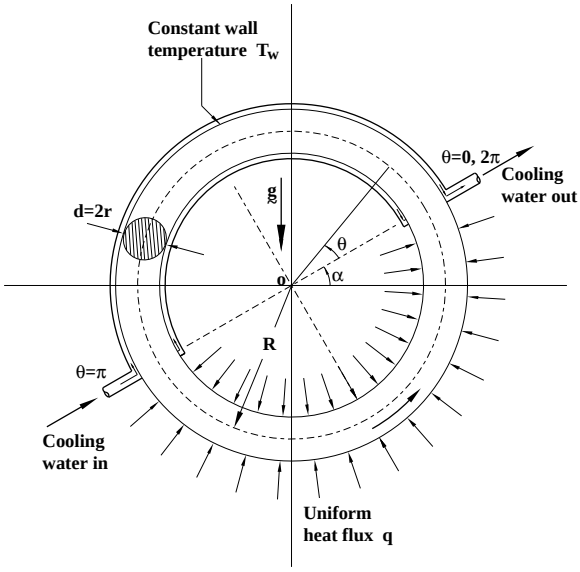

Figure 6.25: Schematic of a convection loop heated with constant heat flux in one half and cooled at constant temperature in the other half.

6.4.1 Modeling

[1]

If we consider a one-dimensional incompressible flow, the equation of continuity indicates that the velocity v is a function of time alone. Thus,

$$v = v(t). \tag{6.235}$$

Taking an infinitesimal cylindrical control volume of fluid in the loop $\pi r^2 d\theta$, see Figure (6.25), the momentum equation in the θ-direction can be written as

$$\rho\pi r^2 R d\theta \frac{dv}{dt} = -\pi r^2 d\theta \frac{dp}{d\theta} - \rho g \pi r^2 R d\theta \cos(\theta + \alpha) - \tau_w 2\pi r R d\theta \tag{6.236}$$

Integrating Eq. (6.236) around the loop using the Boussinesq approximation $\rho = \rho_w[1 - \beta(T - T_w)]$, with the shear stress at the wall being approximated by that corresponding to Poiseuille flow in a straight pipe $\tau_w = 8\mu v/\rho_w r^2$, the expression of the balance in Eq. (6.236) modifies to

$$\frac{dv}{dt} + \frac{8\mu}{\rho_w r^2} v = \frac{\beta g}{2\pi} \int_0^{2\pi} (T - T_w) \cos(\theta + \alpha)\, d\theta \tag{6.237}$$

Neglecting axial heat conduction, the temperature of the fluid satisfies the following energy balance equation

$$\rho_w c_p \left(\frac{\partial T}{\partial t} + \frac{v}{R} \frac{\partial T}{\partial \theta} \right) = \begin{cases} -\frac{2h}{r}(T - T_w), & 0 \le \theta \le \pi \\ \frac{2}{r} q, & \pi < \theta < 2\pi \end{cases} \tag{6.238}$$

Following the notation used by Greif et al. (1979), the nondimensional time, velocity and temperature are defined as

$$\tau = \frac{t}{2\pi R/V}, \quad w = \frac{v}{V}, \quad \phi = \frac{T - T_w}{q/h} \tag{6.239}$$

respectively, where

$$V = \left(\frac{g\beta Rrq}{2\pi c_p \mu}\right)^{1/2}. \tag{6.240}$$

Accordingly, Eqs. (6.237) and (6.238) become

$$\frac{dw}{d\tau} + \Gamma w = \frac{\pi\Gamma}{4D}\int_0^{2\pi} \phi \, \cos(\theta + \alpha)\, d\theta \tag{6.241}$$

and

$$\frac{\partial\phi}{\partial\tau} + 2\pi w\frac{\partial\phi}{\partial\theta} = \begin{cases} -2D\phi, & 0 \le \theta \le \pi \\ 2D, & \pi < \theta < 2\pi \end{cases} \tag{6.242}$$

where the parameters D and Γ are defined by

$$D = \frac{2\pi Rh}{\rho_w c_p r V} \qquad \Gamma = \frac{16\pi\mu R}{\rho_w r^2 V} \tag{6.243}$$

6.4.2 Steady State

The steady-state governing equations without axial conduction are

$$\overline{w} = \frac{\pi}{4D}\int_0^{2\pi} \overline{\phi} \, \cos(\theta + \alpha)\, d\theta \tag{6.244}$$

and

$$\frac{d\overline{\phi}}{d\theta} = \begin{cases} -\frac{D}{\pi\overline{w}}\,\overline{\phi}, & 0 \le \theta \le \pi \\ \frac{D}{\pi\overline{w}}, & \pi < \theta < 2\pi \end{cases} \tag{6.245}$$

where $\overline{w}$ and $\overline{\phi}$ are the steady-state values of velocity and temperature respectively. Eq. (6.245) can be integrated to give

$$\overline{\phi}(\theta) = \begin{cases} A\, e^{-(D\theta/\pi\overline{w})}, & 0 \le \theta \le \pi \\ \frac{D}{\pi\overline{w}}\,\theta + B, & \pi < \theta < 2\pi \end{cases} \tag{6.246}$$

Applying the condition of continuity in the temperature, such that $\phi(0) = \phi(2\pi)$ and $\phi(\pi^-) = \phi(\pi^+)$ the constants A and B can be determined. These are

$$A = \frac{D}{\overline{w}}\frac{1}{1 - e^{(-D/\overline{w})}} \qquad B = \frac{D}{\overline{w}}\left[\frac{2\, e^{(-D/\overline{w})} - 1}{1 - e^{(-D/\overline{w})}}\right] \tag{6.247}$$

The resulting temperature filed is

$$\overline{\phi}(\theta) = \begin{cases} \frac{D}{\overline{w}}\frac{e^{-(D\theta/\pi\overline{w})}}{1-e^{-(D/\overline{w})}}, & 0 \le \theta \le \pi \\ \frac{D}{\overline{w}}\left[\frac{\theta}{\pi} + \frac{2e^{-(D/\overline{w})}-1}{1-e^{-(D/\overline{w})}}\right], & \pi < \theta < 2\pi \end{cases} \tag{6.248}$$

Substituion of Eq. (6.245) in Eq. (6.244), followed by an expansion of $\cos(\theta+\alpha)$, leads to

$$\begin{aligned}\overline{w} = \frac{\pi}{4D}\cos\alpha\left\{\int_0^{\pi}\frac{D}{\overline{w}}\frac{e^{-(D\theta/\pi\overline{w})}}{1-e^{-(D/\overline{w})}}\cos\theta\,d\theta\right.\\ \left.+\int_{\pi}^{2\pi}\frac{D}{\overline{w}}\left[\frac{\theta}{\pi}+\frac{2e^{-(D/\overline{w})}-1}{1-e^{-(D/\overline{w})}}\right]\cos\theta\,d\theta\right\}\\ -\frac{\pi}{4D}\sin\alpha\left\{\int_0^{\pi}\frac{D}{\overline{w}}\frac{e^{-(D\theta/\pi\overline{w})}}{1-e^{-(D/\overline{w})}}\sin\theta\,d\theta\right.\\ \left.+\int_{\pi}^{2\pi}\frac{D}{\overline{w}}\left[\frac{\theta}{\pi}+\frac{2e^{-(D/\overline{w})}-1}{1-e^{-(D/\overline{w})}}\right]\sin\theta\,d\theta\right\}\end{aligned} \tag{6.249}$$

and integration around the loop, gives the steady-state velocity as

$$\overline{w}^2 = \frac{\cos\alpha}{2}+\frac{(D/\overline{w})\cos\alpha+\pi(D/\overline{w})^2\sin\alpha}{4\left[1+\left(\frac{D}{\pi\overline{w}}\right)^2\right]}\left(\frac{1+e^{-(D/\overline{w})}}{1-e^{-(D/\overline{w})}}\right). \tag{6.250}$$

As a final step, multiplying the numerator and denominator by $e^{(D/2\overline{w})}$ and rearranging terms leads to the expresion for the function of the steady-state velocity

$$G(\overline{w},\alpha,D) = \overline{w}^2-\frac{\cos\alpha}{2}-\frac{(D/\overline{w})\cos\alpha+\pi(D/\overline{w})^2\sin\alpha}{4\left[1+\left(\frac{D}{\pi\overline{w}}\right)^2\right]}\coth(D/2\ \overline{w}) = 0 \tag{6.251}$$

For $\alpha = 0$, symmetric steady-state solutions for the fluid velocity are possible since $G(w,0,D)$ is an even function of w. In this case Eq.(6.251) reduces to

$$\overline{w}^2 = \frac{1}{2}+\frac{(D/\overline{w})\left[1+e^{-(D/\overline{w})}\right]}{4\left[1+\left(\frac{D}{\pi\overline{w}}\right)^2\right]\left[1-e^{-(D/\overline{w})}\right]}. \tag{6.252}$$

The steady-state solutions of the velocity field and temperature are shown next. Figure 6.26 shows the $\overline{w}-\alpha$ curves for different values of the parameter D. Regions of zero, one, two and three solutions can be identified. The regions of no possible steady-state velocity are: $-180^\circ < \alpha < -147.5^\circ$ and $147.5^\circ < \alpha < 180^\circ$. There is only one velocity for the ranges $-147.5^\circ < \alpha < -\alpha_0$ and $\alpha_0 < \alpha < 147.5^\circ$ where α_0 varies from 90° at a value of $D = 0.001$ to $\alpha_0 = 32.5^\circ$ when $D = 100$. Three velocities are obtained for $-\alpha_0 < \alpha < -32.5^\circ$ and $32.5^\circ < \alpha < \alpha_0$, except for the zero-inclination case which has two possible steady-state velocities. The temperature distribution in the loop, for three values of the parameter D and $\alpha = 0$ is presented in Figure 6.27. From the $\overline{\phi}-\theta$ curves it can be seen the dependence of the temperature with D. As D increases the variation in temperature between two opposit points also increases. When has a value $D = 0.1$ the heating and cooling curves are almost straight lines, while at a value of $D = 1.0$ the temperature decays exponentially and rises linearly. Similar but more drastic change in temperature is seen when $D = 2.5$. Figure 6.28 shows the $\overline{\phi}-\theta$ curves for three different inclination angles with $D = 2.5$. It can be seen the increase in the temperature as α takes values of $\alpha = 0^\circ$, $\alpha = 90^\circ$ and $\alpha = 135^\circ$. This behaviour is somewhat expected since the steady-state velocity is decreasing in value such that the fluid stays longer in both parts of the loop. Figure 6.29 shows the steady-state velocity as a function of D for different angles of inclination α. For $\alpha = 0$ we have two branches of the velocity-curve which are symmetric. The positive and negative values of the velocity are equal in magnitude for any value of D. For $\alpha = 45^\circ$, the two branches are not symmetric while for $\alpha = 90^\circ$ and $\alpha = 135^\circ$, only the positive branch exist.

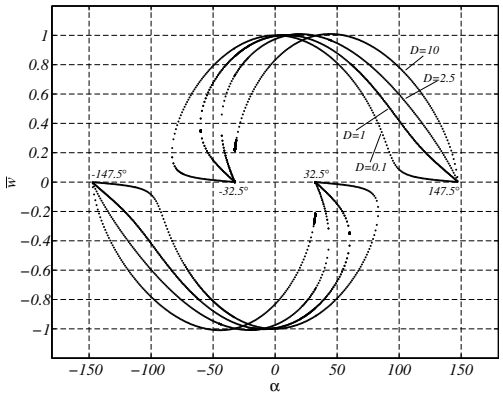

Figure 6.26: Steady-State velocity field.

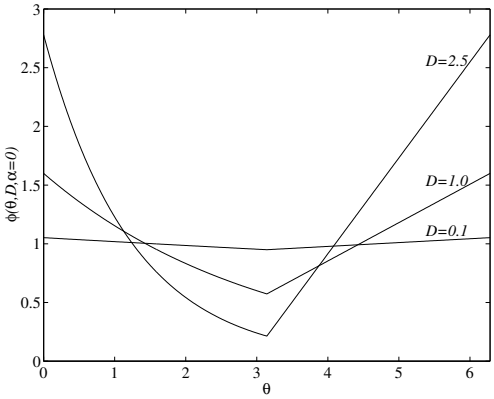

Figure 6.27: Nondimensional temperature distribution as a function of the parameter D for $\alpha = 0$.

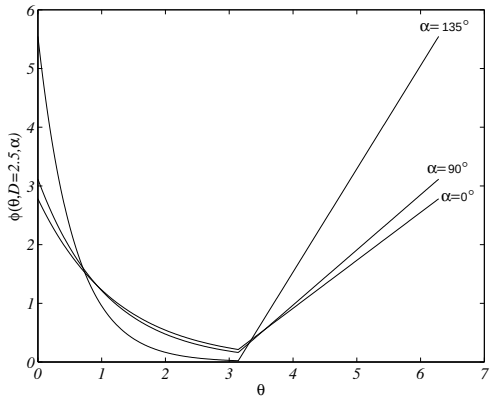

Figure 6.28: Nondimensional temperature distribution as a function of thermosyphon inclination α for $D = 2.5$.

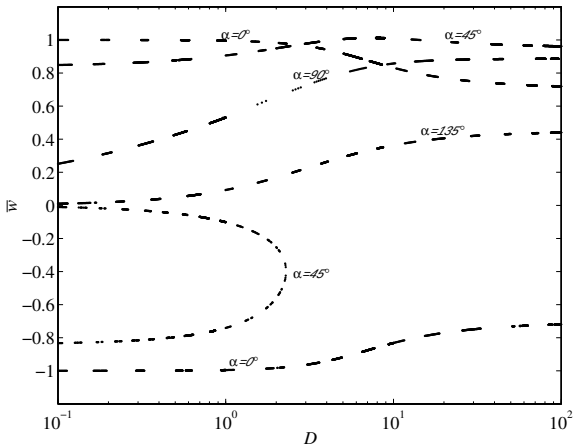

Figure 6.29: Velocity $\overline{w}$ as a function of D for different thermosyphon inclinations α.

6.4.3 Dynamic Analysis

The temperature can be expanded in Fourier series, such that

$$\phi = \phi_0 + \sum_{n=1}^{\infty} \left[\phi_n^c(t)\cos(n\theta) + \phi_n^s(t)\sin(n\theta)\right] \tag{6.253}$$

Substituiting into Eqs. (6.241) and (6.242), we have

$$\frac{dw}{d\tau} + \Gamma w = \frac{\pi^2\Gamma}{4D}\cos\alpha\phi_1^c - \frac{\pi^2\Gamma}{4D}\sin\alpha\phi_1^s \tag{6.254}$$

and

$$\begin{aligned} &\frac{d\phi_0^c}{d\tau} + \sum_{n=1}^{\infty}\left[\frac{d\phi_n^c}{d\tau}\cos(n\theta) + \frac{d\phi_n^s}{d\tau}\sin(n\theta)\right] \\ &+2\pi w\sum_{n=1}^{\infty}\left[-n\phi_n^c\sin(n\theta) + n\phi_n^s\cos(n\theta)\right] \\ &= \begin{cases} -2D\left\{\phi_0^c + \sum_{n=1}^{\infty}\left[\phi_n^c(t)\cos(n\theta) + \phi_n^s(t)\sin(n\theta)\right]\right\}, & 0 \le \theta \le \pi \\ 2D, & \pi < \theta < 2\pi \end{cases} \end{aligned} \tag{6.255}$$

Integrating Eq. (6.255) from $\theta = 0$ to $\theta = 2\pi$ we get

$$\frac{d\phi_0^c}{d\tau} = -D\left[\phi_0^c - \frac{1}{\pi}\sum_{n=1}^{\infty}\frac{\phi_n^s}{n}\left[(-1)^n - 1\right] - 1\right] \tag{6.256}$$

Multiplying by $\cos(m\theta)$ and integrating from $\theta = 0$ to $\theta = 2\pi$

$$\frac{d\phi_m^c}{d\tau} + 2\pi m\, w\, \phi_m^s = -D\phi_m^c + \frac{D}{\pi}\sum_{\substack{n=1\\ n\neq m}}^{\infty}\phi_n^s\left[(-1)^{m+n} - 1\right]\frac{2n}{n^2 - m^2} \tag{6.257}$$

Now multiplying by $\sin(m\theta)$ and integrating from $\theta = 0$ to $\theta = 2\pi$

$$\begin{aligned} \frac{d\phi_m^s}{d\tau} - 2\pi m\, w\, \phi_m^c = -D\phi_m^s + \frac{D}{\pi}\sum_{\substack{n=0\\ n\neq m}}^{\infty}\phi_n^c\left[(-1)^{m+n} - 1\right]\frac{2m}{m^2 - n^2} \\ -\frac{2D}{\pi m}\left[1 - (-1)^m\right] \end{aligned} \tag{6.258}$$

for $m \geq 1$.

Choosing the variables

$$w = w \tag{6.259}$$
$$C_0 = \phi_0^c \tag{6.260}$$
$$C_m = \phi_m^c \tag{6.261}$$
$$S_m = \phi_m^s \tag{6.262}$$

we get an infinte-dimensional dynamical system

$$\frac{dw}{d\tau} = -\Gamma w + \frac{\pi^2\Gamma}{4D}\cos\alpha\, C_1 - \frac{\pi^2\Gamma}{4D}\sin\alpha\, S_1 \tag{6.263}$$

$$\frac{dC_0}{d\tau} = -D\, C_0 + \frac{D}{\pi}\sum_{n=1}^{\infty}\frac{S_n}{n}\left[(-1)^n - 1\right] + D \tag{6.264}$$

$$\frac{dC_m}{d\tau} = -2\pi m\, w\, S_m - D\, C_m + \frac{D}{\pi}\sum_{\substack{n=1\\ n\neq m}}^{\infty} S_n\left[(-1)^{m+n} - 1\right]\frac{2n}{n^2-m^2} \tag{6.265}$$

$$\begin{aligned}\frac{dS_m}{d\tau} &= 2\pi m\, w\, C_m - D\, S_m + \frac{D}{\pi}\sum_{\substack{n=0\\ n\neq m}}^{\infty} C_n\left[(-1)^{m+n} - 1\right]\frac{2m}{m^2-n^2} \\ &+ \frac{2D}{\pi m}\left[(-1)^m - 1\right]\end{aligned} \tag{6.266}$$

for $m \geq 1$. The physical significance of the variables are: w is the fluid velocity, C is the horizontal temperature difference, and S is the vertical temperature difference. The parameters of the system are D, Γ and α. D and Γ are positive, while α can have any sign.

The critical points are found by equating the vector filed to zero, so that

$$\overline{w} - \frac{\pi^2}{4D}\cos\alpha\,\overline{C}_1 + \frac{\pi^2}{4D}\sin\alpha\,\overline{S}_1 = 0 \tag{6.267}$$

$$(\overline{C}_0 - 1) - \frac{1}{\pi}\sum_{n=1}^{\infty}\frac{\overline{S}_n}{n}\left[(-1)^n - 1\right] = 0 \tag{6.268}$$

$$2\pi m\,\overline{w}\,\overline{S}_m + D\,\overline{C}_m - \frac{D}{\pi}\sum_{\substack{n=1\\ n\neq m}}^{\infty}\overline{S}_n\left[(-1)^{m+n} - 1\right]\frac{2n}{n^2-m^2} = 0 \tag{6.269}$$

$$\begin{aligned}2\pi m\,\overline{w}\,\overline{C}_m - D\,\overline{S}_m + \frac{D}{\pi}\sum_{\substack{n=0\\ n\neq m}}^{\infty}\overline{C}_n\left[(-1)^{m+n} - 1\right]\frac{2m}{m^2-n^2} \\ + \frac{2D}{\pi m}\left[(-1)^m - 1\right] = 0\end{aligned} \tag{6.270}$$

However, a convenient alternative way to determine the critical points is by using a Fourier series expansion of the steady-state temperature field solution given in Eq. (6.248). The Fourier series expansion is

$$\overline{\phi} = \sum_{n=0}^{\infty}\left[\overline{C}_n\cos(n\theta) + \overline{S}_n\sin(n\theta)\right] \tag{6.271}$$

Performing the inner product between Eq. (6.248) and $\cos(m\theta)$ we have

$$\begin{aligned}&\frac{D}{\overline{w}}\frac{1}{1-e^{-(D/\overline{w})}}\int_0^{\pi} e^{-(D\theta/\pi\overline{w})}\,\cos(m\theta)\,d\theta \\ &+\frac{D}{\overline{w}}\int_{\pi}^{2\pi}\left[\frac{\theta}{\pi} + \frac{2e^{-(D/\overline{w})} - 1}{1-e^{-(D/\overline{w})}}\right]\cos(m\theta)\,d\theta \\ &= \sum_{n=0}^{\infty}\overline{C}_n\int_0^{2\pi}\cos(n\theta)\cos(m\theta)\,d\theta + \sum_{n=0}^{\infty}\overline{S}_n\int_0^{2\pi}\sin(n\theta)\,\cos(m\theta)d\theta\end{aligned} \tag{6.272}$$

Now the inner product between Eq. (6.248) and $\sin(m\theta)$ gives

$$\begin{aligned}
&\frac{D}{\overline{w}}\frac{1}{1-e^{-(D/\overline{w})}}\int_0^{\pi} e^{-(D\theta/\pi\overline{w})}\,\sin(m\theta)\,d\theta \\
&+\frac{D}{\overline{w}}\int_{\pi}^{2\pi}\left[\frac{\theta}{\pi}+\frac{2e^{-(D/\overline{w})}-1}{1-e^{-(D/\overline{w})}}\right]\sin(m\theta)\,d\theta \\
=\sum_{n=0}^{\infty}\overline{C}_n\int_0^{2\pi}\cos(n\theta)\sin(m\theta)\,d\theta &+\sum_{n=0}^{\infty}\overline{S}_n\int_0^{2\pi}\sin(n\theta)\,\sin(m\theta)d\theta \qquad (6.273)
\end{aligned}$$

from which we get

$$\overline{C}_0 = \frac{1}{2}\left[1+\frac{D}{\overline{w}}\left(\frac{3}{2}+\frac{2e^{-(D/\overline{w})}-1}{1-e^{-(D/\overline{w})}}\right)\right] \qquad (6.274)$$

$$\overline{C}_m = \frac{\left(\frac{D}{\pi\overline{w}}\right)^2}{\left[m^2+\left(\frac{D}{\pi\overline{w}}\right)^2\right]}\frac{1-e^{-(D/\overline{w})}\cos(m\pi)}{1-e^{-(D/\overline{w})}}+\frac{D}{\pi^2m^2\overline{w}}\left[1-\cos(m\pi)\right] \qquad (6.275)$$

$$\overline{S}_m = -\left\{\frac{\left(\frac{D}{\pi\overline{w}}\right)^3}{m\left[m^2+\left(\frac{D}{\pi\overline{w}}\right)^2\right]}\frac{1-e^{-(D/\overline{w})}\cos(m\pi)}{1-e^{-(D/\overline{w})}}\right\} \qquad (6.276)$$

To analyze the stability of a critical point $(\overline{w},\overline{C}_0,\overline{C}_1,\cdots,\overline{C}_m,\overline{S}_1,\cdots,\overline{S}_m)$ we add perturbations of the form

$$w = \overline{w}+w' \qquad (6.277)$$
$$C_0 = \overline{C}_0+C_0' \qquad (6.278)$$
$$C_1 = \overline{C}_1+C_1' \qquad (6.279)$$
$$\vdots \qquad (6.280)$$
$$C_m = \overline{C}_m+C_m' \qquad (6.281)$$
$$S_1 = \overline{S}_1+S_1' \qquad (6.282)$$
$$\vdots \qquad (6.283)$$
$$S_m = \overline{S}_m+S_m' \qquad (6.284)$$

Substituting in Eqs. (6.263) to (6.266), we obtain the local form

$$\frac{dw'}{d\tau} = -\Gamma w' + \frac{\pi^2\Gamma}{4D}\cos\alpha\, C'_1 - \frac{\pi^2\Gamma}{4D}\sin\alpha\, S'_1 \tag{6.285}$$

$$\frac{dC'_0}{d\tau} = -D\, C'_0 + \frac{D}{\pi}\sum_{n=1}^{\infty}\frac{(-1)^n - 1}{n} S'_n \tag{6.286}$$

$$\begin{aligned}\frac{dC'_m}{d\tau} &= -2\pi m\,\overline{w}\, S'_m - 2\pi m\,\overline{S}_m\, w' - D\, C'_m \\ &+ \frac{D}{\pi}\sum_{\substack{n=1\\ n\neq m}}^{\infty}\frac{2n}{n^2-m^2}\left[(-1)^{m+n}-1\right] S'_n - 2\pi m\, w'\, S'_m \qquad m \geq 1\end{aligned} \tag{6.287}$$

$$\begin{aligned}\frac{dS'_m}{d\tau} &= 2\pi m\,\overline{w}\, C'_m + 2\pi m\,\overline{C}_m\, w' - D\, S'_m \\ &+ \frac{D}{\pi}\sum_{\substack{n=0\\ n\neq m}}^{\infty}\frac{2m}{m^2-n^2}\left[(-1)^{m+n}-1\right] C'_n + 2\pi m\, w'\, C'_m \qquad m \geq 1\end{aligned} \tag{6.288}$$

The linearized version is

$$\frac{dw'}{d\tau} = -\Gamma w' + \frac{\pi^2\Gamma}{4D}\cos\alpha\, C'_1 - \frac{\pi^2\Gamma}{4D}\sin\alpha\, S'_1 \tag{6.289}$$

$$\frac{dC'_0}{d\tau} = -D\, C'_0 + \frac{D}{\pi}\sum_{n=1}^{\infty}\frac{(-1)^n - 1}{n} S'_n \tag{6.290}$$

$$\begin{aligned}\frac{dC'_m}{d\tau} &= -2\pi m\,\overline{w}\, S'_m - 2\pi m\,\overline{S}_m\, w' - D\, C'_m \\ &+ \frac{D}{\pi}\sum_{\substack{n=1\\ n\neq m}}^{\infty}\frac{2n}{n^2-m^2}\left[(-1)^{m+n}-1\right] S'_n \qquad m \geq 1\end{aligned} \tag{6.291}$$

$$\begin{aligned}\frac{dS'_m}{d\tau} &= 2\pi m\,\overline{w}\, C'_m + 2\pi m\,\overline{C}_m\, w' - D\, S'_m \\ &+ \frac{D}{\pi}\sum_{\substack{n=0\\ n\neq m}}^{\infty}\frac{2m}{m^2-n^2}\left[(-1)^{m+n}-1\right] C'_n \qquad m \geq 1\end{aligned} \tag{6.292}$$

In general, the system given by Eqs. (6.263) to (6.266) can be written as

$$\frac{d\mathbf{x}}{dt} = \mathbf{f}(\mathbf{x}) \tag{6.293}$$

The eigenvalues of the linearized system given by Eqs. (6.289) to (6.292), and in general form as

$$\frac{d\mathbf{x}}{dt} = \mathbf{A}\mathbf{x} \tag{6.294}$$

are obtained numerically, such that

$$|\mathbf{A} - \lambda\mathbf{I}| = 0 \tag{6.295}$$

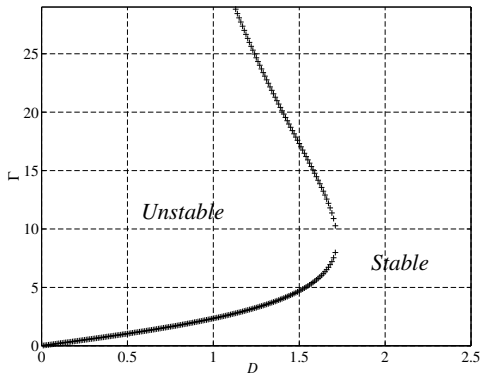

Figure 6.30: Stability curve D and Γ for a thermosyphon inclination $\alpha = 0$.

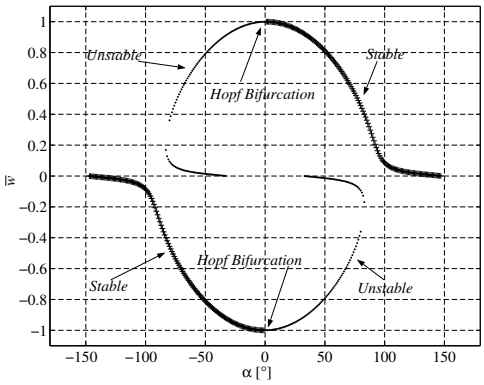

Figure 6.31: Stability curve $\overline{w}$ vs. α for $D = 0.1$, and $\Gamma = 0.20029$.

where $\mathbf{A}$ is the Jacobian matrix corresponding to the vector field of the linearized system, $\mathbf{I}$ is the identity matrix, and λ are the eigenvalues. The neutral stability curve is obtained numerically from the condition that $\Re(\lambda) = 0$. A schematic of the neutral curve is presented in Figure 6.30 for $\alpha = 0$. In this figure, the stable and unstable regions can be identified. Along the line of neutral stability, a Hopf-type of bifurcation occurs. Figure 6.31 shows the plot of $\overline{w} - \alpha$ curve for a value of the parameters $D = 0.1$ and $\Gamma = 0.20029$. When $\alpha = 0$, a Hopf bifurcation for both the positive and negative branches of the curve can be observed, where stable and unstable regions can be identified. It is clear that the *natural* branches which correspond to the first and third quadrants are stable, whereas the *antinatural* branches, second and fourth quadrants are unstable. The symmetry between the first and third quadrants, and, between the second and fourth quadrants can be notice as well. The corresponding eigenvalues of the bifurcation point are shown in Figure 6.32. The number of eigenvalues in this figure is 42 which are obtained from a dynamical system of dimension 42. This system results from truncating the infinite dimensional system at a number for which the value of the leading eigenvalues does not change when increasing its dimension. When we increase the size of the system, new eigenvalues appear in such a way that they are placed symmetrically farther from the real axis and aligned to the previous set of slave complex eigenmodes. This behaviour seems to be a characteristic of the dynamical system itself. Figure 6.33 illustrates a view of several stability curves, each for a different value of the tilt angle α in a $D - \Gamma$ plane at $\alpha = 0$. In this plot, the neutral curves appear to unfold when decreasing the tilt angle from $75.5°$ to $-32.5°$ increasing the region of instability. On the other hand, Figure 6.34 illustrates the linear stability characteristics of the dynamical system in a $\overline{w} - \alpha$ plot for a fixed Γ and three values of the parameter D. The stable and unstable regions can be observed. Hopf bifurcations occur for each branch of ecah particular curve. However, it is to be notice that the bifurcation occurs at a higher value of the tilt angle when D is smaller.

6.4.4 Nonlinear analysis

Let us select $D = 1.5$, and increase Γ. Figures 6.35 and 6.36 show the $w - \tau$ time series and phase-space curves for $\Gamma = 0.95\Gamma_{cr}$, whereas Figures 6.37 and 6.38 show the results for $\Gamma = 1.01\Gamma_{cr}$. The plots suggest the appearance of a subcritical Hopf bifurcation. Two attractors coexist for $\Gamma \leq \Gamma_{cr}$, these being a critical point and a strange attractor of fractional dimension. For $\Gamma > \Gamma_{cr}$, the only presence is of a strange attractor.

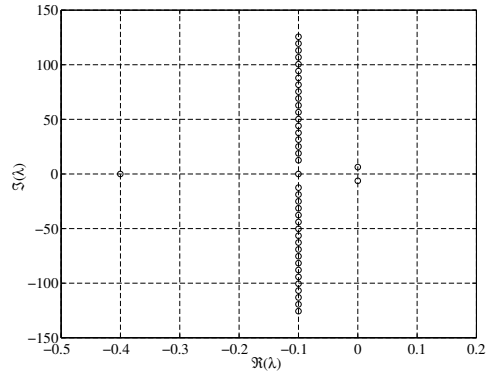

Figure 6.32: Eigenvalues at the neutral curve for $D = 0.1$, $\Gamma = 0.20029$ and $\alpha = 0$.

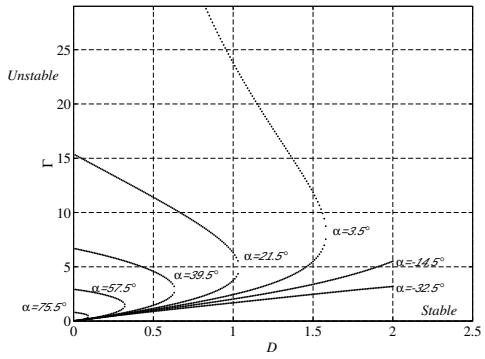

Figure 6.33: Neutral stability curve for different values of the tilt angle α.

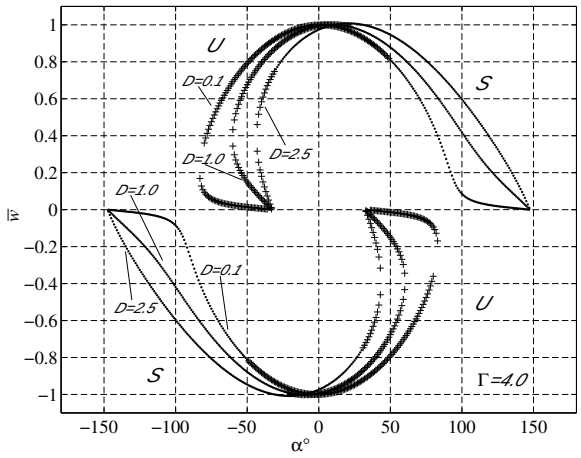

Figure 6.34: Curve $\overline{w}$ vs. α $\Gamma = 4.0$ and $D = 0.1$,$D = 1.0$,$D = 2.5$.

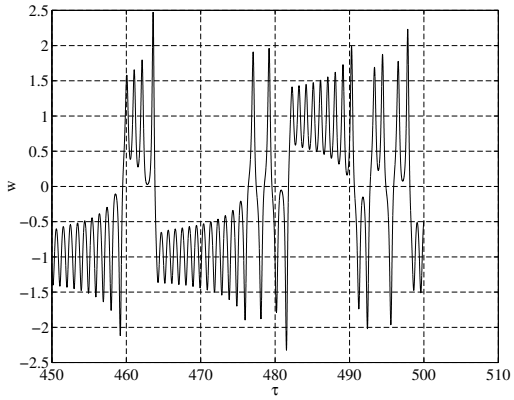

Figure 6.35: Curve w vs. τ for $D = 1.5$, $\Gamma = 0.95\Gamma_{cr}$.

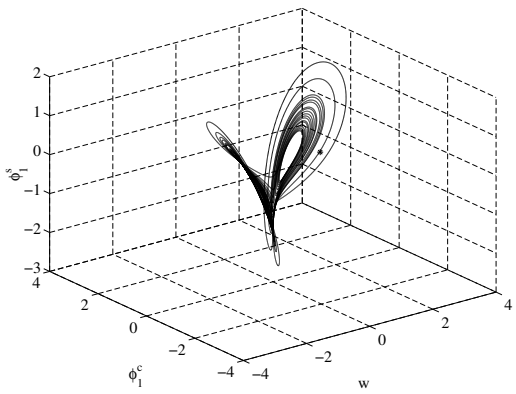

Figure 6.36: Phase-space trajectory for $D = 1.5$, $\Gamma = 0.95\Gamma_{cr}$.

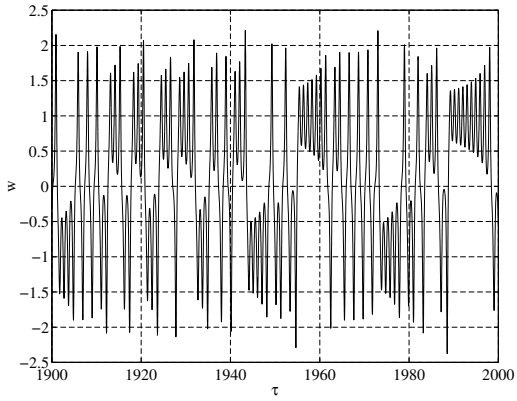

Figure 6.37: Curve w vs. τ for $D = 1.5$, $\Gamma = 1.01\Gamma_{cr}$.

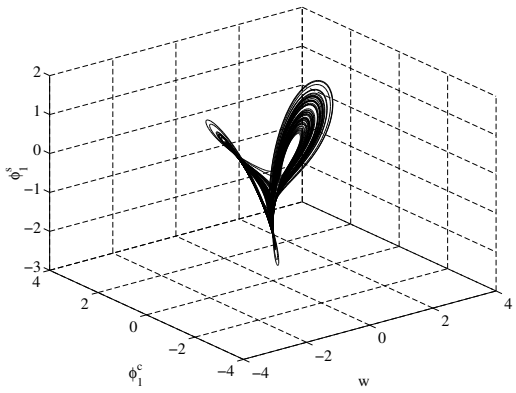

Figure 6.38: Phase-space trajectory for $D = 1.5$, $\Gamma = 1.01\Gamma_{cr}$.

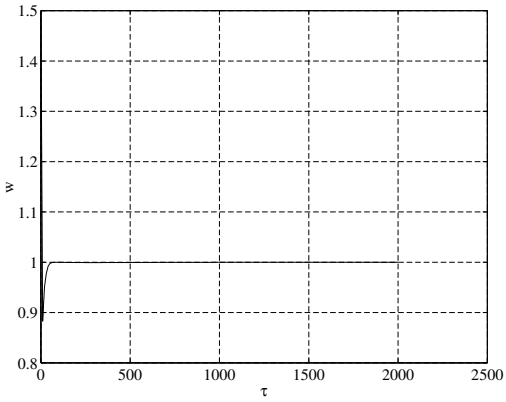

Figure 6.39: Curve w vs. τ for $D = 0.1$, $\Gamma = 0.99\Gamma_{cr}$.

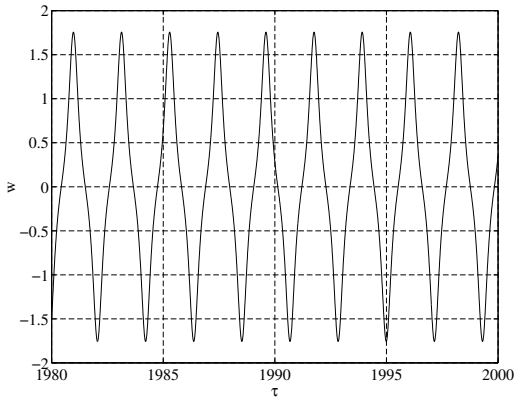

Figure 6.40: Curve w vs. τ for $D = 0.1$, $\Gamma = 1.1\Gamma_{cr}$.

Now we choose $D = 0.1$, and increase Γ. Figure 6.39 presents a plot of the $\overline{w} - \tau$ curve for $\Gamma = 0.99\Gamma_{cr}$. Figures 6.40 and 6.41 show the time series plots and phase space representation for $\Gamma = 1.01\Gamma_{cr}$, and Figures 6.42 and 6.43 for $\Gamma = 20\Gamma_{cr}$. In this case, for $\Gamma < \Gamma_{cr}$ we have stable solutions. For $\Gamma = 1.01\Gamma_{cr}$ the figures show a possible limit cycle undergoes a period doubling. This implies a supercritical Hopf bifurcation. The strange attractor is shown in Figures 6.44 and 6.45.

6.5 Perturbation of one-dimensional flow

6.6 Thermal control

Consider the control of temperature at a given point in the loop by modification of the heating. Both known heat flux and known wall temperatures may be looked at. In terms of control algorithms, one may use PID or on-off control.

Problems

1. Find the pressure distributions for the different cases of the square loop problem.
2. Consider the same square loop but tilted through an angle θ where $0 \leq \theta < 2\pi$. There is constant heating between points a and c, and constant cooling between e and g. For the steady-state problem, determine the temperature distribution and the velocity as a function of θ. Plot (a) typical temperature distributions for different tilt angles, and (b) the velocity as a function of tilt angle.
3. Find the steady-state temperature field and velocity for known heating if the loop has a variable cross-sectional area $A(s)$.
4. Find the temperature field and velocity for known heating if the total heating is not zero.
5. Find the velocity and temperature fields for known heating if the heating and cooling takes place at two different points. What the condition for the existence of a solution?
6. What is the effect on the known heat rate solution of taking a power-law relationship between the frictional force and the fluid velocity?
7. For known wall temperature heating, show that if the wall temperature is constant, the temperature field is uniform and the velocity is zero.

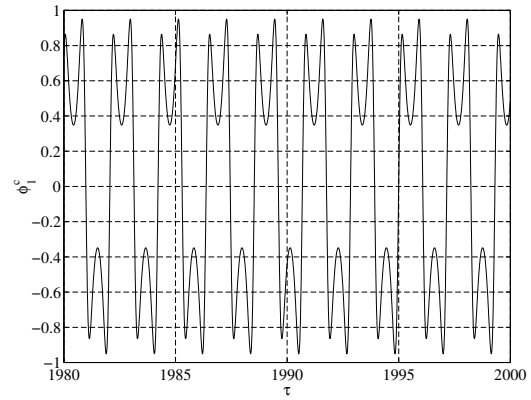

Figure 6.41: Phase-space trajectory for $D = 0.1$, $\Gamma = 1.1\Gamma_{cr}$.

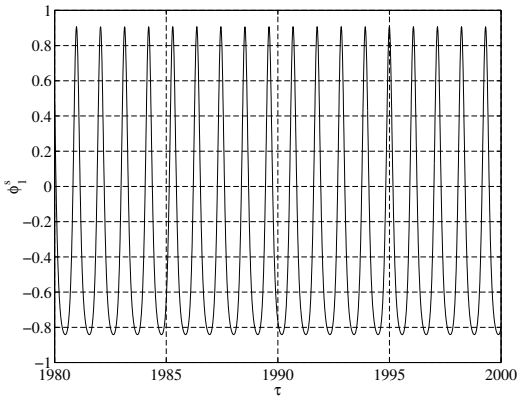

Figure 6.42: Curve w vs. τ for $D = 0.1$, $\Gamma = 1.1\Gamma_{cr}$.

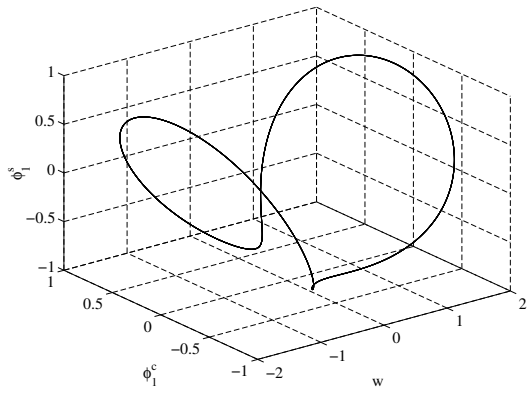

Figure 6.43: Phase-space trajectory for $D = 0.1$, $\Gamma = 1.1\Gamma_{cr}$.

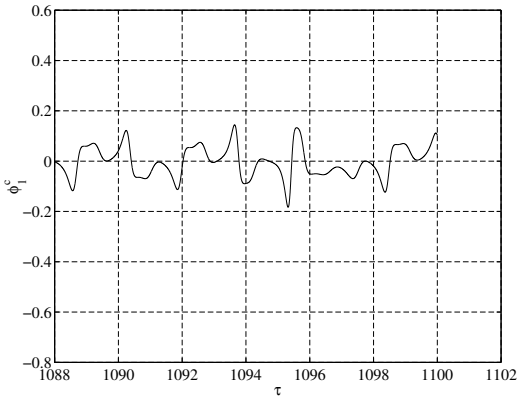

Figure 6.44: Phase-space trajectory for $D = 0.1$, $\Gamma = 20\Gamma_{cr}$.

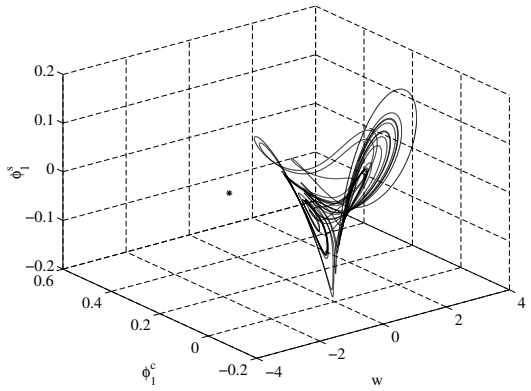

Figure 6.45: Phase-space trajectory for $D = 0.1$, $\Gamma = 20\Gamma_{cr}$.

8. Study the steady states of the toroidal loop with known wall temperature including nondimensionalization of the governing equations, axial conduction and tilting effects, multiplicity of solutions and bifurcation diagrams. Illustrate typical cases with appropriate graphs.
9. Consider a long, thin, vertical tube that is open at both ends. The air in the tube is heated with an electrical resistance running down the center of the tube. Find the flow rate of the air due to natural convection. Make any assumptions you need to.
10. For a thin, vertical pipe compare the wall shear stress to mean flow velocity relation obtained from a two-dimensional analysis to that from Poiseuille flow.
11. Find the combination of fluid parameters that determines the rate of heat transfer from a closed loop with known temperature distribution. Compare the cooling rate achieved by an ionic liquid to water in the same loop and operating under the same temperature difference.
12. Consider a tall natural circulation loop shown in Fig. 6.46 consisting of two vertical pipes of circular cross sections. The heating pipe has a diameter D, and that of the cooling side is $2D$. The heat rate per unit length coming in and going out are both q. Find the steady state velocity in the loop. Neglect the small horizontal sections and state your other assumptions.

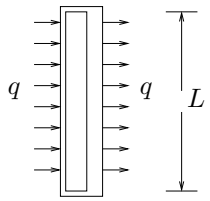

Figure 6.46: Tall natural circulation loop.

13. Set up a controller for PID control of the velocity x to a given value, x_s, in the toroidal natural convection loop equations

$$\begin{aligned} \frac{dx}{dt} &= y - x \\ \frac{dy}{dt} &= a\sin\phi - xz \\ \frac{dz}{dt} &= -b\cos\phi + xy \end{aligned}$$

where a and b are held constant. Use the tilt angle ϕ as control input, and show numerical results.

Chapter 7

Moving boundary

7.1 Stefan problems

[44]

The two phases, indicated by subscripts 1 and 2, are separated by an interface at $x = X(t)$. In each phase, the conduction equations is

$$\frac{\partial^2 T_1}{\partial x^2} - \frac{1}{\kappa_1}\frac{\partial T_1}{\partial t} = 0 \tag{7.1}$$

$$\frac{\partial^2 T_2}{\partial x^2} - \frac{1}{\kappa_2}\frac{\partial T_2}{\partial t} = 0 \tag{7.2}$$

At the interface the temperature should be continuous, so that

$$T_1(X,t) = T_2(X,t) \tag{7.3}$$

Furthermore the difference in heat rate into the interface provides the energy required for phase change. Thus

$$k_1\frac{\partial T_1}{\partial x} - k_2\frac{\partial T_2}{\partial x} = L\rho\frac{dX}{dt} \tag{7.4}$$

7.1.1 Neumann's solution

The material is initially liquid at $T = T_0$. The temperature at the $x = 0$ end is reduced to zero for $t > 0$. Thus

$$T_1 = 0 \quad \text{at} \quad x = 0 \tag{7.5}$$

$$T_2 \to T_0 \quad \text{as} \quad x \to \infty \tag{7.6}$$

Assume $T_1(x,t)$ to be

$$T_1 = A \text{ erf } \frac{x}{2\sqrt{\kappa_1 t}} \tag{7.7}$$

so that it satisfies equations (7.1) and (7.5). Similarly

$$T_1 = A \text{ erf } \frac{x}{2\sqrt{\kappa_1 t}} T_2 = T_0 - B \text{ erf } \frac{x}{2\sqrt{\kappa_2 t}} \tag{7.8}$$

satisfies equation (7.2) and (7.6). The, condition (7.3) requires that

$$A \text{ erf } \frac{x}{2\sqrt{\kappa_1 t}} = T_0 - B \text{ erf } \frac{x}{2\sqrt{\kappa_2 t}} = T_1 \tag{7.9}$$

This shows that

$$X = 2\lambda\sqrt{\kappa_1 t} \tag{7.10}$$

where λ is a constant. Using the remaining condition (7.4), we get

$$k_1 A e^{-\lambda^2} - k_2 B \sqrt{\frac{\kappa_1}{\kappa_2}} e^{-\kappa_1 \lambda^2/\kappa_2} = \lambda L \kappa_1 \rho \sqrt{\pi} \tag{7.11}$$

This can be written as

$$\frac{e^{-\lambda^2}}{\text{erf } \lambda} - \frac{k_2\sqrt{\kappa_1^2}(T_0 - T_1)e^{-\kappa_2\lambda^2/\kappa_2}}{k_1\sqrt{\kappa_2}T_1 \text{ erfc}(\lambda\sqrt{\kappa_1/\kappa_2})} = \frac{\lambda L\sqrt{\pi}}{c_1 T_1 s} \tag{7.12}$$

The temperatures are

$$T_1 = \frac{T_1}{\text{erf } \lambda} \text{ erf } (\frac{x}{2\sqrt{\kappa_1 t}}) \tag{7.13}$$

$$T_2 = T_0 - \frac{T_0 - T_1}{\text{erfc}(\lambda\sqrt{\kappa_1/\kappa_2})} \text{ erfc}(\frac{x}{2\sqrt{\kappa_2 t}}) \tag{7.14}$$

7.1.2 Goodman's integral

Part IV

Multiple spatial dimensions

Chapter 8

Conduction

8.1 Steady-state problems

See [206].

8.2 Transient problems

8.2.1 Two-dimensional fin

The governing equation is

$$c\rho dx\ dyL\frac{\partial T}{\partial t} = Lk\left(\frac{\partial^2 T}{\partial x^2} + \frac{\partial^2 T}{\partial y^2}\right) - hdx\ dy(T - T_\infty) \tag{8.1}$$

which simplifies to

$$\frac{1}{\alpha}\frac{\partial T}{\partial t} = \frac{\partial^2 T}{\partial x^2} + \frac{\partial^2 T}{\partial y^2} - m^2(T - T_\infty) \tag{8.2}$$

where $m^2 = h/kL$, the Biot number.

In the steady state

$$\frac{\partial^2 T}{\partial x^2} + \frac{\partial^2 T}{\partial y^2} - m^2(T - T_\infty) \tag{8.3}$$

Consider a square of unit side with $\theta = T - T_\infty$ being zero all around, except for one edge where it is unity.

Let

$$\theta(x, y) = X(x)Y(y) \tag{8.4}$$

so that

$$\frac{1}{X}\frac{d^2X}{dx^2} = -\frac{1}{X}\frac{d^2Y}{dy^2} + m^2 = -\lambda^2 \tag{8.5}$$

This leads to one equation

$$\frac{d^2X}{dx^2} + \lambda^2 X = 0 \tag{8.6}$$

with $X(0) = X(1) = 1$. Thus

$$X(x) = A\sin\lambda x + B\cos\lambda x \tag{8.7}$$

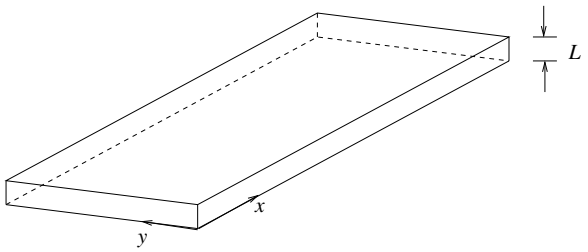

Figure 8.1: Two-dimensional fin.

where due to the boundary conditions, $B = 0$ and $\lambda = n\pi$, $n = 1, 2, \ldots$. Another equation is

$$\frac{d^2Y}{dy^2} - \left(m^2 + \lambda^2\right) Y = 0 \tag{8.8}$$

with

$$Y(y) = A \sinh \sqrt{m^2 + n^2\pi^2}\, y + B \cosh \sqrt{m^2 + n^2\pi^2}\, y \tag{8.9}$$

The condition $Y(0) = 0$ gives $B = 0$. Thus

$$\theta(x, y) = \sum A_n \sin n\pi x \sinh \sqrt{m^2 + n^2\pi^2}\, y \tag{8.10}$$

8.3 Radiating fins

8.4 Non-Cartesian coordinates

Toroidal, bipolar.

Shape factor.

Moving boundary problem at a corner.

Problems

1. Show that the separation of variables solution for $\nabla^2 T = 0$ for a rectangle can also be obtained through an eigenfunction expansion procedure.
2. Consider steady-state conduction in bipolar coordinates shown in
   http://mathworld.wolfram.com/BipolarCylindricalCoordinates.html
   with $a = 1$. The two cylindrical surfaces shown as $v = 1$ and $v = 2$ are kept at temperatures T_1 and T_2, respectively. Sketch the geometry of the annular material between $v = 1$ and $v = 2$ and find the temperature distribution in it by solving the Laplace's equation $\nabla^2 T = 0$.
3. Set up and solve a conduction problem similar to Problem 2, but in parabolic cylindrical coordinates. Use Morse and Feshbach's notation as shown in
   http://www.math.sdu.edu.cn/mathency/math/p/p059.htm
4. Consider an unsteady one-dimensional fin of constant area with base temperature known and tip adiabatic. Use the eigenfunction expansion method to reduce the governing equation to an infinite set of ODEs and solve.
5. Consider conduction in a square plate with Dirichlet boundary conditions. Find the appropriate eigenfunctions for the Laplacian operator for this problem.

Chapter 9

Forced convection

See [206].

9.1 Low Reynolds numbers

9.2 Potential flow

[169]

If the heat flux is written as

$$\mathbf{q} = \rho c \mathbf{u} T - k \nabla T \tag{9.1}$$

the energy equation is

$$\nabla \cdot \mathbf{q} = 0 \tag{9.2}$$

Heat flows along heatlines given by

$$\frac{dx}{\rho c T u_x - k(\partial T/\partial x)} = \frac{dy}{\rho c T u_y - k(\partial T/\partial y)} = \frac{dz}{\rho c T u_z - k(\partial T/\partial z)} \tag{9.3}$$

The tangent to heatlines at every point is the direction of the heat flux vector.

9.2.1 Two-dimensional flow

9.3 Leveque's solution

Leveque (1928)

9.4 Multiple solutions

See [166].

9.5 Plate heat exchangers

There is flow on the two sides of a plate, 1 and 2, with an overall heat transfer coefficient of U. Consider a rectangular plate of size $L_x \times L_y$ in the x- and y-directions, respectively, as shown in Fig.

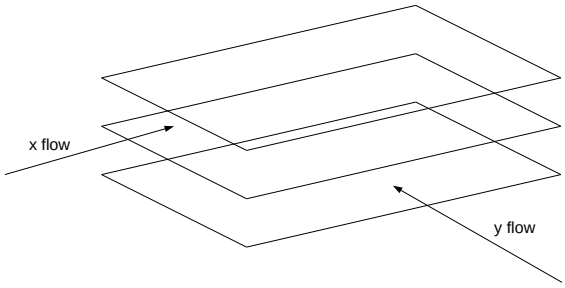

Figure 9.1: Schematic of crossflow plate HX.

9.1. The flow on one side of the plate is in the x-direction with a temperature field $T_x(x, y)$. The mass flow rate of the flow is m_x per unit transverse length. The flow in the other side of the plate is in the y-direction with the corresponding quantities $T_y(x, y)$ and m_y. The overall heat transfer coefficient between the two fluids is U, which we will take to be a constant.

For the flow in the x-direction, the steady heat balance on an elemental rectangle of size $dx \times dy$ gives

$$c_x \; m_x \; dy \; \frac{\partial T_x}{\partial x} \; dx = U \; dx \; dy \; (T_y - T_x) \tag{9.4}$$

where c_x is the specific heat of that fluid. Simplifying, we get

$$2C_x R \frac{\partial T_x}{\partial x} = T_y - T_x \tag{9.5}$$

where $R = 1/2U$ is proportional to the thermal resistance between the two fluids, and $C_x = c_x m_x$. For the other fluid

$$2C_y R \frac{\partial T_y}{\partial y} = T_x - T_y \tag{9.6}$$

These equations have to be solved with suitable boundary conditions to obtain the temperature fields $T_x(x, y)$ and $T_y(x, y)$.

From equation (9.6), we get

$$T_x = T_y + C_y R \frac{\partial T_y}{\partial y} \tag{9.7}$$

Substituting in equation (9.5), we have

$$\frac{1}{C_y} \frac{\partial T_y}{\partial x} + \frac{1}{C_x} \frac{\partial T_y}{\partial y} + 2R \frac{^2 T_y}{\partial x \partial y} = 0 \tag{9.8}$$

Nusselt (Jakob, 1957) gives an interesting solution in the following manner. Let the plate be

of dimensions L and W in the x- and y-directions. Nondimensional variables are

$$\xi = \frac{x}{L} \tag{9.9}$$

$$\eta = \frac{y}{W} \tag{9.10}$$

$$\theta_x = \frac{T_x - T_{y,i}}{T_{x,i} - T_{y,i}} \tag{9.11}$$

$$\theta_y = \frac{T_y - T_{y,i}}{T_{x,i} - T_{y,i}} \tag{9.12}$$

$$a = \frac{UWL}{C_x} \tag{9.13}$$

$$b = \frac{UWL}{C_y} \tag{9.14}$$

The governing equations are then

$$a(\theta_x - \theta_y) = -\frac{\partial \theta_x}{\partial \xi} \tag{9.15}$$

$$b(\theta_x - \theta_y) = \frac{\partial \theta_y}{\partial \eta} \tag{9.16}$$

with boundary conditions

$$\theta_x = 1 \quad \text{at } \xi = 0 \tag{9.17}$$

$$\theta_y = 0 \quad \text{at } \eta = 0 \tag{9.18}$$

Equation (9.16) can be written as

$$\frac{\partial \theta_y}{\partial \eta} + b\theta_y = b\theta_x \tag{9.19}$$

Solving for θ_y we get

$$\theta_y = e^{-b\eta} \left(C(\xi) + b \int_0^\eta \theta_x(\xi, \eta') e^{b\eta'} \, d\eta' \right) \tag{9.20}$$

From the boundary condition (9.18), we get

$$C = 0 \tag{9.21}$$

so that

$$\theta_y(\xi, \eta) = be^{-b\eta} \int_0^\eta \theta_x(\xi, \eta') e^{b\eta'} \, d\eta' \tag{9.22}$$

Using the same procedure, from equation (9.15) we get

$$\theta_x(\xi, \eta) = e^{-a\xi} + ae^{-a\xi} \int_0^\xi \theta_y(\xi', \eta) e^{a\xi'} \, d\xi' \tag{9.23}$$

Substituting for θ_y, we find the Volterra integral equation

$$\theta_x(\xi, \eta) = e^{-a\xi} + abe^{-(a\xi + b\eta)} \int_0^\xi \int_0^\eta \theta_x(\xi', \eta') e^{a\xi' + b\eta'} \, d\xi' \, d\eta' \tag{9.24}$$

for the unknown θ_x.

We will first solve the Volterra equation for an arbitrary λ, where

$$\theta_x(\xi,\eta) = e^{-a\xi} + ab\lambda e^{-(a\xi+b\eta)} \int_0^\xi \int_0^\eta \theta_x(\xi',\eta') e^{a\xi'+b\eta'} \, d\xi' \, d\eta' \tag{9.25}$$

Let us express the solution in terms of a finite power series

$$\theta_x(\xi,\eta) = \phi_0(\xi,\eta) + \lambda\phi_1(\xi,\eta) + \lambda^2\phi_2(\xi,\eta) + \ldots + \lambda^n\phi_n(\xi,\eta) \tag{9.26}$$

This can be substituted in the integral equation. Since λ is arbitrary, the coefficient of each order of λ must vanish. Thus

$$\begin{aligned}
\phi_0(\xi,\eta) &= e^{-a\xi} && (9.27)\\
\phi_1(\xi,\eta) &= abe^{-(a\xi+b\eta)} \int_0^\xi \int_0^\eta \phi_0(\xi',\eta') e^{a\xi'+b\eta'} \, d\xi' \, d\eta' && (9.28)\\
\phi_2(\xi,\eta) &= abe^{-(a\xi+b\eta)} \int_0^\xi \int_0^\eta \phi_1(\xi',\eta') e^{a\xi'+b\eta'} \, d\xi' \, d\eta' && (9.29)\\
&\vdots && (9.30)\\
\phi_n(\xi,\eta) &= abe^{-(a\xi+b\eta)} \int_0^\xi \int_0^\eta \phi_{n-1}(\xi',\eta') e^{a\xi'+b\eta'} \, d\xi' \, d\eta' && (9.31)\\
& && (9.32)
\end{aligned}$$

The solutions are

$$\begin{aligned}
\phi_0 &= e^{-a\xi} && (9.33)\\
\phi_1 &= a\xi e^{-a\xi}(1 - e^{-b\eta}) && (9.34)\\
\phi_2 &= \frac{1}{2}a^2\xi^2 e^{-a\xi}(1 - e^{-b\eta} - b\eta e^{-b\eta}) && (9.35)\\
\phi_3 &= \frac{1}{2\times 3}a^3\xi^3 e^{-a\xi}(1 - e^{-b\eta} - b\eta e^{-b\eta} - \frac{1}{2}b^2\eta^2 e^{-b\eta}) && (9.36)\\
&\vdots && (9.37)\\
\phi_n &= \frac{1}{n!}a^n\xi^n e^{-a\xi}(1 - e^{-b\eta} - b\eta e^{-b\eta} - \ldots - \frac{1}{(n-1)!}b^{n-1}\eta^{n-1}e^{-b\eta}) && (9.38)
\end{aligned}$$

Substituting into the expansion, equation (9.26), and taking $\lambda = 1$, we get

$$\theta_x(\xi,\eta) = \phi_0(\xi,\eta) + \phi_1(\xi,\eta) + \phi_2(\xi,\eta) + \ldots + \phi_n(\xi,\eta) \tag{9.39}$$

where the ϕs are given above.

Example 9.1

Find a solution of the same problem by separation of variables.

Taking

$$T_y(x,y) = X(x)Y(y) \tag{9.40}$$

Substituting and dividing by XY, we get

$$\frac{1}{C_x}\frac{\partial T_x}{\partial x} + \frac{1}{C_y}\frac{dY}{dy} + 2R = 0 \tag{9.41}$$

Since the first term is a function only of x, and the second only of y, each must be a constant. Thus we can write

$$\frac{dX}{dx} + \frac{1}{c_x m_x (a+R)} X = 0 \tag{9.42}$$

$$\frac{dY}{dy} + \frac{1}{c_y m_y (a-R)} Y = 0 \tag{9.43}$$

where a is a constant. Solving the two equations and taking their product, we have

$$T_y = \frac{c}{a+R} \exp\left[-\frac{x}{c_x m_x (a+R)} + \frac{y}{c_y m_y (a-R)} \right] \tag{9.44}$$

where c is a constant. Substituting in equation (9.7), we get

$$T_x = \frac{c}{a-R} \exp\left[-\frac{x}{c_x m_x (a+R)} + \frac{y}{c_y m_y (a-R)} \right] \tag{9.45}$$

The rate of heat transfer over the entire plate, Q, is given by

$$Q = C_x \int_0^{L-y} \left[T_x(L_x, y) - T_x(0, y) \right] \, dy \tag{9.46}$$

$$= cC_x C_y \exp\left[-\frac{l_x}{C_x (a+R)} - \frac{L_y}{C_2 (a-R)} - 2 \right] \tag{9.47}$$

The heat rate can be maximized by varying either of the variables C_x or C_y.

9.6 Falkner-Skan boundary flows

Problems

1. This is a problem

Chapter 10

Natural convection

10.1 Governing equations

10.2 Cavities

10.3 Marangoni convection

See [204].

Problems

1. This is a problem.

Chapter 11

Porous media

[103, 130, 201]

11.1 Governing equations

The continuity equation for incompressible flow in a porous medium is

$$\nabla \cdot \mathbf{V} = 0 \tag{11.1}$$

11.1.1 Darcy's equation

For the momentum equation, the simplest model is that due to Darcy

$$\nabla p = -\frac{\mu}{K}\mathbf{V} + \rho\mathbf{f} \tag{11.2}$$

where $\mathbf{f}$ is the body force per unit mass. Here K is called the permeability of the medium and has units of inverse area. It is similar to the incompressible Navier-Stokes equation with constant properties where the inertia terms are dropped and the viscous force per unit volume is represented by $-(\mu/K)\mathbf{V}$. Sometimes a term $c\rho_0\partial\mathbf{V}/\partial t$ is added to the left side for transient problems, but it is normally left out because it is very small. The condition on the velocity is that of zero normal velocity at a boundary, allowing for slip in the tangential direction.

From equations (11.1) and (11.2), for $\mathbf{f} = 0$ we get

$$\nabla^2 p = 0 \tag{11.3}$$

from which the pressure distribution can be determined.

11.1.2 Forchheimer's equation

Forchheimer's equation which is often used instead of Darcy's equation is

$$\nabla p = -\frac{\mu}{K}\mathbf{V} - c_f K^{-1/2}\rho|\mathbf{V}|\mathbf{V} + \rho\mathbf{f} \tag{11.4}$$

where c_f is a dimensionless constant. There is still slip at a boundary.

11.1.3 Brinkman's equation

Another alternative is Brinkman's equation

$$\nabla p = -\frac{\mu}{K}\mathbf{V} + \tilde{\mu}\nabla^2\mathbf{V} + \rho\mathbf{f} \tag{11.5}$$

where $\tilde{\mu}$ is another viscous coefficient. In this model there is no slip at a solid boundary.

11.1.4 Energy equation

The energy equation is

$$(\rho c)_m \frac{\partial T}{\partial t} + \rho c_p \mathbf{V}\cdot\nabla T = k_m \nabla^2 T \tag{11.6}$$

where k_m is the effective thermal conductivity, and

$$(\rho c)_m = \phi\rho c_p + (1-\phi)(\rho c)_m \tag{11.7}$$

is the average heat capacity. The subscripts m refers to the solid matrix, and ϕ is the porosity of the material. An equivalent form is

$$\sigma\frac{\partial T}{\partial t} + \mathbf{V}\cdot\nabla T = \alpha_m \nabla^2 T \tag{11.8}$$

where

$$\alpha_m = \frac{k_m}{\rho c_p} \tag{11.9}$$

$$\sigma = \frac{(\rho c)_m}{\rho c_p} \tag{11.10}$$

See [1].

11.2 Forced convection

11.2.1 Plane wall at constant temperature

The solution to

$$\frac{\partial u}{\partial x} + \frac{\partial v}{\partial y} = 0 \tag{11.11}$$

$$u = -\frac{K}{\mu}\frac{\partial p}{\partial x} \tag{11.12}$$

$$v = -\frac{K}{\mu}\frac{\partial p}{\partial y} \tag{11.13}$$

is

$$u = U \tag{11.14}$$

$$v = 0 \tag{11.15}$$

For

$$\frac{Ux}{\alpha_m} = Pe_x \gg 1 \tag{11.16}$$

the energy equation is

$$u\frac{\partial T}{\partial x} + v\frac{\partial T}{\partial y} = \alpha_m \frac{\partial^2 T}{\partial y^2} \tag{11.17}$$

or

$$U\frac{\partial T}{\partial x} = \alpha_m \frac{\partial^2 T}{\partial y^2} \tag{11.18}$$

The boundary conditions are

$$T(0) = T_w \tag{11.19}$$
$$T(\infty) = T_\infty \tag{11.20}$$

Writing

$$\eta = y\sqrt{\frac{U}{\alpha_m x}} \tag{11.21}$$
$$\theta(\eta) = \frac{T - T_w}{T_\infty - T_w} \tag{11.22}$$

we get

$$\frac{\partial T}{\partial x} = (T_\infty - T_w)\frac{d\theta}{d\eta}\frac{\partial \eta}{\partial x} \tag{11.23}$$
$$= (T_\infty - T_w)\frac{d\theta}{d\eta}\left(-y\sqrt{\frac{U}{\alpha_m}}\frac{1}{2}x^{-3/2}\right) \tag{11.24}$$
$$\frac{\partial T}{\partial y} = (T_\infty - T_w)\frac{d\theta}{d\eta}\frac{\partial \eta}{\partial y} \tag{11.25}$$
$$= (T_\infty - T_w)\frac{d\theta}{d\eta}\sqrt{\frac{U}{\alpha_m x}} \tag{11.26}$$
$$\frac{\partial^2 T}{\partial y^2} = (T_\infty - T_w)\frac{d^2\theta}{d\eta^2}\frac{U}{\alpha_m x} \tag{11.27}$$

so that the equation becomes

$$\theta'' + \frac{1}{2}\eta\,\theta' = 0 \tag{11.28}$$

with

$$\theta(0) = 0 \tag{11.29}$$
$$\theta(\infty) = 1 \tag{11.30}$$

We multiply by the integrating factor $e^{\eta^2/4}$ to get

$$\frac{d}{d\eta}\left(e^{\eta^2/4}\theta'\right) = 0 \tag{11.31}$$

The first integral is

$$\theta' = C_1 e^{-\eta^2/4} \tag{11.32}$$

Integrating again we have

$$\theta = C_1 \int_0^\eta e^{-\eta'^2/4}\, d\eta' + C_2 \tag{11.33}$$

With the change in variables $x = \eta'/2$, the solution becomes

$$\theta = 2C_1 \int_0^{\eta/2} e^{-x^2}\, dx \tag{11.34}$$

Applying the boundary conditions, we find that $C_1 = 1/\sqrt{\pi}$ and $C_2 = 0$. Thus

$$\begin{aligned} \theta &= \frac{2}{\sqrt{\pi}} \int_0^{\eta/2} e^{-x^2}\, dx && (11.35)\\ &= \operatorname{erf} \frac{\eta}{2} && (11.36) \end{aligned}$$

The heat transfer coefficient is defined as

$$\begin{aligned} h &= \frac{q''}{T_w - T_\infty} && (11.37)\\ &= -\frac{k_m}{T_w - T_\infty} \frac{\partial T}{\partial y} && (11.38)\\ &= k_m \frac{\partial \theta}{\partial y} && (11.39) \end{aligned}$$

The local Nusselt number is given by

$$\begin{aligned} Nu_x &= \frac{hx}{k_m} && (11.40)\\ &= x \left.\frac{\partial \theta}{\partial y}\right|_{y=0} && (11.41)\\ &= \frac{1}{\sqrt{\pi}} \sqrt{\frac{Ux}{\alpha_m}} && (11.42)\\ &= \frac{1}{\sqrt{\pi}} Pe_x^{-1/2} && (11.43) \end{aligned}$$

Example 11.1

Find the temperature distribution for flow in a porous medium parallel to a flat plate with uniform heat flux.

11.2.2 Stagnation-point flow

For flow in a porous medium normal to an infinite flat plate, the velocity field is

$$\begin{aligned} u &= Cx && (11.44)\\ v &= -Cy && (11.45) \end{aligned}$$

The energy equation is

$$Cx \frac{\partial T}{\partial x} - Cy \frac{\partial T}{\partial y} = \alpha_m \frac{\partial^2 T}{\partial y^2} \tag{11.46}$$

11.2.3 Thermal wakes

Line source

For $Pe_x \gg 1$, the governing equation is

$$U\frac{\partial T}{\partial x} = \alpha_m \frac{\partial^2 T}{\partial y^2} \tag{11.47}$$

where the boundary conditions are

$$\frac{\partial T}{\partial y} = 0 \text{ at } y = 0 \tag{11.48}$$

$$q' = (\rho c_p) U \int_{-\infty}^{\infty} (T - T_\infty)\, dy \tag{11.49}$$

Writing

$$\eta = y\sqrt{\frac{U}{\alpha_m x}} \tag{11.50}$$

$$\theta(\eta) = \frac{T - T_\infty}{q'/k_m}\sqrt{\frac{Ux}{\alpha_m}} \tag{11.51}$$

we find that

$$\frac{\partial T}{\partial x} = \theta\frac{q'}{k_m}\sqrt{\frac{\alpha_m}{U}}\left(-\frac{1}{2}x^{-3/2}\right) + \frac{d\theta}{d\eta}y\sqrt{\frac{U}{\alpha_m}}\left(-\frac{1}{2}x^{-3/2}\frac{q'}{k_m}\sqrt{\frac{\alpha_m}{Ux}}\right) \tag{11.52}$$

$$\frac{\partial T}{\partial y} = \frac{q'}{k_m}\sqrt{\frac{\alpha_m}{Ux}}\frac{d\theta}{d\eta}\sqrt{\frac{U}{\alpha_m x}} \tag{11.53}$$

$$\frac{\partial^2 T}{\partial y^2} = \frac{q'}{k_m}\sqrt{\frac{\alpha_m}{Ux}}\frac{d\theta}{d\eta}\frac{U}{\alpha_m x} \tag{11.54}$$

$$\tag{11.55}$$

Substituting in the equation, we get

$$\theta'' = -\frac{1}{2}(\theta + \eta\theta') \tag{11.56}$$

The conditions (11.48)-(11.49) become

$$\frac{\partial \theta}{\partial \eta} = 0 \text{ at } \eta = 0 \tag{11.57}$$

$$\int_{-\infty}^{\infty} \theta\, dy = 1 \tag{11.58}$$

The equation (11.56) can be written as

$$\theta'' = -\frac{1}{2}\frac{d}{d\eta}(\eta\theta) \tag{11.59}$$

which integrates to

$$\theta' = -\frac{1}{2}\eta\theta + C_1 \tag{11.60}$$

Since $\theta' = 0$ at $\eta = 0$, we find that $C_1 = 0$. Integrating again, we get

$$\theta = C_2 e^{-\eta^2/4} \tag{11.61}$$

Substituting in the other boundary condition

$$1 = \int_{-\infty}^{\infty} \theta \; d\eta = C_2 \int_{-\infty}^{\infty} e^{-\eta^2/4} \; d\eta = 2\sqrt{\pi} C_2 \tag{11.62}$$

from which

$$C_2 = \frac{1}{2\sqrt{\pi}} \tag{11.63}$$

Thus the solution is

$$\theta = \frac{1}{2\sqrt{\pi}} e^{-\eta^2/4} \tag{11.64}$$

or

$$T - T_\infty = \frac{1}{2\sqrt{\pi}} \frac{q'}{k_m} \sqrt{(\frac{\alpha_m}{Ux})} \exp(\frac{-Uy^2}{4\alpha_m x}) \tag{11.65}$$

Example 11.2

Show that for a point source

$$T - T_\infty = \frac{q}{4\pi k x} \exp(\frac{-Ur^2}{4\alpha_m x}) \tag{11.66}$$

11.3 Natural convection

11.3.1 Linear stability

This is often called the Horton-Rogers-Lapwood problem, and consists of finding the stability of a horizontal layer of fluid in a porous medium heated from below. The geometry is shown in Fig. 11.1.

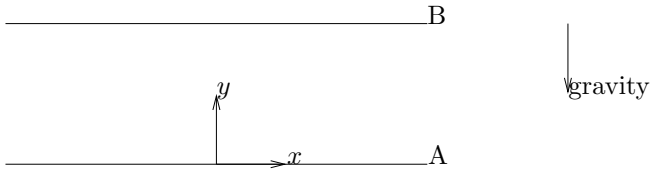

Figure 11.1: Stability of horizontal porous layer.

The governing equations are

$$\nabla \cdot \mathbf{V} = 0 \tag{11.67}$$

$$-\nabla p - \frac{\mu}{K}\mathbf{V} + \rho \mathbf{g} = 0 \tag{11.68}$$

$$\sigma \frac{\partial T}{\partial t} + \mathbf{V} \cdot \nabla T = \alpha_m \nabla^2 T \tag{11.69}$$

$$\rho = \rho_0 \left[1 - \beta \left(T - T_0\right)\right] \tag{11.70}$$

where $\mathbf{g} = -g\mathbf{j}$. The basic steady solution is

$$\overline{\mathbf{V}} = 0 \tag{11.71}$$
$$\overline{T} = T_0 + \Delta T\left(1 - \frac{y}{H}\right) \tag{11.72}$$
$$p = p_0 - \rho_0 g\left[y + \frac{1}{2}\beta\Delta T\left(\frac{y^2}{H} - 2y\right)\right] \tag{11.73}$$

For constant heat flux $\Delta T = q_s''/k_m$. We apply a perturbation to each variable as

$$\mathbf{V} = \overline{\mathbf{V}} + \mathbf{V}' \tag{11.74}$$
$$T = \overline{T} + T' \tag{11.75}$$
$$p = \overline{p} + p' \tag{11.76}$$

Substituting and linearizing

$$\nabla \cdot \mathbf{V}' = 0 \tag{11.77}$$
$$-\nabla p' - \frac{\mu}{K}\mathbf{V}' - \beta\rho_0 T'\mathbf{g} = 0 \tag{11.78}$$
$$\frac{\partial T'}{\partial t} - \frac{\Delta T}{H}w' = \alpha_m \nabla^2 T' \tag{11.79}$$

Using the nondimensional variables

$$\mathbf{x}^* = \frac{\mathbf{x}}{H} \tag{11.80}$$
$$t^* = \frac{\alpha_m t}{\sigma H^2} \tag{11.81}$$
$$\mathbf{V}^* = \frac{H\mathbf{V}'}{\alpha_m} \tag{11.82}$$
$$T^* = \frac{T'}{\Delta T} \tag{11.83}$$
$$p^* = \frac{Kp'}{\mu\alpha_m} \tag{11.84}$$

the equations become, on dropping *s

$$\nabla \cdot \mathbf{V} = 0 \tag{11.85}$$
$$-\nabla p - \mathbf{V} + Ra\ T\mathbf{k} = 0 \tag{11.86}$$
$$\frac{\partial T}{\partial t} - w = \nabla^2 T \tag{11.87}$$

where

$$Ra = \frac{\rho_0 g\beta K H\Delta T}{\mu\alpha_m} \tag{11.88}$$

From these equations we get

$$\nabla^2 w = Ra\nabla_H^2 T \tag{11.89}$$

where

$$\nabla_H = \frac{\partial^2}{\partial x^2} \tag{11.90}$$

Using separation of variables

$$w(x,y,z,t) = W(y)\exp(st+ik_x x) \tag{11.91}$$
$$T(x,y,z,t) = \Theta(y)\exp(st+ik_x x) \tag{11.92}$$

Substituting into the equations we get

$$\left(\frac{d^2}{dy^2}-k^2-s\right)\Theta = -W \tag{11.93}$$
$$\left(\frac{d^2}{dy^2}-k^2\right)W = -k^2 Ra\ \Theta \tag{11.94}$$

where

$$k^2 = k_x^2 + k_y^2 \tag{11.95}$$

Isothermal boundary conditions

The boundary conditions are $W = \Theta = 0$ at either wall. For the solutions to remain bounded as $x, y \to \infty$, the wavenumbers k_x and k_y must be real. Furthermore, since the eigenvalue problem is self-adjoint, as shown below, it can be shown that s is also real.

For a self-adjoint operator L, we must have

$$(u, Lv) = (Lu, v) \tag{11.96}$$

If

$$vL(u) - uL(v) = \frac{\partial P}{\partial x} + \frac{\partial Q}{\partial y} \tag{11.97}$$

then

$$\int_V [vL(u) - uL(v)]\ dV = \int \left(\frac{\partial P}{\partial x} + \frac{\partial Q}{\partial y}\right)\ dV \tag{11.98}$$
$$= \int_V \nabla\cdot(P\mathbf{i}+Q\mathbf{j})\ dV \tag{11.99}$$
$$= \int_S \mathbf{n}\cdot(P\mathbf{i}+Q\mathbf{j}) \tag{11.100}$$

If $\mathbf{n}\cdot(P\mathbf{i}+Q\mathbf{j}) = 0$ at the boundaries (i.e. impermeable), which is the case here, then L is self-adjoint.

Thus, marginal stability occurs when $s = 0$, for which

$$\left(\frac{d^2}{dy^2}-k^2\right)\Theta = -W \tag{11.101}$$
$$\left(\frac{d^2}{dy^2}-k^2\right)W = -k^2 Ra\ \Theta \tag{11.102}$$

from which

$$\left(\frac{d^2}{dy^2}-k^2\right)^2 W = k^2 Ra\ W \tag{11.103}$$

The eigenfunctions are

$$W = \sin n\pi y \tag{11.104}$$

where $n = 1, 2, 3, \ldots$, as long as

$$Ra = \left(\frac{n^2\pi^2}{k} + k \right)^2 \tag{11.105}$$

For each n there is a minimum value of the critical Rayleigh number determined by

$$\frac{dRa}{dk} = 2\left(\frac{n^2\pi^2}{k} + k \right)\left[-\frac{n^2\pi^2}{k^2} + 1 \right] \tag{11.106}$$

The lowest critical Ra is with $k = \pi$ and $n = 1$, which gives

$$Ra_c = 4\pi^2 \tag{11.107}$$

for the onset of instability.

Constant heat flux conditions

Here $W = d\Theta/dy = 0$ at the walls. We write

$$W = W_0 + \alpha^2 W_1 + \ldots \tag{11.108}$$
$$\Theta = \Theta_0 + \alpha^2 \Theta_1 + \ldots \tag{11.109}$$
$$Ra = Ra_0 + \alpha^2 Ra_1 + \ldots \tag{11.110}$$

For the zeroth order system

$$\frac{d^2 W_0}{dy^2} = 0 \tag{11.111}$$

with $W_0 = d\Theta_0/dy = 0$ at the walls. The solutions is $W_0 = 0$, $\Theta_0 = 1$. To the next order

$$\frac{d^2 W_1}{dy^2} = W_0 - Ra_0 \Theta_0 \tag{11.112}$$
$$\frac{d^2 \Theta_1}{dy^2} + W_1 = \Theta_0 \tag{11.113}$$

with $W_1 = d\Theta_1/dy = 0$ at the walls. Finally, we get $Ra_c = 12$.

11.3.2 Steady-state inclined layer solutions

Consider an inclined porous layer of thickness H at angle ϕ with respect to the horizontal shown in Fig. 11.2

Introducing the streamfunction $\psi(x, y)$, where

$$u = \frac{\partial \psi}{\partial y} \tag{11.114}$$
$$v = -\frac{\partial \psi}{\partial x} \tag{11.115}$$

Darcy's equation becomes

$$-\frac{\partial p}{\partial x} - \frac{\mu}{K}\frac{\partial \psi}{\partial y} = \rho_0 g \left[1 - \beta(T - T_0)\right] \sin\phi \tag{11.116}$$
$$-\frac{\partial p}{\partial y} + \frac{\mu}{K}\frac{\partial \psi}{\partial x} = \rho_0 g \left[1 - \beta(T - T_0)\right] \cos\phi \tag{11.117}$$

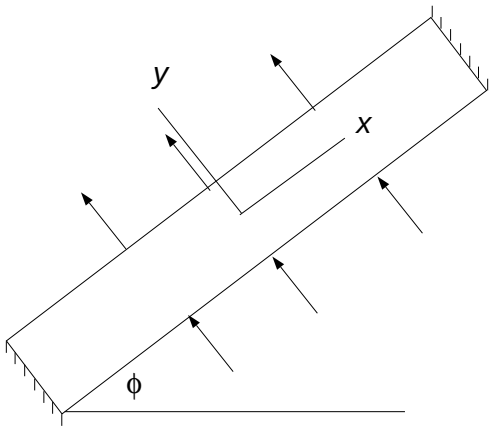

Figure 11.2: Inclined porous layer.

Taking $\partial/\partial y$ of the first and $\partial/\partial x$ of the second and subtracting, we have

$$\frac{\partial^2\psi}{\partial x^2}+\frac{\partial^2\psi}{\partial y^2}=-\frac{\rho_0 g\beta K}{\mu}\left(\frac{\partial T}{\partial x}\cos\phi-\frac{\partial T}{\partial y}\sin\phi\right) \tag{11.118}$$

The energy equation is

$$\left(\frac{\partial\psi}{\partial y}\frac{\partial T}{\partial x}-\frac{\partial\psi}{\partial x}\frac{\partial T}{\partial y}\right)=\alpha_m\left(\frac{\partial^2 T}{\partial x^2}+\frac{\partial^2 T}{\partial y^2}\right) \tag{11.119}$$

Side-wall heating

The non-dimensional equations are

$$\frac{\partial^2\psi}{\partial x^2}+\frac{\partial^2\psi}{\partial y^2} = -Ra\left(\frac{\partial T}{\partial x}\cos\phi-\frac{\partial T}{\partial y}\sin\phi\right) \tag{11.120}$$

$$\frac{\partial\psi}{\partial y}\frac{\partial T}{\partial x}-\frac{\partial\psi}{\partial x}\frac{\partial T}{\partial y} = \frac{\partial^2 T}{\partial x^2}+\frac{\partial^2 T}{\partial y^2} \tag{11.121}$$

where the Rayleigh number is

$$Ra =? \tag{11.122}$$

The boundary conditions are

$$\psi=0,\ \frac{\partial T}{\partial x}=0 \quad \text{at} \quad x=\pm\frac{A}{2} \tag{11.123}$$

$$\psi=0,\ \frac{\partial T}{\partial y}=-1 \quad \text{at} \quad y=\pm\frac{1}{2} \tag{11.124}$$

$$\tag{11.125}$$

With a parallel-flow approximation, we assume [167]

$$\psi = \psi(y) \tag{11.126}$$

$$T = Cx+\theta(y) \tag{11.127}$$

The governing equations become

$$\frac{\partial^2\psi}{\partial y^2} - Ra\ \sin\phi\frac{d\theta}{dy} + RC\cos\phi = 0 \tag{11.128}$$

$$\frac{d^2\theta}{dy^2} - C\frac{d\psi}{dy} = 0 \tag{11.129}$$

An additional constraint is the heat transported across a transversal section should be zero. Thus

$$\int_{-1/2}^{1/2}\left(uT - \frac{\partial T}{\partial x}\right)\ dy = 0 \tag{11.130}$$

Let us look at three cases.

(a) *Horizontal layer*

For $\phi = 0°$ the temperature and streamfunction are

$$T = Cx - y\left[1 + \frac{RaC^2}{24}\left(4y^2 - 3\right)\right] \tag{11.131}$$

$$\psi = -\frac{RaC}{8}\left(4y^2 - 1\right) \tag{11.132}$$

Substituting in condition (11.130), we get

$$C\left(10R - Ra^2C^2 - 120\right) = 0 \tag{11.133}$$

the solutions of which are

$$C = 0 \tag{11.134}$$

$$C = \frac{1}{Ra}\sqrt{10(Ra - 12)} \tag{11.135}$$

$$C = -\frac{1}{Ra}\sqrt{10(Ra - 12)} \tag{11.136}$$

The only real solution that exists for $Ra \leq 12$ is the conductive solution $C = 0$. For $C > 12$, there are two nonzero values of C which lead to convective solutions, for which

$$\psi_c = \frac{RaC}{8} \tag{11.137}$$

$$Nu = \frac{12}{12 - RaC^2} \tag{11.138}$$

For $\phi = 180°$, the only real value of C is zero, so that only the conductive solution exists.

(b) *Natural circulation*

Let us take $C\sin\phi > 0$, for which we get

$$\psi_c = \frac{B}{C}\left(1 - \cosh\frac{\alpha}{2}\right) \tag{11.139}$$

$$Nu = -\frac{\alpha}{2B\sinh\frac{\alpha}{2} + \alpha C\cot\phi} \tag{11.140}$$

where

$$\alpha^2 = RC\sin\phi \tag{11.141}$$

$$B = -\frac{1 + C\cot\phi}{\cosh\frac{\alpha}{2}} \tag{11.142}$$

and the constant C is determined from

$$C - \frac{B^2}{2C}\left(\frac{\sinh\alpha}{\alpha} - 1\right) - B\cot\phi\left(\cosh\frac{\alpha}{2} - \frac{2}{\alpha}\sinh\frac{\alpha}{2}\right) = 0 \tag{11.143}$$

(c) *Antinatural circulation*
For $C\sin\phi < 0$, for which we get

$$\psi_c = \frac{B}{C}\left(1 - \cosh\frac{\beta}{2}\right) \tag{11.144}$$

$$Nu = -\frac{\beta}{2B\sinh\frac{\beta}{2} + \beta C\cot\phi} \tag{11.145}$$

where

$$\beta^2 = -RC\sin\phi \tag{11.146}$$

$$B = -\frac{1 + C\cot\phi}{\cosh\frac{\beta}{2}} \tag{11.147}$$

and the constant C is determined from

$$C - \frac{B^2}{2C}\left(\frac{\sin\beta}{\beta} - 1\right) - B\cot\phi\left(\cosh\frac{\beta}{2} - \frac{2}{\beta}\sinh\frac{\beta}{2}\right) = 0 \tag{11.148}$$

End-wall heating

Darcy's law is

$$\nabla^2\psi = R\left(\frac{\partial T}{\partial x}\sin\phi + \frac{\partial T}{\partial y}\cos\phi\right) \tag{11.149}$$

The boundary conditions are

$$\psi = 0,\ \frac{\partial T}{\partial x} = -1 \quad \text{at} \quad x = \pm\frac{A}{2} \tag{11.150}$$

$$\psi = 0,\ \frac{\partial T}{\partial y} = 0 \quad \text{at} \quad x = \pm\frac{1}{2} \tag{11.151}$$

With a parallel-flow approximation, we assume

$$\psi = \psi(y) \tag{11.152}$$

$$T = Cx + \theta(y) \tag{11.153}$$

The governing equations become

$$\frac{d^\theta}{dy^2} - C\frac{d\psi}{dy} = 0 \tag{11.154}$$

$$\frac{\partial^2\psi}{\partial y^2} - R\cos\phi\frac{d\theta}{dy} - RC\sin\phi = 0 \tag{11.155}$$

An additional constraint is the heat transported across a transversal section. Thus

$$\int_{-1/2}^{1/2}\left(uT - \frac{\partial T}{\partial x}\right)\,dy = 1 \tag{11.156}$$

Let us look at three cases.

(a) *Vertical layer*

For $\phi = 0°$ the temperature and streamfunction are

$$T = Cx + \frac{B_1}{\alpha}\sin(\alpha y) - \frac{B_2}{\alpha}\cos(\alpha y) \tag{11.157}$$

$$\psi = \frac{B_1}{C}\cos(\alpha y) + \frac{B_2}{C}\sin(\alpha y) + B_3 \tag{11.158}$$

where

$$\alpha^2 = -RC \tag{11.159}$$

Substituting in condition (11.130), we get

$$C\left(10R - R^2C^2 - 120\right) = 0 \tag{11.160}$$

the solutions of which are

$$C = 0 \tag{11.161}$$

$$C = \frac{1}{R}\sqrt{10(R-12)} \tag{11.162}$$

$$C = -\frac{1}{R}\sqrt{10(R-12)} \tag{11.163}$$

The only real solution that exists for $R \leq 12$ is the conductive solution $C = 0$. For $C > 12$, there are two nonzero values of C which lead to convective solutions, for which

$$\psi_c = \frac{RC}{8} \tag{11.164}$$

$$Nu = \frac{12}{12 - RC} \tag{11.165}$$

For $\phi = 180°$, the only real value of C is zero, so that only the conductive solution exists.

(b) *Natural circulation*

Let us take $C\sin\phi > 0$, for which we get

$$\psi_c = \frac{B}{C}\left(1 - \cosh\frac{\alpha}{2}\right) \tag{11.166}$$

$$Nu = -\frac{\alpha}{2B\sinh\frac{\alpha}{2} + \alpha C\cot\phi} \tag{11.167}$$

where

$$\alpha^2 = RC\sin\phi \tag{11.168}$$

$$B = -\frac{1 + C\cot\phi}{\cosh\frac{\alpha}{2}} \tag{11.169}$$

and the constant C is determined from

$$C - \frac{B^2}{2C}\left(\frac{\sinh\alpha}{\alpha} - 1\right) - B\cot\phi\left(\cosh\frac{\alpha}{2} - \frac{2}{\alpha}\sinh\frac{\alpha}{2}\right) = 0 \tag{11.170}$$

(c) *Antinatural circulation*

For $C \sin\phi > 0$, for which we get

$$\psi_c = \frac{B}{C}\left(1 - \cosh\frac{\beta}{2}\right) \tag{11.171}$$

$$Nu = -\frac{\beta}{2B\sinh\frac{\beta}{2} + \beta C\cot\phi} \tag{11.172}$$

where

$$\beta^2 = -RC\sin\phi \tag{11.173}$$

$$B = -\frac{1 + C\cot\phi}{\cosh\frac{\beta}{2}} \tag{11.174}$$

and the constant C is determined from

$$C - \frac{B^2}{2C}\left(\frac{\sin\beta}{\beta} - 1\right) - B\cot\phi\left(\cosh\frac{\beta}{2} - \frac{2}{\beta}\sinh\frac{\beta}{2}\right) = 0 \tag{11.175}$$

Problems

1. This is a problem.

Chapter 12

Moving boundary

12.1 Stefan problems

Part V

Complex systems

Chapter 13

Radiation

13.1 Monte Carlo methods

[209]

[219] is a review of the radiative properties of semiconductors.

Problems

1. Consider an unsteady n-body radiative problem. The temperature of the ith body is given by

$$\begin{aligned} M_j c_j \frac{dT_j}{dt} &= -\sum_{i=1}^{n} A_i F_{ij} \sigma (T_i^4 - T_j^4) + Q_j \\ &= A_j \sum_{i=1}^{n} F_{ji} \sigma (T_i^4 - T_j^4) + Q_j \end{aligned}$$

   What kind of dynamic solutions are possible?

2. The steady-state temperature distribution in a one-dimensional radiative fin is given by

$$\frac{dT}{dx} + hT^4 = 0$$

   Is the solution unique and always possible?

3. Show that between one small body 1 and its large surroundings 2, the dynamics of the small-body temperature is governed by

$$M_1 c_1 \frac{dT_1}{dt} = -A_1 F_{12} \sigma (T_1^4 - T_2^4) + Q_1.$$

Chapter 14

Boiling and condensation

14.1 Homogeneous nucleation

Chapter 15

Microscale heat transfer

[108] is a review of microscale heat exchangers, and [36] of photonic devices.
[86, 119, 178, 186, 202, 219]

15.1 Diffusion by random walk

15.1.1 One-dimensional

Consider a walker along an infinite straight line moving with a step size Δx taken forward or backward with equal probability in a time interval Δt. Let the current position of the walker be x, and the probability that the walker is in an interval $[x - dx/2, x + dx/2]$ be $P(x, t)$. Since there is equal probability of the walker in the previous time step to have been in the interval $[x - \Delta x - dx/2, x - \Delta x + dx/2]$ or $[x + \Delta x - dx/2, x + \Delta x + dx/2]$, we have

$$P(x,t) = \frac{1}{2}\left[P(x - \Delta x, t - \Delta t) + P(x + \Delta x, t - \Delta t\right]. \tag{15.1}$$

Assuming that Δx and Δt are small, Taylor series expansions give

$$\begin{aligned} P(x \pm \Delta x, t - \Delta t) \quad = \quad & P \pm \frac{\partial P}{\partial x}\Delta x - \frac{\partial P}{\partial t}\Delta t \\ & + \frac{1}{2}\frac{\partial^2 P}{\partial x^2}\Delta x^2 \pm \frac{\partial^2 P}{\partial x \partial t}\Delta x \Delta t + \frac{1}{2}\frac{\partial^2 P}{\partial t^2}\Delta t^2 \\ & \pm \frac{1}{6}\frac{\partial^3 P}{\partial x^3}\Delta x^3 - \frac{1}{2}\frac{\partial^3 P}{\partial x^2 \partial t}\Delta x^2 \Delta t \pm \frac{1}{2}\frac{\partial^3 P}{\partial x \partial t^2}\Delta x \Delta t^2 - \frac{1}{6}\frac{\partial^3 P}{\partial t^3}\Delta t^3 \\ & + \ldots, \end{aligned} \tag{15.2}$$

where the terms on the right side are evaluated at (x, t). Substituting in Eq. (15.1) we get

$$\frac{\partial P}{\partial t} - D\frac{\partial^2 P}{\partial x^2} = \frac{1}{2}\frac{\partial^2 P}{\partial t^2}\Delta t - \frac{1}{2}\frac{\partial^3 P}{\partial x^2 \partial t}\Delta x^2 + \ldots, \tag{15.3}$$

where $D = \Delta x^2/2\Delta t$. If we let $\Delta x \to 0$ and $\Delta t \to 0$ such that D is constant, we get the diffusion equation

$$\frac{\partial P}{\partial t} = D\frac{\partial^2 P}{\partial x^2}. \tag{15.4}$$

15.1.2 Multi-dimensional

Let $P = P(\mathbf{r}, t)$, and $\Delta\mathbf{r}$ be a step in any direction where $|\Delta\mathbf{r}|$ is a constant. Then

$$P(\mathbf{r}, t) = \int_S P(\mathbf{r} + \Delta\mathbf{r}, t - \Delta t)\ dS \tag{15.5}$$

where S is a sphere of radius $|\Delta\mathbf{r}|$ centered on $\mathbf{r}$. Also

$$P(\mathbf{r} + \Delta\mathbf{r}, t - \Delta t) = P + \frac{\partial P}{\partial r_i}\Delta r_i - \frac{\partial P}{\partial t}\Delta t\frac{1}{2}\frac{\partial^2 P}{\partial r_i \partial r_i} + \ldots \tag{15.6}$$

etc.

15.2 Boltzmann transport equation

The classical distribution function $f(\mathbf{r}, \mathbf{v}, t)$ is defined as number of particles in the volume $d\mathbf{r}\ d\mathbf{v}$ in the six-dimensional space of coordinates $\mathbf{r}$ and velocity $\mathbf{v}$. Following a volume element in this space, we have the balance equation [109, 123, 124]

$$\frac{\partial f}{\partial t} + \mathbf{v}\cdot\nabla f + \mathbf{a}\cdot\frac{\partial f}{\partial \mathbf{v}} = \left(\frac{\partial f}{\partial t}\right)_{scat}, \tag{15.7}$$

where $\mathbf{a} = d\mathbf{v}/dt$ is the acceleration due to an external force. The term on the right side is due to collisions and scattering. The heat flux is then

$$\mathbf{q}(\mathbf{r}, t) = \int \mathbf{v}(\mathbf{r}, t) f(\mathbf{r}, \varepsilon, t)\varepsilon D\ d\varepsilon, \tag{15.8}$$

where $D(\varepsilon)$ is the density of energy states ε.

15.2.1 Relaxation-time approximation

Under this approximation

$$\left(\frac{\partial f}{\partial t}\right)_{scat} = \frac{f_0 - f}{\tau}, \tag{15.9}$$

where $\tau = \tau(\mathbf{r}, \mathbf{v})$. Thus

$$\frac{\partial f}{\partial t} + \mathbf{v}\cdot\nabla f + \mathbf{a}\cdot\frac{\partial f}{\partial \mathbf{v}} = \frac{f_0 - f}{\tau}. \tag{15.10}$$

Several further approximations can be made.

(a) Fourier's law

Assume $\partial/\partial t = 0$, $\mathbf{a} = 0$ and $\nabla f = \nabla f_0$ in the left side of Eq. (15.10) so that

$$f = f_0 - \tau\mathbf{v}\cdot\nabla f_0. \tag{15.11}$$

Introducing explicitly the dependence of f on temperature, we can write

$$\nabla f_0 = \frac{df_0}{dT}\nabla T. \tag{15.12}$$

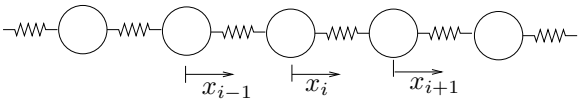

Figure 15.1: Lattice of atoms of a single type

Using Eqs. (15.11) and (15.12) in (15.8), we get

$$\mathbf{q} = -k\nabla T, \tag{15.13}$$

where

$$k = \int \mathbf{v}\left(\tau\mathbf{v}\cdot\frac{df_0}{dT}\right)\varepsilon D\ d\varepsilon, \tag{15.14}$$

since

$$\int \mathbf{v} f_0 \varepsilon D\ d\varepsilon = 0. \tag{15.15}$$

(b) Cattaneo's equation

Assume τ = constant and $\nabla f = (df_0/dT)\nabla T$. Multiply Eq. (15.10) by $\mathbf{v}\varepsilon D\ d\varepsilon$ and integrate to get

$$\frac{\partial}{\partial t}\int \mathbf{v} f \varepsilon D\ d\epsilon + \int\left(\mathbf{v}\cdot\frac{df_0}{dT}\nabla T\right)\mathbf{v}\varepsilon D\ d\varepsilon = -\frac{1}{\tau}\int \mathbf{v} f \varepsilon D\ d\varepsilon. \tag{15.16}$$

Using Eq. (15.8), this gives

$$\mathbf{q} + \tau\frac{\partial \mathbf{q}}{\partial \mathbf{t}} = -k\nabla T, \tag{15.17}$$

where k is given by Eq. (15.14). This is Cattaneo's equation that can be compared to Fourier's law, Eq. (15.13).

15.3 Phonons

15.3.1 Single atom type

A lattice of atoms of a single type is shown in Fig. 15.1. The mass of each atom is m, the spring constants are c, and a is the mean distance between the atoms. For a typical atom n, Newton's second law gives

$$m\frac{d^2x_n}{dt^2} = c(x_{n+1} - x_n) - c(x_n - x_{n-1}) \tag{15.18}$$

$$= c(x_{n+1} - 2x_n + x_{n-1}). \tag{15.19}$$

Let

$$x_i = \widehat{x}e^{i(nka-\omega t)}, \tag{15.20}$$

then the dispersion relation is

$$\omega = \left(\frac{2c}{m}\right)^{1/2}(1-\cos ka)^{1/2}. \tag{15.21}$$

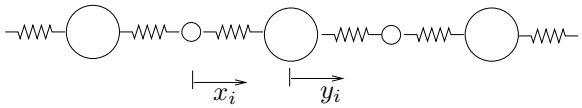

Figure 15.2: Lattice of atoms of two different type

The phase velocity is

$$v_p = \left(\frac{2c}{mk^2}\right)^{1/2} (1-\cos ka)^{1/2}, \tag{15.22}$$

and the group velocity is

$$v_g = \left(\frac{c}{2m}\right)^{1/2} \frac{a\sin ka}{(1-\cos ka)^{1/2}}. \tag{15.23}$$

For $ka \to 0$, we have

$$v_g = a\left(\frac{c}{m}\right)^{1/2}. \tag{15.24}$$

The thermal conductivity

$$k = k_e + k_p \tag{15.25}$$

where k_e and k_p are those due to electron and phonon transports. We can also write

$$k = \frac{1}{3} c v_g l \tag{15.26}$$

where c is the specific heat, and l is the mean free path.

15.3.2 Two atom types

Newton's second law gives

$$\begin{aligned} m_1 \frac{d^2 x_i}{dt^2} &= c(y_i - x_i) - c(x_i - y_{i-1}) && (15.27)\\ &= c(y_i - 2x_i + y_{i-1}), && (15.28)\\ m_2 \frac{d^2 y_i}{dt^2} &= c(x_{i+1} - y_i) - c(y_i - x_i) && (15.29)\\ &= c(x_{i+1} - 2y_i + x_i). && (15.30)\\ & && (15.31) \end{aligned}$$

Let

$$\begin{aligned} x_i &= \widehat{x} e^{i(nka-\omega t)}, && (15.32)\\ y_i &= \widehat{y} e^{i(nka-\omega t)}, && (15.33)\\ & && (15.34) \end{aligned}$$

so that

$$\begin{aligned} -m_1 \widehat{x}\omega^2 &= c\left(\widehat{y} - 2\widehat{x} + \widehat{y} e^{-ika}\right), && (15.35)\\ -m_2 \widehat{y}\omega^2 &= c\left(\widehat{x} e^{ika} - 2\widehat{y} + \widehat{x}\right), && (15.36) \end{aligned}$$

which can also be written as

$$\begin{bmatrix} 2c - m_1\omega^2 & -c(1+e^{-ika}) \\ -c(1+e^{ika}) & 2c - m_2\omega^2 \end{bmatrix} \begin{bmatrix} \widehat{x} \\ \widehat{y} \end{bmatrix} = \begin{bmatrix} 0 \\ 0 \end{bmatrix}. \tag{15.37}$$

This means that

$$(2c - m_1\omega^2)(2c - m_2\omega^2) - c^2(1+e^{-ika})(1+e^{ika}) = 0, \tag{15.38}$$

which simplifies to

$$m_1 m_2 \omega^4 - 2c(m_1+m_2)\omega^2 + 2c^2(1-\cos ka) = 0. \tag{15.39}$$

The solution is

$$\omega^2 = \frac{1}{2m_1m_2}\left[2c(m_1+m_2) \pm 2c\sqrt{m_1^2+m_2^2+2m_1m_2\cos ka}\right]. \tag{15.40}$$

The positive sign corresponds to the optical and the negative to the acoustic mode.

15.4 Thin films

Chapter 16

Bioheat transfer

16.1 Mathematical models

Good references are [35, 53].

Chapter 17

Heat exchangers

17.1 Fin analysis

Analysis of Kraus (1990) for variable heat transfer coefficients.

17.2 Porous medium analogy

See Nield and Bejan, p. 87 [130].

17.3 Heat transfer augmentation

17.4 Maldistribution effects

Rohsenow (1981)

17.5 Microchannel heat exchangers

Phillips (1990).

17.6 Radiation effects

See Ozisik (1981).
Shah (1981)

17.7 Transient behavior

Ontko and Harris (1990)
For both fluids mixed

$$Mc\frac{dT}{dt} + \dot{m}_1 c_1 (T_1^{in} - T_1^{out}) + \dot{m} c_2 (T_2^{in} - T_2^{out}) = 0 \tag{17.1}$$

For one fluid mixed and the other unmixed, we have

$$\rho A c_2 \frac{\partial T_2}{\partial t} + \rho V_2 A c_2 \frac{\partial T_2}{\partial x} + hP(T - T_1) = 0 \tag{17.2}$$

17.8 Correlations

17.8.1 Least squares method

Possible correlations are

$$y(x) = \sum_{k=0}^{n} a_k x^k \tag{17.3}$$

$$y(x) = a_0 + a_{1/2}x^{1/2} + a_1 x + a_{3/2}x^{3/2} + a_2 x^2 + \ldots \tag{17.4}$$

$$y(x) = ax^m + bx^n + \ldots \tag{17.5}$$

$$y(x) = \int_{k=0}^{n} a(k)x^k \, dk \qquad \text{where } -1 < x < 1 \tag{17.6}$$

A power-law correlation of the form

$$y = cx^n \tag{17.7}$$

satisfies the invariance condition given by equation (A.1).

17.9 Compressible flow

17.10 Thermal control

A cross-flow heat exchanger model, schematically shown in Fig. 17.1, has been studied using finite differences [4–6]. Water is the in-tube and air the over-tube fluid in the heat exchanger. This example includes all the conductive, advective and convective effects discussed before. The governing equations on the outside of the tube, in the water, and in the wall of the tube are

$$\frac{\dot{m}_a}{L} c_a (T^a_{in} - T^a_{out}) = h_o 2\pi r_o (T_a - T_t), \tag{17.8}$$

$$\rho_w c_w \pi r_i^2 \frac{\partial T_w}{\partial t} + \dot{m}_w c_w \frac{\partial T_w}{\partial \xi} = h_i 2\pi r_i (T_t - T_w), \tag{17.9}$$

$$\rho_t c_t \pi (r_o^2 - r_i^2) \frac{\partial T_t}{\partial t} = k_t \pi (r_o^2 - r_i^2) \frac{\partial^2 T_t}{\partial \xi^2} + 2\pi r_o h_o (T_a - T_t) - 2\pi r_i h_i (T_t - T_w), \tag{17.10}$$

respectively. L is the length of the tube; $\dot{m}_a(t)$ and $\dot{m}_w(t)$ are the mass flow rates of air and water; T^a_{in} and $T^a_{out}(t)$ are the inlet and outlet air temperatures; $T_a(t)$ is the air temperature surrounding the tube; $T_t(\xi, t)$ and $T_w(\xi, t)$ are the tube-wall and water temperatures; h_i and h_o the heat transfer coefficients in the inner and outer surfaces of the tube; r_i and r_o are the inner and outer radii of the tube; c_a, c_w and c_t are the specific heats of the air, water and tube material; ρ_w and ρ_t are the water and tube material densities; and k_t is the thermal conductivity of the tube material. In addition, the air temperature is assumed to be $T_a = (T^a_{in} + T^a_{out})/2$. The boundary and initial conditions are $T_t(0, t) = T_w(0, t) = T^w_{in}$, $T_t(L, t) = T_w(L.t)$, and $T_t(\xi, 0) = T_w(\xi, 0)$. Suitable numerical values were assumed for the computations.

The inlet temperatures T^a_{in} and T^w_{in}, and the flow rates $\dot{m}_a$ and $\dot{m}_w$ can all be used as control inputs to obtain a desired outlet temperature, T^a_{out} or T^w_{out}. The flow rates present a special difficulty; they appear in nonlinear form in Eqs. (17.8) and (17.9), and the outlet temperature is bounded. Fig. 17.2 shows the steady-state range of values of T^w_{out} that can be achieved on varying $\dot{m}_w$; temperatures outside this range cannot be obtained. It is also seen that the outlet water temperature is hard to control for large water flow rates. As an example of control dynamics, Fig. 17.3 shows the results of applying PI control on $\dot{m}_w$ to obtain a given reference temperature $T^w_{out} = 23°\text{C}$.

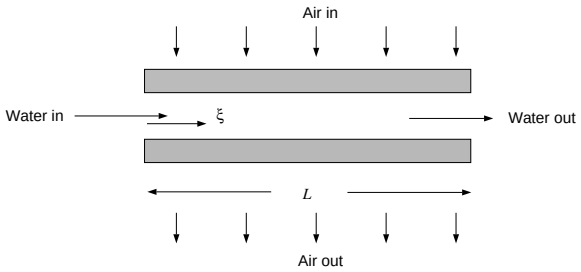

Figure 17.1: Schematic of single-tube cross-flow heat exchanger.

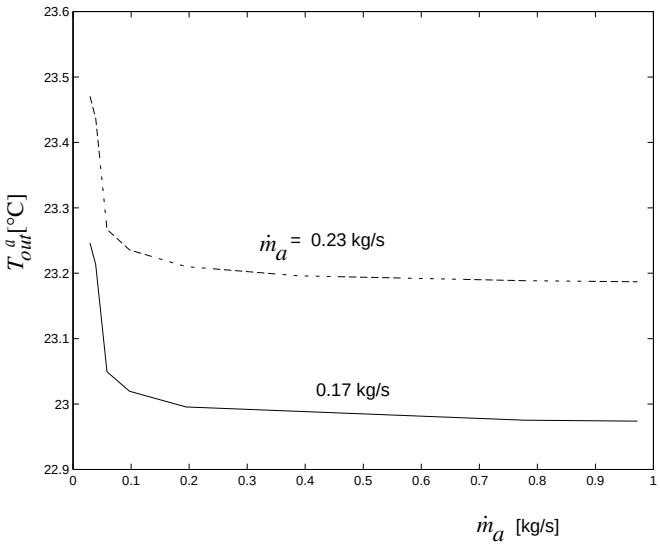

Figure 17.2: The relation between T_{out}^{a} and $\dot{m}_w$ for different $\dot{m}_a$ [4].

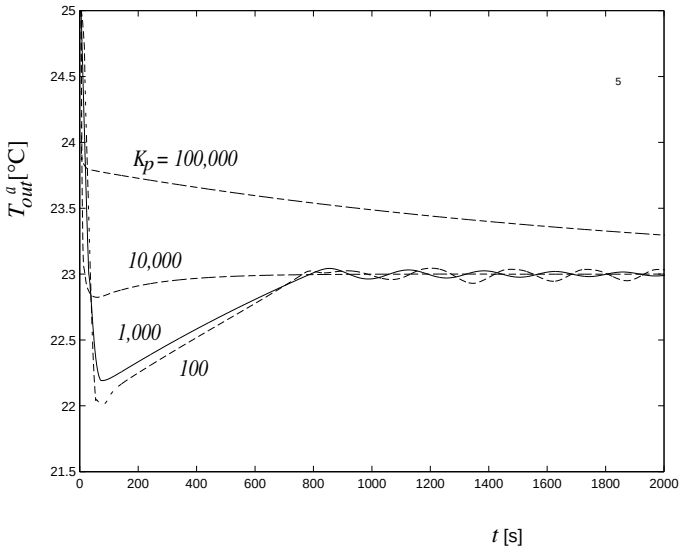

Figure 17.3: Behavior of T_{out}^{a} as a function of time for $K_i = 50$ and different K_p [4].

17.11 Control of complex thermal systems

The previous sections examined systems that were fairly simple in the sense that mathematical models could be written down and their behaviors studied. For most practical thermal systems, this is difficult to do with any degree of precision. In the following, we will look first at thermal components and then combine them in networks.

17.11.1 Hydronic networks

The science of networks of all kinds has been put forward as a new emerging science [15]. In the present context this means that a complete understanding of the behavior of components does not necessarily mean that large networks formed out of these components can be modeled and computed in real time for control purposes. Controllability issues of heat exchanger networks are reported in [203]. Mathematical models of the dynamics of a piping network lead to differential-algebraic systems [61]. The momentum equation governing the flow in each pipe is differential, while the conservation of mass condition at each of the junctions is algebraic. Thus, it turns out that only certain flow rates may be controllable, the others being dependent on these.

There are at present many different strategies for the thermal control of networks, and comparative studies based on mathematical models can be carried out. Fig. 17.4 shows a network in which three specific control strategies can be compared [61, 62]; each control method works differently and are labeled VF, MCF and BT in the following figures (details are in [61]). The network has a primary loop, a secondary loop and a bypass that has the three strategies as special cases. The primary loop includes a chiller, while the secondary has a water-air cooling coil which serves as a thermal load. Integral controllers are used to operate the valves V_α, V_β, and V_γ to control the air temperature leaving the cooling coil, $T_a^L(t)$. Figs. 17.5 and 17.6 show the dynamic response of $T_a^L(t)$, the leaving water temperatures $T_w^L(t)$, and the bypass pressure difference Δp_{bp} to step

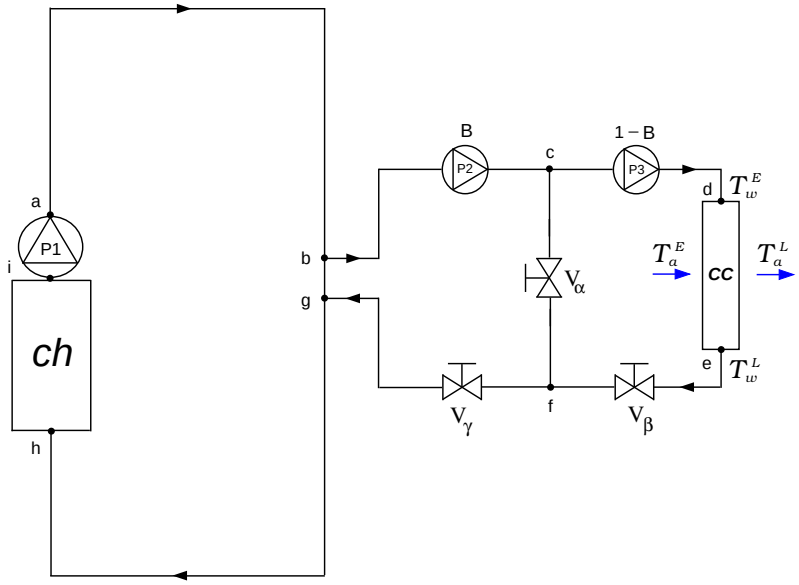

Figure 17.4: Network used to study control strategies [61].

changes in the air velocity over the coil. $\alpha(t)$, $\beta(t)$, and $\gamma(t)$ are the respective closing fractions of the valves which change dynamically in response to the error signal. There are some oscillations in all the variables before they settle down to stable, steady values.

Laboratory experiments with a network of water-to-water heat exchangers have been reported in [61–63]; the configuration is shown in Fig. 17.7. The hot water flow is diminished by changing its controller set point. Figure 17.8 shows the secondary hot water flow rates q_8, q_7 and q_4 to the heat exchangers for the three different control strategies. Each curve represents one independent run; that is, water flow to HX_{BT} and HX_{CF} is zero when testing VF, and so on. The system is taken to the nominal operating conditions, and then the hot water flow is decreased by a constant value every 1800 s. The controls drive the system to different operational points while coping with the changes. The input voltages v_7, v_4 and v_1 that control flow and the hot water temperature at the heat exchanger inlet T_{21} are also shown. It is seen that for certain control parameters, the system is becomes unstable and the variables oscillate in time.

17.11.2 Other applications

There are a large number of other thermal problems in which control theory has been applied. Agent-based controls have been proposed by complex thermal systems such as in buildings [213], microwave heating [120], thermal radiation [143], and materials processing and manufacturing [55, 160]. Control of convection is an important and active topic; this includes the study of convection loops [175,176,205,215,217], stabilization and control of convection in horizontal fluid layers [18,83, 125,145,190–195], and in porous media [189].

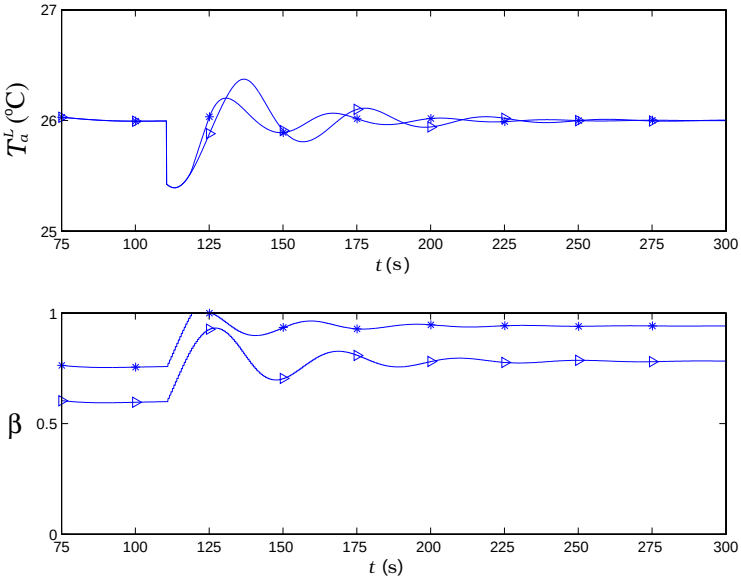

Figure 17.5: Dynamic response of control system to drop in air velocity, $-*-$ method VF, and $-\triangleright-$ method MCF; $T^L_{a,set} = 26°\text{C}$, $T^E_a = 30°\text{C}$ [61].

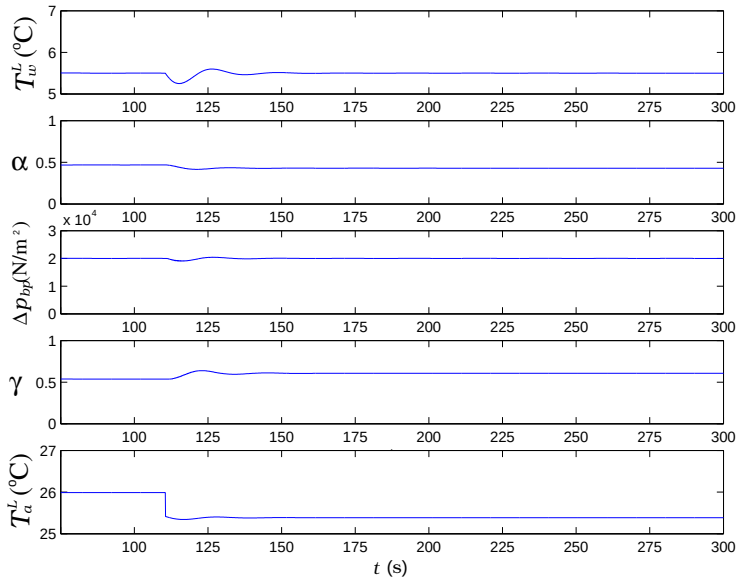

Figure 17.6: Dynamic response of control system to drop in air velocity with method BT; $T^L_{w,set} = 5.5°\text{C}$, $\Delta p_{bp,set} = 20000$ (N/m^2); $T^E_a = 30°\text{C}$ [61].

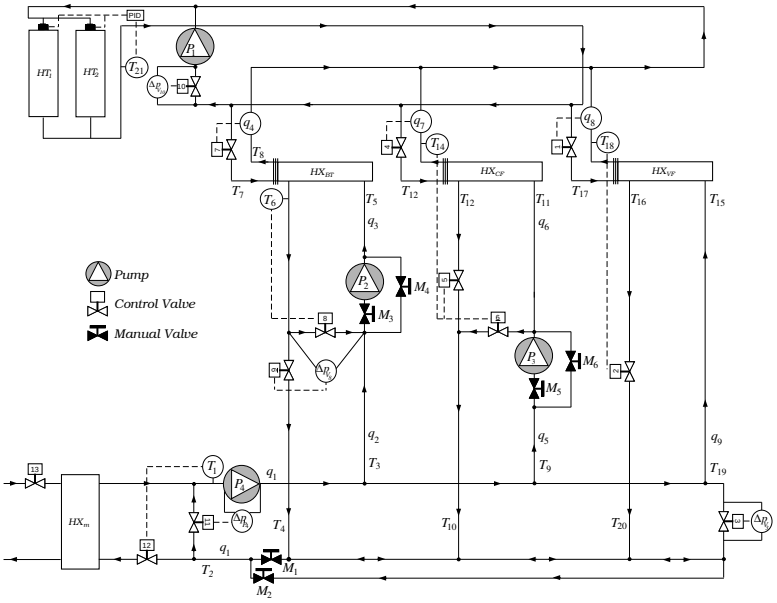

Figure 17.7: Layout of hydronic network [61].

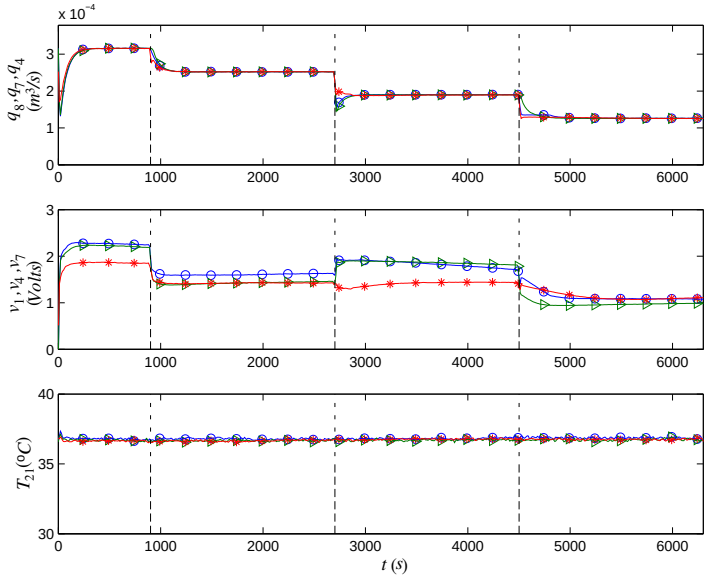

Figure 17.8: Secondary hot water flows and T_{21}: $-\circ-BT$, $-\triangleright-CF$, $-*-VF$. The dashed vertical lines are instants at which the thermal load is changed [61].

17.12 Conclusions

This has been a very brief introduction to the theory of thermal control. The fundamental ideas in this subject are firmly grounded on the mathematics of systems and control theory which should be the starting point. There are, however, a few aspects that are particularly characteristic of thermal systems. Phenomena such as diffusion, convection and advection are common and the systems are usually complex, nonlinear and poorly predictable dynamically. The governing equations cover a wide range of possibilities, from ordinary and partial differential equations to functional and differential-algebraic systems. Furthermore, control theory itself is a vast subject, with specialized branches like optimal [79], robust [38], and stochastic control [37] that are well developed. Many of the tools in these areas find applications in thermal systems.

The study of thermal control will continue to grow from the point of view of fundamentals as well as engineering applications. There are many outstanding problems and issues that need to be addressed. To cite one specific example, networking between a large number of coupled components will become increasingly important; it is known that unexpected synchronization may result even when multiple dynamical systems are coupled weakly [181]. It is hoped that the reader will use this brief overview as a starting point for further study and apply control theory in other thermal applications.

Problems

1. This is a problem

Chapter 18

Soft computing

18.1 Genetic algorithms

[141]

18.2 Artificial neural networks

18.2.1 Heat exchangers

The most important of the components are heat exchangers, which are generally very complex in that they cannot be realistically computed in real time for control purposes [92, 153, 182]. An approach that is becoming popular in these cases is that of artificial neural networks (ANN) [73] for prediction of system behavior both for time-independent [48, 139, 140, 142] and time-dependent operation. It is particularly suitable for systems for which experimental information that can be used for training is available. Reviews of artificial neural network applications to thermal engineering [163, 168] and other soft control methodologies [32, 131, 220] and applications [216] are available.

A stabilized neurocontrol technique for heat exchangers has been described in [47, 49–52]. Fig. 18.1 shows the test facility in which the experiments were conducted. The objective is to control the outlet air temperature T^a_{out}. Figs. 18.2 shows the results of using neurocontrol compared with PID; both are effective. Fig. 18.3 shows the result of an disturbance rejection experiment. The heat exchanger is stabilized at $T^a_{out} = 36°\text{C}$, and then the water flow is shut down between $t = 40\text{s}$ and $t = 70\text{s}$; after that the neurocontroller brings the system back to normal operation. A neural network-based controller is able to adapt easily to changing circumstances; in thermal systems this may come from effects such as the presence of fouling over time or from changes in system configuration as could happen in building heating and cooling systems.

[51, 166]

[162]

Problems

1. This is a problem

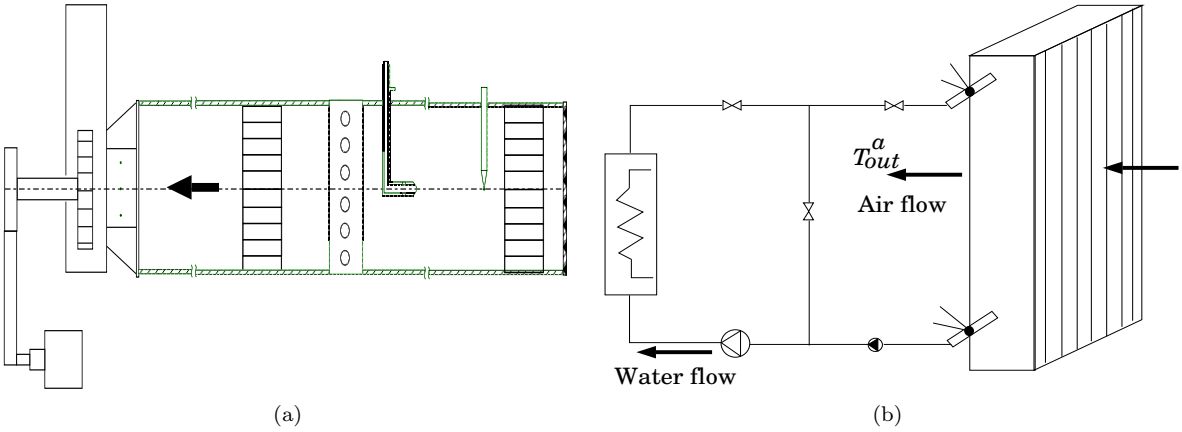

Figure 18.1: Experimental setup: (a) heat exchanger test facility with wind tunnel and in-draft fan, (b) heat exchanger with water and air flows indicated; T^a_{out} is the air outlet temperature [47].

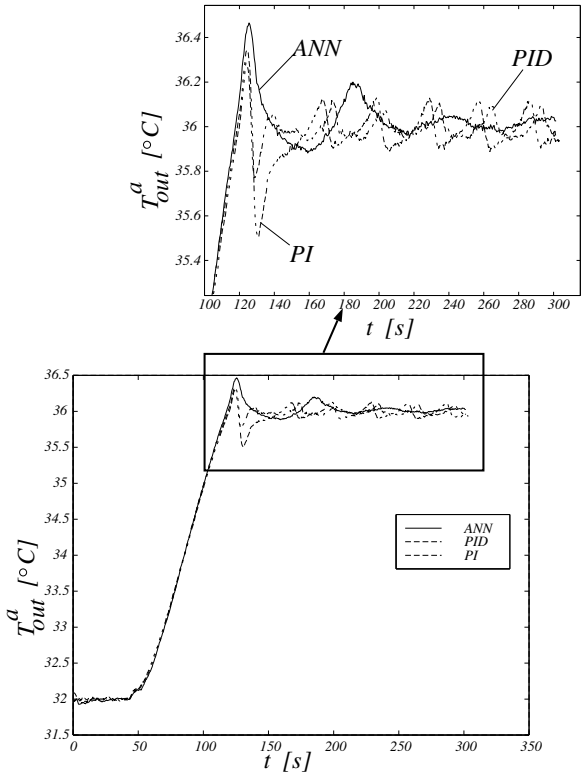

Figure 18.2: Time-dependent behavior of heat exchanger using ANN, PID and PI control methodologies [47].

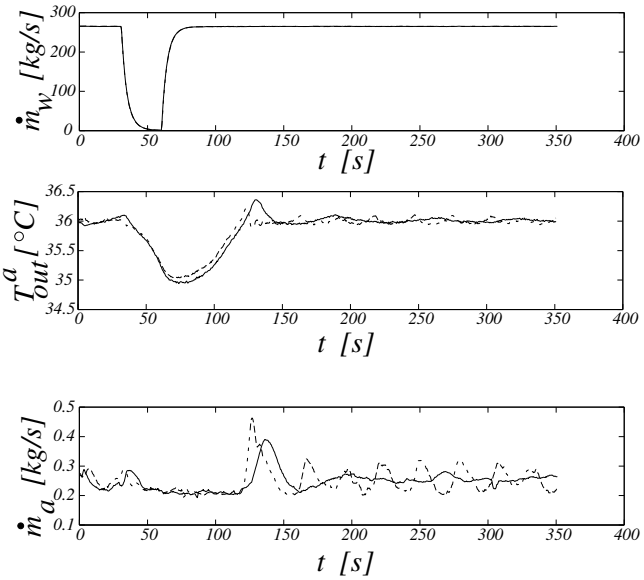

Figure 18.3: Time-dependent behavior of heat exchanger with neurocontrol for disturbance rejection experiment showing flow rates and air outlet temperature [47].

Part VI

Appendices

Appendix A

Mathematical review

A.1 Fractals

[60]

Fractals are objects that are not smooth; they are geometrical shapes in which the parts are in some way similar to the whole. This self-similarity may be exact, i.e. a piece of the fractal, if magnified, may look exactly like the whole fractal.

A function $f(x)$ is invariant under change of scale if there exists constants a and b, such that [199]

$$f(ax) = bf(x) \tag{A.1}$$

A fractal curve must be nowhere rectifiable (i.e. any part of it cannot be of finite length) and homogeneous (i.e. any par6 is similar to the whole).

Before discussing examples we need to put forward a working definition of dimension. Though there are many definitions in current use, we present here the Hausdorff-Besicovitch dimension D. If N_ϵ is the number of 'boxes' of side ϵ needed to cover an object, then

$$D = \lim_{\epsilon \to 0} \frac{\ln N_\epsilon}{\ln(1/\epsilon)} \tag{A.2}$$

We can check that this definition corresponds to the common geometrical shapes.

1. Point: $N_\epsilon = 1, D = 0$
2. Line of length l: $N_\epsilon = l/\epsilon, D = 1$
3. Surface of size $l \times l$: $N_\epsilon = (l/\epsilon)^2, D = 2$
4. Volume of size $l \times l \times l$: $N_\epsilon = (l/\epsilon)^3, D = 3$

A fractal has a dimension that is not an integer. Many physical objects are fractal-like, in that they are fractal within a range of length scales. Coastlines are among the geographical features that are of this shape. If there are N_ϵ units of a measuring stick of length ϵ, the measured length of the coastline will be of the power-law form $\epsilon N_\epsilon = \epsilon^{1-D}$, where D is the dimension.

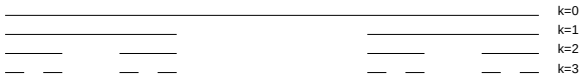

Figure A.1: The Cantor set.

Figure A.2: The Koch curve.

A.1.1 Cantor set

Consider the line [0,1] corresponding to $k = 0$ in Figure A.1. Take away the middle third to leave the two portions; this is shown as $k = 1$. Repeat the process to get $k = 2, 3, \ldots$. If $k \to \infty$, what is left is called the Cantor set. Since $N_\epsilon = 2^k$ and $\epsilon = 1/3^k$,its dimension is $D = \ln 2/\ln 3 = 0.63\ldots$.

If we define a function $C_k(t)$ at the kth level so that $C_k(t) = (3/2)^k$ if t belongs to the set and zero otherwise, its integral over the interval is unity. In terms of this function we can also define

$$D(t) = \int_0^t \lim_{k\to\infty} C_k(t')\ dt' \tag{A.3}$$

that is called the *devil's staircase*.

A.1.2 Koch curve

Here we start with an equilateral triangle shown in Figure A.2 as $k = 0$. The middle third of each side of the triangle is removed, and two sides of a triangle drawn on that. This is shown as $k = 1$. The process is continued, and in the limit gives a continuous, closed curve that is nowhere smooth. Since $N_\epsilon = 3 \times 4^k$ and $\epsilon = 1/3^k$, the dimension of the Koch curve is $D = \ln 4/\ln 3 = 1.26\ldots$.

A.1.3 Knopp function

This is the function

$$K(t) = \sum_{n=0}^{\infty} 2^{-nH} g(2^n t) \tag{A.4}$$

where $0 < H < 1$, and $g(t)$ is the periodic triangular function

$$g(t) = \begin{cases} 2t & \text{for} \quad 0 \le t \le 1/2 \\ 2(1-t) & \text{for} \quad 1/2 < t \le 1 \end{cases} \tag{A.5}$$

defined on [0,1].

A.1.4 Weierstrass function

This is the function

$$W(t) = \sum_{n=0}^{\infty} \omega^{-nH} \cos\left(\omega^n t + \phi_n\right) \tag{A.6}$$

Figure A.3: Mandelbrot set

where a is real, b is odd, and $ab > 1 + 3\pi/2$. It is everywhere continuous, but nowhere differentiable. The related Weierstrass-Mandelbrot function

$$W_m(t) = \sum_{n=-\infty}^{\infty} \omega^{-nH} \left(1 - \cos \omega^n t\right) \tag{A.7}$$

satisfies the invariance relation A.1.

A.1.5 Julia set

An example of this comes from the application of Newton's method to find the complex root of the equation $z^3 = 1$. In this method the following iterative scheme is set up:

$$z_{k+1} = z_k - \frac{z_k^3 - 1}{3z_k^2} \tag{A.8}$$

Each one of the three roots has a basin of attraction, the boundaries of which are fractal.

A.1.6 Mandelbrot set

This is the set of complex numbers c for which

$$z_{k+1} = z_k^2 + c \tag{A.9}$$

stays bounded as $k \to \infty$. The boundaries of this set shown in Figure A.3 are again fractal.

A.2 Perturbation methods

A.3 Vector spaces

Functional analysis, norms, inner product, complete space, Banach and Hilbert spaces, operators, eigenvalues problem, adjoint and self-adjoint operators.

Finite-dimensional spaces, linear algebra.

Eigenfunction expansions.

[13, 78, 107]

A.4 Dynamical systems

A dynamical system is a set of differential equations such as

$$\frac{dx_i}{dt} = f_i(x_1, x_2, \ldots, t; \lambda_1, \lambda_2, \ldots, \lambda_p) \quad \text{for } i = 1, \ldots, n \tag{A.10}$$

The $x_1, \ldots, x_n$s are state variables and the $\lambda_1, \ldots, \lambda_p$ are bifurcation parameters. The mapping $f : X \times \mathcal{R}^p \to Y$ is a *vector field*. If $f_1, \ldots, f_n$ do not depend on time t, the system is autonomous.

A nonautonomous system can be converted into autonomous one by the change in variable $x_{n+1} = t$, from which we can get the additional equation

$$\frac{dx_{n+1}}{dt} = 1 \tag{A.11}$$

We will assume that the solutions of the system are always bounded. The system is *conservative* if the divergence of the vector field $\sum \partial f_i/\partial x_i$ is zero, and *dissipative* if it is negative. An *attractor* of a dissipative dynamical system is the set of $\{x_i\}$ as $t \to \infty$. The *critical* (or *singular*, *equilibrium* or *fixed*) points, $\overline{x}_i$, of equation (A.10) are those for which

$$f_i(x_1, x_2, \ldots, t; \lambda_1, \lambda_2, \ldots, \lambda_p) = 0 \tag{A.12}$$

There may be multiple solutions to this algebraic or transcendental equation.

Defining a new coordinate $x_i' = x_i - \overline{x}_i$ that is centered at the critical point, we get the *local form*

$$\frac{dx_i'}{dt} = f_i(x_1 - \overline{x}_1, \ldots, x_n - \overline{x}_n) \tag{A.13}$$

Sometimes we will use the notation

$$\frac{dx_i}{dt} = g(x_1, \ldots, x_n) \tag{A.14}$$

to indicate the local form, the origin being one critical point of this system.

A.4.1 Stability

The stability of the critical points is of major interest. A critical point is stable if, given an initial perturbation, the solutions tends to it as $t \to \infty$.

Linear stability

The vector field in equation (A.14) can be expanded in a Taylor series to give

$$\frac{dx_i}{dt} = \sum_j \left.\frac{\partial g_i}{\partial x_j}\right|_0 x_j + \ldots \tag{A.15}$$

The eigenvalues of the Jacobian matrix

$$\mathbf{A} = \frac{\partial g_i}{\partial x_j} \tag{A.16}$$

determine the linear stability of the critical point. The critical point is stable if all eigenvalues have negative real parts, and unstable if one or more eigenvalues have positive real parts.

A.4.2 Routh-Hurwitz criteria

The polynomial equation

$$a_0 s^n + a_1 s^{n-1} + \ldots + a_{n-1} s + a_n = 0$$

has roots with negative real parts if and only if the following conditions are satisfied:
(i) $a_1/a_0, a_2/a_0, \ldots, a_n/a_0 > 0$
(ii) $D_i > 0$, $i = 1, \ldots, n$

The Hurwitz determinants D_i are defined by

$$
\begin{aligned}
D_1 &= a_1 \\
D_2 &= \begin{vmatrix} a_1 & a_3 \\ a_0 & a_2 \end{vmatrix} \\
D_3 &= \begin{vmatrix} a_1 & a_3 & a_5 \\ a_0 & a_2 & a_4 \\ 0 & a_1 & a_3 \end{vmatrix} \\
D_n &= \begin{vmatrix} a_1 & a_3 & a_5 & \dots & a_{2n-1} \\ a_0 & a_2 & a_4 & \dots & a_{2n-2} \\ 0 & a_1 & a_3 & \dots & a_{2n-3} \\ 0 & a_0 & a_2 & \dots & a_{2n-4} \\ \vdots & \vdots & \vdots & \vdots & \vdots \\ 0 & 0 & 0 & \dots & a_n \end{vmatrix}
\end{aligned}
$$

with $a_i = 0$, if $i > n$.

Global stability

Consider the dynamical system in local form, equation (A.14). If there exists a function $V(x_1, \dots, x_n)$ such that $V \geq 0$ and $dV/dt \leq 0$, then the origin is *globally* stable, that is, it is stable to all perturbations, large or small. V is called a *Liapunov function.*

[56]

A.4.3 Bifurcations

The critical point is one possible attractor. There are other time-dependent solutions which can also be attractors in phase space, as indicated in the list below.

- Point (steady, time-independent)
- Closed curve (limit cycle, periodic)
- Torus (periodic or quasi-periodic)
- Strange (chaotic)

For a given dynamical system, several attractors may co-exist. In this case each attractor has a basin of attraction, i.e. the set of initial conditions that lead to this attractor. A *bifurcation* is a qualitative change in the solution as the bifurcation parameters λ_i are changed.

A.4.4 One-dimensional systems

A one-dimensional dynamical system is of the type

$$\frac{dx}{dt} = f(x) \tag{A.17}$$

Example A.1

Consider the linear equation

$$\frac{dx}{dt} = ax + b \tag{A.18}$$

The critical point is

$$\overline{x} = -\frac{b}{a} \tag{A.19}$$

On defining $x' = x - \overline{x}$, the local form is obtained as

$$\frac{dx'}{dt} = ax' \tag{A.20}$$

We can take one of two approaches.

(a) Solving

$$x' = x'_0 e^{at} \tag{A.21}$$

The critical point is a repeller if $a > 0$, and an attractor if $a < 0$.

(b) Alternatively, we can multiply equation (A.20) by $2x'$ to get

$$\frac{dV}{dt} = 2aV \tag{A.22}$$

where $V = x'^2$. Since V is always nonnegative, the sign of dV/dt is the sign of a. Thus V will increase with time if $a > 0$, and decrease if $a < 0$.

In either case we find that the critical point is unstable if $a > 0$ and stable if $a < 0$.

Example A.2

The nonlinear equation

$$\frac{dx}{dt} = -x\left[x^2 - (\lambda - \lambda_0)\right] \tag{A.23}$$

has critical point which are solutions of the cubic equation

$$\overline{x}\left[\overline{x}^2 - (\lambda - \lambda_0)\right] = 0 \tag{A.24}$$

Thus

$$x_{(1)} = 0 \tag{A.25}$$

$$x_{(2)} = \sqrt{\lambda - \lambda_0} \tag{A.26}$$

$$x_{(3)} = -\sqrt{\lambda - \lambda_0} \tag{A.27}$$

where $x_{(i)}$ $(i = 1, 2, 3)$ are the three critical points. The bifurcation diagram is shown in Fig. A.4.

(i) Critical point $\overline{x}_{(1)} = 0$

To analyze the local stability of $\overline{x}_{(1)} = 0$, we obtain the local form

$$\frac{dx'}{dt} = x'(\lambda - \lambda_0) - x'^3 \tag{A.28}$$

Neglecting the cubic term x'^3, this becomes

$$\frac{dx'}{dt} = x'(\lambda - \lambda_0) \tag{A.29}$$

Thus $\overline{x}_{(1)} = 0$ is locally stable if $\lambda < \lambda_0$, and unstable if $\lambda > \lambda_0$.

To analyze the global stability, equation (A.28) can be written as

$$\frac{1}{2}\frac{dV}{dt} = V(\lambda - \lambda_0) - V^2 \tag{A.30}$$

where $V = x'^2$. For $\lambda < \lambda_0$, $V \geq 0$, $dV/dt \leq 0$, so that $\overline{x}_{(1)} = 0$ is globally stable.

(ii) Critical point $\overline{x}_{(2)} = \sqrt{\lambda - \lambda_0}$

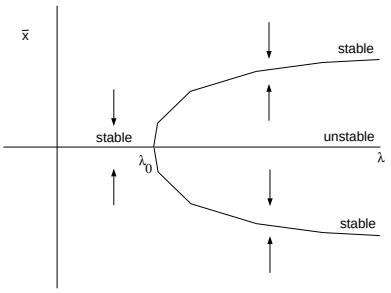

Figure A.4: Supercritical pitchfork bifurcations

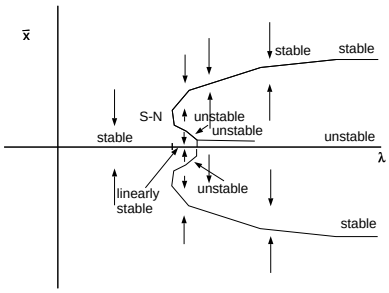

Figure A.5: Subcritical version of Fig. A.4

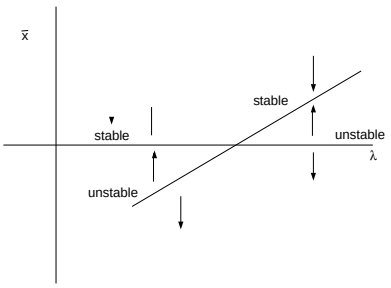

Figure A.6: Transcritical bifurcation.

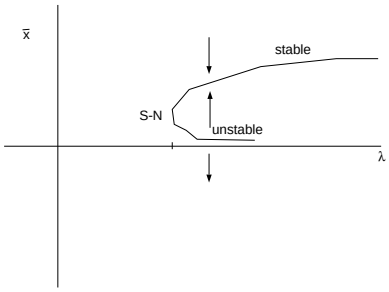

Figure A.7: Saddle-node bifurcation.

The local form of the equation around this critical point is

$$\frac{dx'}{dt} = -\left(\sqrt{\lambda-\lambda_0}+x'\right)\left[\left(\sqrt{\lambda-\lambda_0}+x'\right)^2-(\lambda-\lambda_0)\right] \tag{A.31}$$

Linearizing, we get

$$\frac{dx'}{dt} = -2(\lambda-\lambda_0)x' \tag{A.32}$$

so that this critical point is linearly stable.

(iii) Critical point $\overline{x}_{(3)} = -\sqrt{\lambda-\lambda_0}$
This is similar to the above.

A.4.5 Examples of bifurcations

- Supercritical: Fig. A.4.
- Subcritical: Fig. A.5.
- Transcritical: Fig. A.6.
- Saddle-node: Fig. A.7.

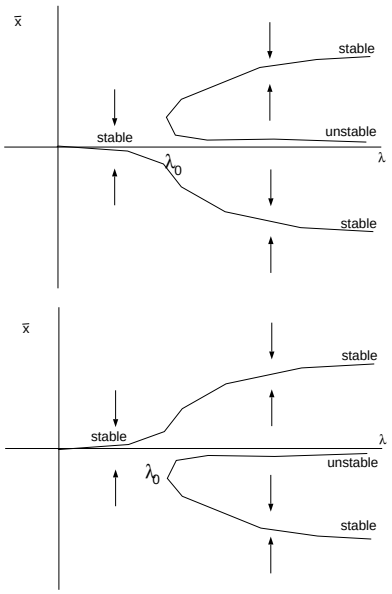

Figure A.8: Imperfect bifurcations; (a) $\epsilon > 0$, (b) $\epsilon < 0$.

A.4.6 Unfolding and structural instability

Adding a small constant to the vector field in equation (A.23), we get

$$f(x) = -x\left[x^2 - (\lambda - \lambda_0)\right] + \epsilon \tag{A.33}$$

The critical points are solutions of

$$\overline{x}^3 - (\lambda - \lambda_0)\overline{x} - \epsilon = 0 \tag{A.34}$$

To see the nature of the curve, we make an expansion around $\overline{x} = 0$, $\lambda = \lambda_0$ and write

$$\overline{x} = x' \tag{A.35}$$
$$\lambda = \lambda_0 + \lambda' \tag{A.36}$$

For small x' and λ, we get

$$\lambda' x' = -\epsilon \tag{A.37}$$

Figure A.8 shows the result of adding the imperfection ϵ. The dynamical system without ϵ is thus *structurally unstable*.

A.4.7 Two-dimensional systems

Consider

$$\frac{dx}{dt} = f_x(x, y) \tag{A.38}$$
$$\frac{dy}{dt} = f_y(x, x) \tag{A.39}$$

The linearized equation in local form has a Jacobian matrix

$$\mathbf{A} = \begin{pmatrix} a_{xx} & a_{xy} \\ a_{yx} & a_{yy} \end{pmatrix} \tag{A.40}$$

The eigenvalues satisfy a quadratic equation

$$\lambda^2 + P\lambda + Q = 0 \tag{A.41}$$

from which

$$\lambda = \frac{1}{2}\left[-P \pm \sqrt{P^2 - 4Q}\right] \tag{A.42}$$

The sign of the discriminant

$$D = P^2 - 4Q \tag{A.43}$$

determines the nature of the solution. If $D < 0$, the eigenvalues are complex and the solution in phase space is a spiral; if in addition $P > 0$, the spiral is stable, and if $P < 0$, it is unstable. If, on the other hand, $D > 0$, the eigenvalues are real; the solutions do not oscillate in time but move exponentially towards (if all eigenvalues are negative) or away (if at least one eigenvalue is positive) from the critical point.

Example A.3

$$\frac{dx}{dt} = y \tag{A.44}$$

$$\frac{dy}{dt} = -(\lambda - \lambda_0)x \tag{A.45}$$

This is a conservative system which is equivalent to

$$\frac{d^2x}{dt^2} + (\lambda - \lambda_0)x = 0 \tag{A.46}$$

The solutions are exponential if $\lambda < \lambda_0$, and periodic if $\lambda > \lambda_0$.

Example A.4

$$\frac{dx}{dt} = y \tag{A.47}$$

$$\frac{dy}{dt} = -\omega^2 x - \sigma y \tag{A.48}$$

For $\sigma > 0$, the system is dissipative, and the solutions are damped oscillations.

The occurrence of periodic solutions in two-dimensional systems, permits a *Hopf bifurcation,* which is a transition from a time-independent to a periodic behavior through a pair of complex conjugate imaginary eigenvalues.

Example A.5

The dynamical system

$$\frac{dx}{dt} = (\lambda - \lambda_0)x - y - (x^2 + y^2)x \tag{A.49}$$

$$\frac{dy}{dt} = x + (\lambda - \lambda_0)y - (x^2 + y^2)y \tag{A.50}$$

can be converted to polar coordinates. Substituting $x = r\cos\theta$ and $y = r\sin\theta$, we get

$$-r\sin\theta\frac{d\theta}{dt} + \cos\theta\frac{dr}{dt} = (\lambda - \lambda_0)r\cos\theta - r\sin\theta - r^3\cos\theta \tag{A.51}$$

$$r\cos\theta\frac{d\theta}{dt} + \sin\theta\frac{dr}{dt} = r\cos\theta + (\lambda - \lambda_0)r\sin\theta - r^3\sin\theta \tag{A.52}$$

which simplifies to

$$\frac{dr}{dt} = r\left(\lambda - \lambda_0 - r^2\right) \tag{A.53}$$

$$\frac{d\theta}{dt} = 1 \tag{A.54}$$

There are two values of r, i..e $r = 0$ and $r = \sqrt{\lambda - \lambda_0}$, at which $dr/dt = 0$. The first is a critical point at the origin, and the second a circular periodic orbit that exists only for $\lambda > \lambda_0$. A linear analysis of equations (A.49) and (AHopftwo) shows that the origin is stable for $\lambda < \lambda_0$. For $\lambda > \lambda_0$, a similar analysis of equation (A.53) indicates that $r = \sqrt{\lambda - \lambda_0}$ is a stable orbit. There is thus a Hopf bifurcation at $\lambda = \lambda_0$.

Example A.6

$$\frac{dx}{dt} = y \tag{A.55}$$

$$\frac{dy}{dt} = -\omega^2 x - \sigma\left(\lambda - x^2 - y^2\right) \tag{A.56}$$

This is a Hopf bifurcation at $\lambda = \lambda_0$, at which point the solution goes from time-independent to periodic.

A.4.8 Three-dimensional systems

Forced Duffing equation

Since a non-autonomous equation can be converted into a three-dimensional autonomous system, we will include the case of the forced Duffing equation here[1].

$$\frac{dx}{dt} = y \tag{A.57}$$

$$\frac{dy}{dt} = x - x^3 + f(t) \tag{A.58}$$

[1]Sometimes defined with a negative sign in front of x in the second equation.

Lorenz equations

An important example is the Lorenz equations:

$$\frac{dx}{dt} = \sigma(y-x) \tag{A.59}$$
$$\frac{dx}{dt} = \lambda x - y - xz \tag{A.60}$$
$$\frac{dx}{dt} = -bz + xy \tag{A.61}$$

where σ and b are taken to be positive constants, with $\sigma > b+1$. The bifurcation parameter will be λ.

The critical points are obtained from

$$\begin{aligned} \overline{y} - \overline{x} &= 0 \\ \lambda\overline{x} - \overline{y} - \overline{xz} &= 0 \\ -b\overline{z} + \overline{xy} &= 0 \end{aligned}$$

which give

$$\begin{pmatrix} \overline{x} \\ \overline{y} \\ \overline{z} \end{pmatrix} = \begin{pmatrix} 0 \\ 0 \\ 0 \end{pmatrix}, \begin{pmatrix} \sqrt{b(\lambda-1)} \\ \sqrt{b(\lambda-1)} \\ \lambda - 1 \end{pmatrix}, \begin{pmatrix} -\sqrt{b(\lambda-1)} \\ -\sqrt{b(\lambda-1)} \\ \lambda - 1 \end{pmatrix} \tag{A.62}$$

A linear stability analysis of each critical point follows.

(a) $\overline{x} = \overline{y} = \overline{z} = 0$

Small perturbations around this point give

$$\frac{d}{dt}\begin{pmatrix} x' \\ y' \\ z' \end{pmatrix} = \begin{pmatrix} -\sigma & \sigma & 0 \\ \lambda & -1 & 0 \\ 0 & 0 & -b \end{pmatrix}\begin{pmatrix} x' \\ y' \\ z' \end{pmatrix} \tag{A.63}$$

The characteristic equation is

$$(\lambda + b)[\lambda^2 + \lambda(\sigma+1) - \sigma(\lambda-1)] = 0 \tag{A.64}$$

from which we get the eigenvalues $-b, \frac{1}{2}[-(1+\sigma) \pm \sqrt{(1+\sigma)^2 - 4\sigma(1-\lambda)}]$. For $0 < \lambda < 1$, the eigenvalues are real and negative, since $(1+\sigma)^2 > 4\sigma(1-\lambda)$. At $\lambda = \lambda_1$, where $\lambda_1 = 1$, there is a pitchfork bifurcation with one zero eigenvalue. For $\lambda > \lambda_1$, the origin becomes unstable.

(b) $\overline{x} = \overline{y} = \sqrt{b(\lambda-1)}$, $\overline{z} = \lambda - 1$

Small perturbations give

$$\frac{d}{dt}\begin{pmatrix} x' \\ y' \\ z' \end{pmatrix} = \begin{pmatrix} -\sigma & \sigma & 0 \\ 1 & -1 & -\sqrt{b(\lambda-1)} \\ \sqrt{b(\lambda-1)} & \sqrt{b(\lambda-1)} & -b \end{pmatrix}\begin{pmatrix} x' \\ y' \\ z' \end{pmatrix} \tag{A.65}$$

The characteristic equation is

$$\lambda^3 + (\sigma + b + 1)\lambda^2 + (\sigma + \lambda)b\lambda + 2\sigma b(\lambda - 1) = 0 \tag{A.66}$$

Using the Hurwitz criteria we can determine the sign of the real parts of the solutions of this cubic equation without actually solving it. The Hurwitz determinants are

$$\begin{aligned} D_1 &= \sigma + b + 1 \\ D_2 &= \begin{vmatrix} \sigma + b + 1 & 2\sigma b(\lambda + 1) \\ 1 & (\sigma + \lambda)b \end{vmatrix} \\ &= \sigma b(\sigma + b + 3) - \lambda b(\sigma - b - 1) \\ D_3 &= \begin{vmatrix} \sigma + b + 1 & 2\sigma b(\lambda - 1) & 0 \\ 1 & (\sigma + \lambda)b & 0 \\ 0 & \sigma + b + 1 & 2\sigma b(\lambda - 1) \end{vmatrix} \\ &= 2\sigma b(\lambda - 1)[\sigma b(\sigma + b + 3) - \lambda b(\sigma - b - 1)] \end{aligned}$$

Thus the real parts of the eigenvalues are negative if $\lambda < \lambda_3$, where

$$\lambda_3 = \frac{\sigma(\sigma + b + 3)}{\sigma - b - 1} \tag{A.67}$$

At $\lambda = \lambda_3$ the characteristic equation (A.66) can be factorized to give the eigenvalues $-(\sigma + b + 1)$, and $\pm i\ 2\sigma(\sigma + 1)/(\sigma - b - 1)$, corresponding to a Hopf bifurcation. The periodic solution which is created at this value of λ can be shown to be unstable so that the bifurcation is subcritical.

Here is a summary of the series of bifurcation with respect to the parameter λ:

- Origin is a stable critical point for $\lambda < \lambda_1$; becomes unstable at $\lambda = \lambda_1$.
- Two other critical points are created for $\lambda > \lambda_1$; these are linearly stable in the range $\lambda_1 < \lambda < \lambda_3$.
- Just below λ_3, i.e. in the range $\lambda_2 < \lambda < \lambda_3$, the two critical points are stable to small perturbations, but for large enough perturbations produce chaos.
- For $\lambda > \lambda_3$, all initial conditions produce chaos (except for periodic windows).

A.4.9 Nonlinear analysis

Center manifold theorem

[30]

Consider a vector field $f_i(x)$ with $f_i(0) = 0$. The eigenvalues λ of $\partial f_i/\partial x_j$ at the origin are of three kinds:
(a) $Re(\lambda) > 0$ with the generalized eigenspace E^u.
(b) $Re(\lambda) < 0$ with the generalized eigenspace E^s.
(c) $Re(\lambda) = 0$ with the generalized eigenspace E^c.
There exist manifolds W^u, W^s, and W^c to which E^u, E^s and E^c, respectively, are tangents. W^u, W^s, and W^c are the unstable, stable and center manifolds, respectively.

A.5 Singularity theory

We have seen that the critical points of a dynamical system, equation (A.10), are found by solving an equation of the type (A.12), i.e. by finding the singularities of the function f_i. The type of bifurcations that occur with a single bifurcation parameter λ has been discussed in the previous

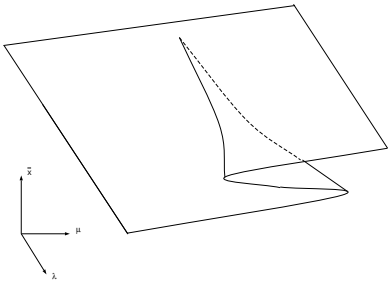

Figure A.9: Surface $\overline{x} = \overline{x}(\lambda, \mu)$.

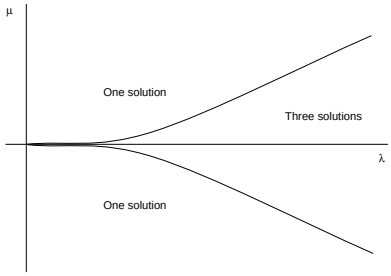

Figure A.10: Bifurcation set.

section. Here we increase the number of parameters to $\lambda_1, \ldots, \lambda_p$ and look at the consequent changes in the bifurcations. A bifurcation (or catastrophe) set is the set of points in parametric space $\lambda_1, \ldots, \lambda_p$ at which equation (A.12) is satisfied.

Example A.7

Examine the one-dimensional vector field

$$f(x) = -(x^3 + px + q) \tag{A.68}$$

Figure A.9 shows the surface $\overline{x} = \overline{x}(\lambda, \mu)$. There are three real solutions if the discriminant $D = 4\lambda^3 + 27\mu^2 > 0$, and only one otherwise. A section of this surface at $\mu = 0$ will give Fig. A.4 and $\mu = \epsilon$ will give Fig. A.8.

The bifurcation set is shown in Fig. A.10 in (λ, μ) coordinates. It is projection of the $\overline{x} = \overline{x}(\lambda, \mu)$ surface in the (λ, μ) plane.

The quadratic surface

$$a_1x^2 + a_2y^2 + a_3z^3 + a_4xy + a_5xz + a_6yz + a_7x + a_8y + a_9z + a_{10} = 0 \tag{A.69}$$

can be classified in terms of eleven canonical surfaces. For gradient systems, i.e. systems in which $f_I = \partial\phi/\partial x_i$, there are only seven.

A.6 Partial differential equations

Classification

Boundary conditions

A.6.1 Eigenfunction expansion

Let $T = T(\mathbf{x}, t)$ and

$$\frac{\partial T}{\partial t} = \mathcal{L}(T) \tag{A.70}$$

in a domain Ω, where $\mathcal{L}$ is a linear operator with spatial partial derivatives. The boundary and initial conditions are $T = 0$ at $\partial\Omega$ and $T = f(\mathbf{x})$ at $t = 0$.

Let $\phi_i(\mathbf{x})$ be the eigenfunctions of $\mathcal{L}$, such that

$$\mathcal{L}\phi_i = \lambda_i\phi. \tag{A.71}$$

Expand $T(\mathbf{x}, t)$ in the form

$$T(\mathbf{x}, t) = \sum_{i=1}^{\infty} a_i(t)\phi_i(\mathbf{x}). \tag{A.72}$$

Substituting in the equation, we get

$$\sum_{i=1}^{\infty} \frac{da_i}{dt}\phi_i = \sum_{i=1}^{\infty} a_i(t)\mathcal{L}(\phi_i). \tag{A.73}$$

Taking the inner product with ϕ_j, we find that

$$\sum_{i=1}^{\infty} \frac{da_i}{dt}\langle\phi_i, \phi_j\rangle = \sum_{i=1}^{\infty} a_i(t)\langle\mathcal{L}(\phi_i), \phi_j\rangle. \tag{A.74}$$

At this point we restrict ourselves to the special case in which $\mathcal{L}$ is a self-adjoint operator, so that the λ_i are real and the ϕ_i are orthonormal. Thus

$$\langle\phi_i, \phi_j\rangle = \delta_{ij}. \tag{A.75}$$

Using eq. (A.71), we get

$$\frac{da_j}{dt} = \lambda_j a_j. \tag{A.76}$$

A.7 Waves

A wave can be of the form [208]

$$f(x, t) = Ae^{i(kx-\omega t)}. \tag{A.77}$$

If we follow a point at constant phase $\phi = kx - \omega t = k(x - \omega t/k)$, we will be moving with the phase velocity v_p, where

$$v_p = \frac{\omega}{k}. \tag{A.78}$$

The relation between the frequency ω and the wave number k

$$\omega = \omega(k) \tag{A.79}$$

is called the dispersion relation. The group velocity is the velocity at which the energy of the wave moves, and is given by

$$v_g = \frac{d\omega}{dk}. \tag{A.80}$$

Problems

1. Show that
$$\frac{dx}{dt} = -x\left[x - (\lambda - \lambda_0)\right]$$
has a transcritical bifurcation.
2. Carry out an imperfection analysis on the transcritical bifurcation above.
3. Show that
$$\frac{dx}{dt} = -x^2 + (\lambda - \lambda_0)$$
has a saddle-node bifurcation.
4. Investigate the bifurcations in
$$\frac{dx}{dt} = -x\left(x^4 - 2x^2 + 2 + \lambda\right)$$

Appendix B

Numerical methods

[33, 96, 97, 126, 146, 171, 196]

Method of weighted residuals

Let us apply the following numerical methods to the one-dimensional fin equation

$$\frac{d^2T}{dx^2} - T = 0 \tag{B.1}$$

with the boundary conditions $T(0) = T_L$ and $T(1) = T_R$.

B.1 Finite difference methods

Divide $[0, 1]$ into N intervals, each of length $\Delta x = 1/N$, and number the nodes as $i = 0, 1, 2, \ldots, N$ so that $x_i = i\Delta x$. Write the second derivative at $x = x_i$ as

$$T''(x_i) = \frac{1}{\Delta x^2}\left(T_{i+1} - 2T_i + T_{i-1}\right) \tag{B.2}$$

where $T_i = T(x_i)$, so that from Eq. B.1, we get

$$-T_{i+1} + (2 + \Delta x^2)T_i - T_{i-1} = 0 \tag{B.3}$$

at $i = 1, 2, \ldots, N-1$. Applying the boundary conditions, we get $N - 1$ algebraic equations in the unknowns $T_1, T_2, \ldots, T_{N-1}$. Thus we have

$$\begin{bmatrix} c & -1 & 0 & \ldots & 0 \\ -1 & c & -1 & 0 & \ldots \\ 0 & -1 & c & -1 & \ldots \\ \vdots & \vdots & \vdots & \vdots & \vdots \\ 0 & 0 & \ldots & -1 & c \end{bmatrix} \begin{Bmatrix} T_1 \\ T_2 \\ \vdots \\ T_{N-2} \\ T_{N-1} \end{Bmatrix} = \begin{Bmatrix} T_L \\ 0 \\ \vdots \\ 0 \\ T_R \end{Bmatrix} \tag{B.4}$$

where $c = 2 + \Delta x^2$, which can be solved.

B.2 Finite element methods

[161]

Figure B.1: Finite differencing.

Figure B.2: Finite element.

Once again, divide $[0,1]$ into N intervals or finite elements, each of length $\Delta x = 1/N$. Number the nodes as $i = 0, 1, 2, \ldots, N$ so that $x_i = i\Delta x$. In each element use a local coordinate ξ that goes from $\xi = 0$ to $\xi = \Delta x$ and correspond to the global coordinate $x = x_i$ and $x = x_{i+1} = x_i + \Delta x$, respectively.

Let us use the linear test functions

$$\phi_1(\xi) = 1 - \frac{\xi}{\Delta x} \tag{B.5}$$

$$\phi_2(\xi) = \frac{\xi}{\Delta x} \tag{B.6}$$

within element i. Notice that $\phi_1(0) = \phi_2(\Delta x) = 1$ and $\phi_1(\Delta x) = \phi_2(0) = 0$, so that we can write

$$T(\xi) = T_{i-1}\phi_1(\xi) + T_i\phi_2(\xi),$$

where $T_{i-1} = T_{x=x_{i-1}} = T_{\xi=0}$ and $T_i = T_{x=x_i} = T_{\xi=\Delta x}$. Using the Galerkin method

$$\int_0^{\Delta x} \left(\frac{d^2T}{d\xi^2} - T \right) \phi_k(\xi)\, d\xi = 0,$$

where $k = 1, 2$. Integrating by parts

$$T'\phi_k \Big|_0^{\Delta x} - \int_0^{\Delta x} \left[\frac{dT}{d\xi}\frac{d\phi_k}{d\xi} + T\phi_k \right] d\xi = 0.$$

where $T' = dT/d\xi$. For $k = 1$ and $k = 2$, we have the two equations

$$\begin{aligned} -T'_{i-1} - T_{i-1}\left(\frac{1}{\Delta x} + \frac{\Delta x}{3}\right) + T_i\left(\frac{1}{\Delta x} - \frac{\Delta x}{6}\right) &= 0, \\ T'_i + T_{i-1}\left(\frac{1}{\Delta x} - \frac{\Delta x}{6}\right) - T_i\left(\frac{1}{\Delta x} + \frac{\Delta x}{3}\right) &= 0, \end{aligned}$$

respectively. Doing this for each of the N element, (and multiplying by $-\Delta x$ for convenience) we

end up with $2N$ algebraic equations.

$$\begin{aligned}
\Delta x\ T_0' + (1+\frac{\Delta x^2}{3})T_0 - (1-\frac{\Delta x^2}{6})T_1 &= 0 && \text{(B.7)}\\
-\Delta x\ T_1' - (1-\frac{\Delta x^2}{6})T_0 + (1+\frac{\Delta x^2}{3})T_1 &= 0 && \text{(B.8)}\\
\Delta x\ T_1' + (1+\frac{\Delta x^2}{3})T_1 - (1-\frac{\Delta x^2}{6})T_2 &= 0 && \text{(B.9)}\\
-\Delta x\ T_2' - (1-\frac{\Delta x^2}{6})T_1 + (1+\frac{\Delta x^2}{3})T_2 &= 0 && \text{(B.10)}\\
\vdots && && \text{(B.11)}\\
\Delta x\ T_{N-1}' + (1+\frac{\Delta x^2}{3})T_{N-1} - (1-\frac{\Delta x^2}{6})T_N &= 0 && \text{(B.12)}\\
-\Delta x\ T_N' - (1-\frac{\Delta x^2}{6})T_{N-1} + (1+\frac{\Delta x^2}{3})T_N &= 0 && \text{(B.13)}
\end{aligned}$$

There are $2N$ unknowns including T and T' at each of the $N+1$ node minus the values of T_0 and T_N at the two ends that are known, so that we can solve for the unknowns at this stage if we wish. However, it can be noticed that adding Eqs. (B.8) and (B.9) cancels the T_1' term. So we discard the first and last equations, add the rest in pairs to get the reduced set

$$\begin{bmatrix} c_1 & -c_2 & 0 & \dots & 0 \\ -c_2 & c_1 & -c_2 & 0 & \dots \\ 0 & -c_2 & c_1 & -c_2 & \dots \\ \vdots & \vdots & \vdots & \vdots & \vdots \\ 0 & 0 & \dots & -c_2 & c_1 \end{bmatrix} \begin{Bmatrix} T_1 \\ T_2 \\ \vdots \\ T_{N-2} \\ T_{N-1} \end{Bmatrix} = \begin{Bmatrix} c_2 T_L \\ 0 \\ \vdots \\ 0 \\ c_2 T_R \end{Bmatrix} \qquad \text{(B.14)}$$

where $c_1 = 2(1+\Delta x^2/3), c_2 = 1-\Delta x^2/6$.

B.3 Spectral methods

For the following, let

$$\theta = T - T_L - (T_R - T_L)x \qquad \text{(B.15)}$$

so that

$$\begin{aligned}
\frac{d^2\theta}{dx^2} - \theta &= T_L + (T_R - T_L)x \\
&= g(x) && \text{(B.16)}
\end{aligned}$$

with the homogeneous boundary conditions $\theta(0) = \theta(1) = 0$.

The dependent variable is expanded in terms of orthonormal functions $\phi_n(x)$ that satisfy the boundary conditions. Thus

$$\theta(x) = \sum_{n=1}^{N} a_n \phi_n(x). \qquad \text{(B.17)}$$

Substituting in the differential equation gives the residual

$$\sum_{n=1}^{N} a_n \left(\frac{d^2\phi_n}{dx^2} - \phi_n \right) - g = \epsilon. \qquad \text{(B.18)}$$

Making the residual and functions $\psi_m(x)$ orthogonal gives

$$\langle \epsilon, \psi_m \rangle = 0 \tag{B.19}$$

This reduces to an algebraic equation for each m. Solve.

B.3.1 Trigonometric Galerkin

Here

$$\phi_n(x) = \psi_n(x) = \sqrt{2}\sin(n\pi x) \tag{B.20}$$

with respect to the $\mathcal{L}_2$ inner product.

B.3.2 Trigonometric collocation

Equate the residual in Eq. (B.18) to zero in N equally-spaced points. This gives algebraic equations; solve.

B.3.3 Chebyshev Galerkin

Using $\xi = 2x - 1$, transform the independent variable to the domain $[-1, 1]$. The orthonormal Chebychev functions are $\phi_n(\xi) = 2^n T_n(\xi)/\sqrt{2\pi}$, where the Chebychev polynomials T_n are

$$\begin{aligned} T_1 &= 1 \\ T_2 &= \xi \\ T_3 &= 2\xi^2 - 1 \\ T_4 &= 4\xi^3 - 3\xi \\ &\vdots \end{aligned}$$

Take $\psi_n(\xi) = \phi_n(\xi)$ and an inner product with respect to the weight function $1/\sqrt{1-\xi^2}$.

B.3.4 Legendre Galerkin

B.3.5 Moments

Let $\phi(x) = x(1-x)$, so that it satisfies the boundary conditions and $\theta(x) = a\phi(x)$. Take $\psi(x) = 1$ to determine a.

For higher-order accuracy, take $\phi_1(x) = x(1-x), \phi_2(x) = x^2(1-x), \phi_3(x) = x(1-x)^2, \ldots$ and $\psi_1(x) = 1, \psi_2(x) = x, \psi_3(x) = x^2, \ldots$

B.4 MATLAB

The PDE Toolbox uses a finite-element code to solve basic partial differential equations needed for conduction heat transfer.

Problems

1. Consider the convective fin equation
$$\frac{d^2T}{dx^2} - T = 0,$$
where $0 \leq x \leq 1$, with $T(0) = 1$, $T(1) = 0$. Solve using the following methods. You may have to transform the dependent or independent variable differently for each method. In each case show convergence.

   (a) *Finite differences:* Divide into N parts, write derivatives in terms of finite differences, reduce to algebraic equations, apply boundary conditions, and solve.

   (b) *Trigonometric Galerkin:* Expand in terms of N trigonometric functions, substitute in equation, take inner products, reduce to algebraic equations, and solve.

   (c) *Chebyshev Galerkin:* Expand in terms of N Chebyshev polynomials, substitute in equation, take inner products, reduce to algebraic equations, and solve.

   (d) *Trigonometric collocation:* Expand in terms of N trigonometric functions, substitute in equation, take inner products, apply collocation, and solve.

   (e) *Galerkin finite elements:* Divide into N elements, assume linear functions, integrate by parts, assemble all equations, apply boundary conditions, and solve.

   (f) *Polynomial moments:* Assume dependent variable to be a Nth-order polynomial that satisfies boundary conditions, obtain algebraic equations by taking moments, and solve.

2. Consider the convective fin equation with heat generation
$$\frac{d^2T}{dx^2} - T = 1,$$
where $0 \leq x \leq 1$, with $T(0) = 1$, $T'(1) = 0$. Solve using the above methods.

Appendix C

Additional problems

1. Plot all real $\overline{\theta}(\beta, \epsilon)$ surfaces for the convection with radiation problem, and comment on the existence of solutions.

2. Complete the problem of radiation in an enclosure (linear stability, numerical solutions).

3. Two bodies at temperatures $T_1(t)$ and $T_2(t)$, respectively, are in thermal contact with each other and with the environment. The temperatures are governed by

$$M_1 c_1 \frac{dT_1}{dt} + hA_c(T_1 - T_2) + hA(T_1 - T_\infty) = 0 \tag{C.1}$$

$$M_2 c_2 \frac{dT_2}{dt} + hA_c(T_2 - T_1) + hA(T_2 - T_\infty) = 0 \tag{C.2}$$

   Derive the equations above and explain the parameters. Find the steady-state temperatures and explore the stability of the system for constant T_∞.

4. Consider the change in temperature of a lumped system with convective heat transfer where the ambient temperature, $T_\infty(t)$, varies with time in the form shown. Find (a) the long-time solution of the system temperature, $T(t)$, and (b) the amplitude of oscillation of the system temperature, $T(t)$, for a small period δt.

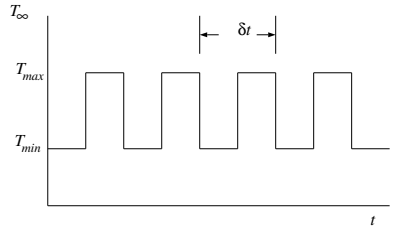

Figure C.1: Ambient temperature variation.

5. Two bodies at temperatures $T_1(t)$ and $T_2(t)$, respectively, are in thermal contact with each

other and with the environment. The temperatures are governed by

$$\begin{aligned} M_1 c_1 \frac{dT_1}{dt} + h_c A_c (T_1 - T_2) + hA(T_1 - T_\infty(t)) &= Q_1(t) \\ M_2 c_2 \frac{dT_2}{dt} + h_c A_c (T_2 - T_1) + hA(T_2 - T_\infty(t)) &= Q_2(t) \end{aligned}$$

where Q_1 and Q_2 are internal heat generations, each one of which can be independently controlled. Using PID control, show numerical results for the different types of responses possible (damped, oscillatory, unstable, stable, etc.). Take the ambient temperature, T_∞, to be (a) constant and (b) oscillatory.

6. Two bodies at temperatures $T_1(t)$ and $T_2(t)$, respectively, are in thermal contact with each other and with the environment. The temperatures are governed by

$$\begin{aligned} M_1 c_1 \frac{dT_1}{dt} + h_c A_c (T_1 - T_2) + hA(T_1 - T_\infty(t)) &= Q_1(t) \\ M_2 c_2 \frac{dT_2}{dt} + h_c A_c (T_2 - T_1) + hA(T_2 - T_\infty(t)) &= Q_2(t) \end{aligned}$$

where Q_1 and Q_2 are internal heat generation sources, each one of which can be independently controlled. Using on-off control, show analytical or numerical results for the temperature responses of the two bodies. If you do the problem analytically, take the ambient temperature, T_∞, to be constant, but if you do it numerically, then you can take it to be (a) constant, and (b) oscillatory.

7. Consider a rectangular fin with convection, radiation and Dirichlet boundary conditions. Calculate numerically the evolution of an initial temperature distribution at different instants of time. Graph the results for several values of the parameters.

8. Consider a longitudinal fin of concave parabolic profile as shown in the figure, where $\delta = [1 - (x/L)]^2 \delta_b$. δ_b is the thickness of the fin at the base. Assume that the base temperature is known. Neglect convection from the thin sides. Find (a) the temperature distribution in the fin, and (b) the heat flow at the base of the fin. Optimize the fin assuming the fin volume to be constant and maximizing the heat rate at the base. Find (c) the optimum base thickness δ_b, and (d) the optimum fin height L.

9. Analyze an annular fin with a prescribed base temperature and adiabatic tip. Determine its fin efficiency and plot.

10. Consider a square plate of side 1 m. The temperatures on each side are (a) 10°C, (b) 10°C, (c) 10°C, and (d) $10 + \sin(\pi x)$ °C, where x is the coordinate along the edge. Find the steady-state temperature distribution analytically.

11. Write a computer program to do the previous problem numerically using finite differences and compare with the analytical results. Choose different grid sizes and show convergence.

12. A plane wall initially at a uniform temperature is suddenly immersed in a fluid at a different temperature. Find the temperature profile as a function of time. Assume all parameter values to be unity.

13. Write a computer program to do the previous problem numerically using finite differences and compare with the analytical results.

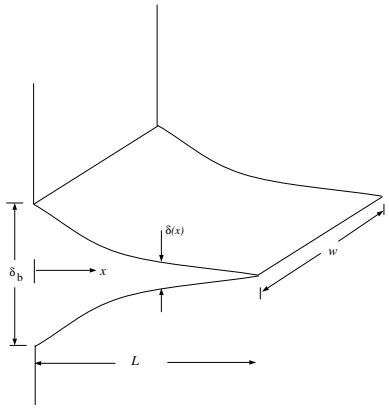

Figure C.2: Longitudinal fin of concave parabolic profile.

14. Consider the hydrodynamic and thermal boundary layers in a flow over a flat plate at constant temperature. Starting from the boundary layer equations

$$\frac{\partial u}{\partial x} + \frac{\partial v}{\partial y} = 0 \tag{C.3}$$

$$u\frac{\partial u}{\partial x} + v\frac{\partial u}{\partial y} = \nu\frac{\partial^2 u}{\partial y^2} \tag{C.4}$$

$$u\frac{\partial T}{\partial x} + v\frac{\partial T}{\partial y} = \alpha\frac{\partial^2 T}{\partial y^2} \tag{C.5}$$

change to variables $f(\eta)$ and $\theta(\eta)$ and derive the boundary layer equations

$$2f''' + ff'' = 0 \tag{C.6}$$

$$\theta'' + \frac{Pr}{2}f\theta' = 0 \tag{C.7}$$

and the boundary conditions.

15. Solve equations (C.6) and (C.7) numerically by the shooting method for different Pr and compare with results in the literature.

16. For Problem 1, derive the momentum and energy integral equations. Using cubic expansions for u/u_∞ and θ, derive expressions for the boundary layer thicknesses.

17. For natural convection near a vertical plate, show that the governing boundary layer equations

$$\frac{\partial u}{\partial x} + \frac{\partial v}{\partial y} = 0 \tag{C.8}$$

$$u\frac{\partial u}{\partial x} + v\frac{\partial u}{\partial y} = g\beta(T - T_\infty) + \nu\frac{\partial^2 u}{\partial y^2} \tag{C.9}$$

$$u\frac{\partial T}{\partial x} + v\frac{\partial T}{\partial y} = \alpha\frac{\partial^2 T}{\partial y^2} \tag{C.10}$$

can be reduced to

$$f''' + 3ff'' - 2(f')^2 + \theta = 0 \quad (C.11)$$
$$\theta'' + 3\ Pr\ f\ \theta' = 0 \quad (C.12)$$

with appropriate boundary conditions.

18. Solve equations (C.11) and (C.12) numerically by the shooting method for different Pr and compare with results in the literature.

19. Write the governing equations for natural convection flow in an inclined rectangular cavity, and nondimensionalize them. The thermal conditions at the walls of the cavity are: (a) AB heating with heat flux q_s'', (b) BC adiabatic, (c) CD cooling with heat flux q_s'', (d) DA adiabatic.

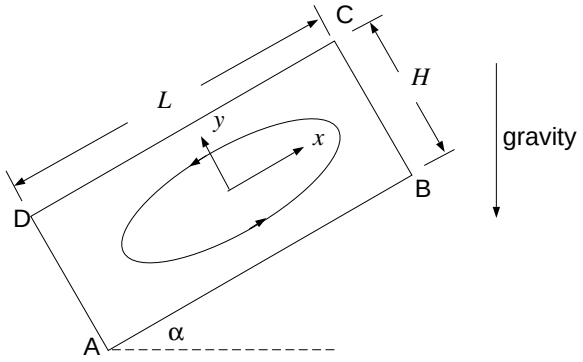

20. Derive the Nusselt result for laminar film condensation on a vertical flat plate. Find from the literature if there is any experimental confirmation of the result.

21. For parallel and counterflow heat exchangers, I obtained the temperature distributions

$$T_h(x) = T_{h,1} - \frac{T_{h,1} - T_{c,1}}{1 \pm (\dot{m}_h c_h / \dot{m}_c c_c)} \left[1 - \exp\{-UP\left(\frac{1}{\dot{m}_h c_h} \pm \frac{1}{\dot{m}_c c_c}\right) x\}\right],$$
$$T_c(x) = T_{c,1} \pm \frac{T_{h,1} - T_{c,1}}{(\dot{m}_c c_c / \dot{m}_h c_h) \pm 1} \left[1 - \exp\{-UP\left(\frac{1}{\dot{m}_h c_h} \pm \frac{1}{\dot{m}_c c_c}\right) x\}\right]$$

for the hot and cold fluids, respectively. As usual the upper sign is for parallel and the lower for counterflow; 1 is the end where the hot fluid enters (from where x is measured) and 2 is where it leaves. Please check.

22. For a counterflow heat exchanger, derive the expression for the effectiveness as a function of the NTU, and also the NTU as function of the effectiveness.

23. (From Incropera and DeWitt) A single-pass, cross-flow heat exchanger uses hot exhaust gases (mixed) to heat water (unmixed) from 30 to 80°C at a rate of 3 kg/s. The exhaust gases, having thermophysical properties similar to air, enter and exit the exchanger at 225 and 100°C, respectively. If the overall heat transfer coefficient is 200 W/m^{2}K, estimate the required area.

24. (From Incropera and DeWitt) A cross-flow heat exchanger used in cardiopulmonary bypass procedure cools blood flowing at 5 liters/min from a body temperature of 37°C to 25°C in order to induce body hypothermia, which reduces metabolic and oxygen requirements. The coolant is ice water at 0°C and its flow rate is adjusted to provide an outlet temperature of 15°C. The heat exchanger operates with both fluids unmixed, and the overall heat transfer coefficient is 750 W/m^{2}K. The density and specific heat of the blood are 1050 kg/m^2 and 3740 J/kg K, respectively. (a) Determine the heat transfer rate for the exchanger. (b) Calculate the water flow rate. (c) What is the surface area of the heat exchanger?

25. Show that the energy spectrum for blackbody radiation (Planck's law)

$$E_\lambda = \frac{C_1}{\lambda^5 \left(\exp \frac{C_2}{\lambda T} - 1\right)}$$

has a maximum at $\lambda = \lambda_m$ where (Wien's law)

$$\lambda_m T = 0.1987\ C_2$$

Also show that (Stefan-Boltzmann's law)

$$\int_0^\infty E_\lambda\ d\lambda = \frac{C_1 \pi^4}{15 C_2^4}\ T^4$$

You can use a symbolic algebra program in this problem.

26. Write a numerical code to evaluate the view factor between two rectangular surfaces (each of size $L \times 2L$) at 90° with a common edge of length $2L$; see Fig. C.3. Compare with the analytical result.

27. Calculate the view factor again but with a sphere (diameter $L/2$, center at a distance of $L/2$ from each rectangle, and centered along the length of the rectangles) as an obstacle between the two rectangles; see Fig. C.4.

28. (From Incropera and DeWitt) Consider a diffuse, gray, four-surface enclosure shaped in the form of a tetrahedron (made of four equilateral triangles). The temperatures and emissivities of three sides are

$$\begin{aligned} T_1 &= 700\text{K}, \quad \epsilon_1 = 0.7 \\ T_2 &= 500\text{K}, \quad \epsilon_2 = 0.5 \\ T_3 &= 300\text{K}, \quad \epsilon_3 = 0.3 \end{aligned}$$

The fourth side is well insulated and can be treated as a reradiating surface. Determine its temperature.

29. An "Aoki" curve is defined as shown in Fig. C.5. Show that when $n \to \infty$, the dimension of the curve is $D = 1$ and the length $L \to \infty$.

30. Consider conductive rods of thermal conductivity k joined together in the form of a fractal tree (generation $n = 3$ is shown in Fig. C.6; the fractal is obtained in the limit $n \to \infty$). The base and tip temperatures are T_0 and T_∞, respectively. The length and cross-sectional area of

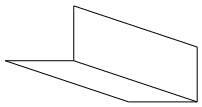

Figure C.3: Two rectangular surfaces.

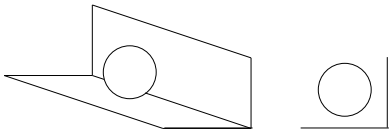

Figure C.4: Two rectangular surfaces with sphere.

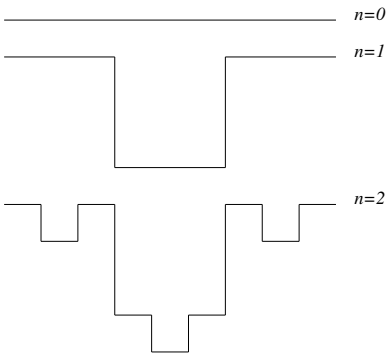

Figure C.5: Aoki curve.

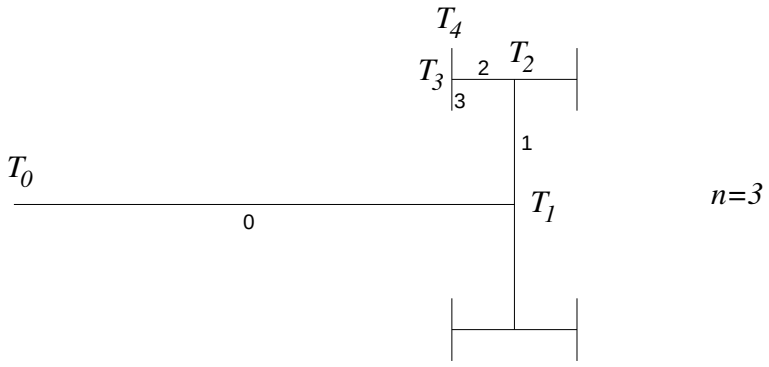

Figure C.6: Fractal tree.

bar 0 is L and A, respectively, and those of bar 1 are $2L/\beta$ and A/β^2, where $1 \leq \beta < 2$, and so on. Show that the conductive heat transfer through rod 0 is

$$q = \frac{kA}{L}(T_0 - T_\infty)\left(1 - \frac{\beta}{2}\right)$$

31. The dependence of the rate of chemical reaction on the temperature T is often represented by the Arrhenius function $f(T) = e^{-E/T}$, where E is the activation energy. Writing $T^* = T/E$, show that $f(T^*)$ has a point of inflexion at $T^* = 1/2$. Plot $f(T^*)$ in the range $T^* = 1/16$ to $T^* = 4$ as well as its Taylor series approximation to various orders around $T^* = 1/2$. Plot also the L_2-error in the same range for different orders of the approximation.

32. If $e^{-E/T}$ is proportional to the heat generated within a tank by chemical reaction, and there is heat loss by convection from the tank, show that the temperature of the tank T is determined by

$$Mc\frac{dT}{dt} = ae^{-E/T} - hA(T - T_\infty)$$

where M is the mass, c is the specific heat, a is a proportionality constant, h is the convective heat transfer coefficient, A is the convective heat transfer area, and T_∞ is the ambient temperature. Nondimensionalize the equation to

$$\frac{dT^*}{dt^*} = e^{-1/T^*} - H(T^* - T^*_\infty)$$

For $T^*_\infty = 0.1$, draw the bifurcation diagram with H as the bifurcation parameter, and determine the bifurcation points.

33. Two bodies at temperatures $T_1(t)$ and $T_2(t)$, respectively, are in thermal contact with each other and with the environment. Show that the temperatures are governed by

$$\begin{aligned} M_1c_1\frac{dT_1}{dt} + C(T_1 - T_2) + C_{1,\infty}(T_1 - T_\infty) &= Q_1 \\ M_2c_2\frac{dT_2}{dt} + C(T_2 - T_1) + C_{2,\infty}(T_2 - T_\infty) &= Q_2 \end{aligned}$$

where M_i is the mass, c_i is the specific heat, the Cs are thermal conductances, and Q_i is internal heat generation. Find the steady state $(\overline{T}_1, \overline{T}_2)$ and determine its stability.

34. Using a complete basis, expand the solution of the one-dimensional heat equation

$$\frac{\partial T}{\partial t} = \alpha\frac{\partial^2 T}{\partial x^2}$$

with boundary conditions

$$\begin{aligned} -k\frac{\partial T}{\partial x} &= q_0 \text{ at } x = 0, \\ T &= T_1 \text{ at } x = L \end{aligned}$$

as an infinite set of ODEs.

35. Show that the governing equation of the unsteady, variable-area, convective fin can be written in the form

$$\frac{\partial T}{\partial t} - \frac{\partial}{\partial x}\left(a(x)\frac{\partial T}{\partial x}\right) + b(x)T = 0$$

Show that the steady-state temperature distribution with fixed temperatures at the two ends $x = 0$ and $x = L$ is globally stable.

36. Show numerically that there are two different types of attractors for the following dynamical system.

$$\begin{aligned}\frac{dx}{dt} &= (\lambda - \lambda_0)x - y - (x^2 + y^2)x,\\ \frac{dy}{dt} &= x + (\lambda - \lambda_0)y - (x^2 + y^2)y.\end{aligned}$$

Choose $\lambda_0 = 1$ and (a) $\lambda = 0.5$ and (b) $\lambda = 2$.

37. For the two-dimensional, unsteady velocity field $u\mathbf{i} + v\mathbf{j}$, where

$$\begin{aligned}u &= y\\ v &= x - x^3 + a\cos t\end{aligned}$$

determine the pathline of a fluid particle which is at position (1,1) at time $t = 0$. Consider two cases: (a) $a = 0$, and (b) $a = 1$. For these two cases find where 11×11 points uniformly distributed within a square of size 0.01 and centered on (1,1) end up. Choose a suitably long final time.

38. Find the dimension of the strange attractor for the Lorenz equations

$$\begin{aligned}\frac{dx}{dt} &= \sigma(y - x)\\ \frac{dy}{dt} &= \lambda x - y - xz\\ \frac{dz}{dt} &= -bz + xy\end{aligned}$$

where $\sigma = 10$, $\lambda = 28$ and $b = 8/3$. Use the method of counting the number of points $N(r)$ within a sphere of radius r from which $D = \ln N / \ln r$.

39. Nondimensionalize and solve the radiative cooling problem

$$Mc\frac{dT}{dt} + \sigma A\left(T^4 - T_\infty^4\right) = 0$$

with $T(0) = T_i$.

40. For heat transfer from a heated body with convection and weak radiation, i.e. for

$$\frac{d\theta}{d\tau} + \theta + \epsilon\left\{(\theta + \beta)^4 - \beta^4\right\} = q$$

with $\theta(0) = 1$, using symbolic algebra determine the regular perturbation solution up to and including terms of order ϵ^4. Assuming $\epsilon = 0.1$, $\beta = 1$, $q = 1$, plot the five solutions (with one term, with two terms, with three terms, etc.) in the range $0 \le \tau \le 1$.

41. Consider a body in thermal contact with the environment

$$Mc\frac{dT}{dt} + hA(T - T_\infty) = 0$$

where the ambient temperature, $T_\infty(t)$, varies with time in the form shown below. Find (a) the long-time solution of the system temperature, $T(t)$, and (b) the amplitude of oscillation of the system temperature, $T(t)$, for a small period δt.

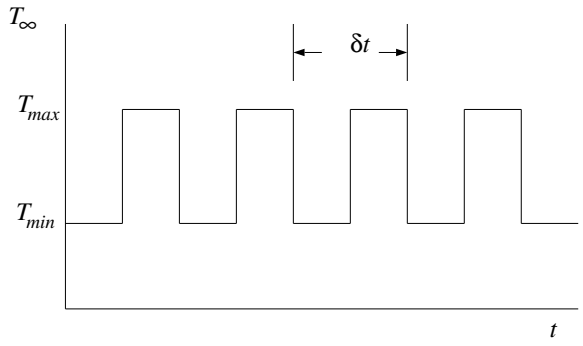

Figure C.7: Ambient temperature variation.

42. For a heated body in thermal contact with a constant temperature environment

$$Mc\frac{dT}{dt} + hA(T - T_\infty) = Q$$

analyze the conditions for linear stability of PID control.

43. Two heated bodies at temperatures $T_1(t)$ and $T_2(t)$, respectively, are in thermal contact with each other and with a constant temperature environment. The temperatures are governed by

$$\begin{aligned} M_1c_1\frac{dT_1}{dt} + C(T_1 - T_2) + C_{1,\infty}(T_1 - T_\infty) &= Q_1(t) \\ M_2c_2\frac{dT_2}{dt} + C(T_2 - T_1) + C_{2,\infty}(T_2 - T_\infty) &= Q_2(t) \end{aligned}$$

where $Q_1(t)$ and $Q_2(t)$ are internal heat generations, each one of which can be independently controlled. Using PID control, choose numerical values of the parameters and PID constants to show numerical results for the different types of responses possible (damped, oscillatory, etc.).

44. Show numerical results for the behavior of two heated bodies in thermal contact with each other and with a constant temperature environment for on-off control with (a) one thermostat, and (b) two thermostats.

45. Analyze the system controllability of two heated bodies in thermal contact with each other and with a constant temperature environment for (a) $Q_1(t)$ and $Q_2(t)$ being the two manipulated variables, and (b) with $Q_1(t)$ as the only manipulated variable and Q_2 constant.

46. Run the neural network FORTRAN code in

    http://www.nd.edu/ msen/Teaching/IntSyst/Programs/ANN/

    for 2 hidden layers with 5 nodes each and 20,000 epochs. Plot the results in the form of exact z vs. predicted z.

47. Consider the heat equation

$$\frac{\partial T}{\partial t} = \frac{\partial^2 T}{\partial x^2}$$

    with one boundary condition $T(0) = 0$. At the other end the temperature, $T(1) = u(t)$ is used as the manipulated variable. Divide the domain into 5 parts and use finite differences to write the equation as a matrix ODE. Find the controllability matrix and check for system controllability.

48. Determine the semi-derivative and semi-integral of (a) C (a constant), (b) x, and (c) x^μ where $\mu > -1$.

49. Find the time-dependent temperature field for flow in a duct wih constant T_∞ and T_{in}, but with variable flow rate $V(t) = V_0 + \Delta V \sin(\omega t)$ such that V is always positive.

50. Write a computer program to solve the PDE for the previous problem, and compare numerical and analytical results.

51. Derive an expression for heat transfer in a fractal tree-like microchannel net[1].

52. Find the steady-state temperature distribution and velocity in a square-loop thermosyphon. The total length of the loop is L and the distribution of the heat rate per unit length is

$$q(x) = \begin{cases} Q & \text{for} \quad L/8 \le x \le L/4, \\ -Q & \text{for} \quad 5L/8 \le x \le 3L/4, \\ 0 & \text{otherwise.} \end{cases}$$

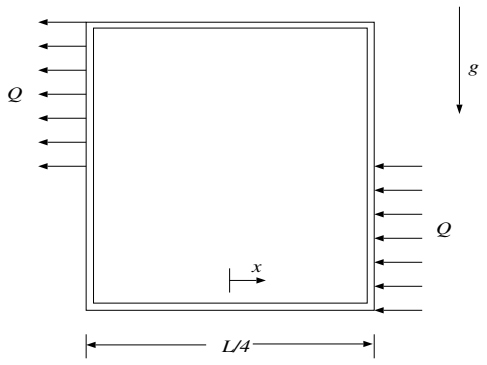

[1] Y. Chen and P. Cheng, Heat transfer and pressure drop in fractal tree-like microchannel nets, *International Journal of Heat and Mass Transfer,* Vol. 45, pp. 2643–2648, 2002

53. Show that the dynamical system governing the toroidal thermosyphon with known wall temperature can be reduced to the Lorenz equations.

54. Draw the steady-state velocity vs. inclination angle diagram for the inclined toroidal thermosyphon with mixed heating. Do two cases: (a) without axial condution[2], and (b) with axial conduction.

55. Model natural convection in a long, vertical pipe that is being heated from the side at a constant rate. What is the steady-state fluid velocity in the pipe? Assume one-dimensionality and that the viscous force is proportional to the velocity.

56. Using the center manifold projection, find the nonlinear behavior of

$$\begin{aligned} \frac{dx}{dt} &= x^2 y - x^5, \\ \frac{dy}{dt} &= -y + x^2, \end{aligned}$$

and hence determine whether the origin is stable.

57. The Brinkman model for the axial flow velocity, $u^*(r^*)$, in a porous cylinder of radius R is

$$\mu_{eff} \left[\frac{d^2 u^*}{dr^{*2}} + \frac{1}{r^*} \frac{du^*}{dr^*} \right] - \frac{\mu}{K} u^* + G = 0,$$

where $u^* = 0$ at $r^* = R$ (no-slip at the wall), and $\partial u^*/\partial r^* = 0$ at $r^* = 0$ (symmetry at the centerline). μ_{eff} is the effective viscosity, μ is the fluid viscosity, K is the permeability, and G is the applied pressure gradient. Show that this can be reduced to the nondimensional form

$$\frac{d^2 u}{dr^2} + \frac{1}{r} \frac{du}{dr} - s^2 u + \frac{1}{M} = 0, \tag{C.13}$$

where $M = \mu_{eff}/\mu$, $Da = K/R^2$, $s^2 = (M\ Da)^{-1}$.

58. Using a regular perturbation expansion, show that for $s \ll 1$, the velocity profile from equation (C.13) is

$$u = \frac{1 - r^2}{4M} \left[1 - \frac{s^2}{16} \left(3 - r^2 \right) \right] + \ldots$$

59. Using the WKB method, show that the solution of equation (1) for $s \gg 1$ is

$$u = Da \ \left[1 - \frac{\exp\{-s(1-r)\}}{\sqrt{r}} \right] + \ldots$$

60. Consider steady state natural convection in a tilted cavity as shown. DA and BC are adiabatic while AB and CD have a constant heat flux per unit length. It can be shown that the governing equations in terms of the vorticity ω and the streamfunction ψ are

$$\begin{aligned} \frac{\partial^2 \psi}{\partial x^2} + \frac{\partial^2 \psi}{\partial x^2} + \omega &= 0 \\ \frac{\partial \psi}{\partial y} \frac{\partial \omega}{\partial x} - \frac{\partial \psi}{\partial x} \frac{\partial \omega}{\partial y} - Pr \ \left[\frac{\partial^2 \omega}{\partial x^2} + \frac{\partial^2 \omega}{\partial y^2} \right] - Ra\ Pr \left[\frac{\partial T}{\partial x} \cos\alpha - \frac{\partial T}{\partial y} \sin\alpha \right] &= 0 \\ \frac{\partial \psi}{\partial y} \frac{\partial T}{\partial x} - \frac{\partial \psi}{\partial x} \frac{\partial T}{\partial y} - \frac{\partial^2 T}{\partial x^2} - \frac{\partial^2 T}{\partial y^2} &= 0 \end{aligned}$$

[2] M. Sen, E. Ramos and C. Treviño, On the steady-state velocity of the inclined toroidal thermosyphon, *ASME J. of Heat Transfer,* Vol. 107, pp. 974–977, 1985.

where Pr and Ra are the Prandtl and Rayleigh numbers, respectively. The boundary conditions are:

$$\begin{aligned} \text{at } x = \pm\frac{A}{2}, \quad \psi = \frac{\partial \psi}{\partial x} = 0, \quad \frac{\partial T}{\partial x} = 0, \\ \text{at } y = \pm\frac{1}{2}, \quad \psi = \frac{\partial \psi}{\partial y} = 0, \quad \frac{\partial T}{\partial y} = 1. \end{aligned}$$

where $A = L/H$ is the aspect ratio. Find a parallel flow solution for ψ using

$$\begin{aligned} \psi &= \psi(y) \\ T(x,y) &= Cx + \theta(y) \end{aligned}$$

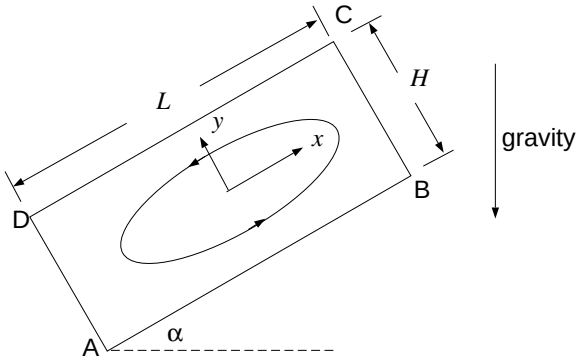

Figure C.8: Problem 5.

61. Determine the stability of a fluid layer placed between two horizontal, isothermal walls and heated from below.

62. Obtain the response to on-off control of a lumped, convectively-cooled body with sinusoidal variation in the ambient temperature.

63. Determine the steady-state temperature field in a slab of constant thermal conductivity in which the heat generated is proportional to the exponential of the temperature such that

$$\frac{d^2T}{dx^2} = \exp(\epsilon T),$$

where $0 \leq x \leq 1$, with the boundary conditions $T(0) = T'(0) = 0$.

64. In the previous problem, assume that ϵ is small. Find a perturbation solution and compare with the analytical. Do up to $O(\epsilon)$ by hand and write a Maple (or Mathematica) code to do up to $O(\epsilon^{10})$.

65. The temperature equation for a fin of constant area and convection to the surroundings at a constant heat transfer coefficient is

$$\left(\frac{d^2}{dx^2} - m^2\right)\theta = 0,$$

where $\theta = T - T_\infty$. Determine the eigenfunctions of the differential operator for each combination of Dirichlet and Neumann boundary conditions at the two ends $x = 0$ and $x = L$.

66. Add radiation to a convective fin with constant area and solve for small radiative effects with boundary conditions corresponding to a known base temperature and adiabatic tip.

67. Find the temperature distribution in a slightly tapered 2-dimensional convective fin with known base temperature and adiabatic tip.

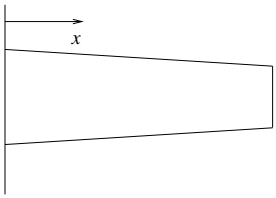

68. Prove Hottel's crossed string method to find the view factor F_{AB} between two-dimensional surfaces A and B with some obstacles between them as shown. The dotted lines are tightly stretched strings. The steps are:

    (a) Assuming the strings to be imaginary surfaces, apply the summation rule to each one of the sides of figure *abc*.

    (b) Manipulating these equations and applying reciprocity, show that

    $$F_{ab-ac} = \frac{A_{ab} + A_{ac} - A_{bc}}{2A_{ab}}.$$

    (c) For *abd* find F_{ab-bd} in a similar way.

    (d) Use the summation rule to show that

    $$F_{ab-cd} = \frac{A_{bc} + A_{ad} - A_{ac} - A_{bd}}{2A_{ab}}$$

    (e) Show that $F_{ab-cd} = A_A F_{AB}/A_{ab}$.

    (f) Show the final result

    $$F_{A-B} = \frac{A_{bc} + A_{ad} - A_{ac} - A_{bd}}{2A_A}$$

69. Complete the details to derive the Nusselt result for laminar film condensation on a vertical flat plate. Find from the literature if there is any experimental confirmation of the result.

70. Consider the hydrodynamic and thermal boundary layers in a flow over a flat plate at constant temperature. Use a similarity transformation on the boundary layer equations to get

    $$\begin{aligned} 2f''' + ff'' &= 0, \\ \theta'' + \frac{Pr}{2} f\theta' &= 0. \end{aligned}$$

    Using the shooting method and the appropriate boundary conditions, solve the equations for different Pr and compare with the results in the literature.

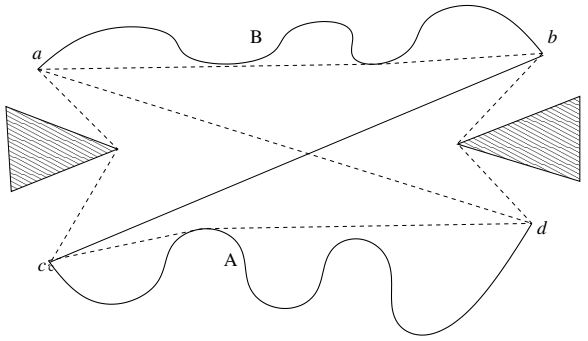

71. Solve the steady state conduction equation $\nabla^2 T = 0$ in the area in the figure between the square and the circle using the MATLAB Toolbox. Edges DA and BC have temperatures of 100 and 0 units, respectively, AB and CD are adiabatic and the circle is at a temperature of 200 units. Draw the isotherms. Save the M-file and e-mail it to: wcai@nd.edu.

72. (From Brauner and Shacham, 1995) Using Eq. 11, write a program to redraw Fig. 2 on a sunny day ($C_l = 0$) and a cloudy day ($C_l = 1$). Assume $T_a = 37°$C. Use Eq. 8 to calculate h_c. Note: since the physical properties are to be taken at the mean temperature between T_s and T_a, Eq. 11 must be solved numerically.

73. The steady-state temperature distribution in a plane wall of thermal conductivity k and thickness L is given by $T(x) = 4x^3 + 5x^2 + 2x + 3$, where T is in K, x in m, and the constants in appropriate units. (a) What is the heat generation rate per unit volume, $q(x)$, in the wall? (b) Determine the heat fluxes, q''_x, at the two faces $x = 0$ and $x = L$.

74. (From Incropera and DeWitt, 5th edition) Consider a square plate of side 1 m. Going around, the temperatures on the sides are (a) 50°C, (b) 100°C, (c) 200°C, and (d) 300°C. Find the steady-state temperature distribution analytically.

75. Write a computer program to do the previous problem numerically using finite differences and compare with the analytical result. Choose different grid sizes and show convergence of the heat flux at any wall. Plot the 75, 150, and 250°C isotherms.

76. A plane wall of thickness 1 m is initially at a uniform temperature of 85°C. Suddenly one side of the wall is lowered to a temperature of 20°C, while the other side is perfectly insulated. Find the time-dependent temperature profile $T(x, t)$. Assume the thermal diffusivity to be 1 m^2/s.

77. Write a computer program to do the previous problem numerically using finite differences and compare with the analytical result.

78. At a corner of a square where the temperature is discontinuous, show how the finite difference solution of the steady-state temperature behaves ompared to the separation-of-variables solution.

79. Find the view factor of a semi-circular arc with respect to itself.

80. Derive the unsteady governing equation for a two-dimensional fin with convection and radiation.

81. Determine the steady temperature distribution in a two-dimensional convecting fin.

82. A number of identical rooms are arranged in a circle as shown, with each at a uniform temperature $T_i(t)$. Each room exchanges heat by convection with the outside which is at T_∞, and with its neighbors with a conductive thermal resistance R. To maintain temperatures, each room has a heater that is controlled by independent but identical proportional controllers. (a) Derive the governing equations for the system, and nondimensionalize. (b) Find the steady state temperatures. (c) Write the dynamical system in the form $\dot{\mathbf{x}} = \mathbf{A}\mathbf{x}$ and determine the condition for stability[3].

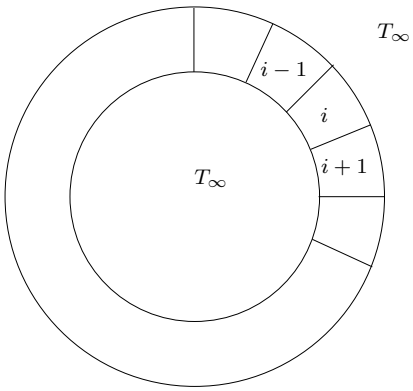

83. A sphere, initially at temperature T_i is being cooled by natural convection to fluid at T_∞. Churchill's correlation for natural convection from a sphere is

$$\overline{Nu} = 2 + \frac{0.589\ Ra_D^{1/4}}{\left[1 + (0.469/Pr)^{9/16}\right]^{4/9}},$$

where

$$Ra_D = \frac{g\beta(T_s - T_\infty)D^3}{\nu\alpha}.$$

Assume that the temperature within the sphere $T(t)$ is uniform, and that the material properties are all constant. Derive the governing equation, and find a two-term perturbation solution.

84. (a) Show that the transient governing equation for a constant area fin with constant properties that is losing heat convectively with the surroundings can be written as

$$\frac{1}{\alpha}\,\frac{\partial\theta}{\partial t} = \frac{\partial^2\theta}{\partial x^2} - m^2\theta.$$

[3]Eigenvalues of an $N \times N$, circulant, banded matrix of the form [3]

$$\begin{bmatrix} b & c & 0 & \dots & 0 & a \\ a & b & c & \dots & 0 & 0 \\ 0 & a & b & \dots & 0 & 0 \\ \vdots & \vdots & \vdots & \vdots & \vdots & \\ 0 & \dots & 0 & a & b & c \\ c & 0 & \dots & 0 & a & b \end{bmatrix}$$

are $\lambda_j = b + (a+c)\cos\{2\pi(j-1)/N\} - i(a-c)\sin\{2\pi(j-1)/N\}$, where $j = 1, 2, \dots, N$.

(b) With prescribed base and tip temperatures, use an eigenfunction expansion to reduce to an infinite set of ordinary differential equations. (c) Show that the steady state is attracting for all initial conditions.

85. **Cantor Sets:** Construct a fractal that is similar to the Cantor set shown in class, but instead remove the middle 1/2 from each line. Show that the fractal dimension is 1/2.

86. **Menger's Sponge:** Shown below is Menger's Sponge. Calculate its Hausdorff dimension using each of the following methods: (a) $D_h = \log P / \log S$, (b) Box Counting (analytical), (c) Box Counting (graphical).

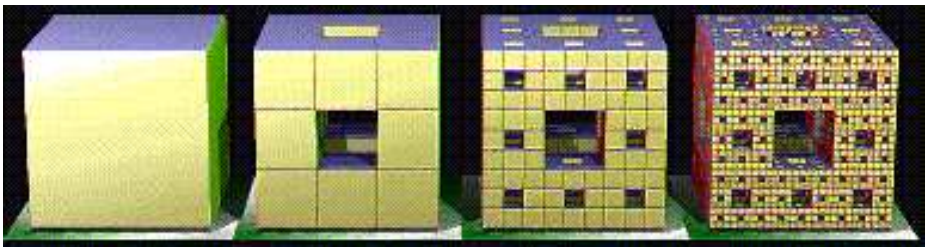

Figure C.9: Menger's Sponge

87. **Space Filling Curves:** Shown below is a Peano curve, a single line that completely fills a unit square. Calculate its Hausdorff dimension and state if the Peano curve is indeed a fractal.

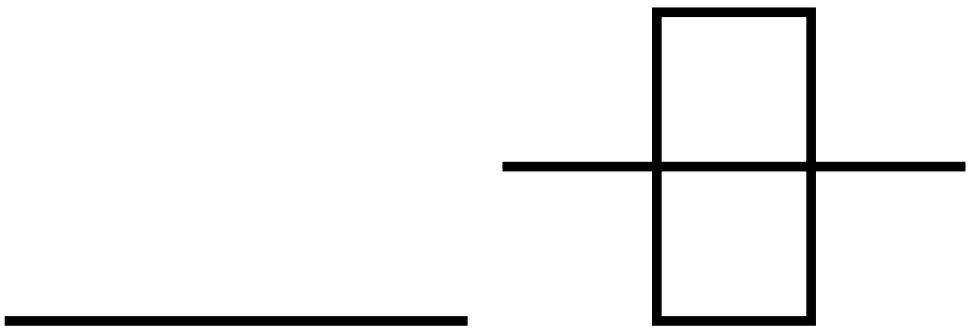

(a) *Initator* (b) *Generator*

Figure C.10: Initiator and generator for a Peano (space filling) curve. The generator is recursively applied to generate the Peano curve.

88. A duct carrying fluid has the cross-section of Koch's curve. Show that the perimeter of the cross-section is infinite while the flow area is finite.

89. **Cauchy's formula:** Verify Cauchy's formula for repeated integration by (a) integrating $f(t)$ five times, (b) applying Cauchy's formula once with $n = 5$, (c) applying Cauchy's formula

twice, once to $f(t)$ with $n = 2$ and then to the result with $n = 3$, showing that

$$\int\int\int\int\int_0^t f(\tau)d\tau = J^5 f(t) = J^3 J^2 f(t)$$

for $f(t) = 16t^3$.

90. **Caputo Derivative:** Take $f(t) = 2t^5$ and using the Caputo RHD, (a) calculate $D^3 f(t)$ (take $m = 4$, $\alpha = 3$) and verify that you get the same result as traditional differentation by comparing to $d^3 f/dt^3$. (b) Calculate $D^{2.5} f(t)$ and plot the function.

91. **Numerical Evaluation of a Fractional Derivative:** Consider the example worked in class of calculating the heat flux in a blast furnace. The heat flux was calculated to be

$$q''(t) = \sqrt{cp\lambda}\ {}_0D_t^{1/2} g(t),$$

where

$$g(t) = T_{surf}(t) - T_0,$$

which is simply the derivative of order $\alpha = 1/2$ of the temperature difference at the surface. Assume that the function $g(t)$ is given as $g(t) = 14\sin(\pi t/60)$ where t is in minutes and the thermocouples sample once per minute, giving the discrete data set $g_i = 14\sin(\pi i/60)$. Calculate the fractional derivative numerically using the first 2 hours of data and plot both the heat flux at the surface and $g(t)$.

Hint: It is easiest to calculate the binomial coefficients recursively, according to the recursion formula:

$$\begin{aligned} \binom{\alpha}{0} &= 1, \\ \binom{\alpha}{k+1} &= \binom{\alpha}{k}\frac{\alpha - k + 1}{k}. \end{aligned}$$

Note: In large time intervals (t very large), which would be of interest in this problem, the calculation we used would not be suitable because of the enormous number of summands in the calculation of the derivative and because of the accumulation of round off errors. In these situations, the principle of "short memory" is often applied in which the derivative only depends on the previous N points within the last L time units. The derivative with this "short memory" assumption is typically written as ${}_{(t-L)}D_t^{\alpha}$.

92. Consider the periodic heating and cooling of the surface of a smooth lake by radiation. The surface is subject to diurnal heating and nocturnal cooling such that the surface temperature can be described by $T_s(t) = T_o + T_a \sin\omega t$. Assume the heat diffusion to be one-dimensional and find the heat flux at the surface of the lake. The following steps might be useful:

(a) Assume transient one-dimensional heat conduction:

$$\frac{\partial T(x,t)}{\partial t} - \alpha\frac{\partial^2 T(x,t)}{\partial x^2} = 0,$$

with initial and boundary conditions $T(x,0) = T_o$ and $T(0,t) = T_s(t)$. Also assume the lake to be a semi-infinite planer medium (a lake of infinite depth) with $T(\infty,t) = 0$.

(b) Non-dimensionalize the problem with a change of variables $\xi = \alpha^{-1/2}x$ and $\theta(x,t) = T(x,t) - T_o$.

(c) Use the following Laplace transform properties to transform the problem into the Laplace domain:

$$\mathcal{L}\big[\frac{\partial^\alpha f(x,t)}{\partial t^\alpha}\big] = s^\alpha F(x,s) \qquad \text{(with 0 initial conditions)}$$

and

$$\mathcal{L}\big[\frac{\partial^\alpha f(x,t)}{\partial x^\alpha}\big] = \frac{\partial^\alpha}{\partial x^\alpha} F(x,s)$$

(d) Solve the resulting second order differential equation for $\Theta(\xi,s)$ by applying the transformed boundary conditions.

(e) Find $\partial\Theta/\partial\xi$ and then substitute $\Theta(\xi,s)$ into the result. Now take the inverse Laplace transform of $\partial\Theta/\partial\xi$ and convert back to the original variables. Be careful! The derivative of order 1/2 of a constant is not zero! (see simplifications in (g) to simplify)

(f) You should now have an expression for $\partial T(x,t)/\partial x$. Substitute this into Fourier's Law to calculate the heat flux, $q''(x,t) = -k\ \partial T(x,t)/\partial x$.

(g) Evaluate this expression at the surface ($x = 0$) to find the heat flux at the surface of the lake. The following simplifications might be helpful:

$$\frac{\partial^{1/2} C}{\partial t^{1/2}} = \frac{C}{\pi t^{1/2}}$$

$$\frac{\partial^\alpha [Cg(t)]}{\partial t^\alpha} = C\frac{\partial^\alpha g(t)}{\partial t^\alpha}$$

(h) The solution should look now look like

$$q''_s(t) = \frac{k}{\alpha^{1/2}} \frac{d^{1/2}(T_a \sin \omega t)}{dt^{1/2}}$$

93. Describe how you would solve this problem using more typical methods and what other information would be required.

94. Consider radiation between two long concentric cylinders of diameters D_1 (inner) and D_2 (outer). (a) What is the view factor F_{12}. (b) Find F_{22} and F_{21} in terms of the cylinder diameters.

95. Temperatures at the two sides of a plane wall shown in Fig. C.11 are T_L and T_R, respectively. For small ϵ, find a perturbation steady-state temperature distribution $T(x)$ if the dependence of thermal conductivity on the temperature has the form

$$k(T) = k_0 \left(1 + \frac{T - T_L}{T_R - T_L}\ \epsilon\right).$$

96. One side of a plane wall shown in Fig. C.12 has a fixed temperature and the other is adiabatic. With an initial condition $T(x,0) = f(x)$, determine the temperature distribution in the wall $T(x,t)$ at any other time. Assume constant properties.

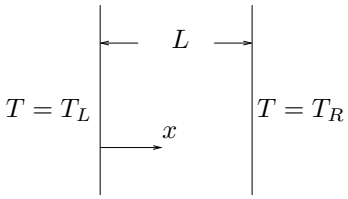

Figure C.11: Plane wall in steady state.

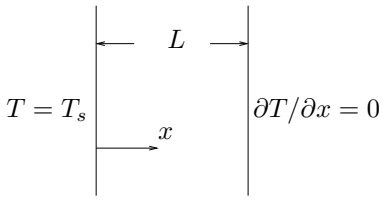

Figure C.12: Plane wall in unsteady state.

97. Using an eigenfunction expansion, reduce the governing PDE in Problem 96 to an infinite set of ODEs.

98. A room that loses heat to the outside by convection is heated by an electric heater controlled by a proportional controller. With a lumped capacitance approximation for the temperature, set up a mathematical model of the system. Determine the constraint on the controller gain for the system response to be stable. What is the temperature of the room after a long time?

99. A turbine blade internally cooled by natural convection is approximated by a rotating natural circulation loop of constant cross-section. The heat rate in and out at the top and bottom, respectively, is Q while the rest of the loop is insulated. Find the steady-state velocity in the loop. Consider rotational forces but not gravity. State your other assumptions.

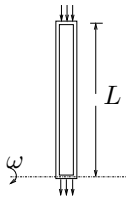

100. An infinite number of conductive rods are set up between two blocks at temperatures T_a and T_b. The first rod has a cross-sectional area $A_1 = A$, the second $A_2 = A/\beta$, the third $A_3 = A/\beta^2$, and so on, where $\beta > 1$. What is the total steady-state heat transfer rate between the two blocks? Assume that the thermal conductivity k is a constant, and that there is no convection.

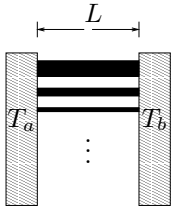

101. Show that the functions $\phi_1(x) = \sqrt{2}\ \sin \pi x$ and $\phi_2(x) = \sqrt{2}\ \sin 2\pi x$ are orthonormal in the interval $[0, 1]$ with respect to the L_2 norm. Using these as test functions, use the Galerkin method to find an approximate solution of the steady-state fin equation

$$T'' - T = 0,$$

with $T(0) = 0, T(1) = 1$.

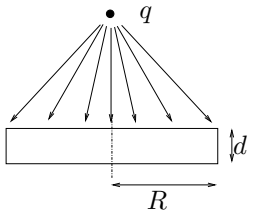

102. A lamp of q W is radiating equally in all directions. Set up the governing equation for the temperature $T(r)$ in the disk.

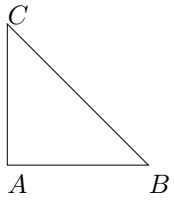

103. Determine the steady-state temperature distribution in the triangle shown, if the hypotenuse is adiabatic, one of the sides is at one temperature and the other is at another.

104. A ball with coefficient of restitution r falls from height H and undergoes repeated bouncing. Determine the temperature of the ball as a function of time $T(t)$ if heat loss is by convection to the atmosphere. Assume that the energy loss at every bounce goes to heat the ball.

105. Heat at the rate of q per unit volume is generated in a spherical shell that lies between R and $R + \delta$. If heat loss is by convection on the external surface only, find the steady-state temperature distribution.

References

[1] R. Acosta, M. Sen, and E. Ramos. Single-phase natural circulation in a tilted square loop. *Wärme- und Stoffübertragung*, 21(5):269–275, 1987.

[2] N.U. Ahmed. *Semigroup Theory with Applications to Systems and Control*. Longman, Harlow, U.K., 1991.

[3] R. Aldrovandi. *Special Matrices of Mathematical Physics: Stochastic, Circulant and Bell Metrices*. World Scientific, Singapore, 2001.

[4] S. Alotaibi. *Temperature Controllability in Cross-Flow Heat Exchangers and Long Ducts*. PhD thesis, Department of Aerospace and Mechanical Engineering, University of Notre Dame, Notre Dame, IN, 2003.

[5] S. Alotaibi, W.J. Goodwine M. Sen, and K.T. Yang. Controllability of cross-flow heat exchangers. *International Journal of Heat and Mass Transfer*, 47:913–924, 2004.

[6] S. Alotaibi, M. Sen, J.W. Goodwine, and K.T. Yang. Numerical simulation of the thermal control of heat exchangers. *Numerical Heat Transfer A*, 41:229–244, 2002.

[7] S. Alotaibi, M. Sen, W.J. Goodwine, and K.T. Yang. Flow-based control of temperature in long ducts. *International Journal of Heat and Mass Transfer*, 47:4995–5009, 2004.

[8] K.A. Antonopoulos and C. Tzivanidis. A correlation for the thermal delay of building. *Renewable Energy*, 6(7):687–699, 1995.

[9] P.J. Antsaklis and A.N. Michel. *Linear Systems*. McGraw-Hill, New York, 1997.

[10] R. Arena, R. Caponetto, L. Fortuna, and D. Porto. *Nonlinear Noninteger Order Circuits and Systems–An Introduction*. World Scientific, Singapore, 2000.

[11] Arpaci and Larson. *Convection Heat Transfer*. Prentice-Hall, 1984.

[12] V.S. Arpaci, S.-H. Kao, and A. Selamet. *Introduction to Heat Transfer*. Prentice-Hall, Upper Saddle River, NJ, 1999.

[13] A. Aziz and T.Y. Na. *Perturbation Methods in Heat Transfer*. Hemisphere Publ. Corp., Washington, DC, 1984.

[14] H.D. Baehr and K. Stephan. *Heat and Mass Transfer*. Springer, New York, 1998.

[15] A.-L. Barabási. *Linked: The New Science of Networks*. Perseus, Cambridge, MA, 2002.

[16] C Baruch and S. Darrell. On stability of systems of delay differential equations. *J. Comp. Appl. Math.*, 117:137–158, 2000.

[17] J.L. Battaglia, L. Le Lay, J.C. Batsale, A. Oustaloup, and O. Cois. Heat flux estimation through inverted non-integer identification models. *International Journal of Thermal Sciences*, 39(3):374–389, 2000.

[18] H.H. Bau. Control of Marangoni-Benard convection. *International Journal of Heat and Mass Transfer*, 42(7):1327–1341, 1999.

[19] Y. Bayazitoglu and M.N. Ozisik. *Elements of Heat Transfer*. McGraw-Hill, New York, 1988.

[20] M. Becker. *Heat Transfer, A Modern Approach*. Plenum Press, New York, 1986.

[21] A. Bejan. *Convection Heat Transfer*. John Wiley, New York, 1984.

[22] A. Bejan. *Heat Transfer*. John Wiley, New York, 1993.

[23] R. Bellman and K.L. Cooke. *Differential-Difference Equations*. Academic Press, New York, 1963.

[24] C.O. Bennett. *Momentum, Heat, and Mass Transfer*. McGraw-Hill, New York, 3rd edition, 1982.

[25] M.Q. Brewster. *Thermal Radiative Transfer and Properties*. John Wiley, New York, 3rd edition, 1992.

[26] L.C. Burmeister. *Heat Transfer*. Dover, New York, 1982.

[27] L.C. Burmeister. *Convection Heat Transfer*. John Wiley, New York, 2nd edition, 1993.

[28] E.F. Camacho and C. Bordons. *Model Predictive Control in the Process Industry*. Springer, London, 2001.

[29] V.P. Carey. *Liquid-Vapor Phase-Change Phenomena*. Hemisphere Publ. Corp., Washington, DC, 1992.

[30] J. Carr. *Applications of Centre Manifold Theory*. Springer-Verlag, New York, 1981.

[31] H.S. Carslaw and J.C. Jaeger. *Conduction of Heat in Solids*. Clarendon Press, Oxford, UK, 1959.

[32] O. Castillo and P. Melin. *Soft Computing for Control of Non-Linear Dynamical Systems*. Physica-Verlag, Heidelberg, 2001.

[33] Cebeci and Bradshaw. *Physical and Computational Aspects of Convective Heat Transfer*. Springer-Verlag, 1984.

[34] A.J. Chapman. *Fundamentals of Heat Transfer*. Macmillan, New York, 1987.

[35] C.K. Charny. Mathematical models of bioheat transfer. In Y.I. Cho, editor, *Advances in Heat Transfer*, volume 22, pages 19–155. Academic Press, New York, 1992.

[36] G. Chen. Heat transfer in micro- and nanoscale photonic devices. In C.-L. Tien, editor, *Annual Review of Heat Transfer*, volume 7, chapter 1. Begell House, New York, 1996.

[37] G. Chen and G. Chen. *Linear Stochastic Control Systems*. CRC Press, Boca Raton, 1995.

[38] P.D. Christofides. *Nonlinear and Robust Control of PDE Systems*. Birkhäuser, Boston, 2002.

[39] P.D. Christofides and Dautidis P. Feed-back control of hyperbolic PDE systems. *AIChE Journal*, 412:3063, 1978.

[40] J. Chu. Application of a discrete optimal tracking controller to an industrial electrical heater with pure delay. *J. Proc. Cont.*, 5(1):3–8, 1995.

[41] J. Chu, Su H., and x. Hu. A time-delay control algorithm for an industrial electrical heater. *J. Proc. Cont.*, 3(4):220–224, 1993.

[42] Collier. *Convective Boiling and Condensation*. McGraw-Hill, 1984.

[43] C. Comstock. On the delayed hot water problem. *Heat and Mass Transfer*, 96:166–171, 1974.

[44] J. Crank. *Free and Moving Boundary Problems*. Clarendon Press, Oxford, U.K., 1984.

[45] L. Dai. *Singular Control Systems*. Springer-Verlag, Berlin, 1989.

[46] D. Díaz, M. Sen, and K.T. Yang. Effect of delay in thermal systems with long ducts. To be published in *International Journal of Thermal Sciences*, 2004.

[47] G. Díaz. *Simulation and Control of Heat Exchangers using Artificial Neural Networks*. PhD thesis, Department of Aerospace and Mechanical Engineering, University of Notre Dame, Notre Dame, IN, 2000.

[48] G. Díaz, K.T. Yang M. Sen, and R.L. McClain. Simulation of heat exchanger performance by artificial neural networks. *International Journal of HVAC&R Research*, 5(3):195–208, 1999.

[49] G. Díaz, M. Sen, K.T. Yang, and R.L. McClain. Adaptive neurocontrol of heat exchangers. *ASME Journal of Heat Transfer*, 123(3):417–612, 2001.

[50] G. Díaz, M. Sen, K.T. Yang, and R.L. McClain. Dynamic prediction and control of heat exchangers using artificial neural networks. *International Journal of Heat and Mass Transfer*, 44(9):1671–1679, 2001.

[51] G. Díaz, M. Sen, K.T. Yang, and R.L. McClain. Stabilization of a neural network-based temperature controller for heat exchangers. *Proceedings of the 12th International Heat Transfer Conference*, 4:225–230, 2002.

[52] G. Díaz, M. Sen, K.T. Yang, and R.L. McClain. Stabilization of thermal neurocontrollers. To be published in *Applied Artificial Intelligence*, 2004.

[53] K.R. Diller. Models of bioheat transfer processes at high and low temperatures. In Y.I. Cho, editor, *Advances in Heat Transfer*, volume 22, pages 157–357. Academic Press, New York, 1992.

[54] C. Doumanidis and N. Fourligkas. Distributed-parameter control of the heat source trajectory in thermal materials processing. *ASME Journal of Manufacturing Science and Engineering*, 118(4):571–578, 1996.

[55] C. Doumanidis and N. Fourligkas. Distributed-parameter control of the heat source trajectory in thermal materials processing. *ASME Journal of Manufacturing Science and Engineering*, 118(4):571–578, 1996.

[56] P.G. Drazin. *Nonlinear Systems*. Cambridge University Press, Cambridge, U.K., 1992.

[57] R.D. Driver. *Ordinary and Delay Differential Equations*. Springer-Verlag, New York, 1977.

[58] D.K. Edwards. *Radiation Heat Transfer Notes*. Hemisphere Pub. Corp., Washington, DC, 3rd edition, 1981.

[59] P. Elgar. *Sensors for Measurement and Control*. Longman, Essex, U.K., 1998.

[60] J. Feder. *Fractals*. Plenum, New York, 1988.

[61] W. Franco. *Hydrodynamics and Control in Thermal-Fluid Networks*. PhD thesis, Department of Aerospace and Mechanical Engineering, University of Notre Dame, Notre Dame, IN, 2003.

[62] W. Franco, M. Sen, K.T. Yang, and R.L. McClain. Comparison of thermal-hydraulic network control strategies. *Proceedings of the Institution of Mechanical Engineers, Part I: Journal of Systems and Control Engineering*, 217:35–47, 2003.

[63] W. Franco, M. Sen, K.T. Yang, and R.L. McClain. Dynamics of thermal-hydraulic network control strategies. *Experimental Heat Transfer*, 17(3):161–179, 2004.

[64] M. Gad-el-Hak. *Flow Control: Passive, Active and Reactive Flow Management*. Cambridge University Press, Cambridge, U.K., 2000.

[65] V. Ganapathy. *Applied Heat Transfer*. PennWell Pub. Co., Tulsa, OK, 1982.

[66] B. Gebhart. *Heat Conduction and Mass Diffusion*. McGraw-Hill, New York, 1993.

[67] B. Gebhart, Y. Jaluria, R.L. Mahajan, and B. Sammakia. *Buoyancy-Induced Flows and Transport*. Hemisphere Publ. Corp., New York, 1988.

[68] U. Grigull. *Heat Conduction*. Hemisphere Pub. Corp., Washington, D.C., 1984.

[69] J. S. Guillermo, D. Aniruddha, and S.P. Bhattacharyya. PI stabilization of first-order systems with time delay. *Automatica*, 37:2020–2031, 2001.

[70] L. Hach and Y. Katoh. Thermal responses in control loop in indirect control of indoor environment of non-air-conditioned space with quasi-steady-state model. *JSME International Journal Series C-Mechanical Systems Machine Elements And Manufacturing*, 46(1):197–211, 2003.

[71] J.K. Hale and S.M. Lunel. *Introduction to Functional Differential Equations*. Springer-Verlag, New York, 1993.

[72] E.G. Hansen. *Hydronic System Design and Operation*. McGraw-Hill, New York, 1985.

[73] S. Haykin. *Neural Networks: A Comprehensive Foundation*. Macmillan, New York, 1999.

[74] G. Henryk, G. Piotr, and K. Adam. *Analysis and Synthesis of Time Delay Systems*. John Wiley Sons, Chichester, 1989.

[75] M.A. Henson and D.E. Seborg, editors. *Nonlinear Process Control*. Prentice Hall, Upper Saddle River, NJ, 1997.

[76] G.F. Hewitt. *Process Heat Transfer*. CRC Press, Boca Raton, 1994.

[77] J.M. Hill and J.N. Dewynne. *Heat Conduction*. Blackwell Scientific Publications, Oxford, U.K., 1987.

[78] E.J. Hinch. *Perturbation Methods*. Cambridge University Press, Cambridge, U.K., 1991.

[79] K.-H. Hoffman and W. Krabs. *Optimal Control of Partial Differential Equations*. Springer-Verlag, Berlin, 1991.

[80] J.P. Holman. *Heat Transfer*. McGraw-Hill, New York, 7th edition, 1990.

[81] M.H. Holmes. *Laminar flow forced convection in ducts, a source book for compact heat exchanger analytical data*. Springer-Verlag, New York, 1995.

[82] M.F. Hordeski. *HVAC Control in the New Millennium*. Fairmont Press, Liburn, GA, 2001.

[83] L.E. Howle. Control of Rayleigh-Benard convection in a small aspect ratio container. *International Journal of Heat and Mass Transfer*, 40(4):817–822, 1997.

[84] C.J. Huang, C.C. Yu, and S.H. Shen. Selection of measurement locations for the control of rapid thermal processor. *Automatica*, 36(5):705–715, 2000.

[85] G. Huang, L. Nie, Y. Zhao, W. Yang, Q. Wu, and L. Liu. Temperature control system of heat exchangers, an application of DPS theory. *Lecture Notes in Control Information Sciences*, 159:68–76, 1991.

[86] H. Ibach and H. Lüth. *Solid-State Physics*. Springer, New York, 1990.

[87] D. Ibrahim. *Microcontroller-Based Temperature Monitoring and Control*. Newnes, Oxford, 2002.

[88] F.P. Incropera and D.P. Dewitt. *Fundamentals of Heat and Mass Transfer*. John Wiley, New York, 5th edition, 2002.

[89] L. Irena and R. Triggiani. *Deterministic Control Theory for Infinite Dimensional Systems, Vols. I and II Encyclopedia of Mathematics*. Cambridge University Press, 1999.

[90] V.P. Isachenko, V.A. Osipova, and A.S. Sukomel. *Heat Transfer*. Mir, Moscow, 1977.

[91] A. Isidori. *Nonlinear Control Systems*. Springer, London, 1995.

[92] A. Ito, H. Kanoh, and M. Masubuchi. MWR approximation and modal control of parallel and counterflow heat exchangers. *Proc, 2nd IFAC Symposium on Distributed-Parameter Systems*, 41, 1978.

[93] O.L.R. Jacobs. *Introduction to Control Theory*. 2nd Ed., Oxford University Press, Oxford, 1993.

[94] M. Jakob. *Heat Transfer*, volume II. John Wiley, New York, 1957.

[95] Y. Jaluria. *Natural Convection Heat and Mass Transfer*. Pergamon Press, New York, 1980.

[96] Y. Jaluria. *Computational Heat Transfer*. Washington, DC, 1986.

[97] Y. Jaluria and K.E. Torrance. *Computational Heat Transfer*. Taylor and Francis, New York, 2nd edition, 2003.

[98] S. Kakac. *Convective Heat Transfer*. CRC Press, Boca Raton, 2nd edition, 1995.

[99] S. Kakac, R.K. Shah, and W. Aung, editors. *Handbook of Single-Phase Convective Heat Transfer*. John Wiley, New York, 1983.

[100] S. Kakac and Y. Yener. *Heat Conduction*. Taylor and Francis, Washington, DC, 3rd edition, 1993.

[101] R.D. Karam. *Satellite Thermal Control for Systems Engineers*. AIAA, Reston, VA, 1998.

[102] M. Kaviany. *Principles of Convective Heat Transfer*. Springer-Verlag, New York, 1994.

[103] M. Kaviany. *Principles of Heat transfer in Porous Media*. Springer-Verlag, New York, 2nd edition, 1995.

[104] W.M. Kays and M.E. Crawford. *Convective Heat and Mass Transfer*. McGraw-Hill, New York, 3rd edition, 1993.

[105] W.M. Kays and A.L. London. *Compact Heat Exchangers*. McGraw-Hill, San Francisco, 3rd edition, 1984.

[106] D.Q. Kern. *Process Heat Transfer*. McGraw-Hill International, Auckland, 1950.

[107] J. Kevorkian and J.D. Cole. *Multiple Scale and Singular Perturbation Methods*. Springer, New York, 1996.

[108] M.-H. Kim, S.Y. Lee, S.S. Mehendale, and R.L. Webb. Microscale heat exchanger design for evaporator and condenser applications. In J.P. Hartnett, T.F. Irvine, Y.I. Cho, and G.A. Greene, editors, *Advances in Heat Transfer*, volume 37, pages 297–429. Academic Press, Amsterdam, 2003.

[109] C. Kittel and H. Kroemer. *Thermal Physics*. W.H. Freeman & Co., San Francisco, 2nd edition, 1980.

[110] J. Klamka. *Controllability of Dynamical Systems*. Kluwer, Dordrecht, Netherlands, 1991.

[111] F. Kreith and W.Z. Black. *Basic Heat Transfer*. Harper and Row, Cambridge, U.K., 1980.

[112] F. Kreith and M.S. Bohn. *Principles of Heat Transfer*. West Publ. Co., St. Paul, MN, 5th edition, 1993.

[113] A. Kumar and P. Daoutidis. *Control of Nonlinear Differential Algebraic Equation Systems*. Chapman and Hall/CRC, Boca Raton, FL, 1999.

[114] J.R. Leigh. *Temperature Measurement and Control*. Peregrinus, London, 1987.

[115] J.I. Levenhagen and D.H. Spethmann. *HVAC Controls and Systems*. Mc-Graw-Hill, New York, 1993.

[116] W.S. Levine, editor. *Control System Fundamentals*. CRC Press, Boca Raton, FL, 2000.

[117] J.H. Lienhard. *A Heat Transfer Textbook*. Prentice-Hall, Englewood Cliffs, NJ, 1981.

[118] J.L. Lions. On the controllability of distributed systems. *Natl. Acad. Sci. USA*, 94:4828–4835, 1997.

[119] W.W. Liou and Y. Fang. *Microfluid Mechanics: Principles and Modeling*. McGraw Hill, New York, 2006.

[120] B. Liu and T.R. Marchant. The occurrence of limit-cycles during feedback control of microwave heating. *Mathematical and Computer Modelling*, 35(9-10):1095–1118, 2002.

[121] L. Ljung. *System Identification: Theory for the User*. Prentice-Hall, Upper Saddle River, N.J., second edition, 1999.

[122] A. Luikov. *Heat and Mass Transfer*. Mir, Moscow, 1980.

[123] A. Majumdar. Microscale energy transport in solids. In C.-L. Tien, A. Majumdar, and F.M. Gerner, editors, *Microscale Energy Transport*, chapter 1. Taylor and Francis, Washington, DC, 1998.

[124] A. Majumdar. Microscale transport phenomena. In W.M. Rohsenow, J.P Hartnett, and Y.I. Cho, editors, *Handbook of Heat Transfer*, chapter 8. McGraw-Hill, New York, 1998.

[125] T. Marimbordes, A.O. El Moctar, and H. Peerhossaini. Active control of natural convection in a fluid layer with volume heat dissipation. *International Journal of Heat and Mass Transfer*, 45(3):667–678, 2002.

[126] W.J. Minkowycz, E.M. Sparrow, G.E. Schneider, and R.H. Pletcher, editors. *Handbook of Numerical Heat Transfer*. John Wiley, New York, 1988.

[127] M. Modest. *Radiative Heat Transfer*. Academic Press, Amsterdam, 2003.

[128] W. Munk. The delayed hot-water problem, brief notes. *ASME J. Applied Mechanics*, 21(10):?–?, 1954.

[129] O. Nelles. *Nonlinear System Identification*. Springer, Berlin, 2001.

[130] D.A. Nield and A. Bejan. *Convection in Porous Media*. Springer-Verlag, New York, 2nd edition, 1999.

[131] M. Nørgaard, O. Ravn, N.K. Poulsen, and L.K. Hansen. *Neural Networks for Modelling and Control of Dynamic Systems*. Springer, London, 2000.

[132] K. Ogata. *Modern Control Engineering*. Prentice-Hall, Englewood Cliffs, N.J., second edition, 1990.

[133] P.H. Oosthuizen and D. Naylor. *Introduction to Convective Heat Transfer Analysis*. McGraw-Hill, New York, 3rd edition, 1998.

[134] A. Oustaloup. *Systèmes Asservis Linéaires d'Ordre Fractionnaire: Théorie et Practique*. Masson, Paris, 1983.

[135] A. Oustaloup. *La Dérivation Non Entière*. Hermès, Paris, 1995.

[136] M.N. Ozisik. *Boundary Value Problems of Heat Conduction*. Dover Publications, New York, 1968.

[137] M.N. Ozisik. *Heat Conduction*. John Wiley, New York, 1980.

[138] M.N. Ozisik. *Heat Transfer, A Basic Approach*. McGraw-Hill, New York, 1985.

[139] A. Pacheco-Vega. *Simulation of Compact Heat Exchangers using Global Regression and Soft Computing*. PhD thesis, Department of Aerospace and Mechanical Engineering, University of Notre Dame, Notre Dame, IN, 2002.

[140] A. Pacheco-Vega, G. Díaz, M. Sen, K.T. Yang, and R.L. McClain. Heat rate predictions in humid air-water heat exchangers using correlations and neural networks. *ASME Journal of Heat Transfer*, 123(2):348–354, 2001.

[141] A. Pacheco-Vega, M. Sen, K.T. Yang, and R.L. McClain. Genetic-algorithm based prediction of a fin-tube heat exchanger performance. *Proceedings of the 11th International Heat Transfer Conference*, 6:137–142, 1998.

[142] A. Pacheco-Vega, M. Sen, K.T. Yang, and R.L. McClain. Neural network analysis of fin-tube refrigerating heat exchanger with limited experimental data. *International Journal of Heat and Mass Transfer*, 44:763–770, 2001.

[143] M.V. Papalexandris and M.H. Milman. Active control and parameter updating techniques for nonlinear thermal network models. *Computational Mechanics*, 27(1):11–22, 2001.

[144] P.N. Paraskevopoulos. *Modern Control Engineering*. Marcel Dekker, New York, 2002.

[145] H.M. Park and W.J. Lee. Feedback control of the Rayleigh-Benard convection by means of mode reduction. *International Journal for Numerical Methods in Fluids*, 40(7):927–949, 2002.

[146] S. Patankar. *Numerical Heat Transfer and Fluid Flow*. McGraw-Hill/Hemisphere, 3rd edition, 1980.

[147] M. Planck. *The Theory of Heat Radiation*. Dover Publications, New York, 1959.

[148] I. Podlubny. *Fractional Differential Equations*. Academic Press, San Diego, CA, 1999.

[149] D. Poulikakos. *Computational Heat Transfer*. Prentice-Hall, Englewood Cliffs, NJ, 1994.

[150] D.C. Price. A review of selected thermal management solutions for military electronic systems. *IEEE Transactions on Components and Packaging Technologies*, 26(1):26–39, 2003.

[151] W. H. Ray. *Advanced Process Control*. McGraw-Hill, New York, 1981.

[152] P. Riederer, D. Marchio, and J.C. Visier. Influence of sensor position in building thermal control: criteria for zone models. *Energy and Buildings*, 34(6):785–798, 2002.

[153] W. Roetzel and Y. Xuan. *Dynamic behaviour of Heat Exchangers*. WIT Press, Boston, 1999.

[154] Rohsenow, Hartnett, and Ganic, editors. *Heat Exchanger Design Handbook*. John Wiley, New York, 2nd edition, 1983.

[155] K.C. Rolle. *Heat and Mass Transfer*. Prentice-Hall, Upper Saddle River, NJ, 2000.

[156] H.H. Rosenbrock. *State-Space and Multivariable Theory*. John Wiley, New York, 1970.

[157] E.O. Roxin. *Control Theory and its Applications*. Gordon and Breach, Amsterdam, 1997.

[158] P.K. Roy, S.M. Merchant, and S. Kaushal. A review: thermal processing in fast ramp furnaces. *Journal of Electronic Materials*, 30(12):1578–1583, 2001.

[159] N. Saman and H. Mahdi. Analysis of the delay hot/cold water problem. *Energy*, 21(5):395–400, 1996.

[160] C.D. Schaper, M.M. Moslehi, K.C. Saraswat, and T. Kailath. Modeling, identification, and control of rapid thermal-processing systems. *Journal of the Electrochemical Society*, 141(11):3200–3209, 1994.

[161] L.J. Segerlind. *Applied Finite Element Analysis*. John Wiley, New York, 2nd edition, 1984.

[162] M. Sen. *Lecture Notes on Intelligent Systems*. Department of Aerospace and Mechanical Engineering, University of Notre Dame, Notre Dame, IN 46556, 2004.

[163] M. Sen and J.W. Goodwine. Soft computing in control. *The MEMS Handbook*, pages 1–37, Chapter 14, 2001.

[164] M. Sen, E. Ramos, and C. Treviño. On the steady-state velocity of the inclined toroidal thermosyphon. *ASME Journal of Heat Transfer*, 107(4):974–977, 1985.

[165] M. Sen, E. Ramos, and C. Treviño. The toroidal thermosyphon with known heat flux. *International Journal of Heat and Mass Transfer*, 28(1):219–233, 1985.

[166] M. Sen and P. Vasseur. Analysis of multiple solutions in plane poiseuille flow with viscous heating and temperature dependent viscosity. *Proceedings of the National Heat Transfer Conference, HTD-Vol. 107, Heat Transfer in Convective Flows*, pages 267–272, 1989.

[167] M. Sen, P. Vasseur, and L. Robillard. Multiple steady states for unicellular natural convection in an inclined porous layer. *International Journal of Heat and Mass Transfer*, 30(10):2097–2113, 1987.

[168] M. Sen and K.T. Yang. Applications of artificial neural networks and genetic algorithms in thermal engineering. *The CRC Handbook of Thermal Engineering*, 123(3):Section 4.24, 620–661, 2000.

[169] M. Sen and K.T. Yang. Laplace's equation for convective scalar transport in potential flow. *Proceedings of the Royal Society A: Mathematical, Physical and Engineering Sciences*, 455(2004):3041– 3045, 2000.

[170] R.K. Shah and A.L. London. *Laminar flow forced convection in ducts, a source book for compact heat exchanger analytical data*. Academic Press, New York, 1978.

[171] T.M. Shih. *Numerical Heat Transfer*. Hemisphere Pub. Corp., Washington, DC, 1984.

[172] K. Shimazaki, A. Ohnishi, and Y. Nagasaka. Development of spectral selective multilayer film for a variable emittance device and its radiation properties measurements. *International Journal of Thermophysics*, 24(3):757–769, 2003.

[173] R. Siegel and J.R. Howell. *Thermal Radiation Heat Transfer*. Hemisphere Publ. Corp., Washington, DC, 3rd edition, 1992.

[174] N. Silviu-lulian. *Delay Effects on Stability*. Lecture Notes in Control and Information Sciences, Springer, London,, 2001.

[175] J. Singer and H.H. Bau. Active control of convection. *Physics of Fluids A-Fluid Dynamics*, 3(12):2859–2865, 1991.

[176] J. Singer, Y.Z. Wang, and H.H. Bau. Controlling a chaotic system. *Physical Review Letters*, 66(9):1123–1125, 1991.

[177] L.E. Sissom and D.R. Pitts. *Elements of Transport Phenomena*. McGraw-Hill, New York, 1972.

[178] H. Smith and H.H. Jensen. *Transport Phenomena*. Clarendon Press, Oxford, U.K., 1989.

[179] E.D. Sontag. *Mathematical Control Theory*. Springer, New York, 1998.

[180] W.F. Stoecker and P.A. Stoecker. *Microcomputer Control of Mechanical and Thermal Systems*. Van Nostrand Reinhold, New York, 1989.

[181] S.H. Strogatz. *Sync: The Emerging Science of Spontaneous Order*. Theia, New York, 2003.

[182] B. Sundén and M. Faghri. *Computer Simulations in Compact Heat Exchangers*. Computational Mechanics Publications, Southhampton, U.K., 1998.

[183] N.V. Suryanarayana. *Engineering Heat Transfer*. West Pub. Co., Minneapolis/St. Paul, 1995.

[184] T.D. Swanson and G.C. Birur. NASA thermal control technologies for robotic spacecraft. *Applied Thermal Engineering*, 23(9):1055–1065, 2003.

[185] M. Sweetland and J.H. Lienhard. Active thermal control of distributed parameter systems with application to testing of packaged IC devices. *ASME Journal of Heat Transfer*, 125(1):164–174, 2003.

[186] P. Tabeling. *Introduction to Microfluidics*. Oxford University Press, Oxford, UK, 2005.

[187] M. Tabib-Azar. *Microactuators: Electrical, Magnetic, Thermal, Optical, Mechanical, Chemical & Smart Structures*. Kluwer Academic, Boston, 1998.

[188] J. Taine. *Heat Transfer*. Prentice-Hall, Englewood Cliffs, N.J., 1993.

[189] J. Tang and H.H. Bau. Feedback-control stabilization of the no-motion state of a fluid confined in a horizontal porous layer heated from below. *Journal of Fluid Mechanics*, 257:485–505, 1993.

[190] J. Tang and H.H. Bau. Stabilization of the no-motion state in Rayleigh-Benard convection through the use of feedback-control. *Physical Review Letters*, 70(12):1795–1798, 1993.

[191] J. Tang and H.H. Bau. Stabilization of the no-motion state in the Rayleigh-Benard problem. *Proceedings of the Royal Society of London Series A-Mathematical and Physical Sciences*, 447(1931):587–607, 1994.

[192] J. Tang and H.H. Bau. Stabilization of the no-motion state of a horizontal fluid layer heated from below with Joule heating. *ASME Journal of Heat Transfer*, 117(2):329–333, 1995.

[193] J. Tang and H.H. Bau. Experiments on the stabilization of the no-motion state of a fluid layer heated from below and cooled from above. *Journal of Fluid Mechanics*, 363:153–171, 1998.

[194] J. Tang and H.H. Bau. Numerical investigation of the stabilization of the no-motion state of a fluid layer heated from below and cooled from above. *Physics of Fluids*, 10(7):1597–1610, 1998.

[195] J. Tang and H.H. Bau. Numerical investigation of the stabilization of the no-motion state of a fluid layer heated from below and cooled from above. *Physics of Fluids*, 10(7):1597–1610, 1998.

[196] J.C. Tannehill, D.A. Anderson, and R.H. Pletcher. *Computational Fluid Mechanics and Heat Transfer*. Taylor and Francis, Washington, DC, 2nd edition, 1997.

[197] C. Tin-Tai. Numerical modeling of thermal behavior of fluid conduit flow with transport delay. *ASHRAE Transactions*, 102(2):?–?, 1996.

[198] L.S. Tong and Y.S. Tang. *Boiling Heat Transfer and Two-Phase Flow*. Taylor and Francis, Washington, DC, 1997.

[199] C. Tricot. *Curves and Fractal Dimension*. Springer-Verlag, New York, 1995.

[200] V. Trivedi and S.J. Pearton. Evaluation of rapid thermal processing systems for use in CMOS fabrication. *Solid-State Electronics*, 46(5):777–783, 2002.

[201] J.W.C. Tseng. *Radiant Heat Transfer in Porous Media*. Springer-Verlag, 2nd edition, 1990.

[202] D.Y. Tzou. *Macro- to Microscale Heat Transfer: The Lagging Behavior*. Taylor and Francis, Washington, DC, 1997.

[203] E.I. Varga, K.M. Hangos, and F. Szigeti. Controllability of heat exchanger networks in the time-varying parameter case. *Control Engineering Practice*, 3(10):1409–1419, 1995.

[204] C.H. Wang, M. Sen, and P. Vasseur. Analytical investigation of bénard-marangoni convection heat transfer in a shallow cavity filled with two immiscible fluids. *Applied Scientific Research*, 48:35–53, 1991.

[205] Y.Z. Wang, J. Singer, and H.H. Bau. Controlling chaos in a thermal-convection loop. *Journal of Fluid Mechanics*, 237:479–498, 1992.

[206] B. Weigand. *Analytical Methods for Heat Transfer and Fluid Flow Problems*. Springer, Berlin, 2004.

[207] F.M. White. *Heat and Mass Transfer*. Addison-Wesley, Reading, MA, 1988.

[208] G.B. Whitham. *Linear and Nonlinear Waves*. John Wiley & Sons, New York, 1974.

[209] J.A. Wiebelt. *Engineering Radiation Heat Transfer*. Holt, Rinehart and Winston, New York, 1966.

[210] R.H.S. Winterton. *Heat Transfer*. Oxford University Press, New York, 1997.

[211] H. Wolf. *Heat Transfer*. Harper and Row, Cambridge, U.K., 1982.

[212] K.-F.V. Wong. *Intermediate Heat Transfer*. Marcel Dekker, New York, 2003.

[213] K.T. Yang and M. Sen. Agent networks for intelligent dynamic control of complex hydronic HVAC building systems–Part 1: Framework for agent network development. *International Journal on Architectural Science*, 3(1):43–50, 2002.

[214] C.-C. Yu. *Autotuning of PID Controllers*. Springer, London, 1999.

[215] P.K. Yuen and H.H. Bau. Rendering a subcritical Hopf bifurcation supercritical. *Journal of Fluid Mechanics*, 317:91–109, 1996.

[216] P.K. Yuen and H.H. Bau. Controlling chaotic convection using neural nets - theory and experiments. *Neural Networks*, 11(3):557–569, 1998.

[217] P.K. Yuen and H.H. Bau. Optimal and adaptive control of chaotic convection - theory and experiments. *Physics of Fluids*, 11(6):1435–1448, 1999.

[218] Z. Zhang and R. M. Nelson. Parametric analysis of a building space conditioned by a VAV system. *ASHRAE Transactions*, 98(1):43–48, 1992.

[219] Z.M. Zhang, C.J. Fu, and Q.Z. Zhu. Optical and thermal radiative properties of semiconductors related to micro/nanotechnology. In J.P. Hartnett, T.F. Irvine, Y.I. Cho, and G.A. Greene, editors, *Advances in Heat Transfer*, volume 37, pages 179–296. Academic Press, Amsterdam, 2003.

[220] A. Zilouchian and M. Jamshidi, editors. *Intelligent Control Systems Using Soft Computing Methodologies*. CRC Press, Boca Raton. FL, 2001.

[221] S. Zumbo, J. Leofanti, S. Corradi, G. Allegri, and M. Marchetti. Design of a small deployable satellite. *Acta Astronautica*, 53(4-10):533–540, 2003.

Index